The University Of Sheffield.

Growth hormone inhibition in Autosomal Dominant Polycystic Kidney Disease

Fiona Macleod

A thesis submitted in partial fulfilment of the requirements for the degree of Doctor of Philosophy

Department of Infection, Immunity & Cardiovascular Diseases

Faculty of Medicine, Dentistry and Health

2021

Table of Contents

List of Figures

List of Tables

Abbreviations

ADPKD	Autosomal-dominant polycystic kidney disease
A_x	Absorbance at x nm
BUN	Blood urea nitrogen
BW	Body weight
cAMP	Cyclic adenosine monophosphate
CCND1	Cyclin D1
CDK	Cyclin-dependent kinase
CV	Column volume
Da	Dalton
DTT	Dithiothreitol
EDTA	Ethylenediaminetetraacetic acid disodium salt
eGFR	Estimated glomerular filtration rate
EMA	European Medicines Agency
ESRD	End-stage renal disease
ESRF	End-stage renal failure
E. coli	*Escherichia coli*
FDA	U.S. Food and Drug Administration
GAIN	GPCR-autoproteolysis inducing

GAS	Interferon gamma-activated sequence
GH	Growth hormone
GHA	Growth hormone receptor antagonist
GHBP	Growth hormone binding protein
GHD	Growth hormone deficiency
GHF-1	Growth hormone factor 1
GHR	Growth hormone receptor
GHS-R	Growth hormone secretagogue receptor
GPCR	G-protein coupled receptor
GPS	GPCR proteolysis site
H&E	Haemotoxylin & Eosin
IGF-1	Insulin like Growth Factor 1
IgG	Immunoglobulin G
IMS	Industrial Methylated Spirits
IPTG	Isopropyl β-D-thiogalactoside
ISRE	Interferon-stimulated response element
JAK	Janus kinase
kDa	Kilodalton
KW	Kidney weight
LB	Lysogeny broth
MWCO	Molecular weight cut-off
NOAEL	No observable adverse effect level
PAPP-A	Pregnancy associated plasma protein A

PBS	Phosphate-buffered saline
PC1	Polycystin 1
PC2	Polycystin 2
PCNA	Proliferating cell nuclear antigen
PH3	Phosphoserine 10 Histone 3
PKD1	Polycystic Kidney Disease 1
PKD2	Polycystic Kidney Disease 2
PLD	Polycystic Liver Disease
PSR	Picrosirius Red
PY	Phosphotyrosine
Q column	Quaternary ammonium anion exchange column
Q/Gln	Glutamine
REJ	Receptor egg jelly
RNA	Ribonucleic acid
RPF	Renal plasma flow
SDS-PAGE	Sodium dodecyl sulfate polyacrylamide gel electrophoresis
SEs	Super Enhancers
siRNA	Silencing RNA
SOCS	Suppressors of cytokine signalling
SP column	Sulphopropyl column
SSA	Somatostatin analogues
SSTR	Somatostatin receptor
STAT	Signal transducer and activator of transcription

TBS	Tris-buffered saline
TBST	Tris-buffered saline with Tween-20
TEMED	N,N,N’,N’-tetramethylethylenediamine
V2R	Vasopressin 2 receptor
WT	Wild-type

Acknowledgements

I would like to give my deepest thanks to my supervisors Dr Maria Fragiadaki and Professor Jon R Sayers who provided me with the opportunity to undertake one of the most challenging and rewarding experiences of my life. Their knowledge, guidance and encouragement were invaluable to my progress and I am incredibly grateful for the support they gave to me. I am truly lucky to have had you both as my supervisors.

I would also like to thank my friends in the department who kept me sane and helped me to keep going when the setbacks felt insurmountable, particularly Emma Brudenell and Stavroula Louka for their unending support and compassion. Thank you also to Monica Neilan and Lisa Chang for being great sources of laughter and the occasional distraction when it was truly needed.

I would like to express my gratitude to Dr Sarbendra Pradhananga for his infinite patience and advice when it came to laboratory techniques, for always being a friendly, approachable and willing to help. Also to Dr Ian Wilkinson and Dr Andrew Streets for their fantastic help and guidance both during my confirmation review and with some of the particularly tricky parts of this project.

A big thank you to all members of the Fragiadaki, Sayers and Ong labs, it was a pleasure working with you all.

A huge thank you to all of the technical staff within the IICD, I really appreciate everything you do. Particularly Janine Phipps and Carl Wright for training me in key techniques for my project.

Last but not least, I would like to give thanks to my husband Christopher for believing in me and for being by my side during the highs and lows. I could not have done it without you.

Abstract

Relevance

Autosomal Dominant Polycystic Kidney Disease (ADPKD) is the most common hereditary renal disease worldwide and the primary genetic cause of end stage-renal failure. ADPKD is characterised by progressive renal hypertrophy and development of renal cysts, leading to loss of function and renal failure requiring dialysis and transplant. There are currently no curative treatments and only one drug (Tolvaptan) available on the market that delays progression of disease which not all people with ADPKD are eligible to take.

Rationale & Hypothesis

Aberrant signalling in the Janus Kinase/Signal Transducers and Activators of Transcription (JAK/STAT) pathway has been implicated in ADPKD pathogenesis and progression, and our laboratory has previously found aberrant activation of JAK2 and STAT5 signalling alongside elevated circulating growth hormone (GH) in a mouse model of ADPKD. This project investigates the hypothesis that growth hormone-induced JAK2/STAT5 signalling promotes proliferation and subsequent cystogenesis in ADPKD and that inhibition of this pathway may slow progression of disease.

Results

Recombinant GH and GH with a mutation resulting in a dominant negative GH receptor antagonist (GHA) were successfully expressed and their ability to modulate STAT5 activity was demonstrated in kidney cells. Stimulation of human and mouse cellular

models of ADPKD with GH significantly increases STAT5 activation and expression of STAT5 transcriptional targets, which is significantly reduced with treatment with GHA or the JAK inhibitor Ruxolitinib. This study presents the novel finding that growth hormone elevates cyst expansion and proliferation in cellular models of ADPKD, and inhibition of GH-JAK2-STAT5 signalling with GHA, Ruxolitinib or genetic knockdown abrogates GH-driven cystic growth and proliferation. *In vivo*, Ruxolitinib treatment protects renal function and reduces renal hypertrophy and fibrosis in a mouse model of ADPKD.

Conclusion

This thesis identifies that growth hormone promotes proliferation and cyst expansion of cystic cells via JAK2-STAT5 signalling. Inhibition of GH-JAK2-STAT5 is beneficial in reducing proliferation, cystic growth and improving renal function.

Chapter 1: INTRODUCTION

Autosomal dominant polycystic kidney disease (ADPKD) is the most prevalent genetic renal disease worldwide and accounts for ~10% of end-stage renal disease (ESRD) requiring dialysis in Europe (Spithoven et al., 2014). Approximately 50% of ADPKD patients will die or develop ESRD (also referred to as stage 5 chronic kidney disease or end-stage renal failure) by an average age of 58 years (Gabow et al., 1992). ADPKD causes a decline in renal function through progressive formation and development of kidney cysts, usually in later life (Grantham *et al*., 2006; Ward *et al*., 1994). In addition to the health burden, ADPKD has a substantial economic impact on healthcare systems primarily through ESRD costs, which are estimated to be 651 million euros per year in Europe (Lentine et al., 2010, Spithoven et al., 2014). This chronic disorder is caused primarily by pathogenic mutations in *PKD1* or *PKD2* genes which encode interacting p polycystin-1 and polycystin-2, respectively. *PKD1* mutations are more prevalent making up approximately 85% of cases of ADPKD, whilst *PKD2* mutations make up an estimated 15% of cases (Harris et al., 2006, Mochizuki et al., 1996, Torra et al., 1996, Ward et al., 1994).

There have been a multitude of studies elucidating the molecular and cellular pathogenesis of ADPKD in the past two decades. Despite this, there is only a single therapeutic strategy that effectively and consistently slows progression (Tolvaptan), available to some, but not all ADPKD patients. This highlights the need to identify new therapies by furthering our understanding of pathogenic mechanisms involved in the disease. There is accumulating evidence that growth hormone (GH) plays a role in progression of ADPKD, via the GH-STAT5-cyclin D1 axis (Fragiadaki et al., 2017).

1.1 Clinical features and epidemiology of autosomal dominant polycystic kidney disease

1.1.1 Prevalence of ADPKD

Based on the European Renal Association–European Dialysis and Transplant Association (ERA–EDTA) registry database, the estimated prevalence of ADPKD is 1 in 3040. However, when combined with population-based studies the estimate was <1 in 2000. Difficulties in accurately estimating prevalence arise due to the complex genetics of ADPKD as well as asymptomatic, undiagnosed cases (Willey et al., 2017). Prevalence estimates vary by approach, location and by their criteria for ADPKD (Davies et al., 1991, Higashihara et al., 1998, Iglesias et al., 1983, Neumann et al., 2013, Solazzo et al., 2018). For example, some studies only include clinically diagnosed cases such as the study by Higashihara *et al*., while Iglesias *et al*. include cases diagnosed clinically or during autopsy. Prevalence estimates are being refined through improved diagnostic techniques and implementation of national registries such as the National Registry of Rare Kidney Diseases (RaDaR) in the UK.

1.1.2 Renal symptoms

The key clinical feature and the major cause of morbidity in ADPKD is progressive formation and enlargement of fluid-filled renal cysts. Cyst formation and their growth gradually enlarges the kidneys and compromises healthy renal tissue leading to fibrosis, deterioration of renal function and ultimately ESRD between 30-60 years of age (Gabow et al., 1992, Grantham et al., 2006, Harris et al., 2006). ADPKD is diagnosed in individuals

with renal ultrasonography where multiple bilateral renal cysts and renal hypertrophy are observed (Bear et al., 1984).

Although the majority of people with ADPKD are asymptomatic until adulthood, renal cysts are detectable as early as *in utero*. In a retrospective study using ultrasound with 27 patients, renal cysts were present in 4 cases prenatally, and 12 cases postnatally by age 12 months (Brun et al., 2004). In children carrying a *PKD1* mutation, renal cysts are detectable in ~60% by five years of age, increasing to 75-80% in children 5-18 years of age (Gabow et al., 1997, Fick et al., 1994).

Acute and chronic pain are common features in ADPKD and frequently lead to the diagnosis (Bajwa *et al*., 2004). Acute pain is associated with nephrolithiasis (the formation of kidney stones), urinary tract infections, and cyst haemorrhage (Torres et al., 1993). Cysts in the kidney, alongside renal hypertrophy can lead to chronic pain in the flank region, back, and abdomen. Uncomfortable abdominal fullness and postural changes in the spine, for example lumbar lordosis, can occur due to cystic enlargement of the kidney and the liver and subsequent mechanical strain (Tellman et al., 2015).

A number of early abnormalities in renal function have been reported in people with ADPKD, such as impaired urinary concentrating capacity and increased vasopressin levels (Gabow et al., 1989). The latter is also referred to as antidiuretic hormone or arginine vasopressin. One of the earliest clinical manifestations in the disease is impaired urinary concentrating mechanisms. Gabow *et al*. (1989) noted a correlation between the presence and severity of the vasopressin-resistant renal concentrating defect with the extent of polycystic disease, which could be attributed to renal cysts causing structural disruption of the medulla and thus impacting urinary concentrating mechanisms.

Increased levels of vasopressin seen in ADPKD are associated with cystogenesis, disease severity and progression (Torres et al., 2012, Yamaguchi et al., 2000).

1.1.3 Extrarenal symptoms

ADPKD is a disease which affects multiple organs. As well as renal cysts, up to 80% of patients with ADPKD also develop polycystic liver disease (PLD), which is characterised by the appearance of cysts in the liver. Cysts in the pancreas, spleen, seminal vesicle, and prostate have also been recorded (Belet et al., 2002, Hogan et al., 2015, Mosetti et al., 2003). ADPKD can impact the central nervous system in the form of benign intracranial arachnoid cysts (~12%) and contributes to morbidity and mortality in the form of intracerebral haemorrhage or intracranial aneurysms, with subsequent subarachnoid haemorrhage and cerebral infarctions affecting mainly patients under 65 (Vlak et al., 2011, Krauer et al., 2012, Orskov et al., 2012). An increased prevalence of colonic diverticular disease has been described (Scheff et al., 1980). Conversely, Sharp *et al*. concluded no increased prevalence of diverticular disease in ADPKD patients (Sharp et al., 1999).

Cardiovascular events are the most frequent cause of death in ADPKD (36%), with death from infection the second most likely cause (17%). The main causes of death from infection are septicaemia (33%; as a percentage of deaths from infection, not deaths from ADPKD), pneumonia (27%) and peritonitis (11%) (Iglesias et al., 1983, Orskov et al., 2012). The leading cardiovascular causes of death are myocardial infarction and ischaemic heart disease, although death by heart failure, valvular disease and pulmonary embolism are also reported (Orskov et al., 2012). Patients with ADPKD have higher prevalence of cardiovascular abnormalities including cardiac valve defects,

hypertension and left ventricular hypertrophy (Chebib et al., 2017, Ward et al., 1994). Hypertension is seen in most patients with ADPKD and, although it occurs prior to decline in renal function, early onset hypertension has been associated with progressive increase in renal volume and renal cysts and earlier onset ESRD (Gabow et al., 1992, Johnson and Gabow, 1997). Hypertension in ADPKD is associated with impaired vascular development, activation of the renin-aldosterone-angiotensin system (RAAS) and increased levels of vasopressin (Chapman et al., 2010, Zittema et al., 2012). Consequent to hypertension, patients with ADPKD are at a greater risk of aortic aneurysm and dissection compared to the general population (Sung *et al*., 2017). Additionally, ADPKD is associated with higher incidence of intracranial aneurysms which can rupture and cause subarachnoid haemorrhage (Vlak et al., 2011, Cagnazzo et al., 2017).

Enhanced, deregulated cell proliferation is a hallmark in both ADPKD and cancer. Both diseases share aberrantly activated signalling pathways such as the mTOR-PI3K-AKT pathway. However, ADPKD shows an increase in apoptosis, whereas a key characteristic of cancer is apoptotic resistance (Hanahan and Weinberg, 2011, Lanoix et al., 1996, Shillingford et al., 2006). Yu *et al* examined the risk of cancer in patients with PKD (autosomal dominant and unspecified type) in Taiwan, excluding PKD patients with a history of cancer, ESRD, or chronic kidney disease. The results of their study suggested that the PKD group had a higher risk of cancers of the kidney, liver, and colon compared to the control group before receiving a transplant or renal replacement therapy (Yu et al., 2016). However, conclusions from this study are limited by a lack of information on environmental/lifestyle factors that could contribute to carcinogenesis. Concordantly, Schrem *et al*. reported that patients with ADPKD were at a slightly higher risk of having post-transplant malignancies, when compared with other patients with ESRD not

related to ADPKD (Schrem et al., 2016). Further studies are needed to make a strong conclusion as to whether patients with ADPKD truly present with higher risk for neoplasia.

1.1.4 Sex distribution and differences

The ratio of males:females affected by ADPKD is closer to 1:1 than other renal diseases with reported ratios ranging 1.085:1 to 1.17:1 (Ishikawa et al., 2000, Solazzo et al., 2018). There is a significant difference between the sexes when it comes to the rate of progression of renal disease with males experiencing worse mean renal function at a given age and earlier age of renal failure and renal death (Gretz et al., 1989, Gabow et al., 1992). Urinary tract infections in males, hepatic cysts in females and three or more pregnancies in hypertensive females were also associated with a faster rate of renal function decline (Gabow et al., 1992, Chapman et al., 1994, Johnson and Gabow, 1997). The mechanisms behind the sex differences are not yet fully elucidated, though it has been postulated that sex hormones play a role (Cowley et al., 1997), but this has not been evidenced in humans. The reasons behind the differences seen in rate of progression between males and females requires further study.

1.1.5 Intrafamilial variation

Despite being a hereditary disease arising from mutation of the same gene, intrafamilial variation in the phenotype of ADPKD has been observed within affected families displayed as considerable differences in disease severity, progression, and the onset of ESRD (Lanktree et al., 2019, Milutinovic et al., 1992). For example, Peral *et al*. describe drastic differences in phenotype between dizygotic (fraternal) twins with the same

germline nonsense mutation in *PKD1*, in which one twin displayed early onset ADPKD wherein enlarged bilateral polycystic kidneys were observed *in utero*, whilst the other twin showed no renal cysts under ultrasound when measured by 5 years of age (Peral et al., 1996). The authors conclude that this discordance was likely due to genetic modifiers.

Concordantly, contribution of genetic modifiers in intrafamilial variability is supported by Persu *et al*., as they demonstrated that there is significantly more variability in disease progression assessed by age at ESRD in affected siblings than in monozygotic twins.

This highlights the variability of ADPKD and illustrates the additional challenges and considerations in predicting risk of disease severity and age of onset ESRD based upon older affected family members alone. Moreover, this provides supporting evidence of the two-hit hypothesis of cyst formation requiring somatic mutation discussed further in section 1.2.3.

1.2 Genetics and molecular pathogenesis in ADPKD

1.2.1 Discovery of the genes PKD1 and PKD2

As a part of The European Polycystic Kidney Disease Consortium, Ward *et al*. describe that *PKD1* is located on chromosome 16p13.3 (mapped by Reeders and colleagues, using positional cloning) and that it encodes a "novel protein whose function is at present unknown", a protein we now know to be polycystin-1 (PC1) (Reeders et al., 1985, Ward et al., 1994). A second gene involved in ADPKD was identified when an Italian family had clinical features of ADPKD with no linkage to chromosome 16p (Romeo et al., 1988).

PKD2 is located on chromosome 4q21-23 (also mapped by positional cloning) and was found to encode polycystin-2 (PC2) (Mochizuki et al., 1996). Although still not fully understood, some of the roles of PC1 and PC2 have been further elucidated in the past two decades described below.

1.2.2 Normal polycystin function in the kidney

Polycystins are widely expressed including in kidney tubular epithelial cells, the liver, vascular endothelium, pancreas, and brain (Ong et al., 1999, IbraghimovBeskrovnaya et al., 1997). Subcellularly, the polycystin complex is located, though not exclusively, in primary cilia, nonmotile extensions on the apical cell surface involved in cell signalling which can have mechanosensory function, sensitive to luminal fluid flow (Dell, 2015).

PC1 is a large integral membrane protein (460 kDa) with features suggestive of receptor function such as multiple extracellular motifs involved in cell-cell and/or cell-matrix interactions, and a heterotrimeric G-protein activation sequence (Hughes et al., 1995, Parnell et al., 1998, Qian et al., 2002, Tsiokas et al., 1999). PC1 undergoes post-translational modification via cleavage at an autoproteolysis sequence known as the G-protein coupled receptor (GPCR) proteolysis site (GPS) motif in a process which requires the receptor for egg jelly (REJ) domain (Ponting et al., 1999, Qian et al., 2002). Previously, the catalytic mechanism was unknown, until Arac *et al*. discovered that the GPS motif is an integral part of what they termed the GPCR-Autoproteolysis INducing (GAIN) domain (Figure 1.1) (Arac et al., 2012). GPS autoproteolytic cleavage is essential for normal functioning of PC1 (Yu et al., 2007).

PC2, also referred to as transient receptor potential polycystin 2 (TRPP2), is an integral membrane glycoprotein (~110 kDa) with six transmembrane domains. It is a non-selective, calcium ion (Ca^{2+}) permeable cation channel that belongs to the transient receptor potential (TRP) channel superfamily (Cai et al., 1999, Tsiokas et al., 1999). PC1 has a coiled-coil domain in the cytoplasmic C terminus which interacts with the cytoplasmic C terminal tail of PC2 (Qian *et al*., 1997). It is thought that the polycystin complex functions as Ca^{2+}-permeable receptor channel, thus mutation in one impacts the function of the other (Hanaoka et al., 2000, Nauli et al., 2003). Gating of PC2 and regulation of assembly of the PC1-PC2 complex has been suggested to be mediated by cyclic adenosine monophosphate (cAMP) signalling and PKA phosphorylation (Cantero et al., 2015).

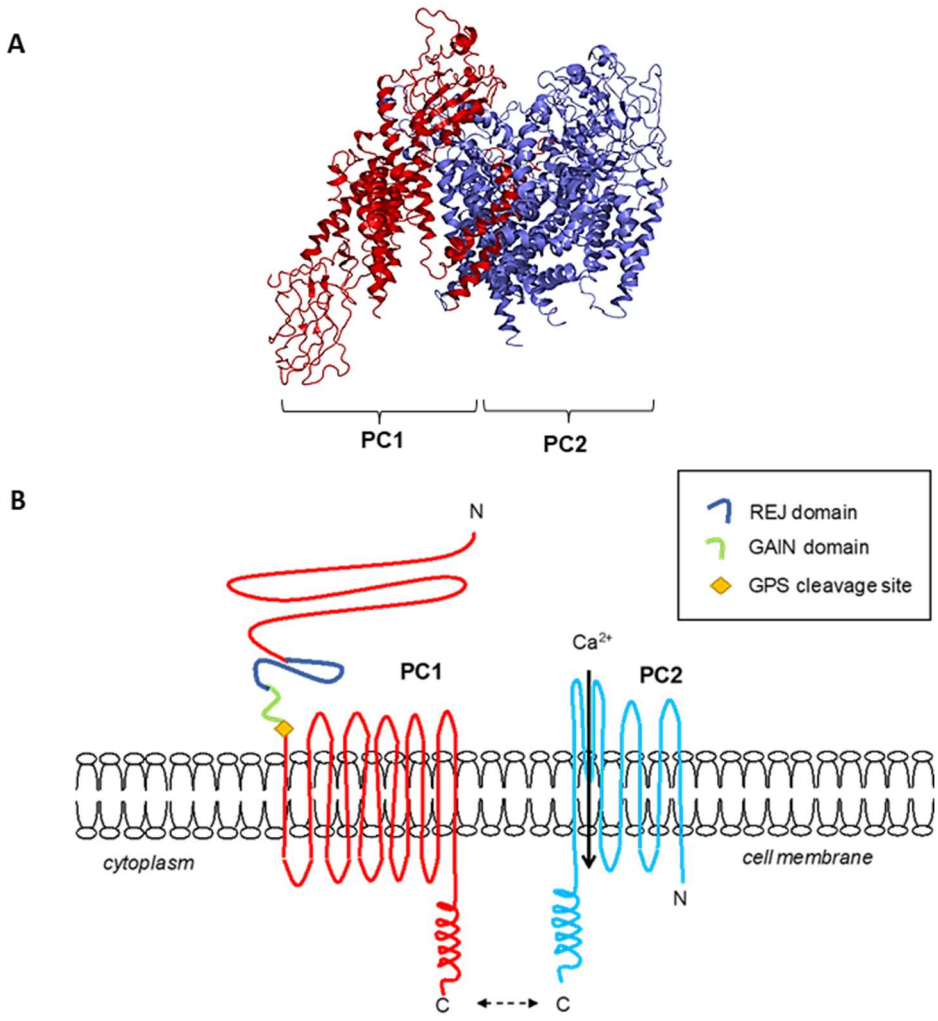

Figure 1.1 Structure of polycystin 1 (PC1) and polycystin 2 (PC2).

(A) Polycystin complex with PC1 (red) and PC2 (blue). Figure was rendered with the 6a70 pdb file (B) Simplified structure of the PC complex. PC1 is a transmembrane protein which undergoes autoproteolytic cleavage at the G-protein coupled receptor (GPCR) proteolysis site (GPS) motif which is part of the GPCR-Autoproteolysis INducing (GAIN) domain in a process which requires the receptor for egg jelly (REJ) domain. PC2 is a non-selective, calcium ion (Ca2+) permeable cation channel. PC1 and PC2 interact via of coiled-coil domains represented as a dashed arrow. (Adapted from (Chapin and Caplan, 2010, Ong and Harris, 2015) with permissions).

1.2.3 Mutations and disease severity

ADPKD is caused by pathogenic mutations occurring in *PKD1* or *PKD2*. ADPKD caused by *PKD1* and *PKD2* mutations are referred to as ADPKD1 and ADPKD2, respectively. Mutations in these genes lead to increased intracellular cAMP and subsequent altered cell polarity, enhanced cell proliferation and apoptosis, and luminal fluid secretion. This results in disruption of the normal differentiated phenotype of the renal tubular epithelium (Belibi et al., 2004, Wilson et al., 1991, Yamaguchi et al., 2000). Moreover, pathogenic mutations in *PKD1*/*PKD2* leads to aberrant cell signalling including cAMP (Yamaguchi et al., 1997), mTOR (Shillingford et al., 2006), Notch (Idowu et al., 2018), Wnt signaling (Happe et al., 2009), and JAK/STAT (discussed further in section 1.4.2 and 1.5.5) (Figure 1.2).

Multiple aspects of mutations in PKD genes affects the severity of the disease, including which gene is mutated, the type of mutation, and the number of mutations. Over 1200 mutations have been reported for *PKD1* and around 200 mutations for *PKD2* (Willey et al., 2017). *PKD1* mutations are the most common in ADPKD and are associated with a more severe phenotype than *PKD2*. Patients with ADPKD1 tend to reach ESRD at a younger age and are more likely to have hypertension and haematuria (Cornec-Le Gall et al., 2013, Gabow et al., 1992, Hateboer et al., 1999, Willey et al., 2017).

Within genes that are pathogenically mutated, the type of mutation can also affect severity of the disease, e.g. in *PKD1*, where a truncating mutation is linked with a more severe form of the disease in comparison to non-truncating mutations (Cornec-Le Gall et al., 2013).

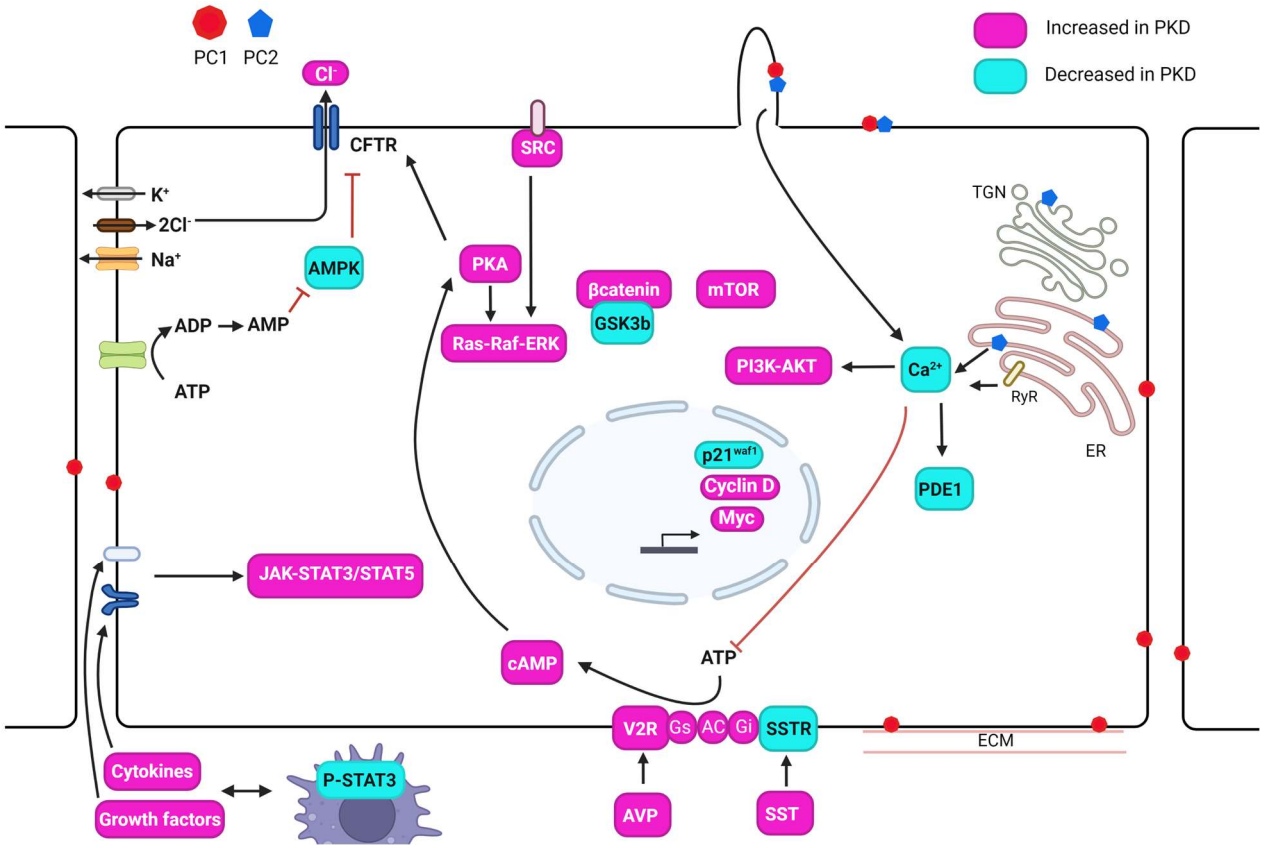

Figure 1.2 Signalling pathways affected in PKD

In PKD there is aberrant activation of JAK/STAT, mTOR, PI3K-AKT, AMPK and Ras-Raf-ERK signalling. There is a decrease in Ca2+ influx alongside elevated cAMP. AC, adenylyl cyclase; AMPK, AMP kinase; AVP, arginine vasopressin; CFTR, cystic fibrosis transmembrane conductance regulator; ER, endoplasmic reticulum; GSK3β, glycogen synthase kinase 3β; PDE1, phosphodiesterase 1; PKA, protein kinase A; SST, somatostatin; SSTR, somatostatin receptor; TGN, trans-golgi network; V2R, vasopressin V2 receptor. Adapted with permissions from (Bergmann et al., 2018, Torres and Harris, 2014, Koslowski et al., 2020).

In a person affected with ADPKD, all cells contain a one-copy germline mutation in *PKD1* or *PKD2*, which resides in one of the two alleles of the gene, but only a subset of these cells will go on to form cysts. Moreover, the high level of intrafamilial variation observed in the severity of ADPKD symptoms has led researchers to postulate that additional germline mutations may not be the underlying cause of heterogeneity. It was proposed by Peter Harris that two fully penetrant germline mutations is predicted to result in embryonic lethality in affected people (Harris, 1999). This is supported by work in mouse models where complete deletion of *Pkd1* or *Pkd2* lead to embryonic lethality (Lu et al., 1997, Wu et al., 2000). Hence the "two-hit" hypothesis model was proposed that postulates that in a subset of cells with a PKD germline mutation an additional somatic mutation takes place known as the "second hit". This somatic mutation results in inactivation of the remaining normal PKD allele, resulting in loss of heterozygosity (LOH). The LOH results in monoclonal proliferation of the PKD null cell and ultimately leads to cyst formation. In every single kidney fewer than 1% of nephrons develop cysts indicating that cyst formation is a focal process. This observation has led Gregory Germino's lab to study the clonality of PKD mutation within the cysts. By isolating epithelial cells from single renal cysts, they have shown that renal cysts in ADPKD are monoclonal (Qian et al., 1996). Furthermore, results of mouse and human studies have indicated that in addition to germinal mutations, somatic mutations leading to a trans-heterozygous state with mutations in both *PKD1* and *PKD2* can also drive cyst formation. This result has been reflected in cyst-derived cells patients with germinal *PKD2* mutation and somatic *PKD1* mutation and vice versa and may increase disease severity with a lower age at ESRD (Koptides et al., 1999, Watnick et al., 2000, Koptides et al., 2000, Wu et al., 2002, Pei et al., 2001). Trans-heterozygosity occurred at a lower rate than somatic

homozygotic mutations, though the prevalence of trans-heterozygosity is unclear and difficult to predict due to small n numbers within the studies of trans-heterozygous mutations.

An additional hypothesis is haploinsufficiency, wherein the remaining wild-type copy of the gene is insufficient for complete function, which offers potential explanation for the occurrence of intracranial aneurysms which are likely not due to secondary somatic mutations. Furthermore, PKD heterozygote cells are particularly sensitive to renal injury and proliferation is also higher in noncystic tubules in both humans and orthologous mouse models of ADPKD (Happe et al., 2009). Ischaemia reperfusion injury (IRI), a common cause of acute kidney injury, in *Pkd1* heterozygous mice leads to more severe renal injury compared to WT mice which further supports the hypothesis that mutations in *PKD1* may increase the sensitivity of the kidney to hypoxia and subsequent damage from IRI (Bastos et al., 2009).

Cyst initiation can occur through either complete loss of polycystin by somatic mutation or sufficient reduction in dosage with a threshold effect possibly combined with stochastic factors such as renal injury. Indeed, the relative contribution of each of these mechanisms in typical human ADPKD remains an open question.

The existence of a third gene locus that could cause ADPKD, termed PKD3, was proposed in the mid-1990s. In studying the French-Canadian population, Daoust *et al*. identified that one family out of the 23 families observed presented with the typical clinical features of ADPKD, but from a mutation at a locus distinct from the previously described loci on chromosomes 16 p and 4q of PKD1 and PKD2, respectively (Daoust et al., 1995). Similarly, no linkage to *PKD1* or *PKD2* loci was identified in a Portuguese family

(Dealmeida et al., 1995), a Bulgarian family (Bogdanova et al., 1995), an Italian family (Turco et al., 1996), and a Spanish family (Ariza et al., 1997). Upon re-analysis of these families thought to have ADPKD3 through direct sequencing, novel variants and mutations of *PKD1* were found in the French-Canadian, Italian and Portuguese families, and frameshift deletion in *PKD2* in the Bulgarian family, which were not captured in the original linkage analysis (Paul et al., 2014). Moreover, in all four of these families there were cases of misdiagnoses from the renal ultrasonography. Nevertheless, the Spanish family had no likely pathogenic mutations form direct sequencing of *PKD1* and *PKD2*, and no linkage to *PKD1* and *PKD2*, though the authors question the diagnosis of ADPKD in this family due to atypical presentation and mild disease. Thus, the possible contribution of PKD3 in ADPKD remains controversial.

1.2.4 Modifier gene mutations

In addition to *PKD1* and *PKD2*, modifier genes can cause or enhance renal cysts as demonstrated in rodent models. Mutations in the RNA binding protein Bicaudal-C (BICC1) or the ankyrin repeat-containing SamCystin protein encoded by *Anks6*, which interact at the protein level, lead to cystogenesis in rodent models of PKD (Nagao et al., 2010, Stagner et al., 2009, Brown et al., 2005, Tran et al., 2010). BICC1 acts as a post-transcriptional regulator of *PKD2* via regulation of miR-17 activity (Tran et al., 2010).

GANAB encoding glucosidase II subunit alpha has been shown to be involved in maturation and localisation of polycystins *in vitro.* Mutations in GANAB have been identified in a small number of people affected with ADPKD that was genetically unresolved through whole exome sequencing (Porath et al., 2016), indicating that it

could play a potential role in a subset of people affected with ADPKD resulting in a milder phenotype.

In addition to whether *PKD1* or *PKD2* is mutated and the type of mutation, modifier gene mutations can have an important effect on the severity and progression of ADPKD. Overall, modifier gene mutations offer potential explanation as a contributing factor in the wide variation seen in ADPKD phenotype.

1.3 Models and treatment of ADPKD

1.3.1 Identification of the harmful effects of vasopressin

Vasopressin and cAMP have been shown to promote renal cyst cell proliferation and fluid secretion into cysts (Wang et al., 2008). Preclinical studies show that suppression/inhibition of vasopressin counteracts these effects, and clinical studies show slower increase in total kidney volume compared to controls. Tolvaptan (Jinarc), a vasopressin V2 receptor antagonist, was granted marketing authorisation in 2015 and is the first approved drug to effectively slow progression of ADPKD and protect renal function (McEwan et al., 2018, Torres et al., 2012).

However, adverse effects can prevent some patients with ADPKD from taking tolvaptan such as hepatotoxicity (Watkins et al., 2015), hypernatremia (Hirai et al., 2016) and allergy. Critically, only a proportion of patients are currently eligible to receive tolvaptan, as such the majority of patients are without a drug. Therefore, there is an urgent and unmet need for alternative therapies (Shoaf et al., 2007, Watkins et al., 2015).

1.3.2 Preclinical models of PKD (mouse and human studies)

A variety of cellular and animal models have been developed to provide better understanding of pathogenic mechanisms and aberrant cell signalling that contribute towards disease initiation and progression.

In vitro

A number of cellular models have been produced for the study of mechanisms underlying ADPKD, from renal epithelia derived from human or animal cysts, to wild-type cells that have undergone genetic manipulation to alter *PKD1*/*PKD2* e.g. through CRISPR-Cas9 gene editing. While cell cultures are useful in the investigation of cellular mechanisms in ADPKD, they have the disadvantage of potentially deviating from how they would normally function in their natural environment within a whole organism.

SKI-001 and OX161 are human renal tubular epithelial cells isolated from patients with ADPKD. In these two patients, cells were isolated from different cysts and pooled together. OX161 clones contain germline *PKD1* mutation (exon 15, E1537X) predicted to be a truncating mutation. SKI-001 carried the germline *PKD1* mutation (IVS43-1G>A) also predicted to be a truncating mutation (Parker et al., 2007). These cells were conditionally immortalised which does have the possibility to alter their typical function, despite this, SKI-001 and OX161 are useful and highly relevant *in vitro* human models of ADPKD that are capable of forming cysts when in a three-dimensional environment.

In vivo

Numerous animal models are used in the study of ADPKD to gain better mechanistic insight into disease pathogenesis and pathophysiological system interactions. Rodent

models are frequently used in ADPKD research as they more closely resemble human physiology than Drosophila or zebrafish models, and reaching the n numbers required for statistical power is more time and cost effective than with other mammals such as the mini-pig (He et al., 2015). Animal models can be non-orthologous but resemble the ADPKD phenotype such as the PCK rat (Lager et al., 2001) or genetically orthologous for example B6-Pkd1$^{nl/nl}$ mice with a hypomorphic deletion of the Pkd1 allele (Lantinga-van Leeuwen et al., 2004, Happe et al., 2013).

1.3.3 Clinical trials and need for new therapeutics

Until recently, treatment of ADPKD was limited to managing symptoms of the disease, followed by offering dialysis and transplantation when possible. Cellular and molecular mechanisms of the disease have been explored in an attempt to find therapeutic targets. Multiple signalling pathways and transcription factors have been implicated in cyst formation and disease progression.

Unsuccessful drug trials

Abnormally high activity of phosphatidylinositol 3-kinase (PI3K)- mammalian target of rapamycin (mTOR) is displayed in both PKD and renal cell carcinomas (RCC). The signalling molecule is a serine/threonine kinase that plays a key role in hypertrophy, hyperplasia, cell differentiation and apoptosis, and has been associated with cyst formation. Excessive mTOR activity is thought to occur through loss of the mTOR negative regulator tuberin which has notably decreased function in *PKD1*-deficient models (Shillingford et al., 2006). Rapamycin (Rapamune), an immunosuppressive drug that inhibits mTOR, and its analogues e.g. everolimus (Afinitor) have been shown to be

effective in experimental models, but was proven to be ineffective in clinical trials when it came to cyst growth, increases in kidney volume and decline in renal function (Stallone et al., 2012, Wahl et al., 2006, Wu et al., 2007, Yu et al., 2016).

Activation of the renin-aldosterone-angiotensin system (RAAS) is associated with hypertension in ADPKD. In hypertensive patients, angiotensin converting enzyme (ACE) inhibitors lowered blood pressure, improved renal blood flow and reduced proteinuria, but were not effective in patients with normal blood pressure. RAAS has also been linked with cyst growth through angiotensin II-promoted cell proliferation and aldosterone-mediated EGFR activation and upregulation of Na^+/K^+-ATPase leading to cystic fluid secretion. ACE-independent production of angiotensin II has also been noted in cyst-derived tissue. However, in clinical trials there was no significant difference in progression to ESRD and increase in kidney volume between the group given angiotensin converting enzyme (ACE) inhibitors and those given dual therapy of ACE inhibitors plus angiotensin II receptor antagonists (Hian et al., 2016, McPherson et al., 2004).

Promising drug trials

In recent preclinical studies, targeting the Ca^{2+}-activated Cl^- channel Transmembrane Member 16A (TMEM16A) has displayed promising results in *in vitro* and murine models of ADPKD. TMEM16A is critical in fluid secretion into cysts and is upregulated in ADPKD. TMEM16A antagonists (niclosamide, benzbromarone or Ani9) reduced proliferation and cystic growth (Cabrita et al., 2020).

Additionally, preclinical studies targeting microRNA 17 (miR17) demonstrated encouraging efficacy in the treatment of ADPKD. The cyst-promoting effect of miR17 has

been demonstrated in ADPKD (Yheskel et al., 2019, Patel et al., 2013, Hajarnis et al., 2017), via a mechanism of modulation of mitochondrial metabolism. In screening the anti-miR17 oligonucleotide RGLS4326, preferentially distributed to the kidney and was able to reduce cell proliferation, renal hypertrophy and attenuate cystic growth in multiple preclinical models (Lee et al., 2019).

In clinical trials of somatostatin analogues such as lanreotide (Somatuline) and Octreotide (Sandostatin), patients exhibited a reduction in total liver and kidney volumes (TLV and TKV, respectively). Somatostatin analogues act on SST2 receptors to reduce cAMP which is thought to be the basis of their volume reducing effects. However, inhibition of GH could offer a potential alternative explanation (Tentler et al., 1997, Gevers et al., 2015). In a 24-week Lanreotide study, a reduction in TKV and stabilisation of estimated glomerular filtration rate was observed in ADPKD patients with PLD. Further work would need to be done to properly assess the efficacy of Lanreotide on the kidneys. In two studies with Octreotide, TKV volume had increased significantly less in the treatment group compared to placebo, which could indicate a slowing of progression. Prolonged somatostatin analogue therapy comes with potential risks, as it has been associated with increased prevalence of gallstones in patients with acromegaly (Gevers et al., 2015).

1.4 The role of JAK/STAT in ADPKD

1.4.1 JAK/STAT signalling

The JAK-STAT cell signalling pathway consists of the Janus Kinase family which is made up of four tyrosine kinases (Tyk2 and JAK1-3), and seven Signal Transducers and Activators of Transcription (STATs; STAT1-4, STAT5a, STAT5b and STAT6) (Firmbachkraft et al., 1990, Ihle, 1996, Rane and Reddy, 1994, Wilks et al., 1991). STAT5a and STAT5b have overlapping and distinct functions, though encoded by separate genes, they are highly related proteins, with approximately 90% homology in their coding sequence. They differ in the C-terminal transcription activation domains and display differences in homodimeric DNA binding specificities (Kanai et al., 2014, Moriggl et al., 1996, Boucheron et al., 1998).

Activated STATs dimerise and translocate to the nucleus to induce transcription through binding the interferon gamma-activated sequence (GAS) elements within promoter regions (Baik et al., 2011) or the interferon-stimulated response element (ISRE) of DNA (Darnell et al., 1994). Downstream signalling and gene transcription vary depending on cytokine stimulation and which STAT is activated. STATs have been shown to play a role in regulating cell cycle progression and differentiation and have also been linked with polycystins and PKD (Baik et al., 2011, Bjorklund et al., 2006).

1.4.1.1 Lessons learned from STAT5 knockouts

Valuable information of STAT function can be gathered from the suppression or knockdown of individual STATs. Using knockout mice with a null allele, STAT5a-deficient mice display defective development of the mammary gland and lactogenesis (Liu et al.,

1997). Suppression of STAT5b indicates that STAT5b is responsible for mediating effects of sexually dimorphic pattern of growth hormone release form the pituitary and GH-stimulated gene expression in the liver (Udy et al., 1997). Knockout of STAT5a and STAT5b in which the locus was completely deleted demonstrates the critical role of STAT5 in normal immune cell development and differentiation(Yao et al., 2006). Despite some distinct functions of STAT5a and STAT5b there are also functional redundancies illustrated by infertility of STAT5a/b mutant female mice due to abnormal ovarian development, but not in the individual mutants of STAT5a or STAT5b (Teglund et al., 1998).

1.4.2 JAK/STAT in ADPKD

Functional PC1 has been linked with STAT1-mediated cell cycle arrest in human cell lines (Bhunia et al., 2002). Bhunia and colleagues observed $p21^{waf1}$-dependent, PC1-mediated inhibition of Cyclin Dependent Kinase 2 (CDK2), which plays a role in cell cycle progression. In human cell lines, increased levels of $p21^{waf1}$ were linked with an increase in tyrosine phosphorylated and dimerised STAT1 which indicates STAT1-induced activation. The group proposed a direct link between PC1 and JAK2-STAT1 because, using *in vivo* immunoprecipitation, they detected that PC1 could link with JAK2. JAK2 was able to bind mutant and wild-type PC1, and could bind PC1 in the absence of PC2. However, phosphorylation and activation of JAK2 occurred only in WT and requires PC2. These results indicate involvement of JAK2-STAT1 in promoting quiescence and cell cycle regulation via direct PKD interactions. Furthermore, Talbot *et al*. also demonstrate the soluble cleaved PC1 tail coactivates STAT1 (Talbot et al., 2011).

PC1 can also regulate the activity of STAT3 via a dual mechanism, whereby membrane-bound PC1 activates STAT3 in a JAK2-dependent manner, and the cleaved PC1 tail acts as a coactivator of STAT3 activity in a mechanism dependent on cytokine/growth factor-induced STAT phosphorylation (Figure 1.3). The cleaved PC1 tail fragments are overexpressed in ADPKD, thus Talbot *et al*. suggest this could contribute to the strong activation of STAT3 observed in cyst-lining cells (Talbot et al., 2011) .

STAT3 inhibition with pyrimethamine or curcumin in orthologous models of disease has been shown to reduce cystogenesis, proliferation and kidney weight (Takakura et al., 2011, Leonhard et al., 2011). However, neither pyrimethamine nor curcumin are specific inhibitors of STAT3. Recently it has been observed by Viau and colleagues that, whilst STAT3 inactivation reduces cystic burden in accordance with what has been seen previously, it had no effect on kidney volume and in fact promoted inflammation and infiltration of macrophages (Viau et al., 2020). Macrophage infiltration has previously been reported in ADPKD and shown to be involved in promotion of cystogenesis and renal hypertrophy (Karihaloo et al., 2011). It appeared that STAT3 repressed expression of proinflammatory cytokines in a cilia-dependent, C-C motif Chemokine Ligand 2 (CCL2)-mediated manner. A question remains of the precise role of STAT3 in ADPKD disease progression.

STAT6 has also been shown to be regulated by the PC1 tail, wherein the PC1 tail interacts with STAT6 and the coactivator P100, all three of which have elevated nuclear levels in cyst lining cells (Low et al., 2006). Olsan *et al*. observed elevated phosphoactivated STAT6 in kidneys of an orthologous *Pkd1* mouse model compared to controls, particularly in the cyst lining cells. In STAT6 -/- mice crossed with bpk mice (mutation in

BICC1 resulting in a non-genetically orthologous PKD phenotype), proliferation, cystic growth and renal hypertrophy was reduced compared to bpk STAT6 +/+ mice, suggesting a role of STAT6 in PKD pathogenesis (Olsan et al., 2011). Conflictingly, Fragiadaki *et al*. found in a siRNA screen that neither STAT3 nor STAT6 silencing were able to reduce proliferation in human ADPKD-derived cells (Fragiadaki et al., 2017). This discordance could potentially be due to differences in the models used or possible indirect actions of STAT3 and STAT6 via immune cells which would not be observed in the human *in vitro* model but could be from murine *in vivo* models.

JAK2 and STAT5 have also been implicated in ADPKD pathogenesis and will be discussed in further detail in section 1.5.5.

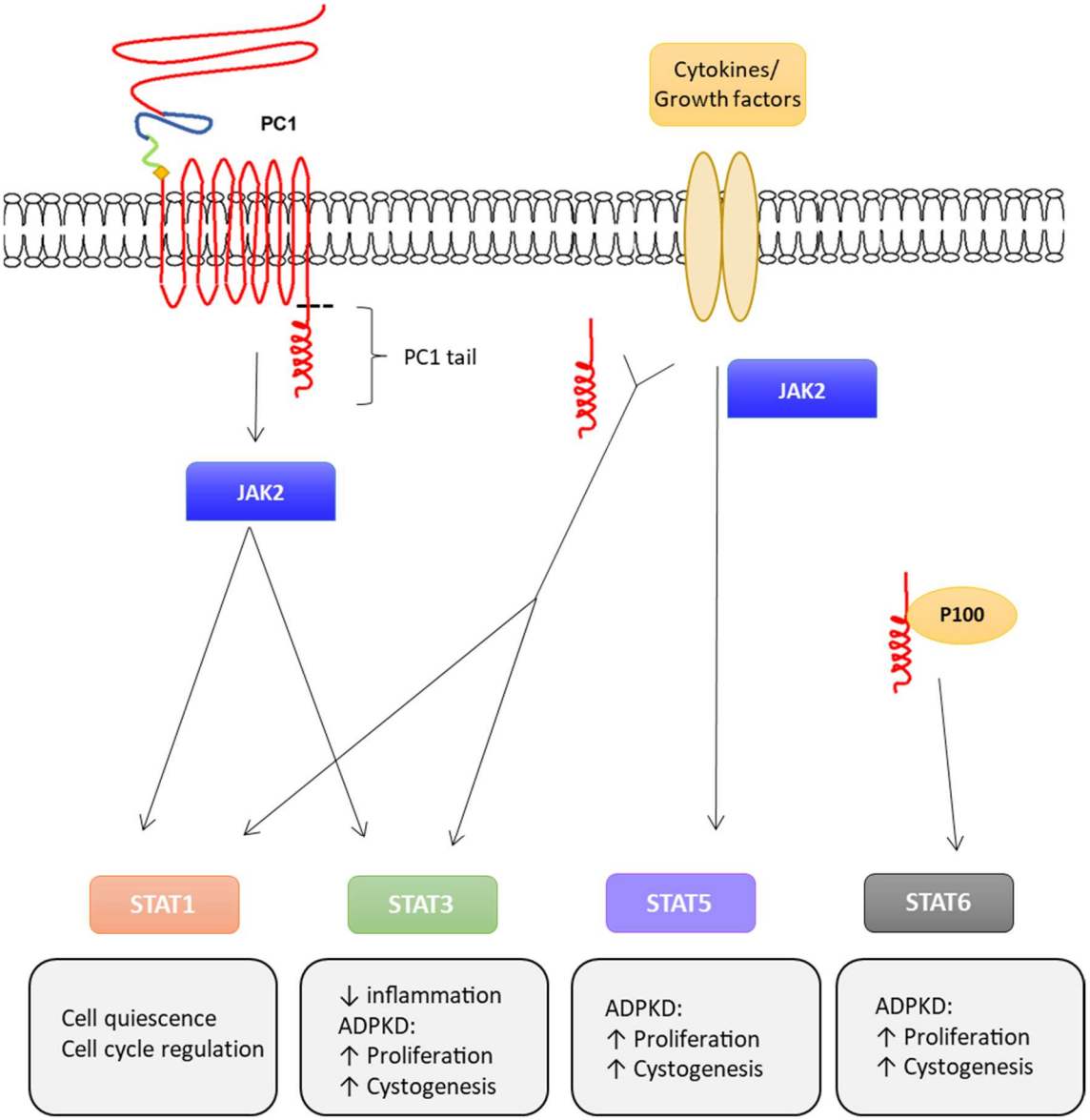

Figure 1.3 JAK-STAT signalling in ADPKD

Polycystin 1 (PC1) regulates STAT1 promoting cell quiescence and STAT3 via JAK2. The cleaved PC1 tail acts as a coactivator of STAT1 and STAT3 alongside cytokines/growth factors. STAT6 is regulated by the cleaved PC1 tail fragment alongside the coactivator P100. STAT3, STAT5 and STAT6 are associated with increased proliferation and cystogenesis in ADPKD.

1.5 Growth hormone

1.5.1 Structure

Human growth hormone is encoded by the *GH1* gene located on chromosome 17q22-24 (Harper et al., 1982, Owerbach et al., 1980). In mice, the growth hormone gene *Gh* is located on the distal half of chromosome 11, which is part of a highly conserved region between mouse chromosome 11 and human chromosome 17 (Jacksongrusby et al., 1988, Elliott et al., 1990). Growth hormone, both mouse and human, is a 191 amino acid protein with a molecular weight of approximately 22 kDa. The human growth hormone structure has a characteristic four-helix bundle structure, in which the helices have an antiparallel up-up-down-down connectivity as opposed to the more common up-down-up-down (Devos et al., 1992). The hGH molecule contains two disulphide bonds located with the first at residues C53-C165 which results in a large loop and the second at C182-C189 which links the COOH-terminus to helix 4 of the four-helix bundle. The C53-165 bridge is required for secretion and biological activity but C182-189 is not essential for the secretion and function of hGH (Graf et al., 1976, Chen et al., 1992, Besson et al., 2005, Devos et al., 1992).

The 22kDa hGH is the most abundant isoform of pituitary hGH, but it should be noted that other isoforms exist as a result of alternative splicing and post-translational modifications. The hGH isoforms have varying biological potency of GH actions compared to 22 kDa hGH with regards to growth promotion, potentiating insulin activity and hyperglycaemic properties, however the physiological roles of the molecular

isoforms of hGH have not been fully elucidated and require further clarification (Bustamante et al., 2009, Salem and Wolff, 1989, Lewis et al., 1991).

1.5.2 Regulation and release

Growth hormone is secreted from the anterior pituitary from somatotroph cells, with pulsatile secretion of GH regulated primarily by two hypothalamic hormones (i) growth hormone releasing hormone (GHRH), (ii) somatostatin (also referred to as growth hormone inhibiting hormone). GHRH stimulates GH production and secretion whilst somatostatin modulates this response by acting as a non-competitive inhibitor of GH release (Brooks and Waters, 2010). Hypothalamic synthesis and release of somatostatin is stimulated in a negative feedback loop both by growth hormone itself, and by insulin like growth factor 1 (IFG-1) which is produced in response to GH stimulation, primarily in the liver (Berelowitz et al., 1981).

In addition to neuroendocrine regulation of growth hormone release, the enteroendocrine hormone ghrelin, known as the “hunger hormone” due to its role in appetite, stimulates pituitary growth hormone secretion via its action as an endogenous ligand to the growth hormone secretagogue receptor (GHS-R) (Kojima et al., 1999). Furthermore, extra-pituitary growth hormone can be expressed in other tissues to act locally in an autocrine/paracrine manner. Pit-1, also known as growth hormone factor 1 (GHF-1) is a transcription factor that is responsible for expression of growth hormone. Although Pit-1 is expressed primarily in somatotroph cells and was originally thought to be pituitary-specific (Suen and Chin, 1993, Cohen et al., 1996), Pit-1 mRNA has been observed in extra-pituitary tissues, which reflects extra-pituitary expression of growth hormone (Perez-Ibave et al., 2014, Delhase et al., 1993, Bamberger et al., 1995).

The typical 24 hour rhythm of pulsatile release of growth hormone is primarily controlled by sleep processes, but also has a weak circadian component. The sleep related GH pulse accounts for around 50% of the total daily GH release (Sassin et al., 1969, Jaffe et al., 1995). Multiple variables impact the profile of growth hormone secretion including sex and age. Ho *et al*., found that the total 24 hour growth hormone secretion was higher in women than men, though when corrected for the effects of oestradiol, was not influenced by sex or age, nonetheless the fraction of GH secreted in pulses in 24 hours was significantly reduced in older adults (>55 yr) versus young adults (18-33 yr) (Ho et al., 1987). Interestingly, the sleep related GH surge is altered in night workers wherein they have a lowered release of GH related to sleep but this is followed by random GH pulses during the waking period ultimately compensating for the lowered sleep-related GH pulse and resulting in the same daily GH release as their day -active counterparts (Brandenberger and Weibel, 2004). This highlights one aspect of variability in growth hormone secretion within the human population due to environmental factors. Exercise also induces growth hormone secretion and can, dependent on exercise intensity, increase 24 hour GH release, although the mechanisms behind exercise-induced GH release are unknown (Godfrey et al., 2003, Wideman et al., 2002).

Growth hormone has a relatively short circulating half-life of approximately 20 minutes (Faria et al., 1989), although binding of growth hormone to the growth hormone binding protein (GHBP), the soluble, extracellular cleaved product of the growth hormone receptor, delays clearance from plasma and prolongs the biological half life (Baumann et al., 1987).

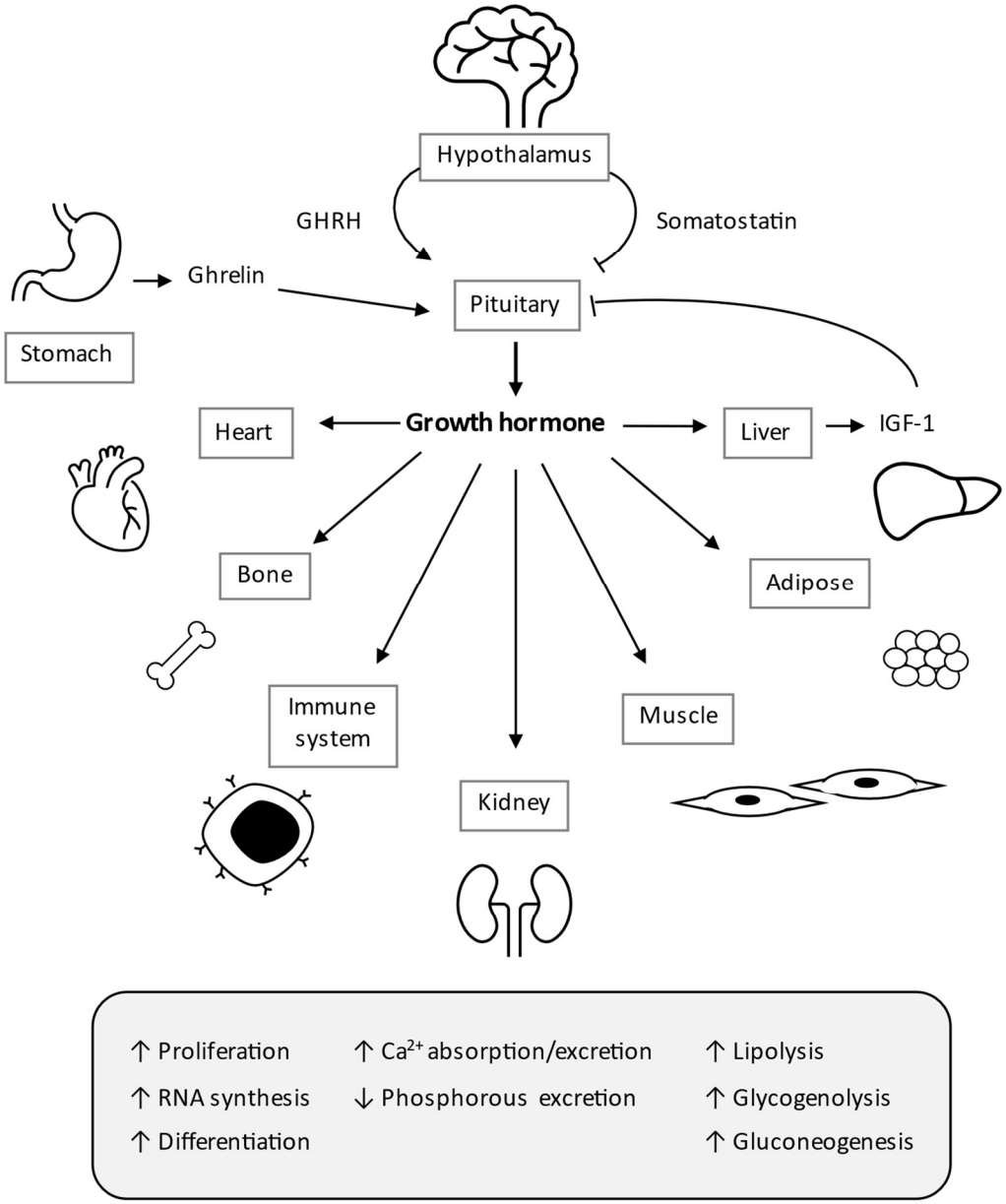

Figure 1.4 Regulation and functions of growth hormone

Pituitary release of growth hormone is positively regulated by growth hormone-releasing hormone (GHRH) and ghrelin, and negatively regulated by somatostatin and insulin-like growth factor 1 (IGF-1). Growth hormone acts on multiple tissues executing metabolic effects and modulating cell processes and development.

1.5.3 Function

Growth hormone modulates proliferation, differentiation, and metabolic processes, affecting skeletal and muscular growth, lipid and glucose metabolism, and immune function (Giustina et al., 2008) (Figure 1.4). It mediates many of its actions through stimulation of downstream production of IGF-1 in multiple tissues, primarily the liver.

1.5.3.1 Development

Growth hormone is detectable in foetal circulation from gestational week 10, rising throughout gestation and peaking at 20-24 weeks (~120 ng/mL) (Kaplan et al., 1972). Although pituitary growth hormone appears to be inessential to foetal development, determined by normal birth weights of anencephalic and growth hormone deficient neonates, there is widespread expression of GHR in foetal tissue, of note in the tubular epithelium of the kidney (Hill et al., 1992, Simard et al., 1996, Salardi et al., 1991). The role of growth hormone in the developing foetus is not yet fully elucidated, but in neonates GH is required for regulation of glucose homeostasis, highlighted by the observations of hypoglycaemia in neonates with severe growth hormone deficiency (GHD) (Mehta et al., 2005).

GH plays an important role in regulation of development of the heart and maintenance of normal cardiac function and morphology directly and indirectly through IGF-1. This function of GH/IGF-1 is illustrated by abnormal cardiac structure and increased risk of cardiovascular morbidity and mortality seen in GHD and acromegaly (Lombardi et al., 1997).

GH also plays a role in growth and development during puberty, in which mean GH levels nearly double, due to increase in pulse amplitude as opposed to pulse frequency (Rose et al., 1991).

1.5.3.2 Metabolism

Growth hormone functions as an anabolic hormone, promoting RNA synthesis, protein synthesis and increased muscle growth (Bergan-Roller and Sheridan, 2018). On the other hand, growth hormone also has catabolic actions, predominantly lipolysis, exhibited as increased free fatty acids (FFAs) and glycerol in response to GH stimulation (Gerich et al., 1976). GH-induced STAT5 is a key contributor in GH-regulated growth and metabolism (Herrington et al., 2000).

Early studies of growth hormone demonstrate its effects on phosphorous and calcium metabolism, in which GH reduces urinary phosphorous excretion and increases intestinal calcium absorption and urinary calcium excretion. It is hypothesised that GH exerts these effects on mineral metabolism through either direct or indirect modulation of vitamin D, although the relationship between the two is not yet fully understood (Wei et al., 1997, Chipman et al., 1980).

Additionally, Growth hormone plays a role in glucose homeostasis and metabolism through its direct action and indirectly through IGF-1. GH elevates gluconeogenesis and glycogenolysis, wherein people with acromegaly or exposed to high doses of exogenous GH display elevated liver and kidney glucose production (Schwarz et al., 2002, Ghanaat and Tayek, 2005, Hoybye et al., 2008)

1.5.3.3 Immune system

Growth hormone has a known role in development and regulation of immune function, wherein GH stimulates lymphocyte proliferation and differentiation (Landreth et al., 1992, Gjerset et al., 1990), synthesis of immunoglobulin (Yoshida et al., 1992) and modulation of cytokine response (Bozzola et al., 2003). Interestingly, evidence suggests GH action on immune function is predominantly through autocrine/paracrine GH as people with GHD do not usually present with immunodeficiency and local GH production has been demonstrated in lymphocytes (Hattori et al., 1990).

1.5.3.4 Skeletal growth

Growth hormone directly and indirectly promotes skeletal growth through an increase in osteoblast and chondrocyte proliferation and differentiation. This function of GH is reflected in deficiency and excess of GH, wherein children with GHD have short stature and decreased bone mass, adults with GHD have reduced bone mineral density and increased prevalence of osteoporosis, whilst people with acromegaly have increased bone turnover (Giustina et al., 2008).

1.5.3.5 Kidney

The kidney expresses growth hormone receptor in the proximal tubules and thick ascending limb, as well as the IGF-1 receptors which are expressed primarily in the glomerulus and the proximal and distal tubules (Hirschberg and Adler, 1998). The kidney is the major organ involved in clearance of GH (Johnson and Maack, 1977, Cameron et al., 1972). Growth hormone impacts renal growth and increases renal plasma flow (RPF) and glomerular filtration rate (GFR) via IGF-1 (Christiansen et al., 1981), exemplified in

hypopituitarism or hypophysectomy which results in reduced GFR and RPF, and decline in kidney size (Falkheden and Wickbom, 1965).

1.5.4 Growth hormone-JAK/STAT signal transduction

The growth hormone receptor (GHR) is ubiquitously expressed in the body, in concordance with the multiple regulatory actions of growth hormone which are exerted mainly through modifications to gene expression. Of note, GHR is expressed in the human kidney, primarily in the the tubulointerstitium (Fragiadaki et al., 2017, Landau et al., 1998). The growth hormone receptor can form a circulating growth hormone binding protein (GHBP) through proteolytic cleavage of the growth hormone receptor extracellular domain (Leung et al., 1987, Sotiropoulos et al., 1993).

To elicit biological response, one molecule of growth hormone binds the extracellular domain of two GHR molecules (Brookes & Waters, 2010). Growth hormone has two receptor binding sites, a distal receptor high affinity binding site (site 1) and a low affinity site (site 2) (Cunningham et al., 1991, Devos et al., 1992), which are allosterically coupled (Walh S *et al*, PNAS 2004). Conformational change of ligand-bound, homodimerised growth hormone receptors results in conformational change of receptor-associated tyrosine kinases (TKs), which transphosphorylate. Activated TKs also phosphorylate tyrosine residues in the cytoplasmic domain of the GHRs, resulting in docking sites for the recruitment of STATs. GHRs can exert different cellular effects through different TKs to initiate multiple signalling pathways. Binding of GH to the GHR initiates ubiquitination, with subsequent internalisation of the complex via endocytosis and proteasome-dependent degradation of the GHR (van Kerkhof et al., 2000), this ensures tight control of the signalling response.

The predominant TKs that associate with GHRs are the Janus Kinase family, particularly JAK2. Binding and activation of JAK2 is facilitated by the proline-rich motif in the cytoplasmic domain of the GHR termed “box 1”. On GH binding the GHR, conformational change brings JAK2 kinase domains together in close proximity, facilitating phosphorylation and activation of JAK2. Activated JAK2 recruits, phosphorylates and subsequently activates signalling molecules containing SH2 domains with STAT5 being the most notable in mediating GH actions (Brookes & Waters, 2010). GH-induced signal transduction is strongly negatively regulated by phosphatases and suppressors of cytokine signalling (SOCS), which are transcriptionally activated by the pathway to ensure the signalling is transient (Figure 1.5).

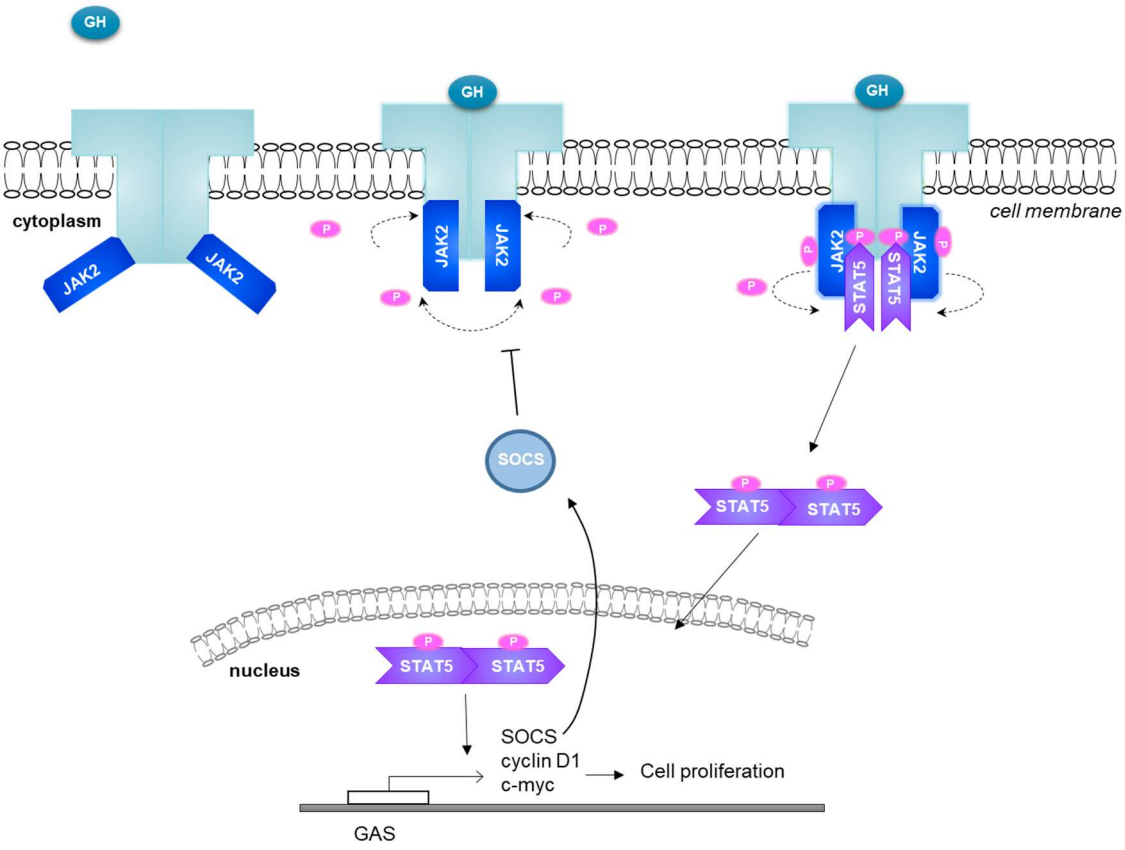

Figure 1.5 Growth hormone-induced activation of STAT5.

Growth hormone binds two growth hormone receptor (GHR) molecules which recruit JAK2. JAK2 transphosphorylates and phosphorylates the GHR molecules. JAK2 is inhibited by suppressors of cytokine signalling (SOCS) which can be activated by oestrogen. Activated JAK2 recruits and phosphorylates STATs, such as STAT5, which then dimerise and translocate to the nucleus to bind the gamma-activated sequence (GAS) in target promoter regions for cell signalling effects such as cell proliferation.

1.5.5 Signalling in ADPKD

The GH-GHR-STAT5 pathway was found to be aberrantly activated in models of ADPKD (Fragiadaki et al., 2017). This work provides compelling evidence for further investigation of the involvement of this pathway as a potential therapeutic target for

ADPKD. Selective STAT5 inhibition and siRNA silencing of STAT5 had no effect on apoptosis but did show decreases in proliferation in ADPKD-derived cell lines, as well as reduction in cyst growth when compared to control. The reduction of proliferation and cyst growth through STAT5 inhibition was replicated in *PKD1* null (-/-) cells, with no effect in *PKD1* wild-type (+/+) cells. These results suggest STAT5 plays a role in proliferation but not apoptosis in ADPKD.

To investigate the involvement of STAT5 further, Fragiadaki and colleagues studied STAT5 expression in *Pkd1* null and wild-type (WT) mouse models. STAT5 was expressed in cyst-lining epithelial cells and shown to be nuclear, indicating activation in *Pkd1* null models, but WT STAT5 expression was primarily cytoplasmic. Similarly, when comparing transgenic GH overexpressing mice (GH^{tg}) to WT, STAT5 was highly nuclear in GH^{tg} and cytoplasmic in WT, independent of *Pkd1* status. Cyclin D1, a pro-proliferative gene known to be a transcriptional target of STAT5 (Matsumura et al., 1999), had higher expression in GH^{tg}. A novel observation was made of significantly increased circulating GH in ADPKD mouse models compared to WT controls. This, in combination with other results, indicates GH-activated STAT5 transcriptionally activates cyclin D1 leading to increased cell proliferation. Enhanced proliferation via the GH-STAT5-cyclin D1 axis was observed in WT kidney epithelial cells but was not tested in ADPKD models, leaving this as an area which warrants further exploration.

Patera *et al*., observed that JAK2 is highly expressed in the cystic epithelial cells of an orthologous mouse model of polycystic kidney disease. Moreover, inhibition of JAK2 activity with curcumin or tofacitinib, both potent JAK inhibitors, reduces *in vitro* cystogenesis (Patera et al., 2019).

Renal hypertrophy in response to chronic, elevated growth hormone has been observed in transgenic growth hormone overexpressing mice and in people with acromegaly. Renal alterations are described in multiple GH^{tg} mouse lines including tubulointerstitial changes, glomerular hypertrophy, and progressive glomerulosclerotic lesions leading to renal failure (von Waldthausen et al., 2008). A novel GH^{tg} mouse strain optimised for analysis of GH-mediated renal pathology was generated by von Waldthausen and colleagues. This strain displayed structural changes in the kidney concordant with PKD pathology such as enlarged kidneys, dilation of tubules, renal epithelial cell proliferation and following development of fluid-filled cysts.

In patients with acromegaly, a disorder caused by pituitary adenoma resulting in excessive growth hormone secretion, formation of cysts was associated with elevated nadir serum GH levels (lowest level after suppression) during an oral glucose tolerance test and excessive secretion of GH (Yamamoto et al., 2016). Taken together, these results support the hypothesis of a role of GH in cyst development and renal alterations.

In further support of this hypothesis, sex differences have been noted in progression of ADPKD, whereby men have earlier onset ESRD and higher mortality than women with ADPKD (Gabow et al., 1992, Harris et al., 2006). Gabow and colleagues originally proposed that this was due to sex differences in hypertension but found that hypertension and sex independently affected disease progression. Sex steroids have been shown to have a regulatory impact on the GH-JAK-STAT pathway. Oestrogen inhibits JAK2 phosphorylation via stimulation of suppressor of cytokine signalling-2 (SOCS-2), which is a negative regulator of GH-activated JAK/STAT signalling. Oestrogen administration results in elevated GH levels but reduced IGF-1 (an indicator of GH signal

transduction). In addition, women were shown to be less responsive to treatment with GH than men (Leung et al., 2003). Sex differences in response to GH could offer a potential explanation for sex differences seen in ADPKD (see section 1.1.4).

In a meta-analysis performed by Malas and colleagues, a PKD signature was created from multiple models of PKD including animal models with an ADPKD or Autosomal Recessive Polycystic Kidney Disease (ARPKD) mutation and from patients with ADPKD to examine genes upregulated and downregulated in PKD (Malas et al., 2018). Interestingly two growth hormone responsive genes were found to be downregulated in all the PKD models tested: growth hormone inducible transmembrane protein (GHTIM) and growth hormone regulated TBC protein 1 (GRTP1). GRTP1 is expressed most highly in the testes and abundance increases post puberty (Lu et al., 2001). When mice were dosed with GH, GRTP1 mRNA decreased in the kidneys (Lu et al., 2001) which is concordant with the decrease in GRTP1 seen in the PKD signature and increased serum GH observed in the Fragiadaki group (Malas et al., 2018, Fragiadaki et al., 2017). GHITM is a ubiquitously expressed protein originally identified in the brown adipose tissue of mice (Li et al., 2001). There is limited knowledge of the function of GHITM, although of note in a study on Tilapia, miR-1338-5p-mediated inhibition of GHITM resulted in increased pituitary release of growth hormone and with an miRNA antagomir the pituitary GH release is reduced as well as hepatic expression of GHR1 (Qiang et al., 2017). This indicates that GHITM plays a role in regulation of growth through GH pituitary release and GHR expression and that in PKD downregulated GHITM could have the potential to affect pituitary GH release as seen in this aquatic model, although this could be a species-specific effect or mediated by different miR-1338-5p targets. Together, these data provides a basis to further explore the involvement of GH-JAK2-STAT5 signalling in

ADPKD pathogenesis, alongside the potential of inhibition of this pathway to delay progression of disease.

1.5.6 Growth hormone analogues for GHR antagonism

In 1990, it was discovered that a glycine to arginine mutation in the third α-helix in low affinity receptor binding site 2 of GH produced a dominant negative GHR antagonist with the ability to antagonise the effects of GH signalling (Chen et al., 1990). A glycine to arginine mutation at the 120 position in site 2 of human GH prevents activation of dimerised GHR molecules and blocks downstream signalling to produce a GHR antagonist effect (Figure 1.6). Disruption of the third α-helix in receptor binding site 2 of growth hormone has been tested in other species such as the rat with a homologous Gly118Arg mutation (Nass et al., 2000b), which was the basis for the development of the mouse growth hormone with a Gly118Arg mutation for mouse GHR receptor antagonism.

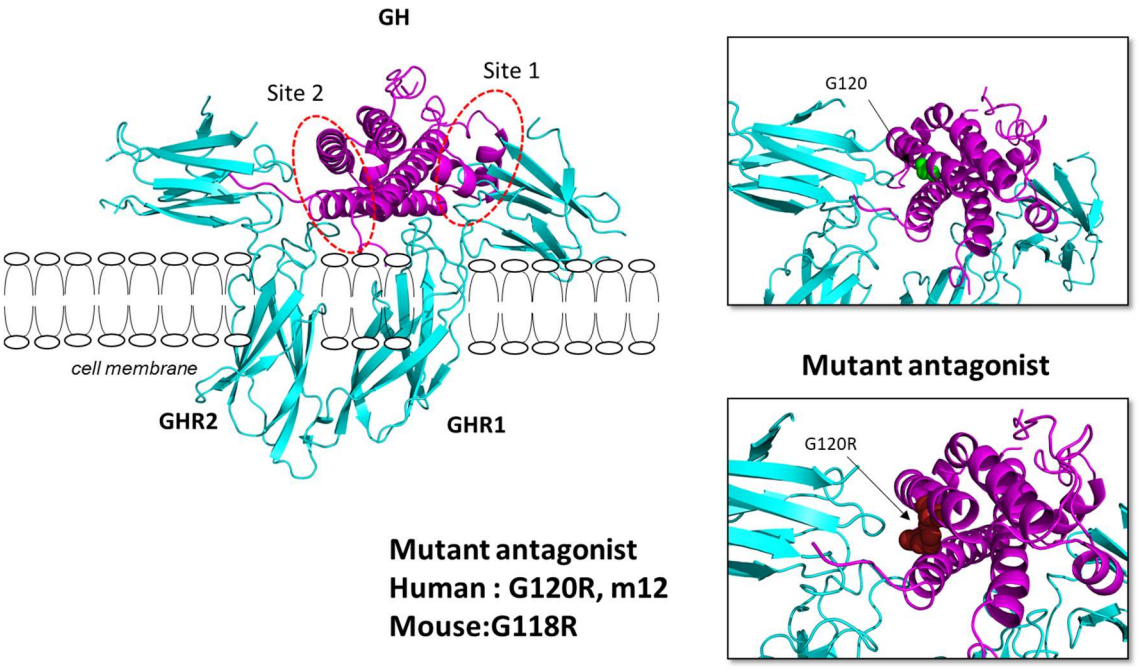

Figure 1.6 Growth hormone analogue interactions with the growth hormone receptor dimer

Wild-type growth hormone (GH) with G120 (green) binds GH receptor molecules (GHR1 and GHR2). GH containing a Gly120Arg mutation (red) in receptor binding site 2 results in a GHR antagonist. Figure was rendered with the 3HHR pdb file.

An additional eight amino acid mutations in receptor binding site 1 (H18D, H21N, R167N, K168A, D171S, K172R, E174S and I179T) result in increased affinity to one GHR molecule (Figure 1.7) (Wilkinson et al., 2016). The multi-mutation GHR antagonist is termed hGH-m12 in our laboratory although is also known as B20, and a highly similar molecule is termed B2036, or when modified with polyethylene glycol (PEG) to prolong its action, Pegvisomant (Somatovert) which is currently used in the treatment of acromegaly (Olson et al., 1997, Trainer et al., 2000, Wang et al., 2020). B2036 contains the same eight site 1 mutations as hGH-m12 though it contains a glycine to lysine mutation at the

120 position to llow for PEGylation as opposed to Gly120Arg. Pegvisomant binds to the GHR dimer and triggers internalisation. However, it blocks downstream signalling independent of receptor internalisation as the proper conformation for productive signalling and alignment for tyrosine phosphorylation is not induced (Maamra et al., 1999, Ross et al., 2001). When PEGylated, B20 has a circulating half-life of 15.2 hours in mice (Wang et al., 2020). Wilkinson and colleagues developed a long-acting GHR antagonist through fusion of the GHR antagonist molecule with the growth hormone binding protein (GHBP) which delays clearance, requires less frequent injection, and is more cost-effective. Fusion to the GHBP extends the terminal half-life to >20 hours and can result in 14% reduction in IGF-1 over 7 days in rabbits (Wilkinson et al., 2016). The hGH-m12 will be expressed and purified as a higher affinity GHR antagonist for use in *in vitro* experiments. Increasing the molecular weight to delay clearance of the GHR antagonist as described will be considered for *in vivo* experiments.

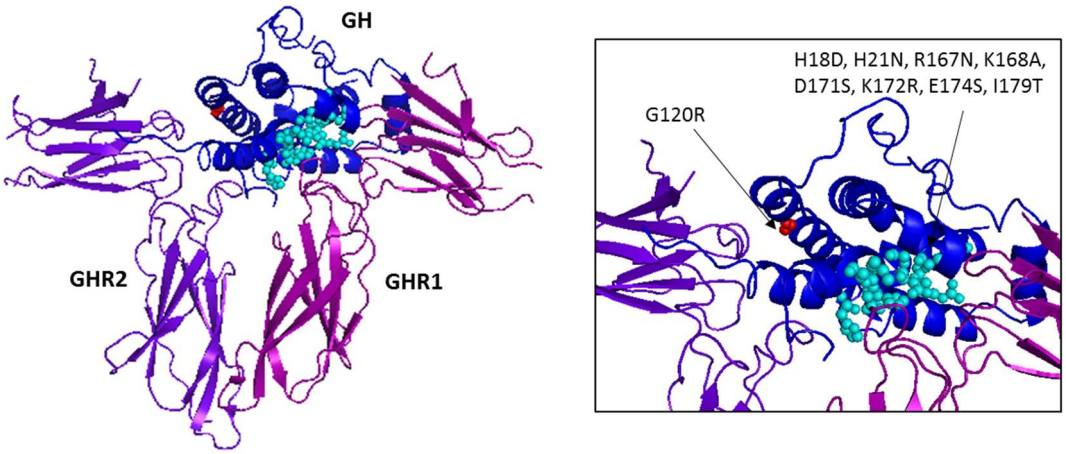

Figure 1.7 GHR antagonist with eight amino acid mutations in site 1:
H18D, H21N, R167N, K168A, D171S, K172R, E174S and I179T (turquoise) which increases binding affinity of the growth hormone (GH) analogue to growth hormone receptor molecule 2 (GHR1); site 2 mutation Gly120Arg mutation (red) which produces an antagonist effect at growth hormone receptor molecule 2 (GHR2). Figure was rendered with the 3HHR pdb file.

1.5.7 Growth hormone inhibition as a novel target in ADPKD

Inhibition of growth hormone signalling offers a potential therapeutic strategy in slowing progression of ADKPD, with the opportunity to target growth hormone (i) upstream with the use of somatostatin analogues such as Lanreotide or Octreotide, (ii) at the receptor level with a growth hormone receptor antagonist, (iii) downstream JAK2/STAT5 signalling with JAK inhibitors such as Tofacitinib or Ruxolitinib, or small molecule STAT5 inhibitors.

Drugs used for the inhibition of growth hormone in the treatment of acromegaly, namely growth hormone receptor antagonist such as Pegvisomant or somatostatin

analogues such as Octreotide are generally well-tolerated (Colao et al., 2006, Yang and Keating, 2010). JAK inhibitors e.g. the small molecule Ruxolitinib is currently used in the treatment of myelofibrosis and is also well-tolerated (Verstovsek et al., 2015). These treatments offer attractive strategies for the potential treatment of ADPKD.

1.6 Hypothesis, aims and objectives

The overarching aim of this project is to investigate how stimulation and inhibition of growth hormone signalling affects development/progression of PKD. I will evaluate the contribution of growth hormone-JAK2/STAT5 signalling to PKD pathogenesis through testing the impact of inhibition of this pathway on key pathogenic processes and markers of progression in PKD such as proliferation and cystogenesis in *in vitro* and *in vivo* models of disease.

I hypothesize that lowering GH-triggered signalling may reduce proliferation and thus cystic growth in murine and human models of ADPKD.

The aims of my project are to (i) express and purify growth hormone and growth hormone receptor antagonists and validate their ability to modulate STAT5 activity (ii) assess the impact of stimulation and inhibition of growth hormone signalling (inhibition at the GHR, JAK2 and STAT5 level on proliferation, cystogenesis and kidney function in ADPKD and (iii) assess the potential therapeutic benefit of GH signalling inhibition in murine and cellular models of ADPKD.

Chapter 2: MATERIALS AND METHODS

2.1 General materials and reagents

Chemicals were purchased from Thermo Fisher Scientific and Sigma Aldrich, unless stated otherwise. Deionised water (18 M Ohm, Milli-Q®) was used to prepare buffer solutions following standard laboratory protocols. All solutions were sterilised via autoclave or filter sterilisation using 0.22 µm pore size filters (Thermo Fisher Scientific) as appropriate. Chromatography columns were purchased from GE Healthcare Life Sciences.

2.2 Subcloning of growth hormone analogues

2.2.1 Plasmid vectors

The pET-21a(+) plasmid vector (Novagen) was used for expression of all growth hormone proteins, provided by Dr Sarbendra Pradhananga (Department of Infection, Immunity and Cardiovascular Disease, University of Sheffield) (Mierendorf et al., 1998) (Mierendorf et al., 1998) (Mierendorf et al., 1998) (Mierendorf et al., 1998) (Mierendorf et al., 1998) (Mierendorf et al., 1998) (Mierendorf et al., 1998) (Mierendorf et al., 1998) (Mierendorf et al., 1998) (Mierendorf et al., 1998) (Mierendorf et al., 1998) (Mierendorf et al., 1998) (Mierendorf *et al.*, 1998). Plasmid DNA was isolated and purified from cell cultures with the Monarch® Plasmid Miniprep Kit (New England BioLabs®; Cat No. T1010)

following the provided manufacturer's protocol, or with the ZymoPURE ® II Plasmid Midiprep Kit (ZYMO RESEARCH CORP; Cat No. D4200) following the centrifugation protocol. Vector maps are provided in Appendix A.

2.2.2 Synthesis and storage of gene strands and oligonucleotides

Gene strands and oligonucleotides for PCR amplification and insertion of restriction sites were custom synthesised by and purchased from Eurofins Genomics. Primer sequences for site-directed mutagenesis were designed using the NEBaseChanger™ tool and purchased from New England BioLabs. Gene strands were codon-optimised for improved gene expression in *E. coli* and included a sequence encoding a C-terminus 6 histidine tag (His-tag) for ease of purification using a codon optimisation tool. Oligonucleotides were briefly centrifuged and resuspended in TE buffer solution (10 mM Tris pH 8.0, 0.1 mM ethylenediaminetetraacetic acid disodium adjusted to pH 8.0 with NaOH) to help maintain a constant pH and prevent nuclease digestion or depurination. Oligonucleotides were made up to a final concentration of 100 µM and stored at -20°C.

2.2.3 PCR amplification

DNA was PCR-amplified with oligonucleotides (Eurofins Genomics), sequences can be found in APPENDIX D. The KAPA system Hifi Hotstart ReadyMix PCR kit (KAPABiosystems; Cat No. KK2602) was used to set up 25 µL reactions following the manufacturer's protocol. Thermocycler conditions were set up according to the manufacturer's protocol using the Eppendorf Mastercycler personal, with the appropriate primer-dependent annealing temperatures based on the primer melting temperature, and the extension

time based on amplicon size. Multiple masses of template DNA were initially tested to find the optimal mass for amplification (2-20 ng), 10 ng of template DNA was used going forward.

2.2.4 Site-directed mutagenesis

The Q5® site-directed mutagenesis kit (New England BioLabs®; Cat No. E0554S) was used according to the manufacturer's protocol.

2.2.5 Restriction digest and ligation

Reactions were set up using PCR-amplified DNA and plasmid vector DNA with KpnI (New England BioLabs®; Cat No. R3142) as restriction enzyme 1 (RE1) and HindIII (New England BioLabs®; Cat No. R31045) as restriction enzyme 2 (RE2), with the exception of the uncut negative control at 5 µL, then briefly centrifuged and pipette-mixed (Table 2.1). The reaction for the plasmid vector was carried out with the individual restriction enzymes separately as single digests to confirm the activity of the individual enzymes. Single digest reactions were incubated for 1 hr at 37°C using a heat block. Fractions of each single digest reaction (15 µL) were combined 1:1 and an additional 1 µL of each restriction enzyme and 2 µL CutSmart buffer® (New England BioLabs®; Cat No. B7204S) was added to aid double digest. The insert DNA negative control and double digest reactions were set up as described in Table 2.1. The negative control and double digest reactions were incubated for 30-60 min at 37°C. Restriction digest products were analysed on a 1.5% agarose gel and gel extracted as described in section 2.2.6.

Table 2.1 Restriction digest reactions

	Negative control	Single digests		Double digest
DNA[1] (µL)	1	5	5	7
CutSmart buffer® (µL)	-	2	2	4
RE1 (µL)	-	1	-	2
RE2 (µL)	-	-	1	2
H_2O (µL)	4	12	12	10

[1] DNA concentration 50-100 ng/ µL

Ligation of restriction digested insert DNA and plasmid DNA was performed using the New England BioLabs® Ligation protocol with T4 DNA ligase (New England BioLabs®; Cat No. M0202) and 10X T4 DNA ligase buffer with 10 mM ATP (New England BioLabs®; Cat No. B0202S). Reactions of 10 µL reactions were prepared as described in Table 2.2. and transformed into chemically competent cells as described in section 2.9.

Table 2.2 Ligation reactions of insert DNA and plasmid DNA.

	Negative control (L-)	Ligation (L+)
Plasmid DNA (µL)	2	2
Insert DNA (µL)	-	6
T4 DNA Ligase Buffer (µL)	1	1
H_2O (µL)	6	-
T4 DNA Ligase (µL)	1	1

2.2.6 DNA analysis

2.2.6.1 Qualitative analysis of DNA

Agarose gel electrophoresis

Agarose gel electrophoresis was used to separate and analyse fragments of DNA based on their molecular weight. Agarose gels were prepared in 1X TAE buffer (40 mM Tris-base, 20 mM acetic acid, 1 mM EDTA pH 8.0) to a final concentration of 1.5% (w/v) agarose, with 0.0001% Midori green (Nippon Genetics Europe; Cat No. MG04) for visualisation. DNA samples were added to gel loading dye purple 6X (New England BioLabs®; Cat No. B7024S) as a 5:1 ratio. Samples were then pipette-mixed and loaded, alongside 5 µL Quick-Load Purple 2-log DNA ladder (New England BioLabs®; Cat No. N0550S) or Quick-Load® 100 bp DNA Ladder (New England BioLabs®; Cat No. N0467) as a standard reference for molecular weight. This was placed in a Cleaver Scientific MutliSUB™ horizontal gel system containing 1X TAE buffer, connected to a BIO-RAD Power Pac 300 set to 65 V for 1-1.5 hours until purple bands were approximately three-quarters of the way down the gel.

DNA purification

DNA at the desired band size was extracted and purified from agarose gels using the Monarch DNA Gel Extraction Kit (New England BioLabs®; Cat No. T1020S) following the provided manufacturer's protocol. The NEB PCR cleanup kit was used to purify DNA from PCR products.

2.2.6.2 Quantitative analysis of DNA

Concentration and purity of DNA was measured using the NanoDrop ND-100 (Thermo Fisher Scientific). The instrument was blanked with nuclease-free water. DNA concentration was measured at 260 nm (A_{260}) with the output in ng/ µL, and DNA purity was measured as a ratio of the absorbance at 260 nm and 280 nm. A volume of 1.5 µL was used for blanking and sample analysis. This was performed in triplicate and a mean average was taken as the final value.

2.3 Transfection

2.3.1 Preparation of chemically competent cells

One single colony of *E. coli* was taken from an LB agar plate and cultured at 37°C shaking at 180 rpm initially in 10 mL LB media with 1% glucose overnight and then into 100 mL until reaching A_{600} of 0.4-0.6, at which point the culture was placed in ice. The culture was centrifuged for 20 minutes at 1000 xg at 4°C and the pellet was resuspended in 40 mL ice cold 100 mM calcium chloride ($CaCl_2$) and incubated on ice for 1 hour. Centrifugation was repeated and the pellet was gently resuspended in 6 mL ice cold 85 mM $CaCl_2$ with 15% glycerol (v/v). Cells were aliquoted into pre-chilled tubes as 300 µL aliquots, flash frozen with liquid nitrogen and stored at -80°C.

2.3.2 Plasmid transformation into competent cells

Chemically competent *E. coli* cells stored at -80°C were thawed on ice. Plasmid DNA (1 µL) was added to 100 µL competent cells and was incubated on ice for 1 hour. Cell

aliquots were then incubated at 42°C for 30 sec. LB media (100 µL) was added to each cell aliquot and these were incubated at 37°C for 10 min. Cell suspensions were then spread/streaked on to LB agar plates (prepared with vegetable tryptone) containing 100 µg/mL ampicillin and % glucose (+/- 0.1% aspartic acid) and incubated overnight at 37°C. As a negative control for transformation, 1 µL MQ water was added to competent cells. As a positive control for transformation, 1 µL plasmid vector containing no gene insert was added to competent cells.

Different *E. coli* strains were used for different purposes. For culture of cells containing plasmid DNA, XL1 Blue cells were used. For expression of plasmid DNA containing the desired insert gene, BL21 (DE3) cells were used for pET21a+ plasmid DNA.

Arctic (DE3) cells were later tested for expression of WT and Gly118Arg mouse growth hormone in an attempt to increase expression of soluble protein. Arctic (DE3) cells underwent a similar transformation protocol in which 1 µL (~50 ng) plasmid DNA was added to 100 µL competent cells and left on ice for 20 min. Cell aliquots were then incubated at 42°C for 30 sec, then placed back on ice for 2 min. Cells were then spread/streaked onto plates as described above.

2.3.3 Lipofection of plasmids into mammalian cells

Cells were reverse transfected using lipofection. Lipofectamine™ 2000 Transfection Reagent (Thermo Fisher Scientific; Cat No. 11668019) was used according to the manufacturer's protocol with Opti-MEM™ Reduced Serum Medium (Gibco; Cat No. 31985062) to transfect plasmids into mammalian cells using a 4:1 lipid:DNA ratio and for a 6 well plate 1- 1.5 µg DNA was used.

Polyethylenimine (PEI; PolySciences) was used for transient transfection (Delafosse et al., 2016) of pCEP4 mGH Gly118Arg fusion plasmid into CHO cells in suspension. Sterile neutralised linear PEI 1 mg/mL and sterile-filtered plasmid were brought to room temperature. The 25 µL PEI was added to 250 µL 150 mM NaCl and 5 µg DNA plasmid was added separately to 250 µL 150 mM NaCl and incubated for 5 minutes at room temperature, these two tubes were then combined and incubated for 15 minutes before adding to 2 x 10^6 cells/mL diluted in RPMI 1640 to 5 mL, then once transfected made up to 20 mL with CHO Hyclone media for expression.

2.3.4 Lipofection of siRNA into mammalian cells

Cells were transfected with silencing RNA (siRNA) using Opti-MEM™ Reduced Serum Medium (Gibco, Cat No. 31985062) and Lipofectamine® RNAiMAX Transfection Reagent (Invitrogen, Cat No. 13778-075), Per well of a 6 well plate:

Table 2.3 Lipofection volumes of siRNA and reagents.

Reagent	Volume
2 µM siRNA	20 µL
RNAimax	7 µL
Opti-MEM	150 µL

150 µL of the lipid-DNA was pipetted dropwise onto confluent cells.

2.4 Bacterial cell culture and protein expression

Individual colonies of BL21 (DE3) pET21a+ growth hormone (mGH-WT, mGH-Gly118Arg, hGH-WT, hGH-Gly120Arg, hGH-m12) were selected from LB agar plates and placed in 3 mL LB media (prepared with vegetable tryptone), 100 µg/mL carbenicillin and 1% glucose (+/- 0.1% aspartic acid). Small-scale cultures were incubated at 37°C, shaking at 180 rpm, for a minimum of 5 hours. Intermediate cultures were then prepared by placing 3 mL of the small-scale cultures into 50-100 mL of the same non-inducing media. Intermediate cultures were incubated at 37°C overnight, shaking at 180 rpm.

Protein expression within BL21 (DE3) cells was induced by allolactose by using auto-induction media superbroth (FORMEDIUM™, Cat No. AIMSB01210) or autoinduction media 2YT broth base (FORMEDIUM™, Cat No. AIM2YT0210), 100 µg/mL carbenicillin, and 0.04% Anti-foam (Sigma-Aldrich; Cat No. A6426). This was performed either in 2 L Pyrex baffled flasks containing 500 mL induction media at 200 rpm, or in a fermenter system containing 3 L induction media at 300 rpm.

Large-scale preparations were initially incubated at 37°C. Absorbance at 600 nm (A_{600}) of cultures was measured to assess bacterial cell density, using the Beckman DU530 UV spectrophotometer. This was performed at regular intervals until an A_{600} reading of ≥ 1.0 was reached, at which point the incubation temperature was reduced to 16-22°C for BL21 (DE3) cells . Expression of the target protein was assessed using SDS-PAGE gels.

Protein expression with ArcticExpress (DE3) cells was under the same conditions, though instead of autoinduction media the cells were cultured in LB media with subsequent

induction performed with Isopropyl β-D-thiogalactoside (IPTG) to a final concentration of 1 mM when the culture reached A_{600}≥ 0.6 to induce expression.

2.4.1 Cell harvest

Bacterial cell cultures were centrifuged at 15,000 x *g* for 30 min at 4°C with using the JLA-8.1000 fixed angle rotor in the Avanti ® J-26XP centrifuge (Beckman Coulter). Supernatant was removed and cell pellets were stored at -80°C.

2.4.2 Bacterial cell lysis

Frozen cell pellets were thawed at room temperature and resuspended in lysis buffer (5 mL lysis buffer per 1 g of cell pellet). The lysis buffer used for obtaining mouse growth hormone consisted of 200 mM NaCl, 50 mM Tris pH 8.0, 1 mM EDTA pH 8.0, 1 mM DTT, 5% (v/v) glycerol. The lysis buffer used for obtaining human growth hormone consisted of 500 mM NaCl, 50 mM sodium phosphate buffer pH 8.0, 5% (v/v) glycerol. Lysozyme from chicken egg white (Sigma-Aldrich; Cat No. L6876) was added to a final concentration of 800 µg/mL and the cell suspension was incubated at room temperature, stirring for 0.5 - 1 hour.

The cell suspension was placed at 4°C and 4-(2-aminoethyl) benzenesulfonyl fluoride hydrochloride (AEBSF), a serine protease inhibitor, was added to a final concentration of 10 µg/mL. Deoxycholic acid was added to a final concentration of 500 µg/mL and the cell suspension was incubated at 4°C, stirring for 0.5 - 1 hour.

The cell suspension was sonicated using the Soniprep 150 Plus (MSE) with 3 rounds of 10 seconds sonication with 10 second cooling intervals to homogenise the suspension and reduce viscosity. The homogenised suspension was centrifuged at 16,000 rpm for

30 min at 4°C to separate soluble and insoluble material. Total cell suspension (pre-centrifuge) and the soluble supernatant fraction were analysed with SDS-PAGE to locate desired proteins.

2.4.2.1 Inclusion body wash

In order to remove inactive, aggregated proteins known as inclusion bodies, cell pellets were thawed and suspended in buffer (20 mM Tris pH 8, 500 mM NaCl, 1 mM DTT, 1% Triton-X-100). Bacterial cells were lysed and homogenised through sonication using the Soniprep 150 Plus (MSE) 3 rounds of 10 seconds sonication, 10 seconds rest. The cell suspension was centrifuged at 25,000 x *g* for 10 min at 4°C using the JLA-16.250 fixed angle rotor. Supernatant was removed and the suspension and centrifugation process was repeated for the pellet twice to remove inclusion body aggregates. The inclusion body wash was initially used for the WT mouse growth hormone and Gly118Arg mouse growth hormone mutant, but was later foregone as these proteins were in inclusion bodies.

2.4.3 Protein solubilisation through denaturation

The bacterial cell pellet was suspended in lysis buffer. To solubilise protein, deionised 8 M urea was added as a chaotropic agent to denature the insoluble protein, to a final concentration of 4 M. Small volumes (20 µL) of concentrated sodium hydroxide were added to increase the pH to improve solubilisation (final pH ~10.0), looking for the suspension to go from cloudy to clear, indicating solubilisation. The suspension was centrifuged at 20,000 x *g* for 10 min, solubility was confirmed through comparison of the suspension and the supernatant on an SDS-PAGE gel. Prior to purification, supernatant was further centrifuged at 20,000 x *g* for 10 min to remove cellular debris.

2.4.4 Refolding of denatured protein

2.4.4.1 Dialysis

Cellulose dialysis membrane tubing (14,000 MWCO) was prepared by boiling in 1 mM EDTA, pH 8.0 and 250 mM sodium hydrogen carbonate to remove preservative agents and sulphides. The tubing was then cooled and stored in 20% ethanol. Prior to use, tubing was rinsed in MQ water. Protein solution was loaded into dialysis tubing and dialysed at 4°C for a minimum of 6 hours to remove urea and allow the growth hormone to refold.

2.4.4.2 Rapid dilution

A small volume of protein solution (1 mL) was slowly added to 20 mL buffer (25 mM tris pH 8.0, 2 mM EDTA, 5 mM DTT) while vortexing the buffer.

2.4.4.3 Refolding on the column

Reverse urea gradient with equilibration buffer containing 4 M urea and equilibration buffer with no urea was performed during purification to gradually remove urea from the protein and allow refolding, see section 2.6.1.

2.4.4.4 Buffer exchange using vivaspin

Protein solution containing 4 M urea was gradually buffer exchanged to reduce and remove urea and allow refolding of the protein, the buffer used for exchange was 500 mM NaCl, 50 mM Tris-HCl pH 8.0, 1 mM EDTA, 1 mM DTT, 5% glycerol. This was performed using a Vivaspin® 15 centrifugal concentrator with a 10,000 dalton MWCO, centrifuged at 3,000 x *g* at 4°C.

2.5 Mammalian protein expression

Using lipofection (protocol described in section 2.3.3), plasmids were transfected into mammalian cells HEK293T cells or Chinese Hamster Ovary (CHO) cells provided by Dr Ian Wilkinson (Oncology & Metabolism department, University of Sheffield). The pCEP4 vector containing the CMV promoter and neomycin resistant region to allow for selection containing inserted mammalian codon-optimisied mGH-WT 6xHis was provided by Dr Ian Wilkinson (Oncology & Metabolism department, University of Sheffield). The pCEP4 vector containing 6xHis mGH-Gly118Arg or 6xHis mGH-Gly118Arg-mGHBP fusion were subcloned using site directed mutagenesis and/or splicing by overlap extension, described in further detail in Chapter 3.

2.6 Purification of protein

2.6.1 Immobilised metal affinity chromatography

Polyhisitidine-tagged growth hormone analogues were purified using nickel chelate affinity chromatography. Supernatant containing soluble target proteins in lysis buffer (500 mM NaCl, 50 mM sodium phosphate buffer, pH 8.0, 5% glycerol) was adjusted to 20 mM imidazole. The protein solution was loaded onto a nickel chelate column (HisTrap™HP nickel chelate column, or a column prepared with nickel affinity resin) which had been equilibrated with 10 column volumes (CV) low imidazole buffer (20 mM imidazole, 500 mM NaCl, 50 mM sodium phosphate buffer, pH 8.0, 5% glycerol). Protein solution was loaded onto the column at a 0.5 CV flow rate to optimise binding to nickel,

and flow-through of the protein load was collected to retain any unbound target protein. Weakly bound or unbound proteins were washed off the column with 10 CV low imidazole buffer. To elute bound protein, an imidazole gradient of 20 mM – 500 mM imidazole was used overa volume of 8 CV and eluted fractions were collected (1 CV). The protein load, flow-through, wash and eluted fractions were analysed using SDS-PAGE to assess location and purity of the target protein.

Initially, the low imidazole buffer and high imidazole buffers were prepared with 4 M deionised urea to maintain solubility of mGH during purification. Refolding the protein on the column was later tested utilising a reverse urea gradient of 4 M – 0 M urea following the wash step with low imidazole buffer containing 4 M urea. Refolded protein was eluted off the nickel chelate column with high imidazole buffer. The column was then washed with 5 CV high imidazole buffer containing 4 M guanidine chloride to solubilise and remove any insoluble target protein.

2.6.2 Ion exchange chromatography

The growth hormone analogues were dialysed (section 2.4.4) in buffer (20 mM Tris buffer, 1 mM DTT, 1 mM EDTA, 5% glycerol, 4 M urea) to reduce NaCl to < 20 mM prior to ion exchange chromatography. Cation exchange chromatography was tested as purification method using a HiTrap™ SP HP Sepharose column and 20 mM Tris buffer pH 6.0, however protein precipitated out of solution when reduced to pH 6.0 to run on the column likely due to the isoelectric point of the proteins.

Anion exchange chromatography was performed with a HiTrap™ Q HP sepharose column, this was tested as a purification method both before and after metal chelate

affinity chromatography, and before and after removal of urea to optimise purification. The target protein-containing solution was loaded onto a Q column which had been equilibrated with 10 CV low salt buffer (see buffer used for dialysis, pH 8.0; presence of 4 M urea dependent on the stage the purification method was tested). Weakly bound or unbound proteins were washed off the column with 10 CV low salt buffer. Bound protein was eluted using a 0 mM – 1 M NaCl gradient. Refolding on the column was also tested as described in section 2.6.1 with the appropriate buffers. Initially pH 8.0 was used for equilibration buffer and elution buffer, but later equilibration buffer pH 8.0 and elution buffer pH 9.0 was used, as increasing pH during elution can improve resolution. SDS-PAGE was used to assess location and purity of the target protein.

2.6.3 Endotoxin removal

Endotoxin detection kit ToxinSensor™ Endotoxin Detection System (Genscript, Cat No. L00350C) was used according to the manufacturer's protocol with a 0.1-1 EU/mL reference scale. EU=endotoxin unit and is equivalent to approximately 0.1-0.2 ng/mL. absorbance was measured at 545 nm (A_{545}) for the endotoxin standard reference scale and the hGH analogues. The EU/mL value was determined from interpolation of the A_{545} values compared to the standard curve, using GraphPad linear regression analysis.

Pierce™ High Capacity Endotoxin Removal Spin Columns, 0.5 mL (ThermoFisher, Cat No. 88274) were used according to the manufacturer's protocol using the "spin method" to remove endotoxin from GH protein purified from *E. coli*. After endotoxin removal, endotoxin detection was performed again to assess adequate removal of endotoxin.

2.6.4 Protein analysis

2.6.4.1 SDS-PAGE

SDS-PAGE was used to analyse the expression, solubility, and purity of proteins. Protein samples were combined 1:1 (v/v) with loading dye (75 mM Tris-HCl pH 6.8, 0.5% bromophenol blue, 5 mM EDTA, 1 mM DTT, 0.2% SDS, 2.5% glycerol). Samples were incubated for 3-5 minutes at 90°C to denature proteins for band separation. Denatured samples were allowed to cool and then loaded onto 10 % SDS-PA gels, alongside the 10-250 kDa Precision Protein Plus™ ladder (Bio-Rad; Cat No. 1610373) as a standard for molecular weight. The resolving fraction of the gel was prepared with 100 mM Tris pH 8.3, 100 mM bicine, 40 µM EDTA, 0.1% SDS, 0.05% (w/v) ammonium persulphate (APS), polyacrylamide and 0.16% N,N,N',N'-tetramethylethylenediamine (TEMED). The stacking fraction of the gel was prepared in 10% acrylamide, 0.1% SDS, 0.05% (w/v) APS, 125 mM Tris/HCl pH 6.9, 0.33% TEMED.

Gels were run in SDS running buffer (100 mM Tris, 100 mM bicine pH 8.3, 200 µM EDTA, 0.1% SDS) at a constant current of 35 mA per gel for approximately 30 minutes. Gels were stained and proteins were fixed in a solution of 2 mg/mL Coomassie Brilliant Blue, 40% methanol and 10% acetic acid to visualise separated protein bands. Gels were destained in 20% methanol, 10% glacial acetic acid solution until stain was removed from the background of the gel to a sufficient level that protein bands were clearly visible. Imaging of gels was carried out using the BIO-RAD Gel Doc™ EZ Imager and Image Lab™ software.

2.6.4.2 Mass spectrometry

Proteins that were visually determined to be ≥90% pure from SDS-PAGE gels were analysed with matrix-assisted laser desorption/ionisation-time of flight (MALDI-TOF) mass spectrometry to confirm their molecular weight. Mass spectrometry was performed by the Facility of Mass Spectrometry, Department of Chemistry, University of Sheffield.

2.6.4.3 Spectrophotometry

The NanoDrop ND-100 (Thermo Fisher Scientific) was blanked with nuclease-free water. Protein concentration was measured as absorbance at 280 nm (A_{280}). A volume of 1.5 µL was used for blanking and sample analysis. This was performed in triplicate and a mean average was taken as the final value. Protein concentration was determined from the mean A_{280} value, the protein's Mw, and its molar extinction coefficient ($M^{-1}cm^{-1}$) (APPENDIX C).

2.6.4.4 Bradford assay

The Bradford assay was used to confirm concentration of proteins. A standard curve was prepared with bovine serum albumin (BSA) diluted 1:10 in Bradford protein assay dye (Bio-Rad; Cat No. 500-006) and absorbance at 595 nm (A_{595}) was measured with the Biospectrometer. A serial dilution of protein solution was prepared and measured at A_{595} Protein sample A_{595} was compared to the standard curve to determine the protein concentration.

2.6.5 Protein concentration and storage

Proteins that were deemed >95% pure from visual assessment of SDS-PAGE gels were buffer exchanged to remove elution buffer and replace it with 1X phosphate buffered saline (PBS) using dialysis and Vivaspin® as described in section 2.4.4.4. Protein was concentrated to 0.5-1 mL using a Vivaspin® 2 centrifugal concentrator with a 10,000 dalton MWCO, centrifuged at 3,000 x *g* at 4°C. The concentrated protein suspension in PBS was collected into the concentrator's recovery cap through inverting the concentrator during centrifugation. Concentration of the protein was determined as described in section 2.6.4.4. Concentrated, purified protein was stored at -20°C in 50% (v/v) glycerol as a cryoprotectant.

2.7 Mammalian cell culture

PKD-derived human kidney epithelial cells (OX161 clone 1 (OX161c1) and SKI-001), HEK293-GHR, murine F1 Pkd1 WT, F1 Pkd1 KO, MEK Pkd1 WT or MEK Pkd1 KO cells were thawed and cultured in HyClone™ Dulbecco's High Glucose Modified Eagles Medium F12 1:1 (GE Healthcare; Cat No. SH30023.01) containing 10 % foetal bovine serum (FBS; Sigma, Cat No. F4135) at 33°C and 5% CO_2. OX161c1 and SKI-001 cells were maintained in T75 flasks and passaged when >90% confluent using trypsin-EDTA (Gibco; Cat No. 11590626). Cells were passaged a maximum of 15 times.

Wild-type renal epithelial cells had been previously isolated from kidney papillae of Pkd1fl/fl mouse (B6.129S4-Pkd1tm2Ggg/J), identified as F1 Pkd1 WT cells. The cells were

previously immortalised using mTert expressing lentiviral vector VVPW/mTert. Cells had the Pkd1 gene deleted using VIRHD/HY/Silntβ1/2363 lentivector and hydromycin selection, identified as F1 Pkd1 KO cells (Lee et al., 2015). Mouse embryonic kidney (MEK) cells are conditionally immortalised renal epithelial cells isolated from E15.5 WT and *Pkd1*$^{nl/nl}$ kidneys (Li et al., 2005), identified as MEK Pkd1 WT and MEK Pkd1 KO, respectively. These cells were used from passage 10.

Conditionally immortalised renal tubular epithelial cells SKI-001 and OX161 are cells isolated from human kidneys from people with ADPKD(Parker et al., 2007). These cells contain *PKD1* mutations and were previously immortalised by transduction with a retroviral vector with defective replication that contains a temperature-sensitive large T antigen and the catalytic subunit of human telomerase (hTert) (O'Hare et al., 2001). SKI-001 were used from passage 21 and OX161c1 from passage 16.

HEK293 overexpressing full-length human growth hormone receptor (HEK293-GHR) used for validation of human growth hormone analogues were provided by Dr Ian Wilkinson (Department of Oncology and Metabolism, University of Sheffield). HEK293 had undergone stable transfection with pcDNA1 plasmid containing the full-length human growth hormone receptor sequence. HEK293-GHR were used from passage 12.

2.7.1 Hormone/drug treatment of cells

OX161c1 and SKI-001 cells were seeded into 6 or 12 well plates and incubated at 33°C until confluent. In some cases, prior to stimulation, media containing FBS was washed with 1X PBS and replaced with the serum-free media to serum starve the cells overnight. The following controls, GH analogues or inhibitors were added and incubated at 33°C:

vehicle (negative control), 100-500 ng/mL human growth hormone (hGH) (recombinant or commercial (R&D systems, Cat No. 1067-GH-025) , 0.1-5 µg/mL laboratory-purified Gly120Arg mutant hGH (hGH-Gly120Arg/hGH-m12), 10 ng/mL Oncostatin-M (OSM), 1 µg/mL mouse growth hormone (mGH) (recombinant or commercial (GeneTex, Cat No. GTX65343-pro), 0.1-10 µM. OSM was used as a positive control for activation of the JAK-STAT pathway. Media containing vehicle/stimulants/inhibitors was removed and the cells were washed twice with 1X TBS (20 mM Tris-HCl pH 7.6, 18 mM NaCl). Lysis buffer (50 mM Tris-HCl pH 7.4, 250 mM NaCl, 5 mM EDTA, 0.3% Triton X-100, cOmplete™ mini protease inhibitor cocktail (Merck, Cat No. 11836153001), and phosphatase inhibitor PhosSTOP™ (Sigma-Aldrich, Cat No. 4906845001) was added 80-200 µL/well to cells for immunoblotting. Stimulated cells for RNA extraction had 800 µL/well of TRIzol™ reagent (Invitrogen; Cat No. 15596026) added. Cells were then scraped and stored at -20°C.

2.8 Western blot

Stimulated eukaryotic cell lysates were sonicated as described in section 2.4.2. Cell lysates or supernatant were then combined 1:1 with 2X Laemmli sample buffer (125 mM Tris-HCl pH 6.8, 20 % glycerol, 4% SDS, 0.005% BB dye, 5% β-mercaptoethanol). SDS-PAGE was performed similarly to the method described in section 2.6.4.1, in some cases precast 15-well 4–20% Mini-PROTEAN® TGX™ Precast Protein Gels (Bio-Rad; Cat No. 4561096) were used and the gel was run at 80 V for 10 minutes then 95 V for 70 minutes. The gel was disassembled, excess gel was trimmed and transfer was performed using either (i) wet transfer using nitrocellulose blotting membrane and transfer papers in 1 X transfer buffer (200 mM Tris, 250 mM glycine, 0.04% SDS) at 80 V for 80 minutes, or (ii)

semi-dry transfer using the Bio-Rad Trans-blot Turbo Transfer system at 25 V 2.5 A for 7 minutes with the Trans-Blot Turbo Transfer pack (Bio-Rad, mini Cat No. 1704157; midi Cat No. 1704158). The membrane was washed in 1X TBST (1X TBS, 0.1% Tween-20) and blocked in 1X TBST containing 5% skimmed milk powder (w/v) for 30 minutes.

Membranes were incubated overnight at 4°C on a tube roller in the following primary antibodies diluted in TBST containing 5% BSA (w/v):

Table 2.4 Primary antibodies used to probe antigen proteins in western blots

Antigen	**Host**	**Manufacturer**	**Dilution**	**Mw (kDa)**
Phosphotyrosine (Y694) STAT5	Rabbit	Cell Signalling Technology Cat No. 9314S	1:1000	90
β-actin	Mouse	abcam	1:2000	42
PCNA	Mouse	Cell Signalling Technology Cat No. 2586S	1:2000	36
6xHistidine	Mouse	NA – aliquot supplied	1:1000	NA
STAT5	Rabbit	Cell Signalling Technology Cat No. 25656	1:1000	90
GHR	Mouse	Santa Cruz Biotechnology Cat No. sc-137185	1:500	110, 140*
Polycystin 1	Rabbit Mouse	Abcam Cat No. ab203240 Santa Cruz Biotechnology Cat No. sc-130554	1:500 1:500	450

*110 kDa for the GHR precursor and 140 kDa for the glycosylated mature GHR

Membranes were divided according to expected band size of the primary antibody. The membrane was washed in 1X TBST and probed with the following secondary antibodies diluted 1:10,000 in TBST containing 5% skimmed milk powder (w/v):

Table 2.5 Secondary antibodies used in western blots

Secondary Antibody	**Manufacturer**
Goat, anti-mouse IgG1, human ads-HRP	Dako Cat No. P0447
Goat, anti-rabbit IgG (H+L) mouse/human ads-HRP	Dako Cat No. P0448

Bands were visualised using ECL western blotting reagents (Cytiva, Cat No. RPN2106) and with the Bio-RAD Chemidoc™ XRS+ Molecular Imager® and Image Lab™ software.

2.9 Luciferase Assay

2.9.1.1 Transfection of plasmids

STAT5RE-luc-LHRR plasmid and *Renilla* plasmids were reverse transfected into cells using lipofection (section 2.3.3).

2.9.1.2 Cell stimulation and dual luciferase assay

Cells were serum starved for 4 hours then stimulated with 100 ng/mL hGH-WT and 500 ng/mL hGH-m12. After 4 hours the cells were lysed and buffers from the Dual-

Luciferase® Assay System kit (Promega; Cat No. E1910) were added according to the manufacturer's protocol. Plates were read using the Fusion plate reader and SkanIt software.

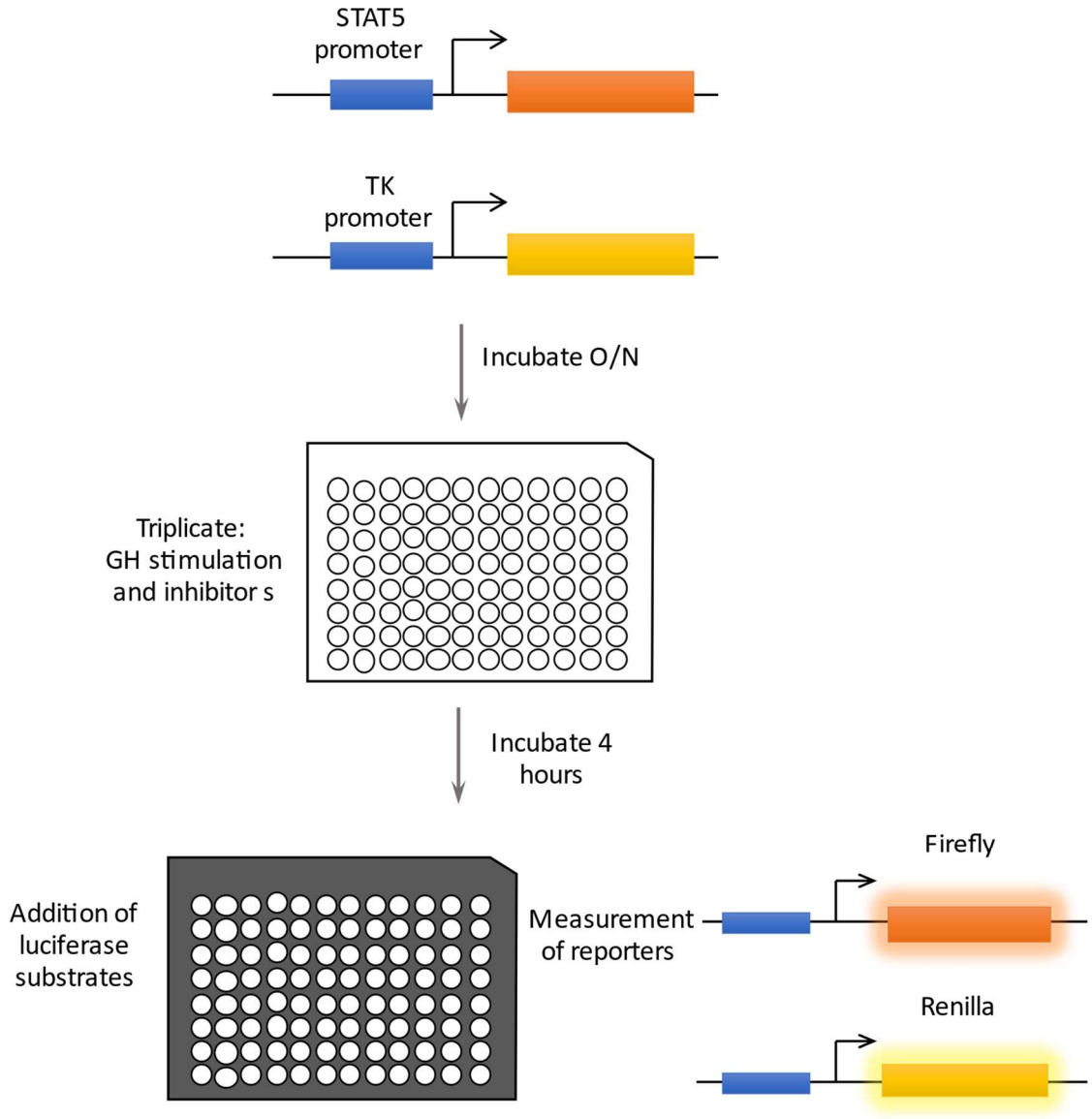

Figure 2.1 Dual luciferase assay for measurement of STAT5 transcriptional activity

Cells were transfected or cotransfected with plasmids containing STAT5 Firefly luciferase or thymidine kinase (TK) Renilla luciferase, seeded onto a 96 well plate and incubated overnight. Cells were then stimulated as untreated controls, with growth hormone (GH) ore growth hormone signalling inhibitors and incubated for 4 hours. Luciferase substrates were added and signal was measured.

2.10 Real-time PCR

2.10.1 RNA extraction

RNA was extracted from cells adapted from the TRIzol™ Reagent User Guide protocol. Media was removed from confluent cells and TRIzol™ reagent (Invitrogen, Cat No. 15596026) or QIAzol™ lysis reagent (Qiagen, Cat No. 79306) was added, using 400-500 µL of reagent per well of a 6 well plate. Cell were incubated with the lysis reagent for 10 minutes, pipette-mixing to homogenise. Chloroform was added using 0.2 mL chloroform per 1 mL lysis reagent, and vortexed for 15 seconds, then incubated for 2 minutes. Prior to centrifugation samples were briefly vortexed, then centrifuged for 15 minutes at 12,000 xg 4°C to separate organic and aqueous phases. The aqueous clear top layer containing RNA was transferred into a new tube and 0.5 mL per 1 mL lysis reagent was added, then incubated for 10 minutes. Samples were then centrifuged for 10-12 minutes at 12,000 x g 4°C allowing RNA to precipitate a pellet at the bottom of the tube. Supernatant was removed and the RNA was resuspended in 1 mL 75 % ethanol per 1 mL lysis reagent and mixed by briefly vortexing. Samples were centrifuged for 5 minutes at 7,500 x g 4°C and the supernatant was discarded. The samples were then incubated 2-5 minutes with the tube lid open to allow the ethanol to evaporate but ensuring the sample did not dry out. The pellet was resuspended in 20-40 µL nuclease free water and incubated for 10 minutes at 55°C. RNA was quantified using the NanoDrop as described in section 2.2.7. RNA was stored at -80°C.

In some cases RNA extraction was performed using an RNA extraction kit (Qiagen, Cat no. 217084) following the manufacture's protocol.

2.10.2 cDNA synthesis

The iScript™ cDNA Synthesis Kit was used to synthesis cDNA from RNA according to the manufacturers protocol.

2.10.3 RT-PCR

Performed according to the SsoAdvanced™ Univerasl SYBR® Green Supermix Instruction Manual with appropriate primers. The cDNA was diluted in nuclease free water 1:500.

Thermocyling condition using the BioRad qPCR machine and primers used for the Real-Time Polymerase Chain Reaction (RT-PCR) are described below. The threshold values were used to determine Delta-Delta Ct value and fold change to assess differential gene expression.

Table 2.6 Thermocycling conditions for Real-Time PCR

Stage	Temp.	Time
Initiation	95.0°C	3 min
40 X		
Denaturation	95.0°C	30 sec
Annealing	Tm – 5°C	30 sec
Melt Curve	65.0°C	5 sec

Tm = Melting temperature of the primers

Table 2.7 Primers for target genes used in RT-PCR

Gene	Forward primer	Reverse Primer
Beta actin	ATCATTGCTCCTCCTGAGCG	GACAGCGAGGCCAGGATG
Hs CCND1 (Cyclin D1)	ATGAACTACCTGGACCGCTT	TTCATTGAAATCGTGCGGGG
Hs IGF-1 (Insulin-like growth factor 1)	CATGTCCTCCTCGCATCTCT	GGTGCGCAATACATCTCCAG
Hs GHR (Growth hormone receptor)	GCCCTGATTATGTTTCTGCTGG	ATCCACTGTACCACCATTGC
Hs STAT5b	GCGTTATATGGCCAGCATTT	TGGGTAGCCTTAATGTTCTC

2.11 Flow cytometry

Flow cytometry was used to assess proliferation of cells. Cells were grown to confluence, washed twice with 1X PBS, and detached using Accutase® Cell Detachment Solution (BioLegend, Cat No. 423201) at room temperature. Cells were centrifuged at 3000 rpm for 5 minutes to form a pellet and resuspended in PBS with 5% FBS to wash the Accutase from the cells. Cells were centrifuged again and fixed in ice cold methanol for 30 minutes at – 20°C. Cells were centrifuged and washed twice in PBS with 5% FBS.

Propidum iodide/RNase (Cell Signalling Technology, Cat No. 4087s) was used for cell cycle analysis as a neat solution by resuspending the cells and incubating at room

temperature in the dark for a minimum of 30 minutes. Cell cycle analysis was performed by assessing the single cell population in the forward scatter (FSC) and side scatter (SSC) graph, gated and read using Blue 660/20 area and width. Cell cycle was analysed in FlowJo software. Proliferative cells were assessed using the Pacific Blue-conjugated phosphoserine Histone 3 (PH3) antibody (Cell Signalling Technology, Cat No. 8552S) which is marker of mitosis. After fixation and washing, cells were resuspended in 100 µL PH3 antibody diluted 1:50 in PBS with 0.5% BSA and 0.25% Triton-X-100, incubated for a minimum of 1 hour at room temperature in the dark. Cells were centrifuged and washed with PBS, then pelleted and resuspended in 500 µL PBS to read using Violet 450/50 area and width. PH3 negative cells were determined using an IgG control to gate the negative cells.

2.12 Cyst assay

Cystic cell lines (OX161c1, SKI-001, F1 Pkd1 KO, F1 Pkd1 WT) were cultured as previously described and either not transfected or transfected with an siRNA control (Non-targeting (NT), GHR siRNA or STAT5AB siRNA). Cells were detached using trypsin-EDTA and diluted to a concentration of 2×10^4 cells/mL. Matrigel (Corning, Cat No. 354234) was thawed at 4°C and kept on ice until seeding to maintain the Matrigel as a liquid, 20 ng/mL EGF (Thermo Fisher Scientific, Cat No. 13247-051) and 200 ng/mL IFNα (mouse: pbl assay science, Cat No. 12100-1; human: pbl assay science, Cat No. 11100-1) was added and the Matrigel was placed into a 96 well plate. Cells were seeded onto the 96 well plate with Matrigel as a 1:1 ratio, and the plate was subsequently incubated at

either 33°C or 37°C for 30 minutes to allow the Matrigel to polymerise. Media containing vehicle negative control (DMSO), growth hormone, growth hormone antagonist or Ruxolitinib was added to the 96 well plate. Images were taken using brightfield microscopy periodically and media containing stimulant/inhibitors was replaced every 3 days, for 9-12 days. One biological replicate of the SKI-001 and OX161c1 cyst assay was blinded, wherein I prepared the drug treatments and a laboratory member Areej Alahmadi placed the treatments in separate tubes with numbers that were then given back to me to apply to the cysts, the key to the number and drug treatments was provided to me after cyst analysis was complete.

Analysis of cyst size and growth was performed using ImageJ software. From multiple photos (minimum 3 separate fields) of the whole well with a z-stack, images of cysts were selected randomly from each well. The diameter of cysts was measured. With a minimum of 20 cysts measured per condition. Cysts were excluded if they were aggregated or in clusters contacting other cysts, or if the cysts were out of focus to an extent the diameter could not accurately be measured.

2.13 Animals

Male and female *Pkd1*$^{nl/nl}$ mice with an intronic neomycin-selectable marker from a C57BL/6J background (Happe et al., 2013), or wild type littermate controls were dosed using intraperitoneal (IP) injection with from 4 weeks of age to 6 weeks of age 1mg/kg/day of the somatostatin analogue Octreotide in saline (Sigma, Cat No. O1014), or from 6 weeks of age to 8 weeks of age with 50 mg/kg/day of Ruxolitinib (ApexBio, Cat

No. A3012) solubilised DMSO (Thermo Fisher Scientific, Cat No. 85190) or vehicle controls at an equal volume (saline, or DMSO with saline, respectively). IP injections were performed on alternating sides to avoid injection site irritation. All mouse experiments were done under the authority of a U.K. Home Office license.

Mice were sacrificed at 6 or 8 weeks old and serum and tissues (liver, spleen, kidney) were collected. Cardiac puncture for collection of blood was performed by Carl Wright (Department of Infection, Immunity and Cardiovascular Disease, University of Sheffield). Blood samples were incubated at room temperature for a minimum of 1 hour and then centrifuged at 10,000 rpm for 5 minutes to separate the serum, which was collected and placed into a new tube. Serum aliquots were snap-frozen in liquid nitrogen and stored at -80°C. Liver, spleen and one half of the left kidney were formalin fixed overnight and placed in PBS for use in histology. The other half of the left kidney and hemisected right kidney was snap-frozen in liquid nitrogen for storage at -80°C to allow for protein or RNA analysis.

Power calculations were performed using https://clincalc.com/stats/samplesize.aspx comparing two independent study groups with continuous data. For the Ruxolitinib study power calculations were based on the BUN values between treatment groups of $Pkd1^{nl/nl}$ mice and for Octreotide the power calculations were based on fibrotic index values between treatment groups of $Pkd1^{nl/nl}$ mice.

2.13.1 Genotyping

Genotyping to determine the Pkd1 status of the mice was performed using ear clips by Monica Neilan (Department of Infection, Immunity and Cardiovascular Disease,

University of Sheffield). Mice that were either *Pkd1* $^{nl/nl}$ or WT, determined by agarose gel electrophoresis, were used in experiments.

2.14 Serum analysis

2.14.1 Blood urea nitrogen

The levels of blood urea nitrogen (BUN) in the serum were determined by analysis performed by Emilia Bettell (Sheffield Children's NHS Foundation Trust).

2.14.2 Growth hormone and IGF-1 ELISA

Growth hormone ELISA or IGF-1 ELISA was used to determine the circulating levels of these biological molecules in the mouse serum. The Rat/Mouse GH ELISA kit (Merck, Cat No. EZRMGH-45K) was used to determine serum growth hormone levels following the manufacturers protocol. Two serum samples were selected for a test run of each ELISA to determine the appropriate serum dilution.

2.15 Histology

Formalin-fixed tissues were paraffin embedded, cut and sections placed onto slides by Fiona Wright (Department of Infection, Immunity and Cardiovascular Disease, University of Sheffield). Dewaxing to remove paraffin prior to histological staining was performed by placing the slides in xylene for 5 minutes twice, then into high alcohol of 99% IMS

twice for 30 seconds, and gradually lowering the alcohol by moving the slides into 95% IMS for 30 seconds and finally 70% IMS. Slides were then rinsed with tap water, making sure the water stream did not make direct contact with the tissue on the slides in order to preserve the tissue. After histological staining, slides were rinsed in tap water and a dehydration protocol was performed in which the slides were placed in 70% IMS for 30 seconds, then 95% IMS for 30 seconds, followed by 99% IMS twice for 30 seconds and finally xylene twice for 2 minutes. Slides were mounted and sealed with a coverslip using DPX mountant for histology (Sigma-Aldrich, Cat No. 06522).

2.15.1 Haematoxylin and Eosin staining

Haematoxylin and Eosin (H&E) staining was performed to aid in visualising the cysts of the kidney. After dewaxing, slides were placed in haematoxylin reagent to stain nuclei and rinsed with tap water to remove excess stain. Slides were then placed in 0.3% acid-alcohol (v/v) (1.2 mL concentrated hydrochloric acid, 120 mL distilled water, 280 mL ethanol) for 1-2 seconds, rinsed in tap water, Scott's tap water substitute (24 mM sodium hydrogen carbonate, 166. mM magnesium sulphate) and rinsed in tap water again. Finally, tissues were stained with eosin for 2 minutes, before rinsing with water.

2.15.2 Picrosirius Red staining

Picrosirius red (PSR) staining was performed to allow for visualisation of collagens to assess fibrosis. Slides were dewaxed and hydrated as described, then nuclei were stained with Weigert's iron haematoxylin (1 g haematoxylin into 100 mL 95% ethanol combined with 2.5 g ferric chloride, 4.5 g ferric sulphate, 2 mL concentrated hydrochloric acid, and 298 mL distilled water) for 8 minutes, then washed with running tap water for

10 minutes. Tissue was then stained in picrosiurus red (Siurus red (Sigma, Cat No. 365548) with 1.3% picric acid solution) for 1 hour. Slides were washed twice with acidified water (5 mL glacial acetic acid in 1 L distilled water) then dehydrated as described.

2.15.3 Immunohistochemistry

Immunohistochemistry was used to visualise specific antigen targets within the tissue. After dewaxing and hydrating, heat-induced epitope retrieval was performed using antigen retrieval buffer (2.9 g trisodium citrate buffer, pH 6.0 and 1 mL Tween-20 in 1 L distilled water) and exposing the slides to 5-6 rounds of 3 minutes in a 850 W microwave, ensuring that the slides were covered with buffer. Slides were then placed under running cold water for approximately 5 minutes before circling the tissue with a wax pen. Tissues were placed in a blocking buffer of 3% milk in 1x TBST for 30 minutes then washed twice with 1x TBST. Slides were probed with the following primary antibody in a humidified environment overnight at 4°C:

Table 2.6 Primary antibodies used for immunohistochemistry

Antigen	**Host**	**Manufacturer**	**Dilution**
Mouse IgG	Mouse	Millipore Cat No. CS200621	1:500
Rabbit IgG	Rabbit	Merck Cat No. CS200621	1:500
GHR	Mouse	Santa Cruz Biotechnology Cat No. sc-137185	1:100
Aquaporin 1	Rabbit	Santa Cruz Biotechnology Cat No. sc-20810	1:10-1:50
Aquaporin 2	Goat	Santa Cruz Biotechnology Cat No. sc-9882	1:50
THP	Goat	Santa Cruz Biotechnology Cat No. sc-19554	1:100

Slides were washed twice in TBST and secondary antibody was applied at 1:200 dilution in 3% BSA in 1xTBST: Alexa fluor 488 goat anti-mouse IgG (Cell Signalling Technology, Cat No. 4408S), Alexa fluor 568 goat anti-rabbit IgG (Invitrogen, Cat No. A11036) and an aliquot provided of Alexa fluor 584 anti-goat IgG. Slides were incubated in a humidified chamber at room temperature for 4- 5 hours. When multiplexing, the second primary antibody would be added after the secondary antibody for the first primary antibody was applied. The nuclear far-red fluorescent stain TO-PRO was added at a dilution of 1:20 in 3% BSA for 30 minutes at room temperature in a humidified chamber and slides were sealed with a coverslip and mounted with Prolong™ Diamond Antifade Mountant.

2.16 Cystic index

Cystic index analysis was performed using H&E-stained kidneys that had been imaged with brightfield microscopy, either with the Zeiss or Leica microscopes. ImageJ software was used to analyse the kidneys wherein the image type was changed to 8-bit to provide a black and white image, and threshold was performed with Li B&W settings. The scale was set using the scale bar burned into the image when exporting from the microscope software. Cysts were measured by using the analyse particles function in ImageJ, with a minimum size of 5000 to avoid non-cystic hole being included. The outline image provided of the automatically measured cysts was compared to the original image to ensure that the output was accurately picking up on cysts and not non-cystic holes. The cyst output was totalled and normalised to the entire kidney size measure in ImageJ to provide the cystic index.

2.17 Fibrotic index

Fibrotic index of the kidneys were assessed using PSR stained kidneys. For the Octreotide *in vivo* study the fibrotic index was determined using ImageJ from brightfield images taken with the Zeiss microscope. The colour channels were split to give the red staining and thresholding was used to assess and quantify the red-stained collagen. For the Ruxolitinib study I had access to the Leica microscope with polarised light function,

which allowed for the collagen stain of the PSR stained kidneys to be imaged with polarised light. ImageJ was used to quantify the polarised light corresponding to the collagen fibres.

2.18 Statistical Analysis

Statistical power

Statistical analysis was performed in GraphPad Prism. When comparing two groups the non-parametric Mann-Whitney test was used. When comparing multiple groups with one independent variable a one-way ANOVA with Bonferroni correction was used for multiple comparisons. Comparison of multiple groups with two independent variables was performed using a two-way ANOVA with Bonferroni correction for multiple comparisons.

Table 2.8 Statistical annotation denoting significance

Annotation	P value
ns	Not significant, $p>0.05$
*	$p<0.05$
**	$p<0.01$
***	$p<0.001$
****	$p<0.0001$

Chapter 3: Expression, purification, and validation of bioactive recombinant growth hormone analogues

3.1 Introduction

This chapter will describe the subcloning, expression and purification of human and mouse growth hormone and mutant growth hormone analogues that act as a competitive inhibitor at the growth hormone receptor (GHR), thus inhibiting growth hormone signalling. This chapter will also detail the validation of the bioactivity of growth hormone and validation of the GHR antagonists (GHA) to inhibit growth hormone signalling.

A glycine to arginine mutation in the third α-helix of receptor binding site 2 of growth hormone produces a dominant negative GHR antagonist (Chen et al., 1990, Chen et al., 1994). The hGH-Gly120Arg GHA can bind to constitutive GHR dimers and promote internalisation however, it is unable to induce productive receptor conformational change and alignment for tyrosine phosphorylation, blocking GHR-mediated JAK2-STAT5 signalling independent of receptor internalisation (Harding et al., 1996, Maamra et al., 1999)

3.1.1 Aims

The purpose of the experiments in this chapter was to produce functional growth hormone analogues to take forward into *in vitro* and *in vivo* experiments to investigate

the effects of stimulation and inhibition of growth hormone signalling within the context of ADPKD.

The following growth hormone analogues were produced: human growth hormone wild-type (hGH-WT), human growth hormone receptor antagonists (hGH-Gly120Arg and hGH-m12), mouse growth hormone wild-type (mGH-WT), mouse growth hormone receptor antagonist (mGH-Gly118Arg) and mouse growth hormone fused to mouse growth hormone binding protein (mGH-Gly118Arg fusion protein).

3.2 Expression and purification of human growth hormone analogues from *E. coli*

The hGH-WT, hGH-Gly120Arg and hGH-m12 analogues had been previously cloned into the pET21a+ vector in which expression of an inserted gene is regulated by the upstream T7lac promoter and induced with the addition of lactose or IPTG. The clones had been codon optimised for expression in *E. coli.* These plasmids were provided by provided by Dr Sarbendra Pradhananga (Department of Infection, Immunity and Cardiovascular Disease, University of Sheffield). DNA sequencing analysis was performed to confirm the identity and accuracy of each target sequence from the provided plasmids (see APPENDIX B for sequences).

The hGH analogues were then transformed into BL21(DE3) chemically competent *E. coli* which carry an inducible gene for T7 RNA polymerase. For expression, superbroth (SB) autoinduction media was used based on the small-scale testing performed with BL21

(DE3) pET21a+ mouse growth hormone (section 3.4.1). The basis for the use of autoinduction media is that glucose is the preferred carbon source and will be preferentially used over lactose, thus when glucose is present it prevents induction by lactose in the log-growth phase. As glucose depletes, there is a natural shift to lactose consumption as a source of carbon and lactose is imported into the cells, as this process is dependent on growth of the bacteria, it is referred to as autoinduction (Studier, 2005).

For large scale expression BL21 (DE3) pET21a+ hGH analogues were grown in LB media prior to induction of expression to increase bacterial cell density. Expression of hGH analogues SB autoinduction media, with uninduced control cultures grown in LB media.

Samples were taken from the induced cultures (I) and compared to uninduced controls (U.I.) using SDS-PAGE gels stained with Coomassie to reveal the protein content. A band of the expected molecular weight for hGH (22kDa) is strongly visible in induced cultures for the hGH-WT, hGH-Gly120Arg and hGH-m12, indicating successful expression of the target proteins (Figure 3.1 A-C). Protein was extracted from the harvested cells through lysis and washing steps for partial removal of contaminants. Solubility of the hGH proteins was determined by comparing the total suspension of bacterial lysate (soluble and insoluble fractions) to the supernatant of the bacterial lysate (soluble fraction). A strongly visible 22 kDa band was observed in the bacterial lysate supernatant which suggests solubility of the hGH analogues (Figure 3.1 D-F).

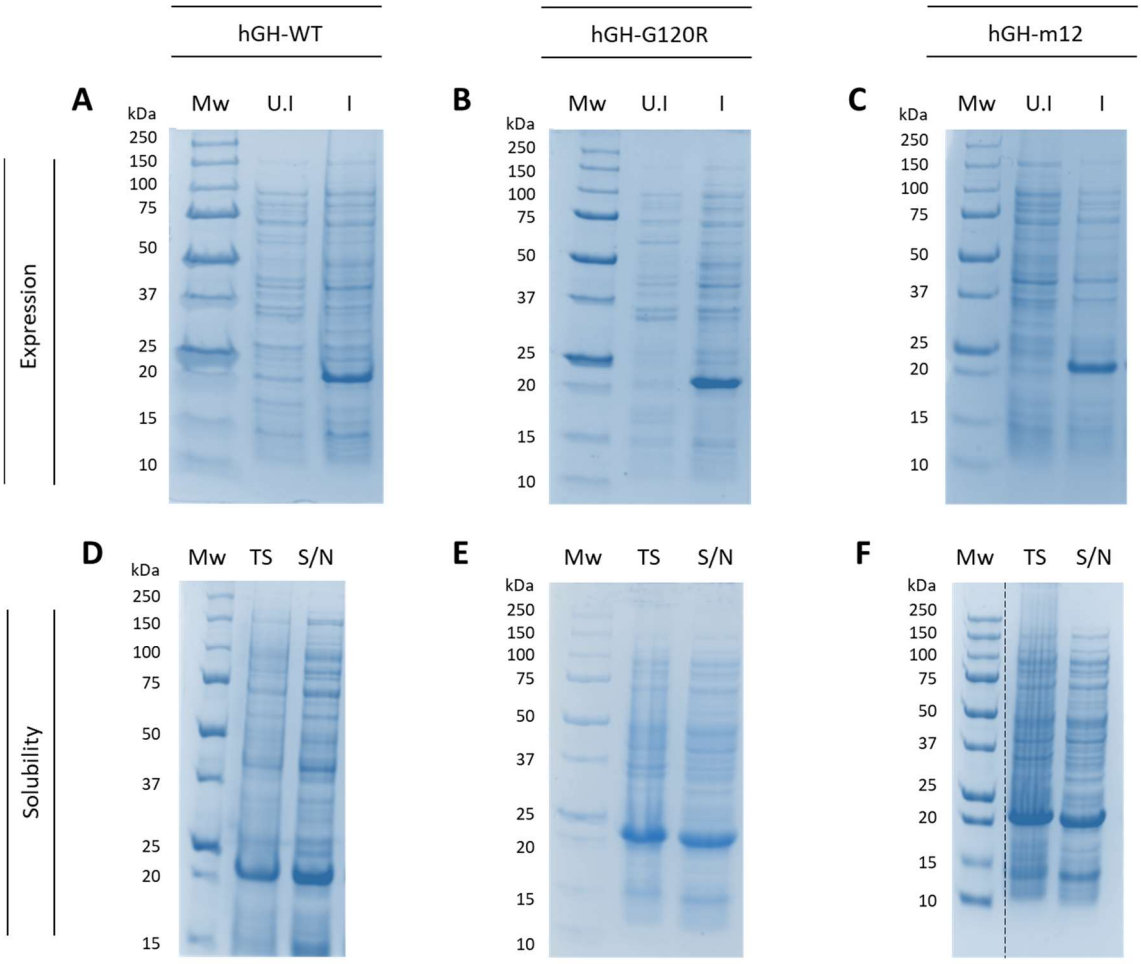

Figure 3.1 Expression and solubility of human growth hormone in BL21 (DE3) E. coli cells.

WT (A), Gly120Arg (B), or m12 (C) human growth hormone-transformed bacterial cell lysates of control uninduced (UI) cells were compared to cells that were induced for expression (I). A 22 kDa band is seen in induced lysates which is not present in uninduced lysates, demonstrating successful expression of hGH analogues. WT (D) or Gly120Arg (E) and m12 (F) human growth hormone total cell lysate suspension (TS) was compared with supernatant (S/N) to assess solubility. hGH-WT, hGH-Gly120Arg and hGH-m12 are present in the soluble fraction. The dotted line denotes removal of unrelated lanes from the image on the gel to place the relevant lanes next to the Mw ladder. Run on an SDS-PAGE (10%) visualised with Coomassie stain.

Preliminary analysis of the protein sequence was performed by entering the amino acid sequence of the hGH analogues into the ExPASy Protparam tool which predicts physico-chemical properties based on the amino acid sequence and provided a theoretical isoelectric point (pI) (APPENDIX C). This analysis informed appropriate pH for subsequent protein purification by ion exchange chromatography, as well as a more precise molecular weight estimated from the amino acid sequence to compare with the mass spectrometry molecular weight results.

Next, the soluble fractions of bacterial cell lysates containing hGH-WT, -Gly120Arg and -m12 were purified to remove contaminants. The hGH analogues are all polyhisitine-tagged thus nickel chelate chromatography was performed as a purification step. Each hGH-containing protein solution was loaded onto separate nickel chelate columns, flow-through was collected in case any target protein did not bind to the column. Columns were washed to remove any weakly bound proteins and remaining protein was eluted on an increasing imidazole gradient (50 mM-500 mM). To detect the location and purity of hGH, the protein load, flow-through, wash and eluted fractions were analysed using a Coomassie-stained SDS-PAGE gel. Imidazole concentrations of approximately 50 – 200 mM were capable of eluting hGH-WT, hGH-Gly120Arg and hGH-m12 from the nickel beads (Figure 3.3), observed as 22 kDa bands on the Coomassie-stained gel. Eluted fractions containing hGH (WT fractions 1-4; Gly120Arg fractions 1-7; m12 fractions 1-4) were pooled, concentrated, and stored in 1XPBS with ~50% glycerol as a cryoprotectant.

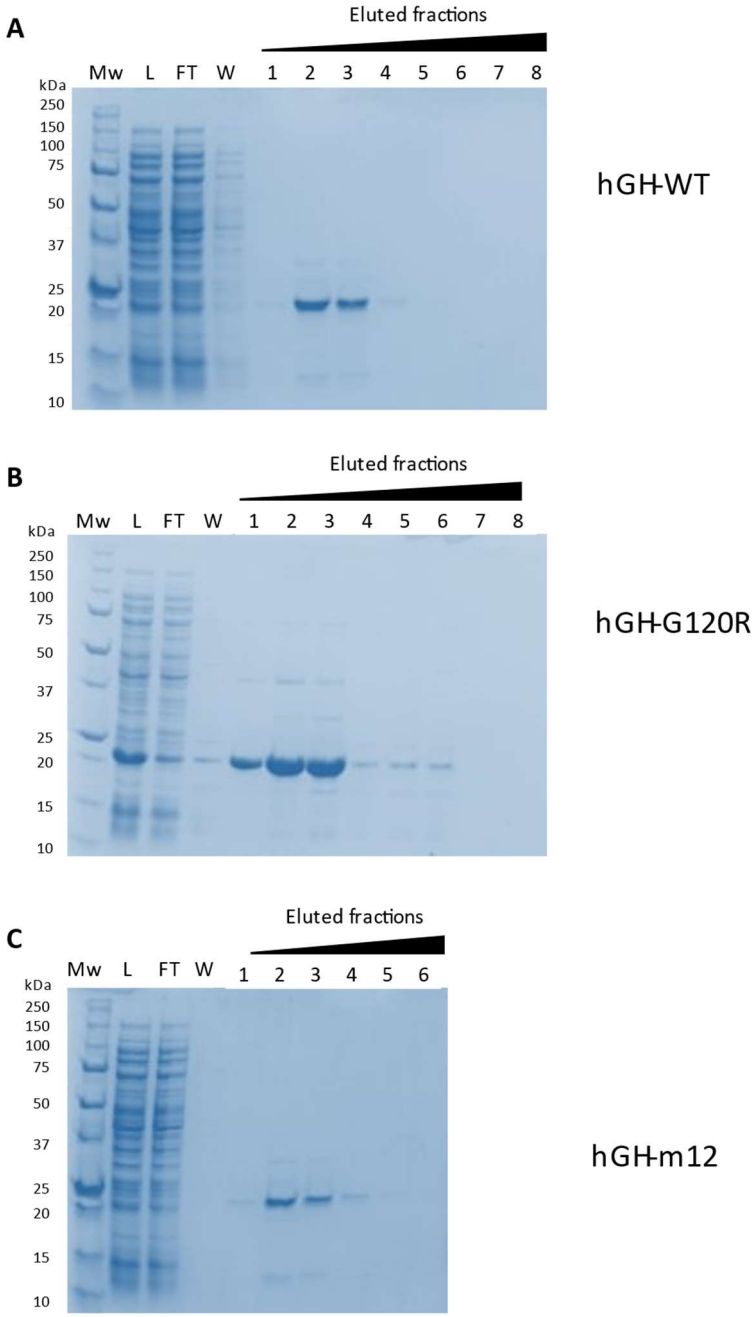

Figure 3.2 Purification of human growth hormone using nickel chelate affinity chromatography.

Purification of hGH-WT (A), hGH-Gly120Arg (B) and hGH-m12 (C) His-tagged human growth hormone in which L is the protein was loaded onto the column; FT, flow-through of protein from load; W, protein eluted with low imidazole buffer wash; Eluted fractions, fractions of protein eluted with a 20 mM – 500 mM imidazole gradient. Run on an SDS-PAGE (10%) visualised with Coomassie stain.

Endotoxin levels of the hGH analogues was measured to ensure they were at a reasonably low level to limit cytotoxicity for *in vitro* experiments using mammalian cells. Although there is not a consensus of a defined acceptable endotoxin level when it comes to *in vitro* applications, the FDA states an acceptable endotoxin level is ≤0.5 endotoxin units (EU)/mL so this was used as a rough guideline. Endotoxin levels were initially measured at 0.66 EU/mL for hGH-WT, 0.86 EU/mL for hGH-m12 and 0.88 EU/mL for hGH-Gly120Arg, these were later reanalysed after an endotoxin removal step was performed.

The endotoxin levels for the hGH solutions carried forward were 0.22 for hGH-WT, 0.39 for hGH-m12, and 0.29 EU/mL for hGH-Gly120Arg. As these values were <0.5 Eu/mL they were considered satisfactory for *in vitro* experiments. The endotoxin levels between the different GH preparations are comparable, hence cellular responses after recombinant protein stimulation are likely to be due to the direct effects of the recombinant proteins and not due to endotoxin levels.

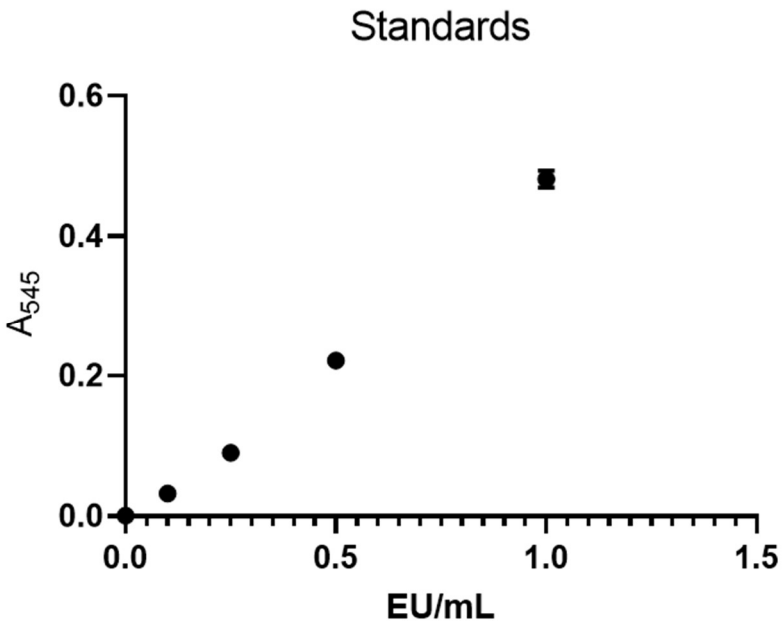

Protein	Pre-removal endotoxin (EU/mL)	Post-removal endotoxin (EU/mL)
hGH-WT	0.66	0.22
hGH-G120R	0.83	0.39
hGH-m12	0.88	0.29

Figure 3.3 Endotoxin detection and removal from human growth hormone analogues
Endotoxin levels of wild-type and mutant antagonist human growth hormone analogues (hGH-WT, hGH-Gly120Arg, hGH-m12) interpolated from a standard curve of absorbance at 545 nm (mean±SEM is plotted for technical repeats measured in triplicate) were measure prior to and post-removal of endotoxin as endotoxin units per mL (EU/mL).

To further study level of contamination and the precise molecular weight of the approximately 22kDa protein seen in eluted fractions, the purified, concentrated hGH-WT and hGH-Gly120Arg samples underwent matrix assisted laser desorption ionization-

time of flight (MALDI-TOF) mass spectrometry. The molecular weight of proteins in the sample was obtained and assessed for purity of the target protein and to examine any mass modifications that may have occurred. The main peaks for the hGH-WT (Figure 3.4 A) and hGH- Gly120Arg (Figure 3.4 B) had a molecular weight of 23322.0 daltons and 23420.9 daltons, respectively. These values correspond to the theoretical molecular weights that were predicted based on the amino acid sequences including the methionine start codon, which provides supporting evidence that the identity of the hGH-WT and hGH-Gly120Arg is correct (APPENDIX C). The values of closer to 23 kDa than 22 kDa as what has been denoted throughout the thesis as the approximate molecular weight of the growth hormone analogues is due to the polyhisitdine tag which accounts for 840.86 daltons.

There are a few contaminant proteins in the human growth hormone samples, however these are negligible when comparing the relative intensity of the contaminant peaks to the main peaks. The contaminants are also considered negligible in terms of bioactivity as the source is the host *E. coli* and potentially cytotoxic endotoxin has already been removed, so they are unlikely to have a bioactive impact on the mammalian experiment cells.

The human growth hormone analogues were concentrated down to ~2 mL at 1 mg/mL (45 µM) hGH-WT, ~1 mL of 3 mg/mL (136 µM) hGH-Gly120Arg, and ~1 mL of 1.6 mg/mL (73 µM) hGH-m12.

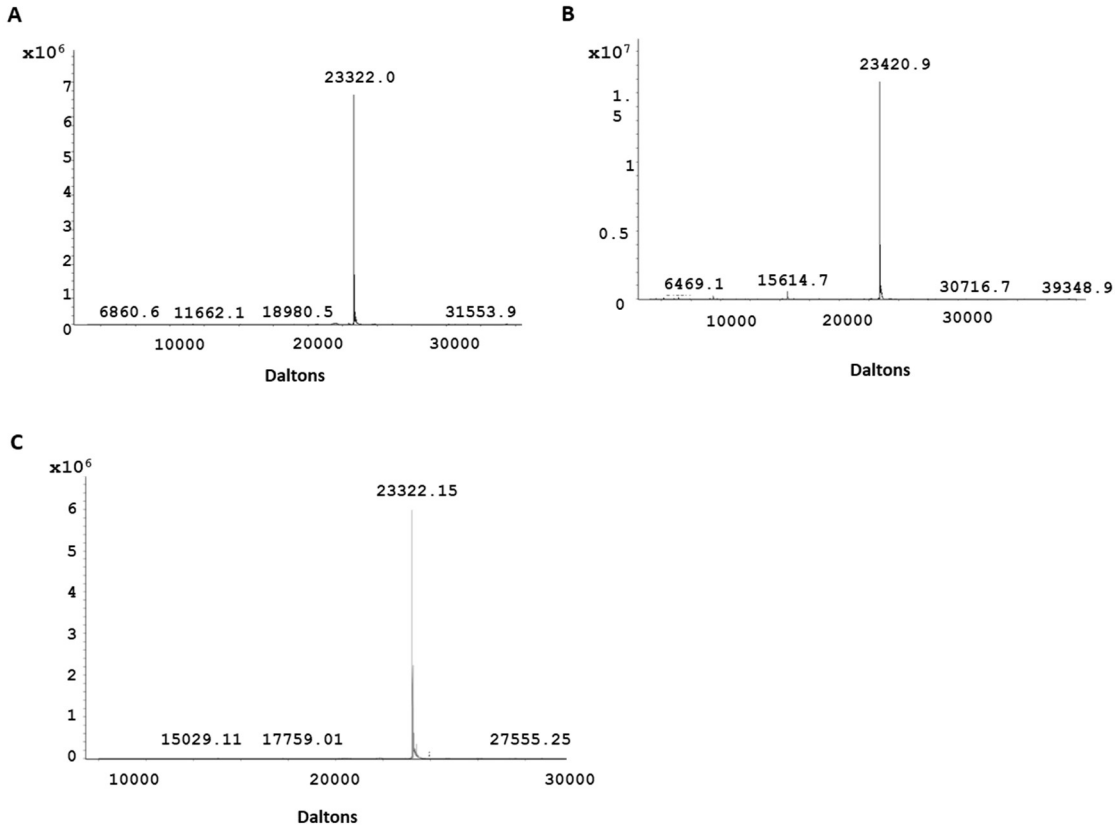

Figure 3.4 Mass spectrometry of human growth hormone using MALDI-TOF

To identify the molecular weights of human growth hormone analogues hexahistidine-tagged (A) hGH-WT with the main peak at 23322.0 daltons, and (B) hGH-Gly120Arg mutant with the main peak at 23420.9 daltons, and (C) hGH-m12 mutant with the main peak at 23322.15 daltons. Original graphs provided by the University of Sheffield Mass Spectrometry Services and modified for simplification

3.3 Examination of the bioactivity of recombinant human growth hormone analogues

Now that the solubility and identity of the laboratory-purified human growth hormone analogues had been confirmed, the next step was to verify that they had properly folded

into a bioactive conformation and were capable of modulating GH-GH receptor (GHR) signal transduction. The bioactivity of human growth hormone analogues was validated using Human Embryonic Kidney cells (HEK293) cells that overexpress full length human growth hormone receptor (HEK293-GHR). STAT5 activity was assessed to determine stimulation and inhibition of GH-induced STAT5 signalling, measured through western blot for phosphotyrosine (pY) STAT5 and through STAT5 luciferase assays to examine STAT5 transcriptional activity. Tyrosine phosphorylation of STAT5 is an obligatory event in activation of canonical STAT5 transcriptional activity, while luciferase transcriptional assays report directly on the activity of STAT5.

To determine the optimal dose and time exposure of hGH to stimulate phosphoactivation of STAT5, HEK293-GHR cells were stimulated with 50-500 ng/mL hGH-WT at three timepoints (15, 30, 45 minutes), analysed using western blot for pY-STAT5. The band intensity of pY-STAT5 was normalised to β-actin for semi-quantitative analysis. At all timepoints tested 100 and 500 ng/mL hGH-WT resulted in a statistically significant increase in STAT5 activity, but 50 ng/mL hGH-WT did not significantly increase pY-STAT5. The 15 minute and 30 minute timepoints are comparable for STAT5 activity across dose groups. STAT5 is most potently activated at 45 minutes post-stimulation with either 100 ng/mL or 500 ng/mL as observed under western blot (Figure 3.5 A).

After semi-quantitative analysis of STAT5 activity by studying pY levels, a more quantitative approach was utilised with the luciferase assay to assess the STAT5 transcriptional response to hGH-WT stimulation. The luciferase assay was employed using STAT5 Firefly luciferase and normalising to Thymidine Kinase (TK) Renilla luciferase.

The laboratory-purified hGH-WT was able to activate STAT5 in a dose-dependent manner within the range tested (25 – 500 ng/mL). As observed with the western blot pYSTAT5 data, stimulation at ≤50 ng/mL of hGH-WT although it did not significantly increase STAT5 activity it trended towards an increase. While 100 and 500 ng/mL of hGH-WT led to a statistically significant increase in STAT5 activity. The laboratory hGH most potently activates STAT5 at 500 ng/mL, increasing 8-fold compared to unstimulated controls (Figure 3.5 B).

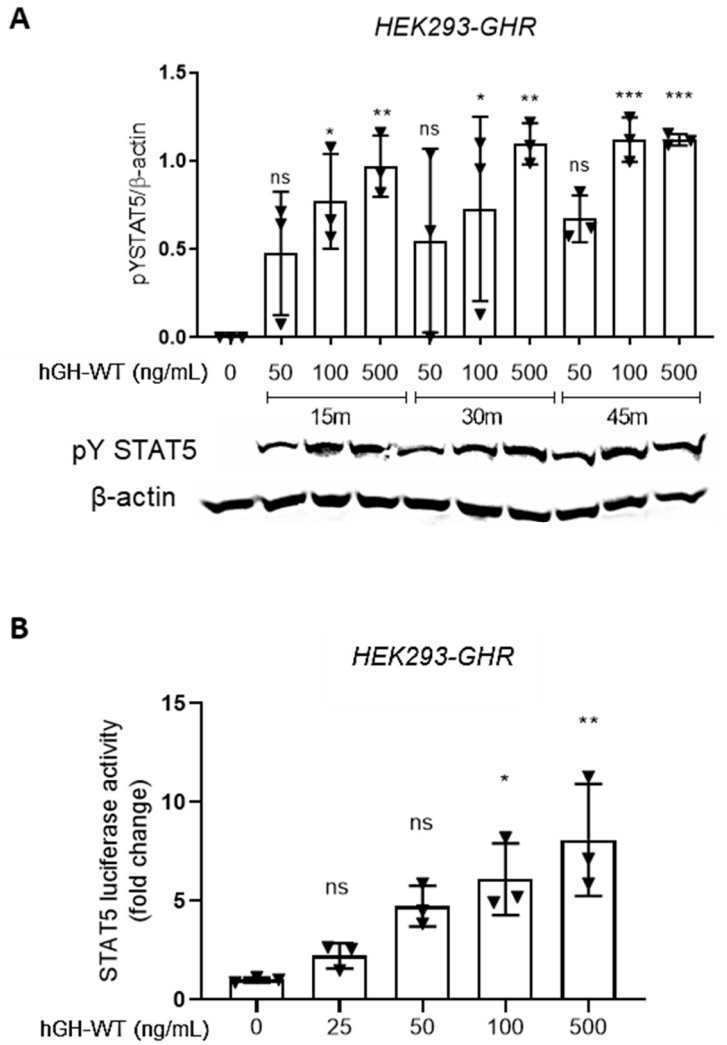

Figure 3.5 Bioactivity of human growth hormone-WT demonstrated by STAT5 activation in HEK293 cells that overexpress full-length hGHR (HEK293-GHR)

(A) Laboratory-purified hGH-WT was able to significantly increase STAT5 activity compared to unstimulated control. Multiple doses were tested to find the optimal dose (50, 100, 500 ng/mL) and three timepoints were tested for hGH-WT to find the optimal time for hGH-induced STAT5 activity (15, 30 and 45 minutes). Doses ⩾ 100 ng/mL hGH-WT at all timepoints show significant increase in STAT5 activity. (B) Similarly in the luciferase assay hGH-WT stimulates STAT5 activity 4 hours post-stimulation in a dose-dependent manner and is significantly higher ⩾ 100 ng/mL. A one-way ANOVA test with a post-hoc Bonferroni correction for multiple comparison was used to determine statistical significance, indicated by asterisks. N=3 (biological repeats) for each dose group tested. Mean ±SEM is plotted. ns = not significant, * P<0.05, ** P<0.01, *** P<0.001.

The hGHR antagonists hGH-m12 /hGH-Gly120Arg were applied to HEK293-GHR cells at 0.5-10 fold of the applied hGH-WT dose to test their ability to inhibit hGH-induced STAT5 activation and determine the optimal dose for reduction of STAT5. In previous studies, experiments have used up to a 10-fold dose of GHA compared GH to antagonise growth hormone signalling (Nass et al., 2000a) which formed the basis of the highest dose tested.

When compared to cells stimulated with hGH-WT only, hGH-Gly120Arg and hGH-m12 were able to significantly decrease STAT5 phosphoactivation (Figure 3.6 A) and transcriptional activity (Figure 3.6 B) in a dose-dependent manner, indicating successful production of functional hGHR antagonists. The hGH-m12 analogue potently decreases STAT5 activity, with a reduction of up to 6-fold at the higher dose levels of 500 and 100 ng/mL, whereas hGH-Gly120Arg achieved a 3-fold decrease in STAT5 activity in these dose groups. This is expected as hGH-m12 has a higher binding affinity to the hGHR

(Figure 3.6 C). Although hGH-m12 is more potent than hGH-Gly120Arg there is not a statistically significant difference between the two when comparing STAT5 activity of each dose group with the exception of the dose of 200 ng/mL, meaning it is likely that inhibitory capacity has been reached after this point. The higher binding affinity of hGH-m12 is reflected in the blot data as pY-STAT5 bands are not visible from 200 ng/mL of hGH-m12 versus from 500 ng/mL with hGH-Gly120Arg. In conclusion hGH-Gly120Arg and hGH-m12 successfully inhibit growth hormone-induced STAT5 activity in HEK293 overexpressing GHR.

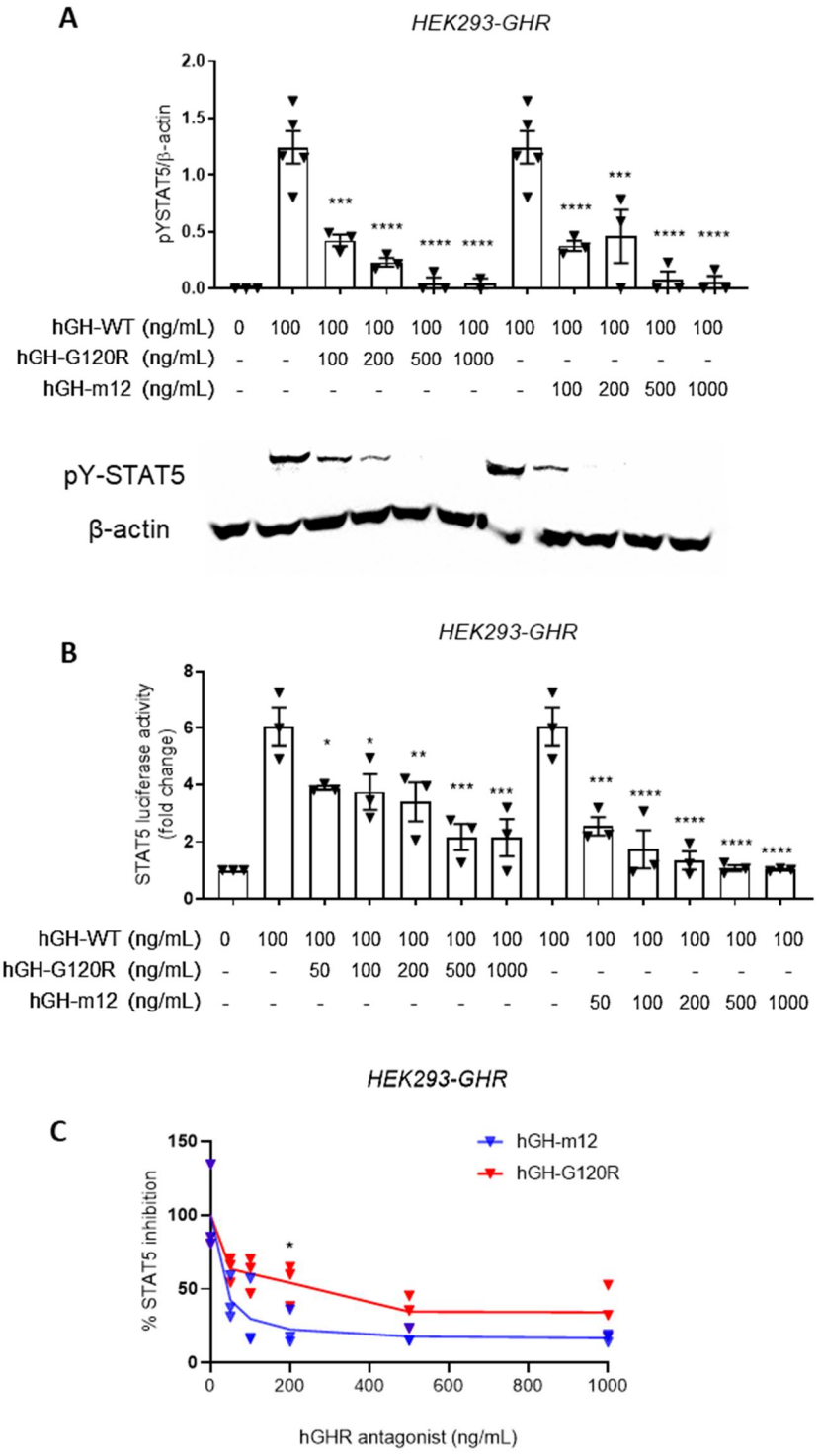

Figure 3.6 Laboratory-produced growth hormone receptor antagonists inhibit growth hormone-induced STAT5 activation in HEK293-GHR

The hGH-Gly120Arg and hGH-m12 hGHR antagonists (GHA) act as competitive inhibitors and lead to significant dose-dependent decrease in hGH-induced STAT5 activity from ⩾ 50 ng/mL when compared to hGH-WT only, stimulated for 30 minutes, observed in

western blot (A) and luciferase assay where luciferase levels were measured 4 hours after stimulation (B). (C) Side by side comparison of the hGH-Gly120Arg and hGH-m12 hGHR antagonists in their ability to inhibit hGH-induced STAT5 activity. The hGH-m12 GHA has a higher binding affinity and reduces the STAT5 significantly more than hGH-Gly120Arg at 200 ng/mL. A one-way ANOVA test with a post-hoc Bonferroni correction for multiple comparison was used to determine statistical significance, indicated by asterisks. N=3 (biological repeats) for each dose group tested. Mean ±SEM is plotted. * P<0.05, ** P<0.01, *** P<0.001, **** P<0.0001.

3.4 Subcloning, expression and purification of mouse growth hormone analogues

3.4.1 Bacterial expression

Initially the same bacterial expression system that had been successfully used to produce the hGH analogues was performed with the mouse growth hormone (mGH) wild-type (WT) and the mutant mGHR antagonist (Gly118ArgGly118Arg), which had been previously cloned in the pET21a+ vector. I began with optimisation of expression of pET21a+ mGH by comparing small scale expression levels of two subclones (mGH-WT and mGH-Gly118Arg) at 22°C in lactose-containing (2YT) autoinduction media and superbroth (SB) autoinduction media, with superbroth being a more enriched media. Autoinduction media was chosen over LB media with IPTG induction as it has been shown to achieve higher cell densities and protein yield than LB media (Studier, 2005, Madurawe et al., 2000).

The level of protein expression was analysed using Coomassie-stained SDS-PAGE gel. Both mGH analogues expressed well as indicated by the thickness of the 22 kDa target protein bands in the gel, and they appeared relatively similar between the 2YT and SB, SB autoinduction media was selected for expression going forward, which is the media that was used for the human analogues.

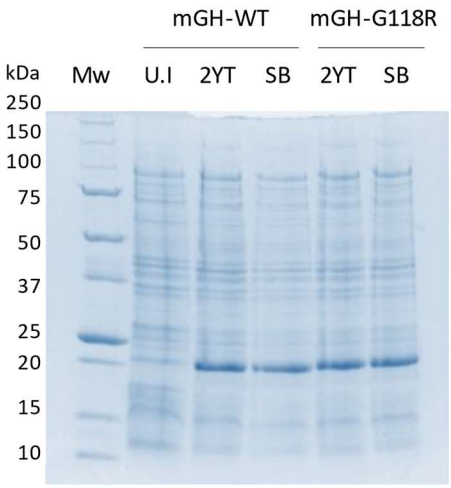

Figure 3.7 Comparison of autoinduction media in small scale expression of mGH-WT and mGH-Gly118Arg

Expression of mGH-WT and mGH-Gly118Arg were compared in two different autoinduction medias: 2YT and superbroth (SB). Run on an SDS-PAGE (10%) visualised with Coomassie stain.

High levels of expression of the mGH analogues was achieved in *E. coli* as shown by the strong 22 kDa band in large scale induced cultures, which is the expected band size of mGH, for the mGH-WT (Figure 3.8 A,) and mGH-Gly118Arg (Figure 3.8 B).

However, when testing solubility both mGH analogues, no 22 kDa band was visible in the soluble fraction of cell lysates for mGH-WT (Figure 3.8 C) or mGH-Gly118Arg (Figure 3.8 D) and was only present in the total suspension, indicating the formation of insoluble highly aggregated protein referred to as inclusion bodies for both mGH analogues.

To recover the mGH analogue proteins from the inclusion bodies the proteins were denatured and solubilised with the use of a chaotrope and then a number of subsequent refolding methods.

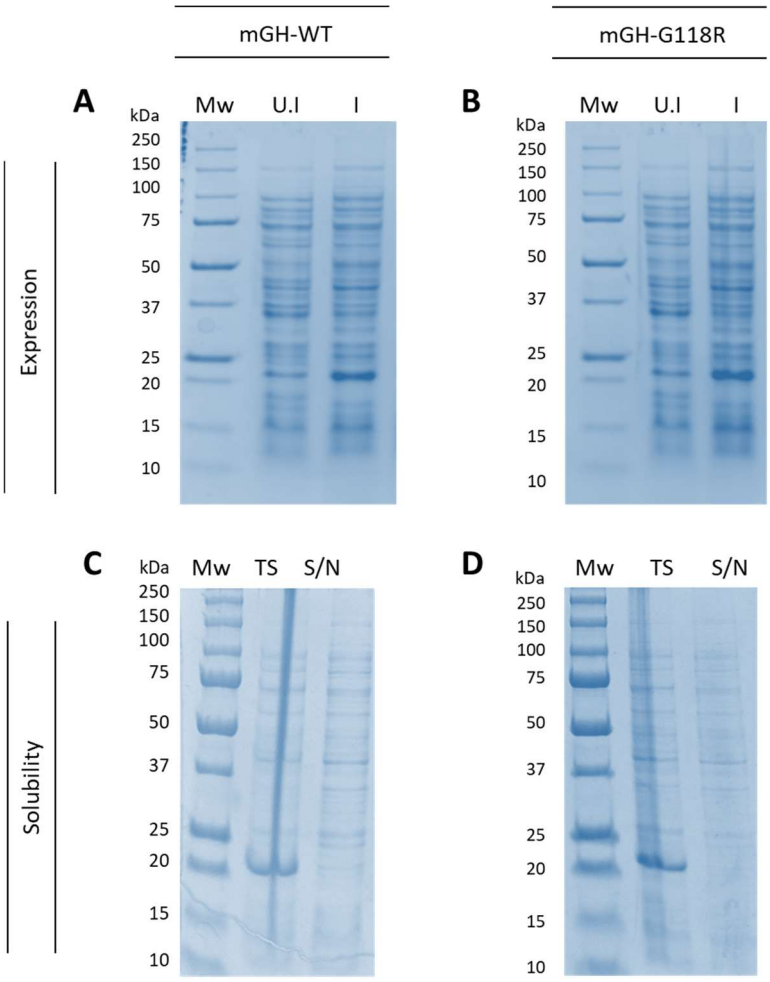

Figure 3.8. Expression and solubility of mouse growth hormone in BL21 (DE3) E. coli cells.

Mouse growth hormone wild-type (A) and Gly118Arg mutant (B) bacterial lysates with induced expression (I) was compared to uninduced control (U.I), which shows a strong 22 kDa in induced samples, indicating expression of mGH analogues. The total suspension of lysate (TS) was compared with the supernatant soluble fraction (S/N) to test solubility of mGH. A 22 kDa band is only visible in the total suspension indicating both the mGH-WT (C) and Gly118Arg (D) are in inclusion bodies. Run on an SDS-PAGE (10%) visualised with Coomassie stain.

Optimal conditions for denaturation of the mGH-WT and mGH-Gly118Arg analogues that were in inclusion bodies was 4 M urea at pH 8.0 (Figure 3.9 A). Protein refolding of denatured mGH through either dialysis showed that 22 kDa bands were present in the total suspension (TS) and pellet (P) but not the supernatant (S/N) from either method indicating that dialysis to remove urea did not yield soluble protein (Figure 3.9 B). Although a 22 kDa band is not present in the rapid dilution total suspension this is likely because it is so dilute that it does not appear on the Coomassie gel. The 22 kDa band for mGH can be seen in the pellet but not in the supernatant or the concentrated supernatant (S/Nc) which suggests that refolding method of rapid dilution also did not yield soluble mGH.

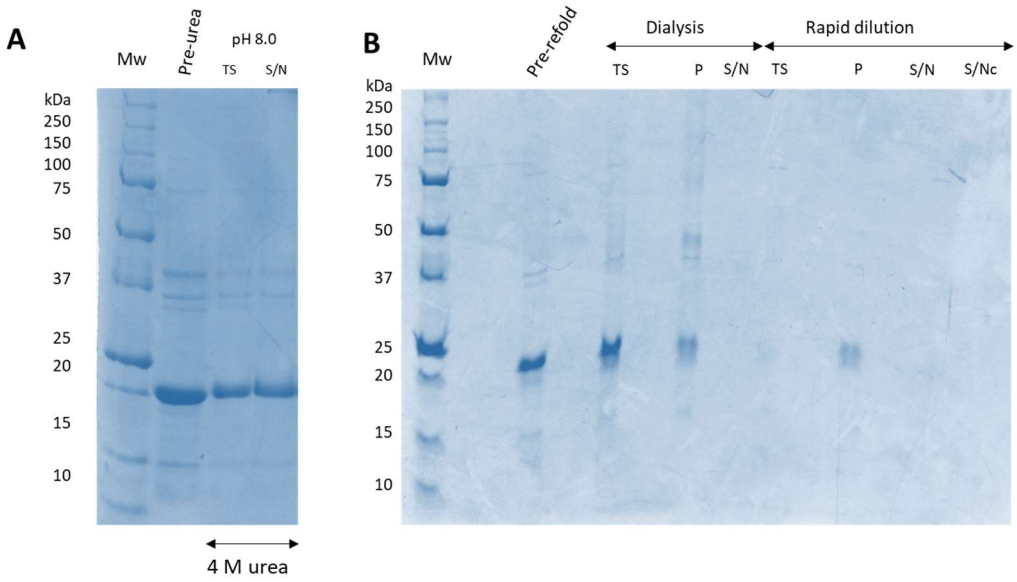

Figure 3.9 Denaturation and refolding of mGH

(A) mGH WT was totally denatured and solubilised at pH 8.0 with 4 M urea shown by the same amount of 22 kDa band in the total suspension (TS) and the supernatant (S/N) (B) Refolding of mGH-WT through dialysis or rapid dilution with the TS, pellet (P) or S/N shows no 22 kDa band in the S/N of either method indicating that mGH is not in the soluble fraction. mGH was not present in the concentrated S/N (S/Nc) from the rapid dilution method. Run on an SDS-PAGE (10%) visualised with Coomassie stain.

Refolding the denatured mGH analogues in 4 M urea during purification was attempted by gradually removing the urea in a 4 M – 0 M urea reverse concentration gradient after the wash step and prior to elution of the protein however the protein precipitated on the column during urea removal.

As soluble mGH proteins were not recovered from inclusion bodies with the method of solubilisation and refolding, changing the conditions of induction of expression to yield soluble, active protein was tested. The aim here was to produce target protein that was already soluble and properly folded in order to avoid manually denaturing and refolding the product which had so far proved unsuccessful. Often inclusion body formation in *E. coli* results from expression with a high temperature and expression under a strong promoter leading to a high translational rate and subsequently leading to misfolding and aggregation of target protein (Singh et al., 2015) . Thus, the temperature was lowered during induction of expression of the BL21 (DE3) pET21a+ mGH from 22°C to 16°C, as high-level expression at standard cultivation temperatures can impair proper refolding of recombinant protein. Even at a lower temperature for induction, mGH remained totally insoluble.

For the same purpose of overcoming protein misfolding and insolubility, expression of mGH-WT and Gly118Arg was also attempted in ArcticExpress (DE3) cells. ArcticExpress (DE3) cells are a specialised *E. coli* which contain a chaperonin plasmid that can be selected for via its gentamycin-resistance gene. This plasmid encodes Cpn10 (10 kDa) and Cpn60 (57 kDa) chaperonins from *Oleispira antarctica* which retain high protein refolding activity at lower temperatures (4 -12°C)., unlike the cold-sensitive *E. coli*

chaperonin GroEL-GroES complex (Ferrer et al., 2003). ArcticExpress (DE3) cells which coexpress the cold-adapted chaperonins were transformed with the pET21a+ mGH plasmids and were IPTG-induced at 11°C.

When tested, this method obtained the same results as induction in BL21 (DE3) cells in which the target mGH proteins were completely insoluble. The soluble fraction from the expression of mGH-Gly118Arg was run across a nickel chelate column in case levels of target protein were below detection so were not visualised on the gel amongst the contaminants, however no 22 kDa mGH was observed in the concentrated eluted fractions.

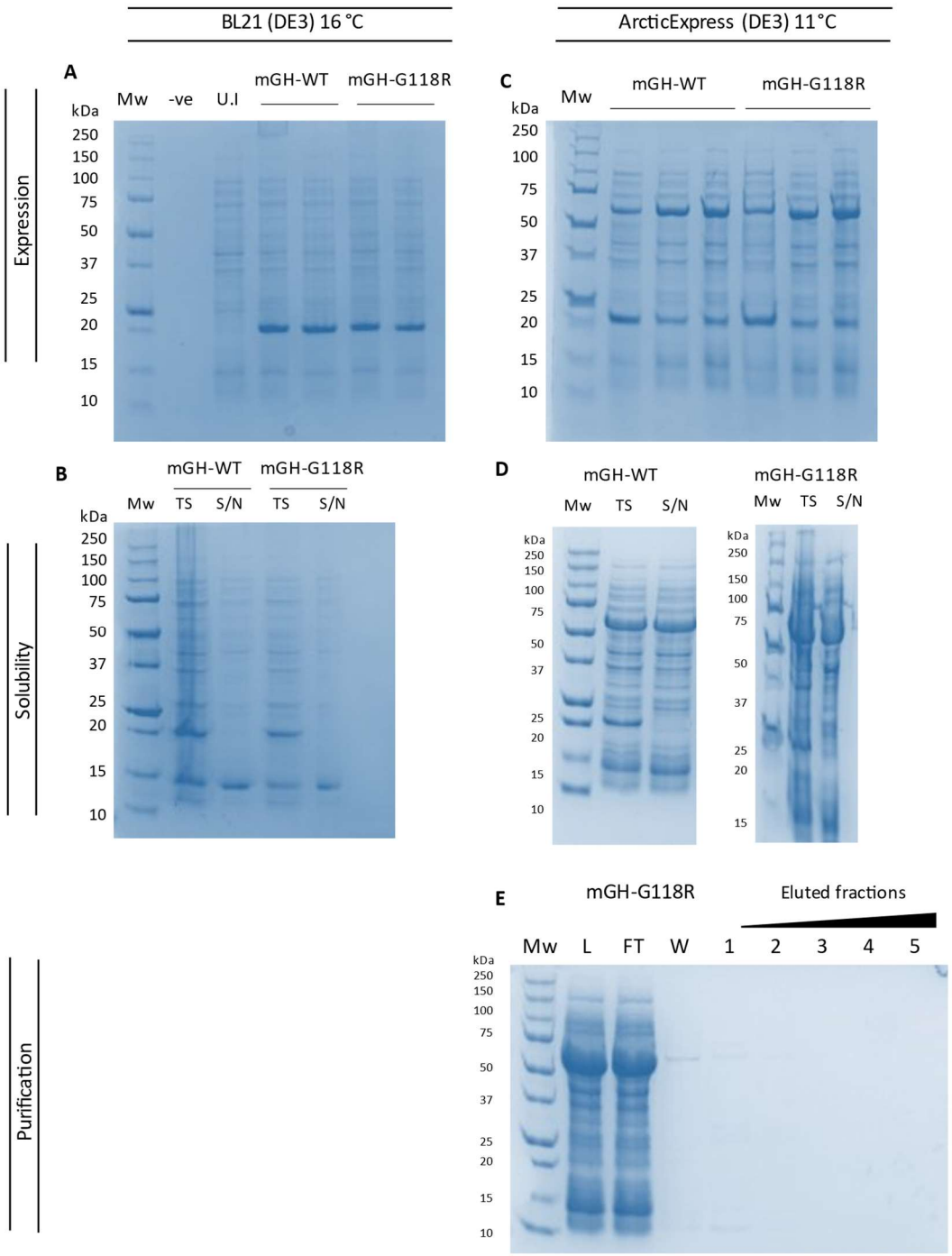

Figure 3.10 Expression, solubility, and purification of mGH in Bl21 (DE3) at 16°C and ArcticExpress (DE3)

Expression (A) and solubility (B) of mGH-WT and mGH-Gly118Arg in Bl21 (DE3) at 16°C. Expression (C), solubility (D) of mGH-WT and mGH-Gly118Arg in ArcticExpress (DE3) cells. The total suspension of lysate (TS) was compared with the supernatant soluble fraction (S/N) to test solubility of mGH. A 22 kDa band is only visible in the total suspension

indicating both the mGH-WT and Gly118Arg are in inclusion bodies in both conditions. (**E**) The S/N of mGH-Gly118Arg expressed in ArcticExpress (DE3) was run across a nickel chelate column in case of low undetectable level of soluble protein to concentrate and purify, though no visible 22 kDa band in the eluted fractions indicates no soluble target protein was present. Run on an SDS-PAGE (10%) visualised with Coomassie stain.

3.4.2 Mammalian expression

No soluble protein was obtained from the bacterial expression and refolding methods described, thus expression in *E. coli* was discontinued and a mammalian expression system was pursued. For mammalian expression, a gene encoding mGH-WT was provided by Dr Ian Wilkinson (Oncology & Metabolism department, University of Sheffield) in a pCEP4 vector which expresses the gene of interest under the CMV promoter. The vector encoding a hexahistidine-tagged mGH-WT was transfected into HEK293T cells for expression. Here, it was able to be expressed in a soluble form directly into the culture supernatant. The 22 kDa band, suspected to be the mGH-WT, probed for hexahistidine (6X His tag) emerges day 1 post-transfection, and by day 7 the mGH has accumulated. This was run across a nickel chelate column to purify, using an imidazole gradient in which the mGH -WT 22 kDa band appears in eluted fractions 1-4 at approximately 50-300 mM imidazole (Figure 3.11 A, C).

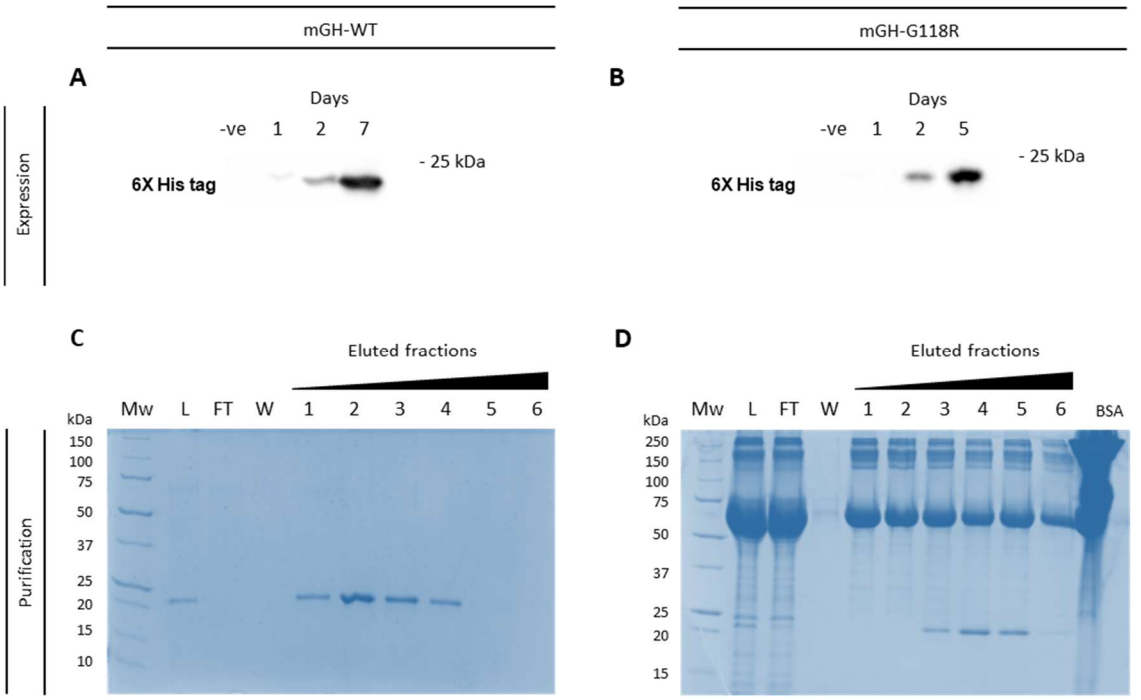

Figure 3.11. Expression of mouse growth hormone in HEK293T and purification with nickel chelate chromatography.

The culture supernatant from HEK293T cells transfected with plasmids containing either mouse growth hormone wild-type (mGH-WT) (A) or and Gly118Arg mutant (mGH-Gly118Arg) (B), was compared to that from an un-transfected control (-ve), which shows presence of a ~22 kDa band in 6XHis tag blot, indicating successful expression of hexahistidine-tagged mGH analogues. Purification using nickel chelate chromatography was performed with mGH-WT (C), and mGH-Gly118Arg (D), whereby L is the protein loaded onto the column; FT, flow-through of protein from load; W, protein eluted with low imidazole buffer wash; Eluted fractions, fractions of protein eluted with a 20 mM – 500 mM imidazole gradient.

Once it was shown that mGH-WT could be produced in a soluble form using mammalian expression, the next step was to produce a pCEP4 plasmid containing the mGH-Gly118Arg, which was codon-optimised for mammalian expression. Initially the mGH-WT was used as a template to perform site-directed mutagenesis to produce a glycine

to arginine mutation (Gly118Arg) in the pCEP4 mGH-WT with primers containing the arginine mutation and amplifying the entire vector backbone, however the expected ~11 kilobase band was not present in the PCR product when visualised in the agarose gel, which may have simply been because the product was too large however increasing the extension time did not yield the expected band.

Instead, using the same primers that were designed for the site-directed mutagenesis (Gly118Arg for, Gly118Arg rev), DNA encoding mGH-Gly118Arg was subcloned into the pCEP4 vector using overlap extension PCR alongside CMV for and EBV rev primers so that only an ~800 bp region containing mGH-Gly118Arg was amplified (Figure 3.12 A).

Restriction digest analysis was performed using KpnI and HindIII in the mGH-WT containing pCEP4 plasmid, as I did not have the empty vector. Restriction digest with the same enzymes was performed with the insert which was the 807 bp mGH-Gly118Arg PCR product yielded from the overlap extension PCR, in order to produce the correct corresponding base pair ends for ligation to the restriction-digested vector (Figure 3.12 B). There appears to be multiple bands in the DNA cute with HindIII indicating possible star activity, in which the enzyme is cutting sequences it should not recognise which may be the case as the HindIII used was not a high fidelity restriction enzyme like KpnI. Only the DNA of the correct band size was gel extracted for use in ligation. T4 ligase was used to ligate the pCEP4 open vector to the mGH-Gly118Arg insert, with a negative control for ligation of the pCEP4 open vector with the same reaction set up but without the insert.

Following ligation, the pCEP4 mGH-Gly118Arg and negative ligation control were transformed into XL1 blue. Colonies formed in the XL1 blue pCEP4 mGH-Gly118Arg were cultured, the plasmid DNA was extracted and sequenced.

After the correct sequence of pCEP4 mGH-Gly118Arg had been verified by sequencing, expression in HEK293T and purification using nickel chelate chromatography of mGH-Gly118Arg was performed for both the mutant and WT mGH (Figure 3.11 C, D). The nickel chelate purification of mGH-Gly118Arg shows 22 kDa band in eluted fractions 3-5, at approximately 200-400 mM imidazole.

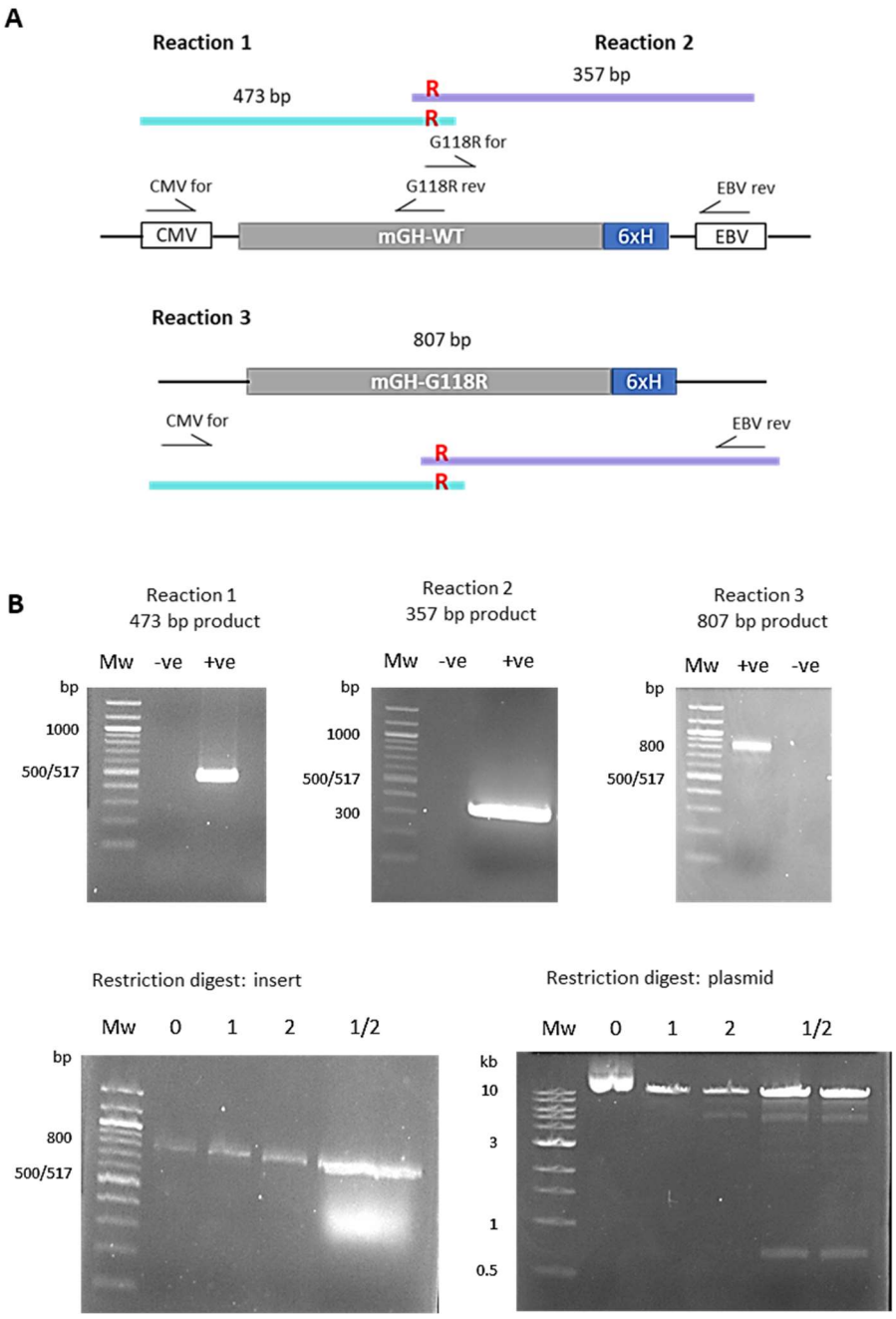

Figure 3.12 Overlap extension PCR of mGH-Gly118Arg and restriction digest with KpnI/HindIII

(A) Graphic summary of the overlap extension PCR reactions to produce mGH-Gly118Arg from mGH-WT, see APPENDIX D for primers. (B) Agarose gel electrophoresis analysis of the overlap extension PCR reactions to produce mGH-Gly118Arg and the restriction digest with KpnI (1) and HindIII (2) of the mGH-Gly118Arg insert (reaction 3 product) and the pCEP4 mGH plasmid, with the negative control (0) which contains no restriction enzymes, only the PCR product of uncut insert or plasmid.

Although, some notable differences between mGH-WT and mGH-Gly118Arg when it came to expression were the HEK293T cells were less adherent when transfected with pCEP4 mGH-Gly118Arg. For this reason, the protocol was adapted to use media containing 10% FBS compared to serum free media used during mGH-WT expression. The HEK293T cells transfected with mGH-Gly118Arg plasmid also detached from the plate and died earlier than with the mGH-WT, hence why the final expression sample for mGH-Gly118Arg is shown as 5 days rather than 7 days as for the mGH-WT. Due to issues with maintaining detectable protein during purification, 3% BSA was added to the loaded mGH-Gly118Arg-containing solution and the collecting tubes for eluted fractions were pre-coated with 3% BSA solution. For these reasons there are more visible contaminants in the Coomassie gel for the mGH-Gly118Arg nickel column run than for the mGH WT nickel column run. The thick band between 50-75 kDa is also present in media from un-transfected HEK293T control so is likely a component of FBS (supplemental figure 3). Figure 3.11 D shows a BSA only control that was used to try to account for bands present from BSA although it was overloaded so individual bands are unclear, but it does serve the purpose of highlighting the additional visible protein present on a Coomassie gel due to the presence of BSA.

Using the Bradford assay the concentrated pooled eluted fractions were determined to be 71.4 µg/mL or 3.2 µM mGH-WT and after adjusting for levels of BSA the mGH-Gly118Arg was determined to be 39.9 µg/mL or 1.8 µM, both in ~500 µL. This amounts to approximately 37 µg of mGH-WT and 20 µg of mGH-Gly118Arg. Here it has been demonstrated that mouse growth hormone protein analogues can be expressed in a mammalian expression system.

Due to limited amount of the mGH-Gly118Arg purified, only the mGH-WT was sent for MALDI-TOF mass spectrometry to determine the precise molecular weight of the protein suspected to be mGH-WT that was purified. The main peak has a molecular weight of 22902.08 daltons (Figure 3.13) which corresponds to the theoretical molecular weight predicted for polyHis-tagged mGH-WT, not including the methionine start codon (APPENDIX C) which suggests that the identity of the mGH-WT is correct.

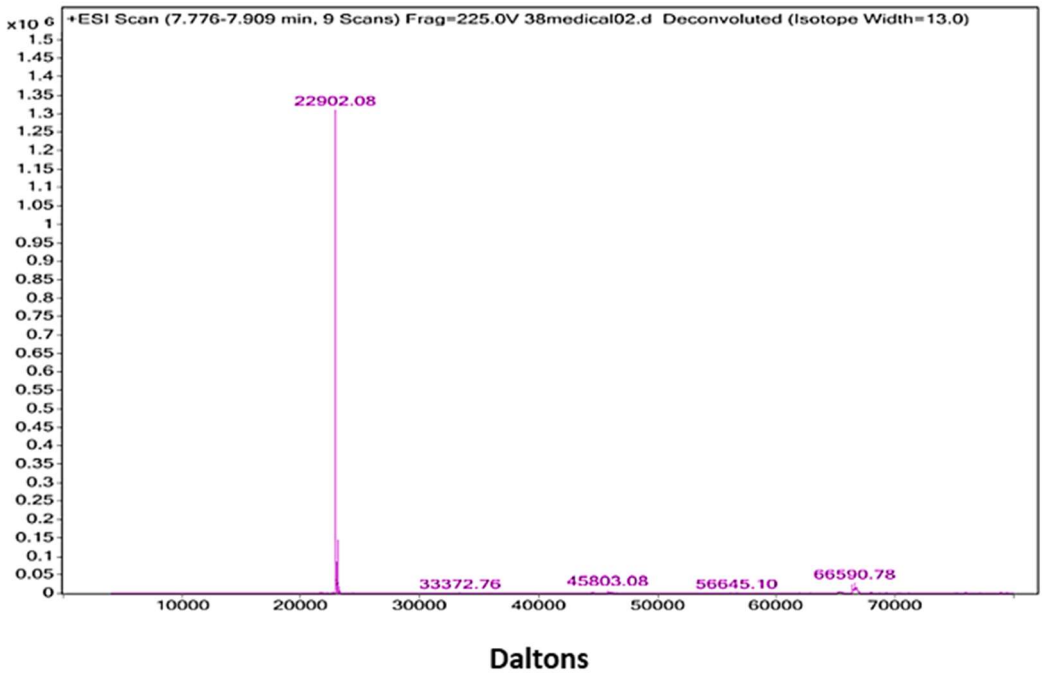

Figure 3.13 Mass spectrometry of wild-type mouse growth hormone

To identify the molecular weights of hexahistidine-tagged WT mouse growth hormone (mGH-WT). The main peak appears ar 22902.08 daltons. Original graphs provided by the University of Sheffield Mass Spectrometry Services and modified for simplification.

3.5 Verification of recombinant mouse growth hormone bioactivity

Mouse growth hormone analogues were validated by assessing impact on STAT5 activation in mouse embryonic kidney (MEK) cells, isogenic MEK Pkd1 +/+ and MEK Pkd1 -/- cells. Laboratory-purified mGH-WT was able to induce signal transduction in MEK cells displayed as phosphoactivation of STAT5 in response to mGH-WT stimulation. MEK cells were stimulated with 1 μg/mL mGH-WT over a time course of 5, 30, 60 and 240 minutes and phosphoactivation of STAT5 was assessed using western blot then compared to unstimulated cell (0 minutes). This was performed to determine optimal time for stimulation of cells to observe STAT5 activation with mGH-WT in a mouse model, in case this was at all altered compared to what was observed with the hGH-WT in the HEK293-GHR cells. These results show that mGH-WT elicited the strongest STAT5 activation response after 30 minutes shown as the highest band intensity in the western blot. STAT5 phosphoactivation is observable after 5 minutes as a weak pYSTAT5 band, peaks at 30 minutes, declines slightly by 1 hour and reduces to near unstimulated levels by 6 hours (Figure 3.14). No significant differences were observed in the ability of MEK cells to respond to GH activation depending on their PKD1 status.

The mGH-Gly118Arg function to reduce GH-induced STAT5 activation was assessed using western blot for pY-STAT5. As there was only a limited amount of the mGH-Gly118Arg only one repeat was performed so no statistical significance can be determined from this data but it does indicate a trend of reduced STAT5 activation to unstimulated levels at doses of 2 μg/mL and 5 μg/mL, 2- and 5-fold the dose of mGH-

WT applied in both F1 Pkd1 +/+ and F1 Pkd1 -/- (Figure 3.15). This suggests that mGH-Gly118Arg has the potential of reducing GH-induced STAT5 signalling though further repeats are required to confirm this conclusion.

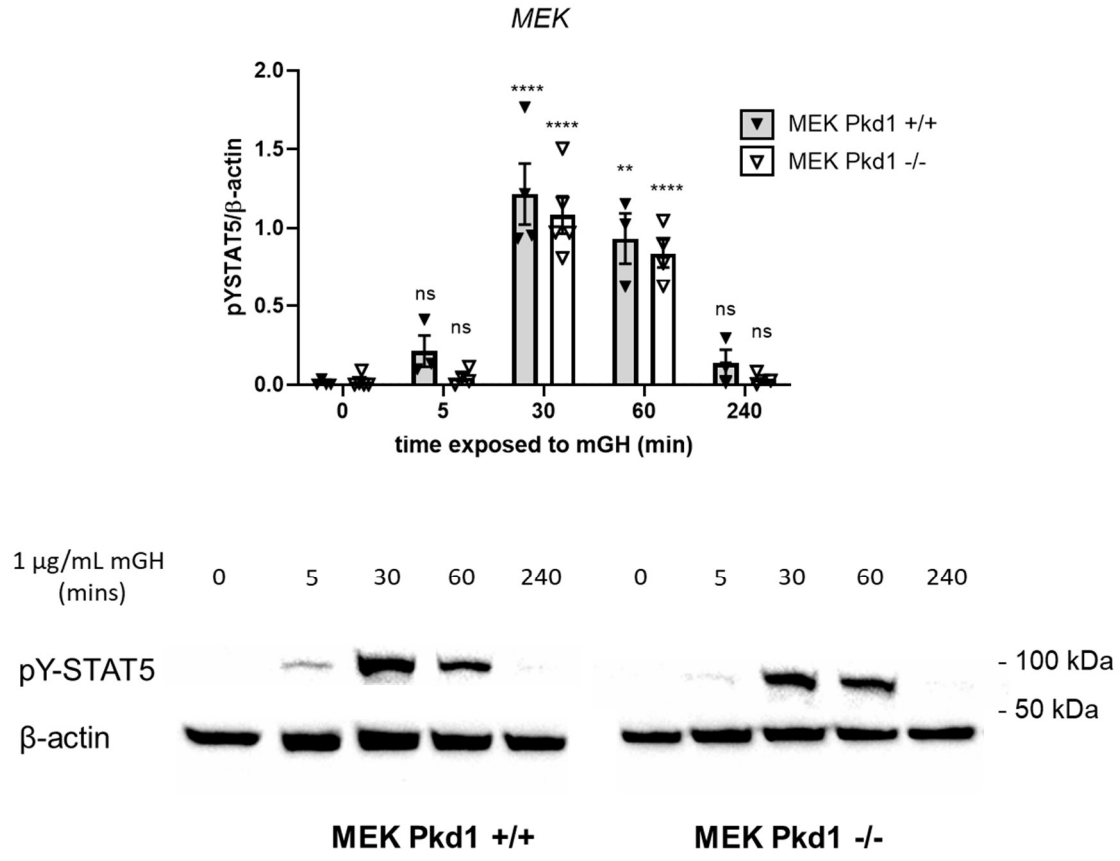

Figure 3.14 Bioactivity of mGH-WT in MEK Pkd1 +/+ and MEK Pkd1 -/- cells

Laboratory-purified mGH-WT was able to significantly increase STAT5 activity compared to unstimulated control. A dose of 1 µg/mL mGH-WT was tested at four timepoints to find the optimal time for mGH-induced STAT5 activity (5, 30, 60 and 240 minutes). Significant increase in STAT5 activity was observed at 30 and 60 minutes of mGH stimulation compared to unstimulated control (0 minutes). A one-way ANOVA test with a post-hoc Bonferroni correction for multiple comparison was used to determine statistical significance, indicated by asterisks. N=3 (biological repeats. Mean ±SEM is plotted. ns = not significant, ** P<0.01, *** P<0.001, **** P<0.0001.

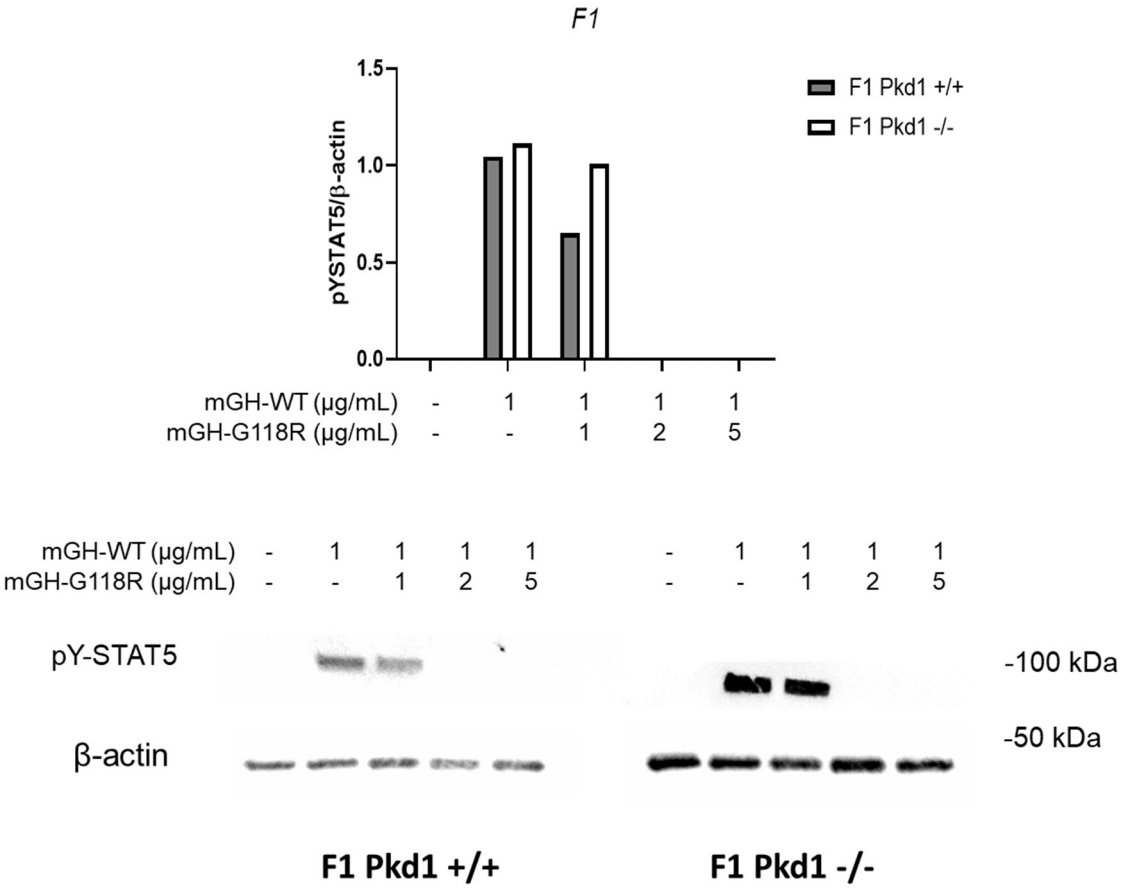

Figure 3.15 Inhibition activity of mGH-Gly118Arg mouse growth hormone receptor antagonist in F1 Pkd1 +/+ and F1 Pkd1 -/- cells

Laboratory-purified mGH-Gly118Arg appears to reduce STAT5 activity at a dose of 2- and 5-fold the amount of mGH-WT added, though a 1:1 ratio of the WT:Gly118Arg mGH only minimally reduces STAT5 activity shown as phosphotyrosine STAT5 (pY-STAT5) in the western blot.

3.6 Cloning, expression, and purification of mouse growth hormone fusion proteins

The purpose of producing a mouse growth hormone fusion protein (mGH linked to a portion of the GH receptor) was to (i) overcome potential issue of instability and degradation facing the mGH-Gly118Arg as fusion protein can improve biophysical stability (Hellebust et al., 1989) (ii) prevent clearance of the growth hormone to take forward for *in vivo* work in order to prolong efficacy and reduce the required amount of doses for effective GHR antagonism.

Mouse growth hormone was fused to the extracellular region of the mouse growth hormone receptor (mGHR) also known as the mGH binding protein (mGHBP) via a flexible Gly_4Ser linker from the C-terminus of the mGH to the N-terminus of the mGHBP. The mGH-WT and mGH-Gly118Arg were fused to the mGHBP to produce mGH-Gly118Arg fusion protein (mGH-Gly118Arg fus) through overlap extension using a gene strand of the mGHBP and the pCEP4 mGH plasmids (Figure 3.16).

The restriction enzymes KpnI and HindIII were used to restriction digest pCEP4 mGH-WT as I did not have the empty pCEP4 vector, in order to excise the mGH-WT and insert the mGH-Gly118Arg-mGHBP fusion protein which was restriction digested with the same enzymes (Figure 3.17). The digested pCEP4 and mGH-Gly118Arg-mGHBP were ligated using a T4 ligase system, transformed into XL1 blue *E. coli* and plated onto LB agar plates containing ampicillin, alongside a ligation negative control. Colonies that grew on the ligation test plate were selected, cultured and the DNA obtained through a miniprep kit for sequencing. The correct sequence for the mGH-Gly118Arg-mGHBP fusion protein

was obtained, as confirmed by DNA sequencing, thus the pCEP4 fusion plasmid was carried forward for expression.

Expression in HEK293T was performed for the mGH-Gly118Arg fusion protein as had been performed previously for the other mGH analogues. Expression was assessed using western blot for the hexahistidine tag and compared to un-transfected (UT) control. The media of the transfected cells displayed a band for 6xHis at ~54 kDa, which is the expected band size of the mGH-Gly118Arg fusion protein (Figure 3.18 A).

The culture supernatant containing the 54 kDa protein indicated that the mGH-Gly118Arg fusion protein was purified using nickel chelate chromatography. The fractions were initially run on a Coomassie gel to see if 54 kDa band protein was present, however a thick band between 50-75 kDa present in the media which is likely a component of the media/FBS (Supplemental figure 1) was obfuscating potential target protein (Figure 3.18 B). Thus, the fractions collected from the nickel chelate column were run in a western blot for the hexahistidine tag which showed that ~54 kDa protein was present in eluted fractions 1-4, mostly strongly in eluted fraction 3. The hGH-WT 6xHis was used as a positive control for the 6xHis antibody. The eluted fractions were pooled, though when attempting to concentrate and quantify the target protein, when adjusted for the media components the levels of target protein were very low at 0.44 µg/mL so protein may have been lost in the concentration process.

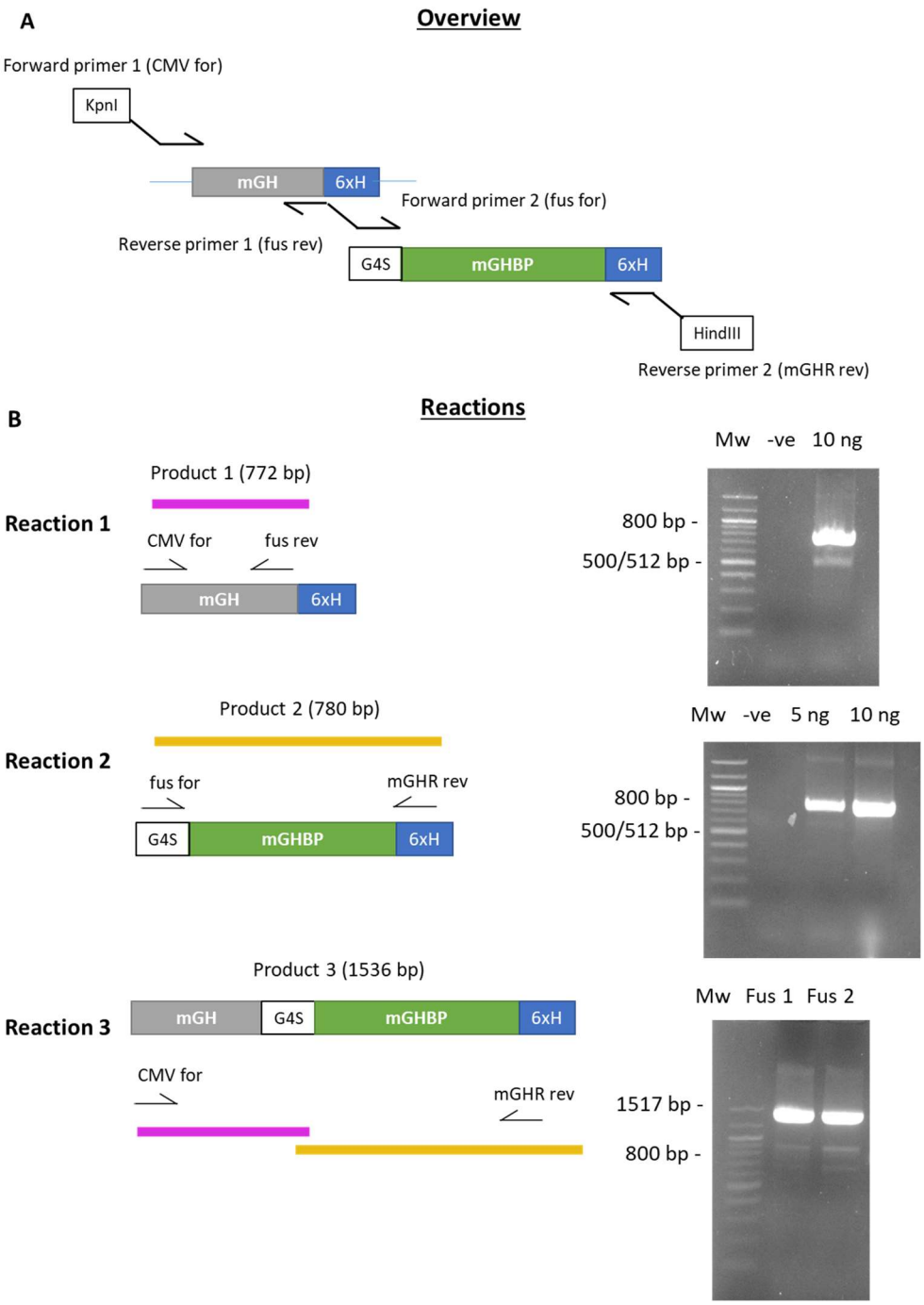

Figure 3.16 Splicing by overlap extension of the mGH-mGHBP fusion proteins

A fusion protein of mGH Gly118Arg-mGHBP connected by a Gly_4Ser linker was produced from a mGHBP gene strand and pCEP4 mGH (A). (B) Three PCR reactions were preformed to produce the mGH-mGHBP fusion protein (Fus).

Figure 3.17 Restriction digest of pCEP4 and mGH-mGHBP with KpnI and HindIII

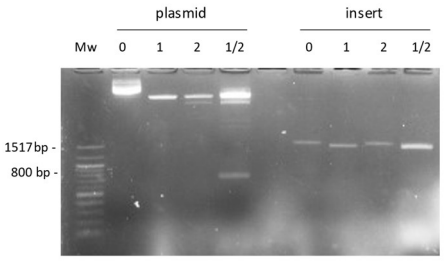

The plasmid pCEP4 mGH-WT (plasmid) and mGH-mGHBP (insert) were restriction digested with KpnI (1) and HindIII (2), an uncut negative control (0) was used with no restriction enzymes.

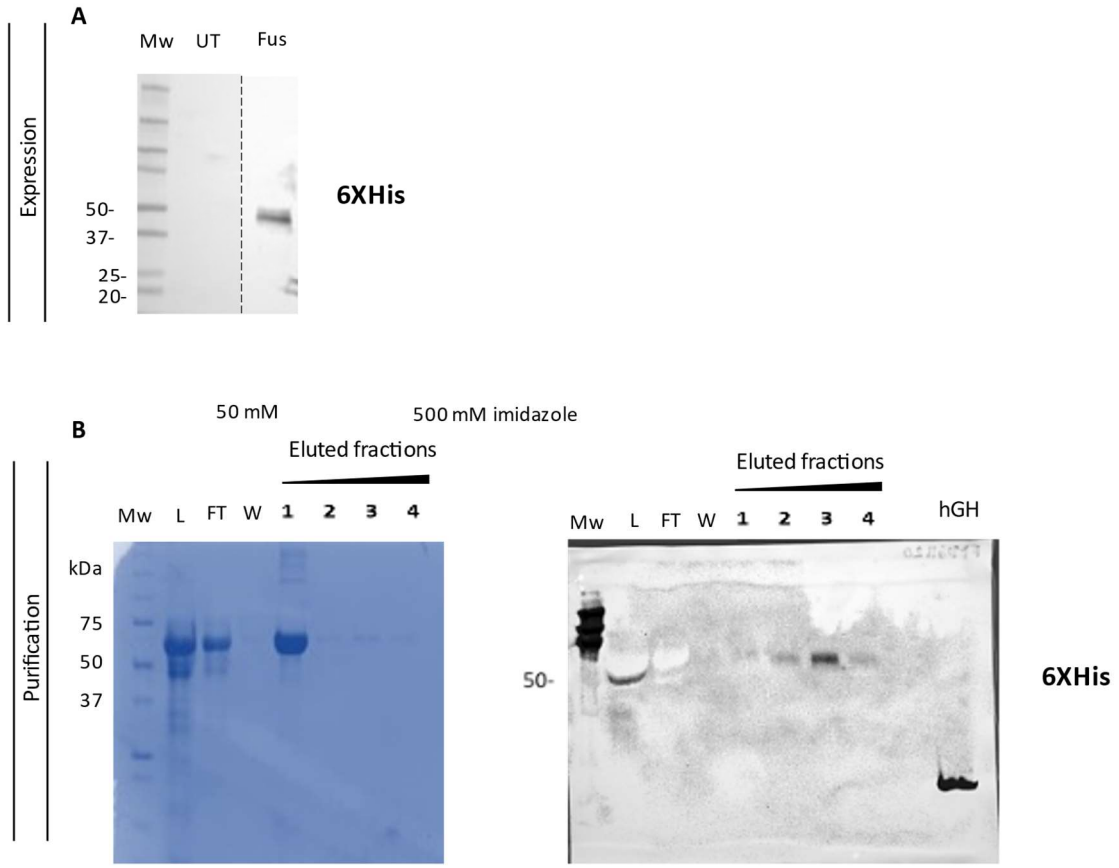

Figure 3.18 Expression and purification of mGH-Gly118Arg-mGHBP fusion proteins

(A) pCEP4 mGH-Gly118Arg mGHBP 6xHis fusion protein (Fus) was expressed in HEK293T and compared to an untransfected control (UT) in a western blot for the 6xHis tag which showed a band at ~54 kDa, the expected band size of the fusion protein. The dotted line denotes removal of unrelated lanes from the image on the blot to place the relevant lanes next to the Mw ladder (B) The fusion protein was run across a nickel chelate column and assessed with Coomassie on the left and a western blot for the 6xHis tag on the right which shows ~54 kDa bands in the eluted fractions 1-4.

3.7 Discussion

3.7.1 Human growth hormone analogues

3.7.1.1 Expression and purification

Human wild-type growth hormone and mutant antagonists (hGH-Gly120Arg and hGH-m12) were successfully expressed and purified from *E. coli* using a T7 induction system in the pET21a+ plasmid (Figures 3.1-3.2). In the T7 induction system the lac repressor (LacI) binds to the lac operon (LacO) in the absence of lactose/IPTG which is adjacent to the T7 promoter, preventing binding of the T7 RNA polymerase to the promoter and expression of the gene of interest. Plasmids containing the T7 promoter require T7 RNA polymerase for transcription, present in BL21 (DE3) cells, the inducible chromosomal gene for the T7 RNA polymerase driven by the *lac*UV5 promoter (Dubendorff and Studier, 1991). This is consistent with previously published work that has shown that other researchers were also able to produce active recombinant human growth hormone in *E. coli* successfully (Olson et al., 1981, Goeddel et al., 1979) . Goeddel *et al*. produced hGH from *E. coli* using the pGH6 plasmid containing two *lac*UV5 promoters in *E. coli* x1776.

A difference in the approach used in this project is that nickel chelate chromatography was performed for purification taking advantage of the fact that the proteins are hexahistidine-tagged. Whereas Olson *et al*. performed initial purification steps employing polyethyleneimine to remove nuclear and membrane components and protein purification with ammonium sulphate precipitation to fractionate proteins and subsequent gel filtration purification.

3.7.1.2 Validation of bioactivity

Multiple studies have demonstrated that STAT5 becomes transcriptionally 'activated' when cells that possess the GHR are stimulated with GH (Waxman et al., 1995, Wood et al., 1995, Chow et al., 1996). The response of STAT5 activity to growth hormone is of particular interest due to STAT5 being the primary contributor in regulating many of the functions of growth hormone relating to growth and metabolism (Herrington et al., 2000), GH modulation of STAT5 signalling is also of particular relevance to this project because of involvement of STAT5 signalling in ADPKD models indicated by Fragiadaki *et al*. (Fragiadaki et al., 2017).

The hGH-WT potently activated STAT5 in HEK293-GHR cells displayed by strong pY-STAT5 and increased STAT5 transcriptional activity (Figure 3.5). Both GHAs hGH-Gly120Arg and hGH-m12 significantly reduced GH-induced STAT5 activity in all doses tested from 0.5-fold – 10-fold the dose of hGH applied (Figure 3.6). The hGH-m12 more potently inhibits STAT5 activity compared to hGH-Gly120Arg due to higher binding affinity from additional mutations in receptor binding site 1 (H18D, H21N, R167N, K168A, D171S, K172R, E174S and I179T) (Figure 3.5 C).

The dose range tested (50 -500 ng/mL) was selected based on previous *in vitro* hGH-stimulation experiments for STAT activation performed by other research groups (Han et al., 1996, Smit et al., 1996) and the time range (15, 30, 45 minutes) was selected based on oncostatin-M (OSM) optimal time (15 min) for STAT5 activity (Hintzen et al., 2008).

The relevance of the doses of hGH tested in the cellular model versus what cells within tissues of a whole organism exposed to physiological levels of hGH is difficult to compare. A number of factors affect physiological circulating levels of hGH including age, sex and

the time at which hGH is measured due to pulsatile secretion (see section 1.5.2). There is also the additional factor to consider of elevated growth hormone levels in ADPKD as observed in a murine ADPKD mouse model (Fragiadaki et al., 2017), which may raise growth hormone levels above the normal physiological range. This highlights one limitation in translating between *in vitro* and *in vivo* models.

3.7.2 Mouse growth hormone analogues

3.7.2.1 Expression and purification

The initial approach to produce mouse growth hormone was to use the same method as the one used to produce human growth hormone, in *E. coli* under a lactose-inducible promoter (Figures 3.7-3.10). One of the challenges was to produce soluble recombinant mouse growth hormone in *E. coli*. There are two potential ways to obtain soluble, active protein which are 1) Denature the protein with a chaotrope and refold the protein into a soluble conformation. The limitation of this method is there is little to no control over how the proteins refold, and no guarantee of obtaining biologically active product using the methods tested thus far. Alternatively, 2) Express the protein in an already soluble conformation. The rmGH was highly expressed in *E. coli* as evidence by thick 22 kDa bands in induced cultures but the protein was in inclusion bodies. The protein was denatured in urea which was improved by increasing the pH as previously demonstrated for rhGH (Sonoda and Sugimura, 2008). Multiple methods of refolding denatured mGH were attempted, however during attempts to refold solubilised mGH, protein would precipitate out of solution. Fradkin *et al*. reported expression of rmGH in *E. coli* produced largely insoluble aggregates, which is concordant with what was observed during my own expression of rmGH. This group achieved successful solubilisation and refolding by

using a high hydrostatic pressure system which has been previously described (Crisman and Randolph, 2009, Fradkin et al., 2010). High-pressure technology reportedly favours refolding of inclusion bodies, though the expense and availability of this technology presents a limitation to employing the use of this method in my own work.

Successful expression of soluble mouse growth hormone analogues was achieved using a transient mammalian expression system in HEK293T cells with the pCEP4 plasmid containing the CMV promoter (Figure 3.11). Whilst prokaryotic expression systems have multiple advantages such as high protein yield and lower cost of reagents, there is also the disadvantage of endotoxin contamination within purified samples that has the potential to cause inflammatory host responses. Mammalian expression has the benefit over bacterial expression in allowing for post-translational modifications which can include removal of the start codon methionine, and reduction or formation of disulphide bonds. This helps to promote proper protein refolding and solubility, so can be beneficial when struggling with obtaining soluble protein from bacterial expression systems.

Low level expression of the mGH-Gly118Arg fusion protein was achieved (Figure 3.18). Fusing the GH to the GHBP has previously shown to protect GH from clearance and degradation, after a single injection in rats human GH fusion protein is still detectable after 8 days versus 6 hours for hGH (Wilkinson *et al*., 2007). The fusion protein was subcloned and produced with future *in vivo* experiments in mind, to allow for longer periods of GHR antagonism from single injections due to reduced clearance. However, only low levels were produced using the pCEP4 HEK293T system so could not be taken forward for testing. The issues faced with expressing larger quantities of the mGH-Gly118Arg and the mGH-Gly118Arg fusion protein could be due to instability of the

protein, or potential cytotoxicity. As a potential future direction for production of mGHR antagonists, alternative expression methods could be tried. Though here only bacterial and mammalian expression systems were tested for the mouse growth hormone analogues, there are alternative eukaryotic expression systems such as insect and yeast. There are also alternative mammalian expression systems that could be tested such as Chinese Hamster Ovary (CHO) cells, different plasmids and promoter systems, or also stable transfections instead of transient transfection for expression. As well as optimising the expression system, alterations to the construct itself could potentially improve stability and protein yield, such as removal of the hexahistidine tag (Booth et al., 2018), or potentially an alternative amino acid mutation to arginine that would still disrupt receptor binding site 2 and prevent signal transduction.

3.7.2.2 Validation of bioactivity

The laboratory-purified mGH-WT was able to induce phosphoactivation of STAT5 in mouse embryonic kidney cells (MEK), in both Pkd1 WT (+/+) and isogenic Pkd1 null (-/-) cells (Figure 3.14), suggesting proper refolding and bioactivity of the mGH-WT and also highlighting successful modulation of STAT5 activity in an ADPKD model. Higher quantities of mGH-WT were required to induce STAT5 activity in MEK cells (1 µg/mL) compared to hGH-WT inducing STAT5 activity in HEK293-GHR cells (100 ng/mL) which is likely because of lower GHR expression, wherein HEK293-GHR cells overexpress the GHR so are more GH-responsive.

A limitation in drawing conclusions from the testing of mGH-Gly118Arg inhibition of GH-induced STAT5 activation was the quantity of mGH-G18R yielded limited the number of repeats able to be performed in the testing. Thus, although mGH-Gly118Arg appears to

reduce mGH-induced STAT5 activation when applied at ≥2-fold the dose of mGH-WT (Figure 3.15), robust conclusions cannot be made from a single experiment. Further repeats are required for statistical significance.

3.7.3 Conclusion

In this chapter it has been demonstrated that recombinant human growth hormone (hGH-WT) and mutant human growth hormone receptor antagonists (hGH-Gly120Arg and hGH-m12), as well as mouse growth hormone (mGH-WT) and mouse growth hormone receptor antagonist (mGH-Gly118Arg) have been successfully expressed and purified and are capable of modulating STAT5 activity in kidney cells.

3.8 Supplemental figures

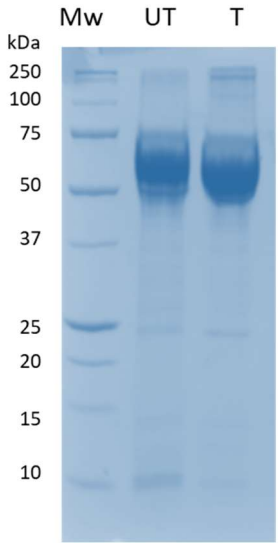

Supplemental figure 1 Untransfected HEK293T media negative control (UT) compared to mGH-Gly118Arg-transfected HEK293T media (T), both containing 10% FBS.

Chapter 4: The effects of stimulation and inhibition of growth hormone signalling in *in vitro* models of ADPKD

4.1 Introduction

In this chapter the impact of stimulation and inhibition of growth hormone-STAT5 signalling within the context of ADPKD will be explored using cellular models of disease to assess STAT5 signalling, proliferation and cystic growth.

Growth hormone levels have been shown to be elevated in a mouse model of ADPKD, alongside nuclear STAT5 expression, suggesting phosphoactivation, nuclear translocation and ultimately STAT5 transcriptional activity (Fragiadaki et al., 2017). Fragiadaki *et al*. have demonstrated that silencing of STAT5 in human cyst-derived cells OX161c1 and SKI-001 prevents proliferation without impacting apoptosis, indicating a role for STAT5 signalling in proliferation in ADPKD. Patera *et al*. observed that JAK2 expression is higher in polycystic kidneys compared to wild-type kidneys (Patera et al., 2019), which is of interest as JAK2 is the key mediator of signal transduction from GH-GHR that activates STAT5. This work provided the basis for the experiments performed in this chapter to discern the impact of growth hormone signalling via STAT5 on proliferation and cystogenesis in cellular models of ADPKD, and whether inhibition of this pathway can impede proliferation and cystic growth.

4.1.1 Aims

The aim of this chapter was to use in vitro cellular models of ADPKD (SKI-001, OX161c1, F1 Pkd1 -/- and isogenic WT control F1 Pkd1 +/+) to examine how these cells respond to stimulation with growth hormone and inhibition of growth hormone signalling with growth hormone receptor antagonism or JAK inhibition with Ruxolitinib (Figure 4.1). The impact of GH signalling stimulation and inhibition on STAT5 phosphoactivation, expression of STAT5 targets, proliferation and cystogenesis will be analysed.

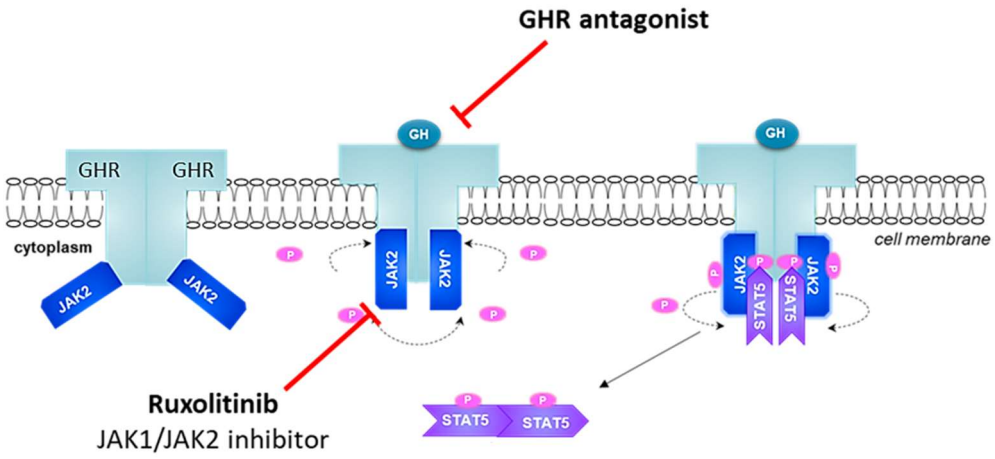

Figure 4.1 Inhibition of growth hormone signalling with a GHR antagonist or JAK inhibitor Ruxolitinib

4.2 Inhibition of growth hormone-induced STAT5 signalling in *in vitro* models of PKD

Since the solubility, identity and bioactivity of the laboratory-purified human growth hormone analogues has been confirmed, the next step was to examine whether the hGH

analogues were capable of modulating STAT5 activity in relevant cellular models of ADPKD.

Initially, to demonstrate presence of the GHR and thus ability to respond to GH in an *in vitro* model of PKD, GHR was assessed in immortalised human ADPKD-derived renal epithelial cells SKI-001 through immunofluorescent staining. Green fluorescence in GHR-stained cells demonstrates the presence of the GHR indicating their ability to respond to growth hormone (Figure 4.2 B). IgG controls were used to control for nonselectivity of the GHR antibody, the IgG controls displayed no green fluorescence which suggests the green fluorescence seen in the GHR-stained cells is for the GHR and not due to non-selective staining. These findings are consistent with GHR staining previously described to be present in the kidney, predominantly in the tubular regions (https://www.proteinatlas.org/ENSG00000112964-GHR/tissue/kidney, July 2021).

Since the ability of hGH-WT and of GHR antagonists to stimulate and inhibit GH-induced STAT5 activity respectively was established in renal cells overexpressing GHR (HEK293-GHR), the hGH analogues were then tested in SKI-001 as a relevant *in vitro* model of ADPKD. STAT5 activity was induced in response to stimulation with growth hormone in SKI-001, with the pYSTAT5 bands appearing with 30 minutes stimulation with 100 ng/mL hGH. When the hGHR antagonist (GHA) hGH-m12 is added at a 1:1 ratio with hGH the STAT5 activity is reduced to approximately a third of the activity observed with hGH-WT (Figure 4.2). These results demonstrate that SKI-001 are responsive to growth hormone and STAT5 is successfully activated, and that the hGHR antagonist effectively abrogates this STAT5 activity in human cystic renal epithelial cells. However, after initial successful results, pYSTAT5 was unable to be detected in subsequent experiments, despite the fact

that the experiment was working as indicated by a strong positive phospho-tyrosine STAT5 band in positive control SKI-001 cells (i.e. SKI-001 cells treated with 20ng/ml of oncostatin M).

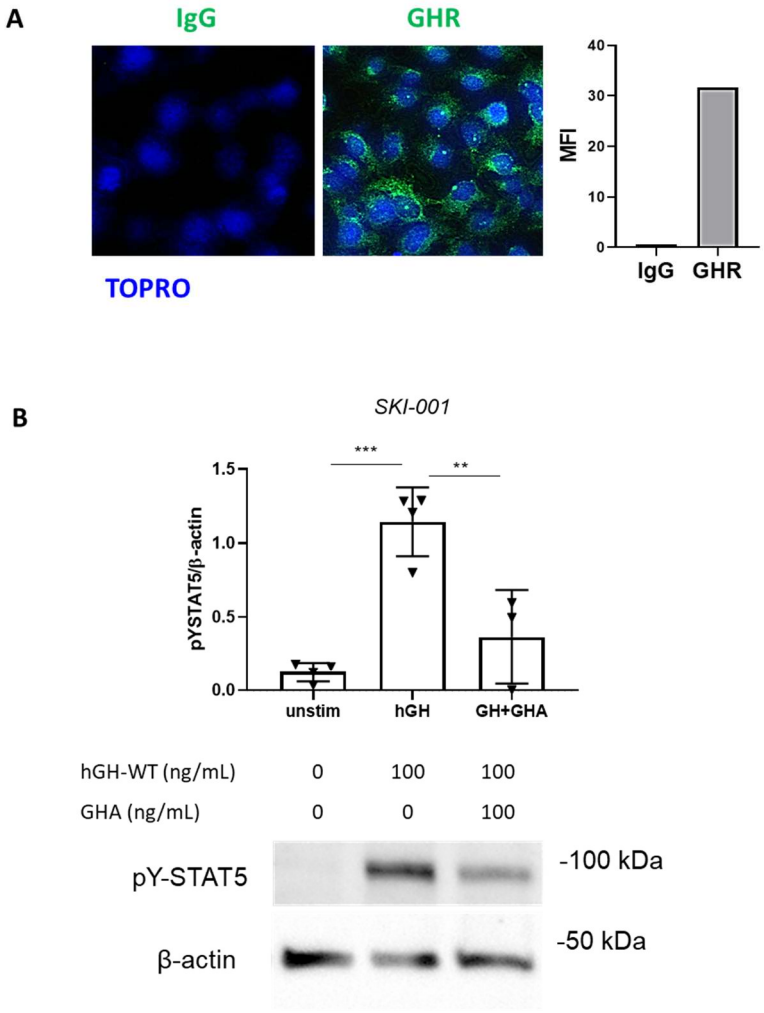

Figure 4.2 SKI-001 STAT5 activity in response to stimulation with hGH-WT and inhibition with GHR antagonist (GHA)

(A) Images of cells stained with either IgG or GHR (green) and nuclear TOPRO staining (blue) at 63X magnification demonstrate the presence of GHR in SKI-001. (B) hGH-WT induces phosphoactivation of STAT5 in SKI-001 when applied for 30 minutes at a dose of 100 ng/mL and the GHA (hGH-m12) reduces STAT5 activity when applied at 100 ng/mL. A one-way ANOVA test with a post-hoc Bonferroni correction for multiple comparison was used to determine statistical significance, indicated by asterisks. N=4 biological repeats. Mean ±SEM is plotted. ns = not significant, ** P<0.01, *** P<0.001.

As there were limited levels of mouse growth hormone receptor antagonist, an alternative method of inhibition of growth hormone-STAT5 signalling was explored with the use of the small molecule and selective JAK1/JAK2 inhibitor Ruxolitinib. Commercial mouse growth hormone was used as there was limited amounts of the laboratory-purified mGH-WT. First the ability of Ruxolitinib to modulate STAT5 activation was tested in HEK293-GHR as proof of concept and to demonstrate the ability of Ruxolitinib to inhibit JAK signalling in a human cellular kidney model. Ruxolitinib was tested at three different concentrations (0.1 µM , 1 µM and 10 µM) applied simultaneously with 100 ng/mL hGH-WT for 30 minutes (Figure 4.3 A). The concentration range of 0.1-10 µM was selected as it corresponds to serum levels of patients treated with Ruxolitinib for myelofibrosis (Heine et al., 2013). The pYSTAT5 bands disappeared at all concentrations of Ruxolitinib tested suggesting that JAK inhibition successfully inhibits GH-induced phosphoactivation of STAT5.

Then, Ruxolitinib was tested in the murine F1 Pkd1 +/+ and F1 Pkd1 -/- cells at the lower concentration of 0.1 µM looking at STAT5 activity using western blot for phosphotyrosine STAT5. In both F1 Pkd1 +/+ and F1 Pkd1 -/- 1 µg/mL mGH significantly increases STAT5 activation shown as stronger pYSTAT5 bands compared to control as expected based on what was observed in MEK cells. Ruxolitinib reduces mGH-induced phosphoactivation of STAT5 at 0.1 µM by ~60%, though only to a statistically significant degree in the F1 Pkd1 -/- (Figure 4.3 B). The difference in GH-induced pYSTAT5 reduction in response to 0.1 µM Ruxolitinib in the F1 cells with a moderate reduction in pYSTAT5 versus the HEK293-GHR cells where pYSTAT5 appears completely suppressed is likely due to the amount of GH initially added wherein the HEK293-GHR cells were exposed to

100 ng/mL hGH whereas the F1 cells were exposed to 1 µg/mL mGH. For this reason, a dose of 1 µM Ruxolitinib was carried forward for the cyst assay experiments in F1 cells to ensure further reduction of STAT5 activity. Together this data demonstrates the ability of Ruxolitinib to inhibit growth hormone-induced phosphoactivation of STAT5 in a cellular model of ADPKD.

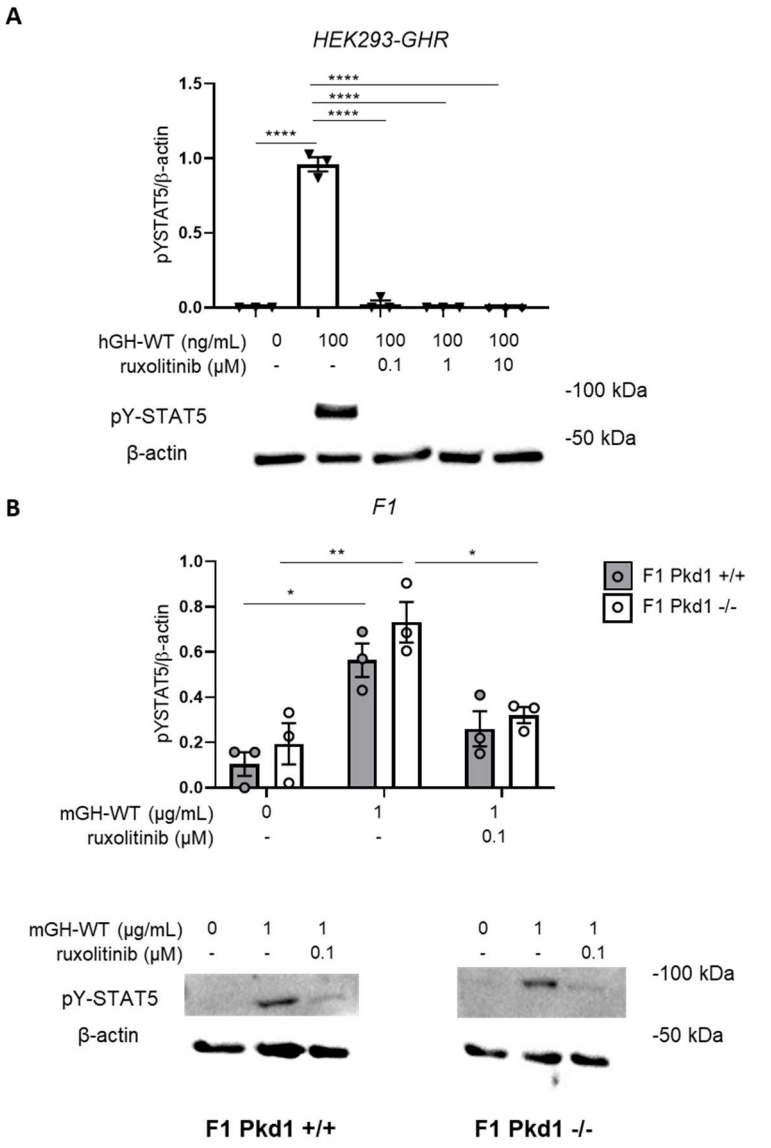

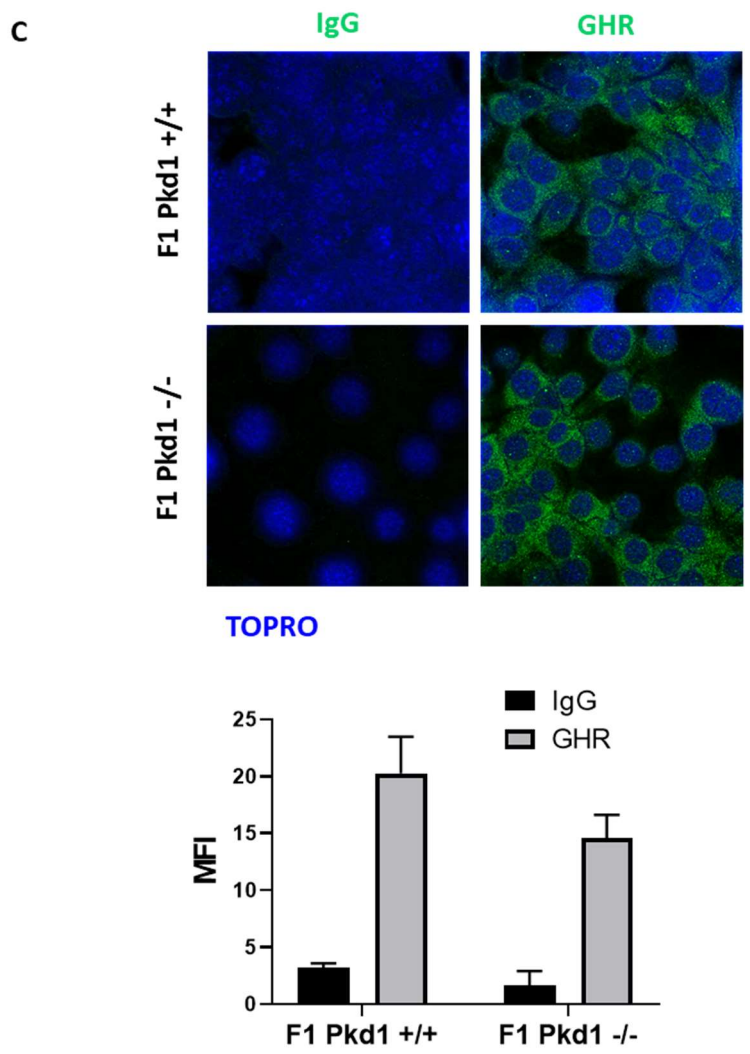

Figure 4.3 Ruxolitinib inhibits growth hormone-stimulated STAT5 activity

(A) In HEK293-GHR Ruxolitinib abrogates hGH-induced pYSTAT5 at the three concentrations tested. (B) In both F1 Pkd1 +/+ and F1 Pkd1 -/- cells 0.1 µM Ruxolitinib reduces pYSTAT5 band intensity compared to cells only stimulated with mGH. A one-way ANOVA test with a post-hoc Bonferroni correction for multiple comparison for A and a two-way ANOVA test with a post-hoc Bonferroni correction for B was used to determine statistical significance, indicated by asterisks. N=3 biological repeats. Mean ±SEM is plotted. * P<0.05, ** P<0.01, **** P<0.0001. (C) Images of cells stained with either IgG or GHR (green) and nuclear TOPRO staining (blue) at 63X magnification demonstrate expression of GHR in F1 Pkd1 +/+ and F1 Pkd1 -/- cells.

4.3 Growth hormone enhances cystogenesis in *in vitro* PKD models which is abrogated by GH-GHR-JAK2-STAT5 inhibition

To assess the potential biological function of GH in disease relevant human ADPKD *in vitro* models cystogenesis assays were employed as has been previously described.

The three-dimensional (3D) cyst assay was used to assess the growth of cysts in response to modulation of growth hormone signalling (Mangookarim et al., 1989). 3D cyst assays offer the advantage of more closely resembling the *in vivo* environment. Matrigel, comprised of basement membrane and extracellular matrix proteins allow the cystic cells to grow into cysts rather than as a 2D monolayer.

To determine whether modulation of growth hormone signalling affects cyst expansion, *in vitro* PKD monocultures were analysed with a 3D cyst assay and assessed cystic growth by measuring cyst diameter over time. Multiple cell lines were employed to ensure robustness of the observed effects, namely the human derived cystic SKI-001 and OX161c1 cells, and the murine isogenic F1 Pkd1 +/+ and F1 Pkd1 -/- cells. Each independent cell line was able to form cysts and successfully grow over time, with untreated cysts significantly increasing in each cell line compared to Day 0. Cysts were measured up to day 12 in all cell types, however by day 12 cysts started to regress and in some cases the cells started to undergo apoptosis, with the typical apoptotic morphological appearance due to shrinkage, fragmentation and blebbing. This occurred more so with OX161c1 cells by this timepoint, although did also occur with later passages of SKI-001 that were used. For this reason, cystic growth is only presented up to day 9.

The SKI-001 and OX161c1 human cystic cells were treated (i) vehicle unstimulated control, (ii) 500 ng/mL hGH-WT, (iii) 500 ng/mL hGH-WT plus 2.5 µg/mL hGH-m12 (GHA 5X), (iv) 500 ng/mL hGH-WT plus 1 µM Ruxolitinib, (v) 1 µM Ruxolitinib only. The treatment group of 1 µM Ruxolitinib on its own without the hGH-WT was performed to assess whether this concentration of Ruxolitinib could impact cystic growth compared to unstimulated controls in the absence of hGH-WT. Images were taken every 3 days alongside media change with fresh treatments.

In both SKI-001 and OX161c1, treatment with recombinant human growth hormone promoted cystic growth compared to untreated controls (Figure 4.4 - 4.5). In human cystic cells treated with human growth hormone there is a clear trend in elevated cystic growth compared to unstimulated controls and cells treated with inhibitors of growth hormone signalling, GHA and Ruxolitinib. The growth hormone-induced cystic growth reaches significance by day 9 in both cell types. Furthermore, when the human growth hormone receptor antagonist (GHA) was added alongside growth hormone treatment, the antagonist prevented the growth hormone-induced cyst expansion, limiting cystic growth to unstimulated levels when applied at five times the amount of the growth hormone. The GHA significantly lowered cyst expansion when compared to growth hormone-treated cysts at day 9. Similarly, the addition of the Ruxolitinib suppressed the cyst expansion stimulated by growth hormone, limiting cystic growth to a significant level at days 9. This was also the case for Ruxolitinib treatment on its own wherein it was significantly lower than hGH-induced cystic growth at day 9 but there were no significant differences between ruxolitnib treatment on its own compared to unstimulated controls and in fact the cysts followed a similar pattern of growth as the treatment group of hGH + Ruxolitinib.

Likewise, the murine cystic models F1 Pkd1 +/+ and F1 Pkd1 -/- were also responsive to growth hormone treatment, whereby mouse growth hormone promoted cyst expansion in both cell lines, showing a clear trend of increased cyst diameter compared to unstimulated controls. Cells treated with Ruxolitinib both in the presence and absence of mGH displayed reduced cystic growth compared to mGH-treated cells (Figure 4.6).

Together this demonstrates that addition of exogenous recombinant growth hormone significantly advances cystic growth in two independent human cystic cell lines and two murine cystic cell lines, and inhibition of growth hormone signalling using growth hormone receptor antagonist or Ruxolitinib, which inhibit at the receptor complex and the JAK kinase levels respectively, abrogates this effect.

Then to test the effects of inhibition of growth hormone signalling through genetic modulation, which was achieved using silencing RNA (siRNA) knockdown to suppress the expression of growth hormone receptor, and STAT5AB in SKI-001 cells.

The efficacy of siRNA in suppressing expression of GHR or STAT5AB was first assessed using qPCR. GHR siRNA (si GHR) reduced GHR expression ~85 % compared to non-targeting siRNA control (siCtrl). STAT5AB siRNA (si STAT5AB) reduced expression of STAT5B and STAT5A ~75 % compared to siCtrl (Figure 4.7 A).

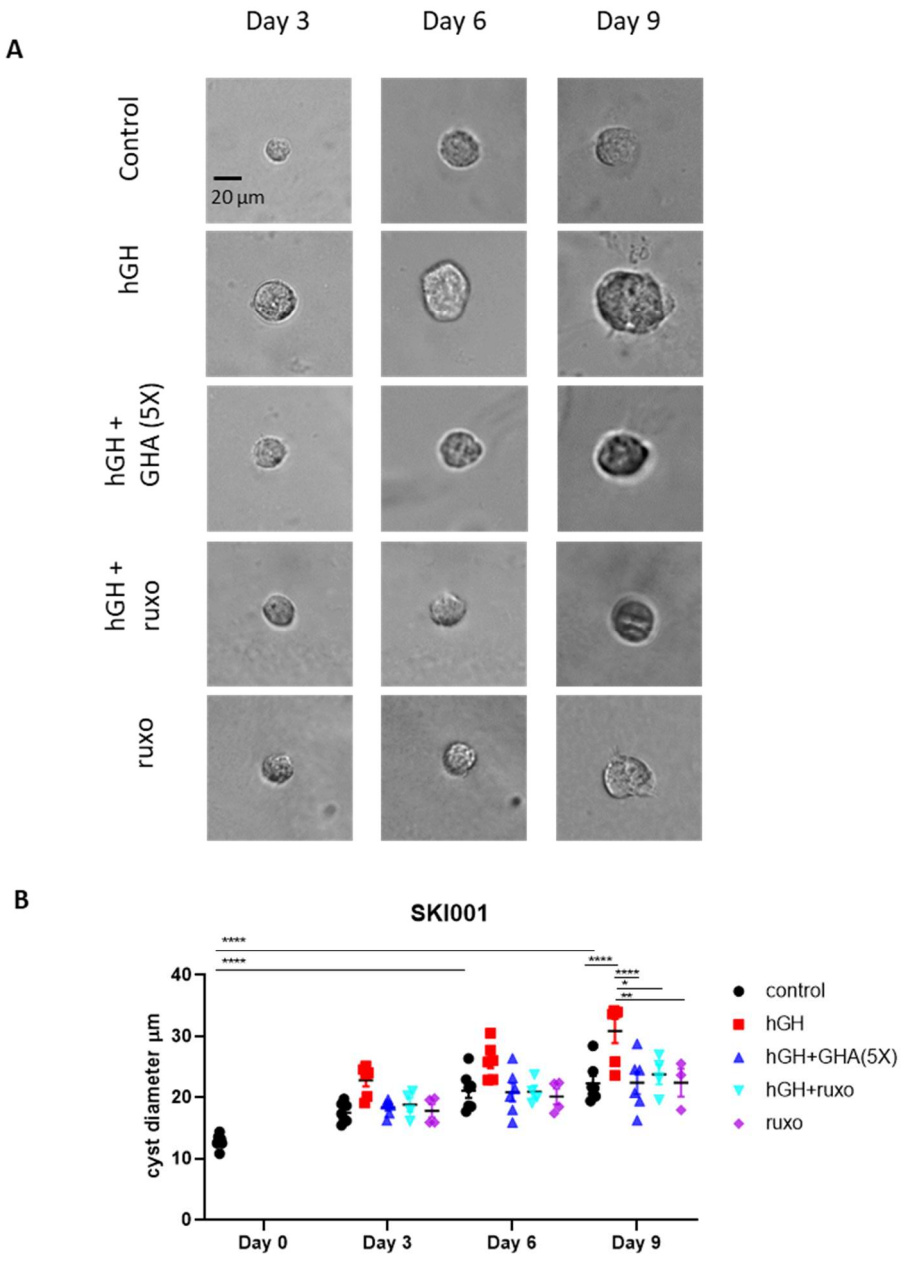

Figure 4.4 SKI-001 cystogenesis in response to growth hormone stimulation and inhibition

(A) Representative images (10X magnification) of SKI-001 cysts taken at day 3, day 6 and day 9 for each treatment group of unstimulated control, 500 ng/mL hGH, 500 ng/mL hGH + 2.5 µg/mL GHA, 500 ng/mL hGH + 1 µM Ruxolitinib, or 1 µM Ruxolitinib. Cyst growth was increased in cells treated with hGH compared to unstimulated control and cells treated with inhibitors. (B) Quantification of cyst growth measured as cyst diameter (µm) over 9 days. Treatment with hGH (red) promoted cyst growth compared to control (black). Cysts treated with additional GHA (blue), Ruxolitinib (cyan) or Ruxolitinib only (purple)

grew at similar levels to the control. A two-way ANOVA test with a post-hoc Bonferroni correction for multiple comparison was used to determine statistical significance, indicated by asterisks. Each plot point represents a biological repeat taken as the mean of means from all cysts measured in that repeat, per replicate n=≥20 cysts. Mean ±SEM is plotted. * P<0.05, ** P<0.01,**** P<0.0001.

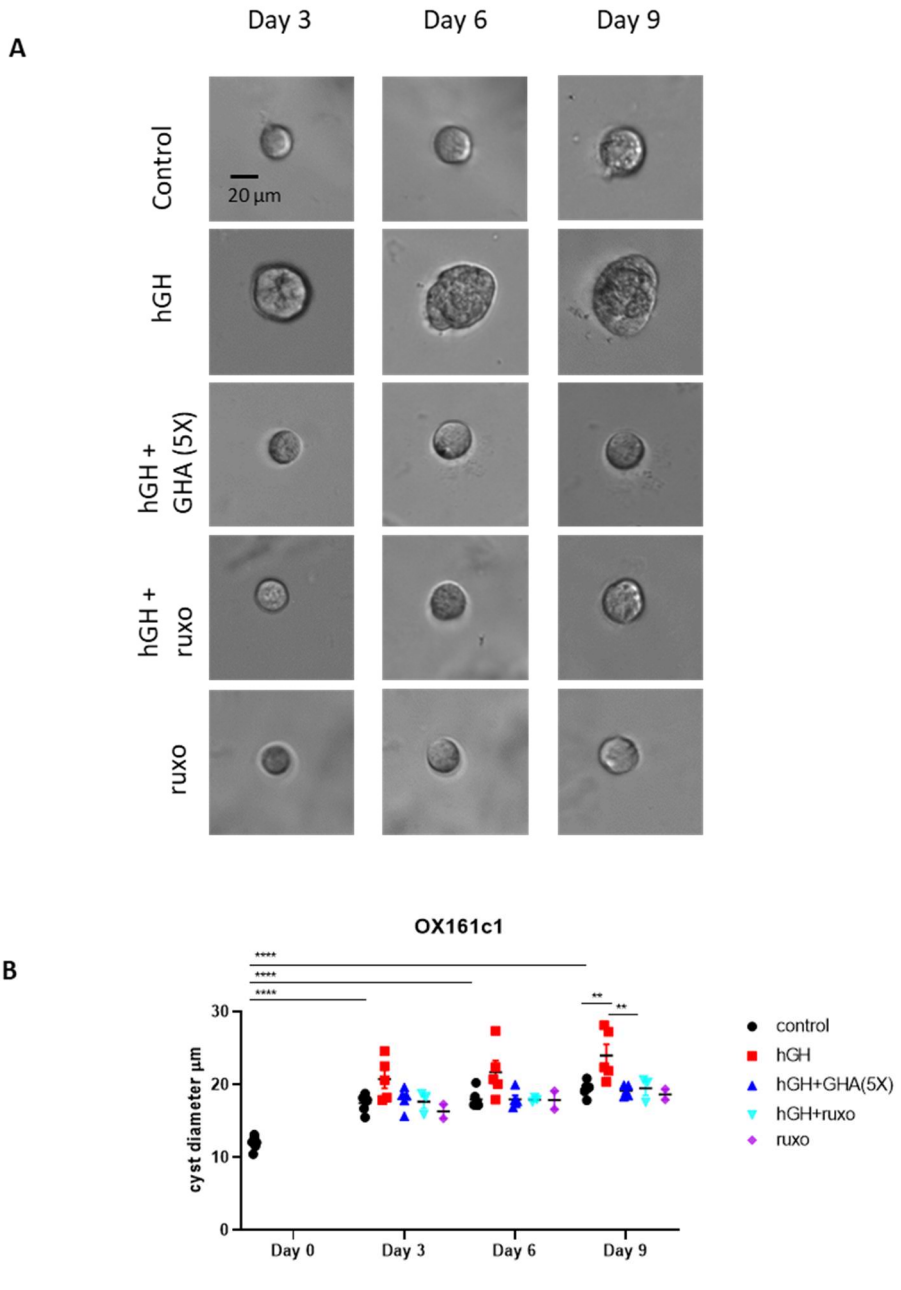

Figure 4.5 OX161c1 cystogenesis in response to growth hormone stimulation and inhibition

(A) Representative images (10X magnification) of OX161c1 cysts taken at day 3, day 6 and day 9 for each treatment group of unstimulated control, 500 ng/mL hGH, 500 ng/mL hGH + 2.5 µg/mL GHA, 500 ng/mL hGH + 1 µM Ruxolitinib, or 1 µM Ruxolitinib. Growth of cysts was increased with hGH stimulation compared to unstimulated control and cells treated with inhibitors. (B) Quantification of cyst growth measured as cyst diameter (µm) over 9 days. Treatment with hGH (red) promoted cyst growth compared to control (black). Treatment with inhibitors GHA (blue), Ruxolitinib (cyan) or Ruxolitinib only (purple) resulted in a similar pattern of cystic growth to control. A two-way ANOVA test with a post-hoc Bonferroni correction for multiple comparison was used to determine statistical significance, indicated by asterisks. Each plot point represents a biological repeat taken as the mean of means from all cysts measured in that repeat, per replicate n=≥20 cysts. Mean ±SEM is plotted. ** P<0.01,**** P<0.0001.

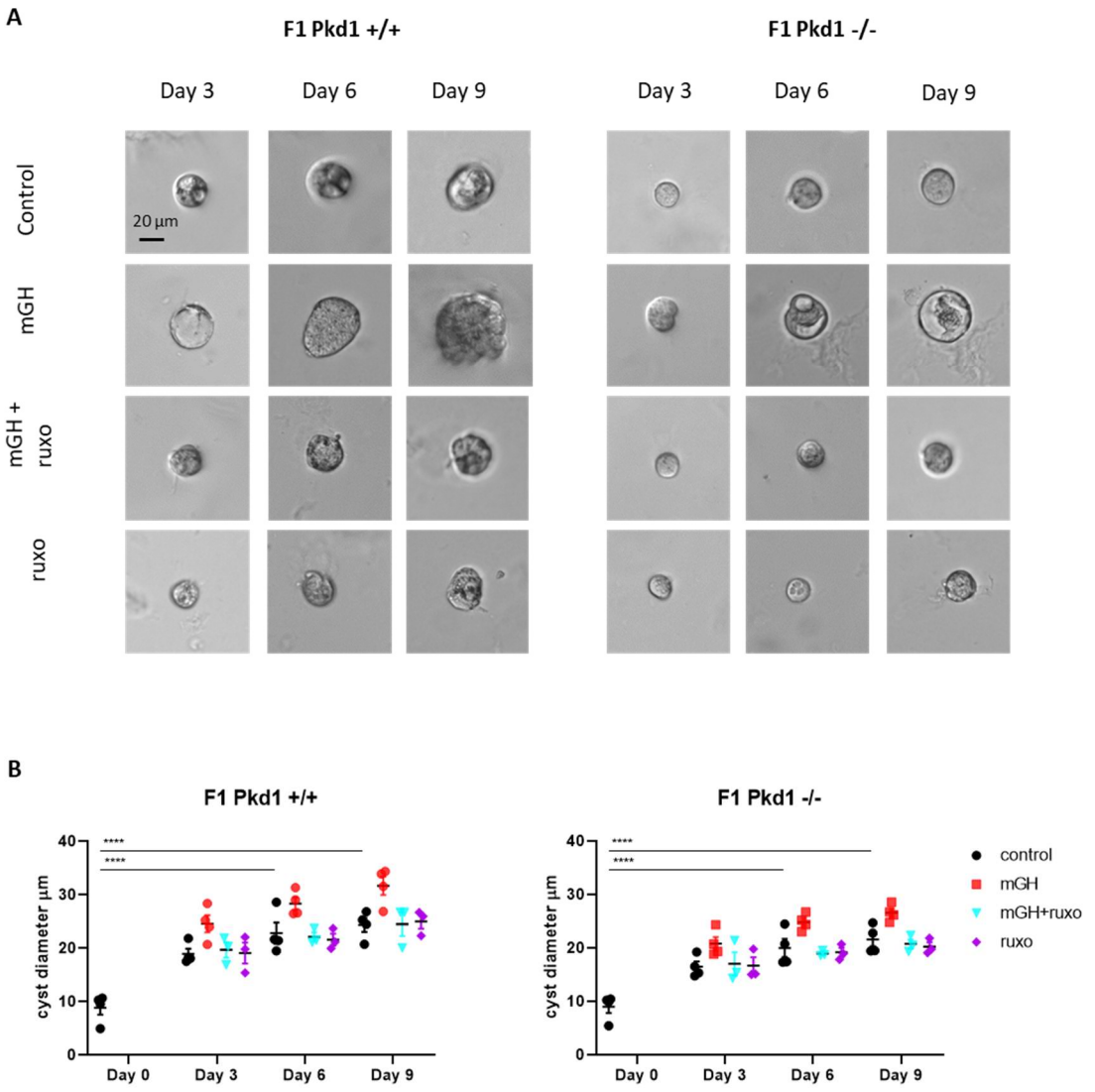

Figure 4.6 Cystogenesis in response to growth hormone stimulation and inhibition in F1 Pkd1 +/+ and F1 Pkd1 -/- cells

(A) Representative images (10X magnification) of F1 Pkd1 +/+ and F1 Pkd1 -/- cysts taken at day 3, day 6 and day 9 for each treatment group of unstimulated control, 1 µg/mL mGH +/- 1 µM Ruxolitinib, or 1 µM Ruxolitinib only. There was a trend of elevated cystic growth with mGH, which was reduced with Ruxolitinib treatment. (B) Quantification of cyst growth measured as cyst diameter (µm) over 9 days. In both cell types mGH (red) promoted cyst growth compared to control (black). Additional Ruxolitinib (cyan) or Ruxolitinib only (purple) prevented mGH-induced cyst growth, with a similar pattern of cystic growth to control. A two-way ANOVA test with a post-hoc Bonferroni correction for multiple comparison was used to determine statistical significance, indicated by

asterisks. Each plot point represents a biological repeat taken as the mean of means from all cysts measured in that repeat, per replicate n=≥20 cysts. Mean ±SEM is plotted.**** P<0.0001.

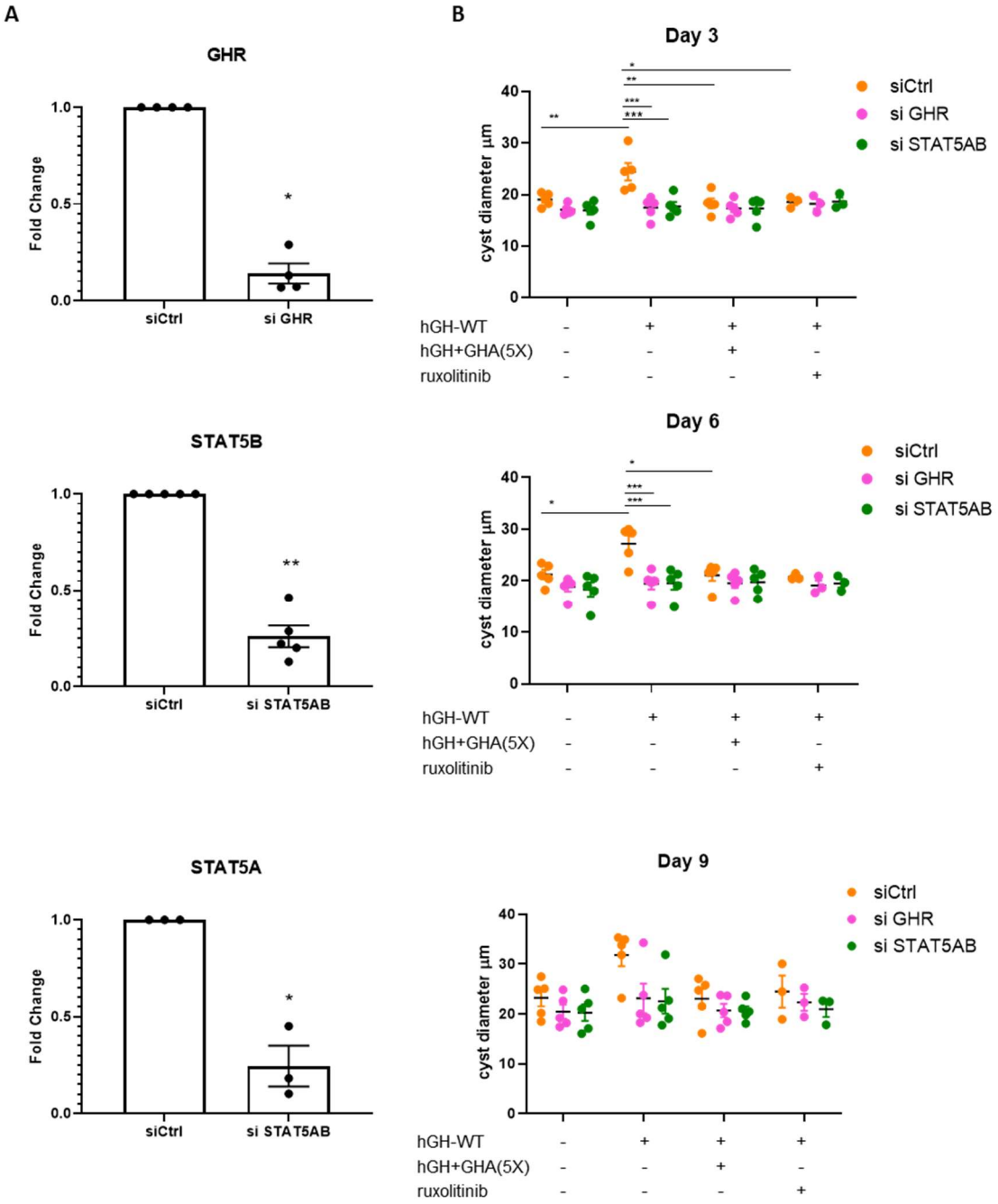

Figure 4.7 Silencing of GHR-STAT5 in SKI-001 reduces cyst growth

(A) The knockdown efficacy of siRNA was confirmed using qPCR to look at fold change differential expression between siCtrl and the si GHR or si STAT5AB. Transfection with si GHR resulted in ~85 % reduction in GHR expression. Transfection with si STAT5AB resulted in ~70-75 % reduction of STAT5A and STAT5B. A one-tailed Mann-Whitney test was used to determine statistical significance. Each plot point represents a biological repeat.

(B) Cyst growth of SKI-001 measured as cyst diameter (μm) at day 3, day 6 and day 9 showed reduced expansion in cells transfected with siRNA for GHR (si GHR, pink) or STAT5AB (si STAT5AB, green) compared to siRNA control (siCtrl, orange) in unstimulated cells and to a significant degree in hGH (500 ng/mL)-treated cells at day 3 and day 6, though this effect is lost by day 9 due to loss of siRNA knockdown. Treatment with inhibitors GHA (2.5 μg/mL) or Ruxolitinib (1 μM) shows the same pattern of cyst growth in siCtrl, si GHR and si STAT5AB. A two-way ANOVA test with a post-hoc Bonferroni correction for multiple comparison was used to determine statistical significance. Each plot point represents a biological repeat taken as the mean of means from all cysts measured in that repeat, per replicate n=≥20 cysts.

Statistical significance is indicated by asterisks. Mean ±SEM is plotted. * P<0.05, ** P<0.01, *** P<0.001.

SKI-001 transfected with siRNA were treated as previously described for up to 9 days. At day 3 and day 6, for SKI-001 cells there was a trend of reduced cystic growth in si GHR and si STAT5AB-transfected cells compared to siCtrl in the unstimulated control group, though this effect was more pronounced and reached statistical significance in the hGH treated group (Figure 4.7 B). By day 9 the siRNA knockdown was losing effect as the cells were only transfected with siRNA once at the beginning of experiment, this was expected as siRNA knockdown usually lasts for a duration of 5-7 days (Han, 2018).

Cyst growth was only elevated in hGH-treated cells compared to unstimulated controls in the siCtrl group and not in the si GHR and si STAT5AB cells at day 3 and day 6, indicating that silencing of GHR or STAT5AB effectively represses GH-induced promotion of cystic growth.

There was no significant difference or obvious pattern of altered cystic growth between the GHA or Ruxolitinib-treated cells when comparing siCtrl to si GHR and si STAT5AB cells. Though the contribution of other growth hormone signalling pathways cannot be completely ruled out, this data suggests that growth hormone promotes cystic growth via the GH-GHR-JAK2-STAT5 signalling pathway. Thus targeting this pathway with GHA or Ruxolitinib prevents cystic growth.

4.4 Inhibition of GHR-JAK2 prevents GH-induced increase in proliferation in *in vitro* PKD models

Following the results showing that human cystic renal epithelial cells display enhanced cystic growth in the presence of exogenous GH and the inhibition of this growth with the hGHR antagonist, the next step was to determine the mechanism behind the cystic growth. It was hypothesised that the elevated cystic growth in response to GH could be associated with proliferation as one of the hallmarks of ADPKD, thought to be a key driver in cyst expansion, and a cellular mechanism altered by GH.

To assess the effect of stimulation and inhibition of growth hormone signalling on proliferation flow cytometry was employed using propidium iodide for cell cycle analysis.

SKI-001 and OX161c1 cells were treated with 500 ng/mL hGH for 24 hours and displayed a moderate increase in the percentage of cells in G2 phase of the cell cycle (%G2), with an increase of ~ 4 % in SKI-001 and ~ 6 % in OX161c1. The baseline of cells undergoing G2 phase in SKI-001 was higher than in OX161c1 which was also reflected during cell culture in which SKI-001 were observed to grow faster and become confluent more quickly than OX161c1. When 2.5 µg/mL GHA was applied in addition to the hGH-WT, the percentage of cells in G2 phase was reduced back to the levels of the unstimulated control (Figure 4.8). No significant differences in percentage of cells in S phase were detected between treatment groups in either SKI-001 or OX161c1.

Next, to confirm the impact of growth hormone signalling modulation on mitosis the percentage of cells positive for the mitotic marker phosphoserine histone 3 (PH3) was examined using flow cytometry in SKI-001. The SKI-001 cells were treated with a single dose for 24 hours of either (i) unstimulated control, (ii) 500 ng/mL hGH, (iii) 500 ng/mL hGH + 2.5 µg/mL GHA, or (iv) 500 ng/mL hGH + 1 µM Ruxolitinib (Figure 4.9).

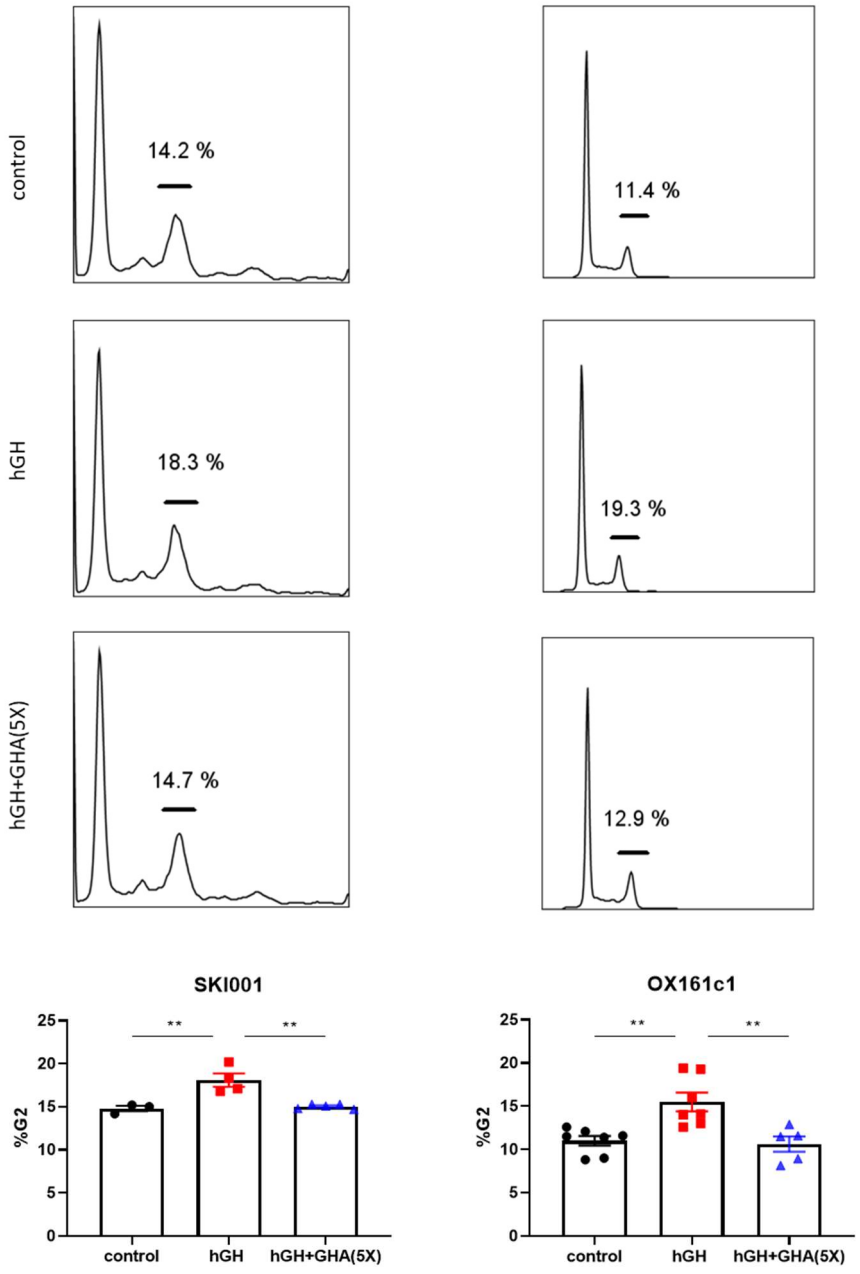

Figure 4.8 Cell cycle analysis with growth hormone signalling stimulation and inhibition in SKI-001 and OX161c1

Representative images of the histograms (Blue 660-20-area) from one biological run of cell cycle analysis with propidium iodide are displayed for each cell type with the percentage of cells in G2 (%G2) from 10,000 events displayed above the G2 peak for each treatment group. The %G2 is shown for each biological repeat in the graphs for SKI-001 and OX161c1. Treatment with hGH (red, 500ng/ml for 24 hours) increased %G2 compared to control (black) and simultaneous addition of the GHA (blue, 2.5ug/ml (5x))

reduced %G2 compared to hGH-stimulated cells. A one-way ANOVA test with a post-hoc Bonferroni correction for multiple comparison was used to determine statistical significance, indicated by asterisks. Each plot point represents a biological repeat, within each biological repeat 10000 events/cells were counted. Mean ±SEM is plotted. ** P<0.01

An IgG control was used to gate for cells negative for PH3 (PH3-) and cells above this gate based on the Violet 450_50 area values were determined to be positive for PH3 (PH3+). The percentage of PH3+ cells was significantly increased with hGH stimulation after 24 hours compared to control. Through inhibition of growth hormone signalling with GHR antagonism or JAK inhibition with Ruxolitinib, the percentage of PH3+ cells was significantly reduced in comparison to cells stimulated with hGH only. Together this data shows that GHA and Ruxolitinib can effectively and significantly prevent growth hormone-induced elevation in cells undergoing G2/mitosis in human cystic cells, suggesting the potential to control proliferation induced by growth hormone.

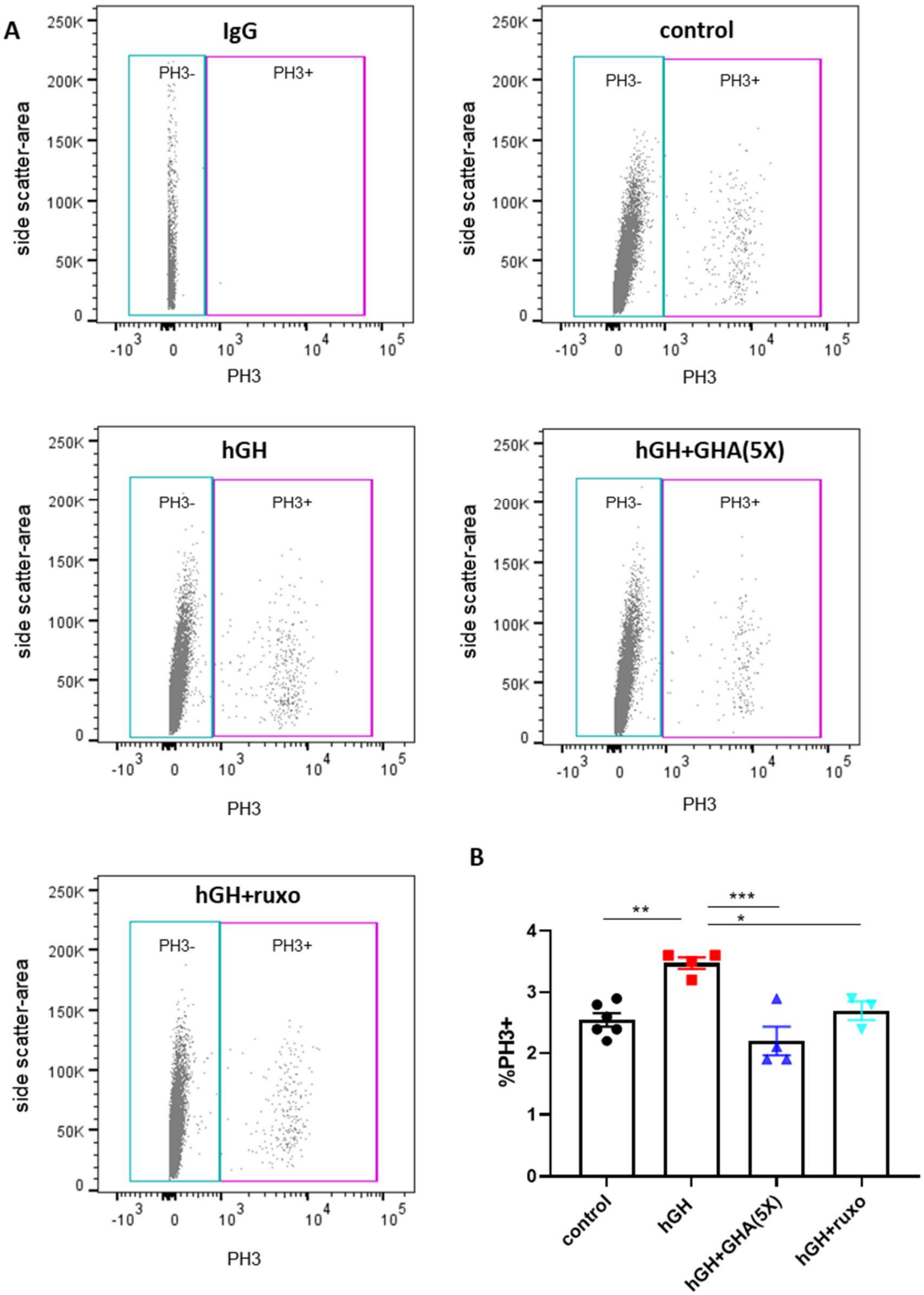
A
IgG
control
hGH
hGH+GHA(5X)
hGH+ruxo
PH3-
PH3+
side scatter-area
PH3
250K
200K
150K
100K
50K
0
-10^3
0
10^3
10^4
10^5
B
%PH3+
**
***
*
4
3
2
1
0
control
hGH
hGH+GHA(5X)
hGH+ruxo

Figure 4.9 Effect of growth hormone stimulation and inhibition on proliferation shown with phosphoserine Histone 3 in SKI-001

The mitotic marker phosphoserine 10 histone 3 (PH3) was probed in SKI-001. (A) One biological repeat with each treatment group is displayed in the images of the gating for PH3, with PH3 negative cells (PH3-) and PH3 positive cells (PH3+) determined from the IgG control. (B) The percentage of PH3+ cells (%PH3+) was analysed for each biological repeat. Treatment with hGH (red, 500 ng/mL 24 hours) increased %PH3+ SKI-001 cells compared to control (black), and the addition of either GHA (blue, 2.5 µg/mL) or Ruxolitinib (cyan, 1 µM) reduced GH-induced increase in %PH3+. A one-way ANOVA test with a post-hoc Bonferroni correction for multiple comparison was used to determine statistical significance, indicated by asterisks. Each plot point represents a biological repeat, within each biological repeat 10000 events/cells were counted. Mean ±SEM is plotted. * $P<0.05$, ** $P<0.01$,*** $P<0.001$.

4.5 Modulation of growth hormone signalling in human ADPKD-derived cystic cells alters expression of pro-proliferative STAT5 targets

Next, the expression of two well-studied STAT5 transcriptional targets was assessed:cyclin D1 (CCND1) and insulin-like growth factor-1 (IGF-1) as these are well established STAT5 targets known to stimulate proliferation (Matsumura et al., 1999, Davey et al., 2001, Parker et al., 2007). When compared to controls, expression of CCND1 and IGF-1 was significantly elevated, by approximately 4-fold, at 24 hours after stimulation with 500 ng/mL hGH-WT (Figure 4.10). This indicates that the phosphoactivated STAT5 that was observed in SKI-001 is transcriptionally active and promoting expression of proliferative CCND1.

Addition of the 2.5 µg/mL GHA, 5 times the concentration of hGH-WT, was applied at the same time as the hGH-WT and demonstrated the ability to reduce expression of CCND1 and IGF-1 compared to hGH-WT-stimulated cells back to around the unstimulated levels of controls. This demonstrated the potential for GHA to modulate expression of STAT5 transcriptional targets involved in proliferation.

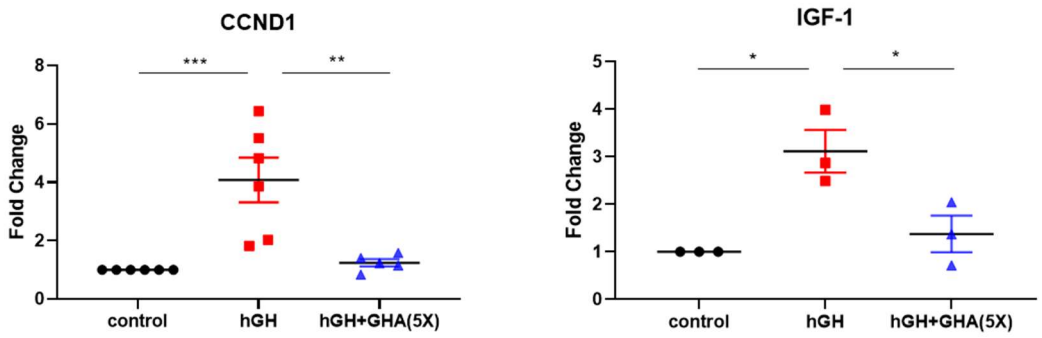

Figure 4.10 Expression of STAT5 targets cyclin D1 (CCND1) and insulin-like growth factor 1 (IGF-1) in SKI-001 in response to human growth hormone (hGH) and growth hormone receptor antagonist (GHA)

Expression of CCND1 and IGF-1 is increased in response to hGH stimulation, and the addition of the GHA reduces expression. Fold change expression of CCND1 and IG-1 was determined from Delta-delta Ct values normalised to β-actin. A one-way ANOVA test with a post-hoc Bonferroni correction for multiple comparison was used to determine statistical significance, indicated by asterisks. Each plot point represents a biological repeat. Mean ±SEM is plotted. * P<0.05, ** P<0.01, *** P<0.001.

4.6 Discussion

4.6.1 General overview

Here it has been conclusively demonstrated with novel data that addition of growth hormone induces enhanced cystic growth in ADPKD-derived human and mouse cells over time, when compared to untreated cells not stimulated with exogenous recombinant GH. on the next step was to investigate the possible mechanism of enhanced cystic expansion in response to the presence of exogenous GH. It was speculated that GH may enhance cell proliferation via STAT5, which would subsequently lead to an increased cell number and would be consistent with increased cystic area in the cystogenesis assay. Indeed, using robust flow cytometric and staining approaches, it was shown that GH causes an increase in cell proliferation of the G2/M phase of the cell cycle in human cystic cells. This interesting finding was also supported by qPCR data showing that GH causes a significant increase in STAT5 transcriptional targets cyclin D1 (CCDN1) and Insulin like growth factor 1 (IGF1), both of which are known activators of proliferation.

4.6.2 Growth hormone enhances cystogenesis in *in vitro* PKD models which is abrogated by GH-GHR-JAK2-STAT5 inhibition

A key novel finding in this chapter is that growth hormone consistently elevates growth of cysts in a number of independent models of ADPKD above unstimulated controls. Inhibition of growth hormone signalling with the use of a growth hormone receptor antagonist (GHA) at 5-fold the dose of growth hormone or the JAK1/JAK2 inhibitor Ruxolitinib (Jakafi/Jakavi) effectively inhibits growth hormone signalling and reduces

cyst growth to the levels of unstimulated controls, indicating the potential of these inhibitory molecules in combatting GH-induced cystic growth.

The cells were also treated with Ruxolitinib only to compare whether the JAK inhibitor was capable of reducing cystic growth below the baseline unstimulated control. However, at the dose of 1 µM Ruxolitinib did not reduce cystic growth compared to controls, which could imply that the dose was too low to have an impact. Previous work from a masters student in the Fragaidaki laboratory (Christopher Byrnes, Department of Infection, Immunity and Cardiovascular Disease, University of Sheffield) showed that cystic growth was only significantly reduced compared to untreated controls with a dose of 15 µM Ruxolitinib. Though at this higher dose there is also increased risk of cellular toxicity. The dose of 1 µM Ruxolitinib is sufficient in reducing GH-induced cyst expansion, even though it does not reduce baseline cyst expansion.

The question could be raised that alterations in other signalling pathways contribute to the reduction in cyst expansion, particularly with Ruxolitinib which inhibits both JAK1 and JAK2 and thus reduced cyst expansion could be due to inhibition of signalling pathways influenced by other cytokines/growth factors present in media/FBS. Though these contributions cannot be completely ruled out, Ruxolitinib appears to be as effective as the GHR antagonist in reducing GH-induced cyst expansion indicating this is a GH-mediated effect. Moreover, genetic modulation via GHR silencing with ~80% knockdown efficiency in combination with Ruxolitinib treatment shows no additional impact on cyst expansion compared to siRNA control cells treated with Ruxolitinib, which is further evidence that the reduction of cystic growth with Ruxolitinib is due to inhibition of growth hormone signalling.

To further explore STAT5 involvement as a potential mediator for GH-induced cyst expansion silencing of STAT5 was performed, as STAT5 had been shown to be activated in ADPKD cells and is a key mediator of growth hormone cellular responses. Silencing of STAT5 with ~75% knockdown efficiency in SKI-001 displayed a trend in reduction in cyst expansion below baseline in unstimulated cells. This is concordant with what has previously been described with silencing of STAT5 or treatment with a STAT5 inhibitor performed in OX161c1, F1 Pkd1 +/+ and F1 Pkd1 -/- which resulted in significantly reduced cystic growth (Fragiadaki et al., 2017). The inhibition of cyst growth with STAT5 knockdown was more pronounced in GH-treated cells, showing significant reduction in cyst expansion compared to siRNA control. STAT5 silenced cells treated with GHA or Ruxolitinib have comparable cyst size to siRNA controls cells with the same treatment, which shows that addition of STAT5 silencing on top of either GHR antagonism or JAK inhibition does not have additional impact on cystic growth. Together this data suggests that GH-induced cystic growth is STAT5-mediated, and inhibition along the GH-GHR-JAK2-STAT5 axis can abrogate this effect.

4.6.3 Inhibition of GHR-JAK2 prevents GH-induced increase in proliferation in *in vitro* PKD models

As enhanced cystogenesis had been shown, I set out to determine the mechanism behind enhanced GH-induced cyst expansion. Increased proliferation was a likely candidate mechanism as it has previously been described as a key driver in cyst expansion. The percentage of cells in G2 phase was significantly higher in GH-stimulated cells and addition of the GHA reduced proliferation to baseline. Furthermore, when delving further into the stage of the cell cycle that is impacted by growth hormone,

phosphoserine histone 3 was used as a G2/M marker as histone 3 is phosphorylated at serine 10 in late G2 phase through mitosis, ending at early telophase (Hans and Dimitrov, 2001). The number of phosphoserine histone 3 positive cells was significantly increased with growth hormone stimulation. This provides evidence that modulation of GH signalling impacts the number of cystic cells entering G2/M phase and proliferation.

4.6.4 Modulation of growth hormone signalling in human ADPKD-derived cystic cells alters expression of pro-proliferative STAT5 targets

Investigation of two well-established STAT5-transcriptional target genes involved in proliferation, cyclin D1 and IGF-1, yielded novel evidence that these two genes are significantly upregulated in response to stimulation with exogenous GH in human ADPKD cells. Cyclin D1 is a nuclear cell cycle regulatory molecule which, in conjunction with cyclin dependent kinsases (CDKs), is essential for progression through G1 phase to S phase leading to proliferation (Baldin et al., 1993). IGF-1 reportedly induces proliferation via the Ras/Raf signalling in renal cells (Parker et al., 2007) though involvement of MAPK and PI3K signalling is also implicated in IGF-1 induced proliferation in other cell types (Davison et al., 2011, Kiepe et al., 2005). Of note, IGF-1 has been implicated in hyperproliferation of cells within the context of ADPKD (Parker et al., 2007), and the potential role of GH-STAT5-IGF-1 signalling in ADPKD pathogenesis will be discussed further in chapter 6. The GHA can successfully inhibit GH-induced upregulated expression of these pro-proliferative genes, further showing the potential of the GHA to impact GH-induced proliferation and subsequent cystogenesis.

4.6.5 Conclusion

In combination, the phosphoactivation of STAT5 and upregulated expression of CCND1 and IGF-1 observed in SKI-001 alongside the elevated levels of cells in G2/M phase with stimulation of exogenous GH, serves to show a GH-STAT5 mediated mechanism of inducing proliferation in human ADPKD-derived cells. Moreover, treatment with a GHR antagonist is capable of reducing proliferation to baseline. Thus, providing a potential mechanism for GH promoting cyst expansion and also a potential treatment to prevent GH-induced hyperproliferation and cystogenesis in ADPKD.

4.7 Supplementary figures

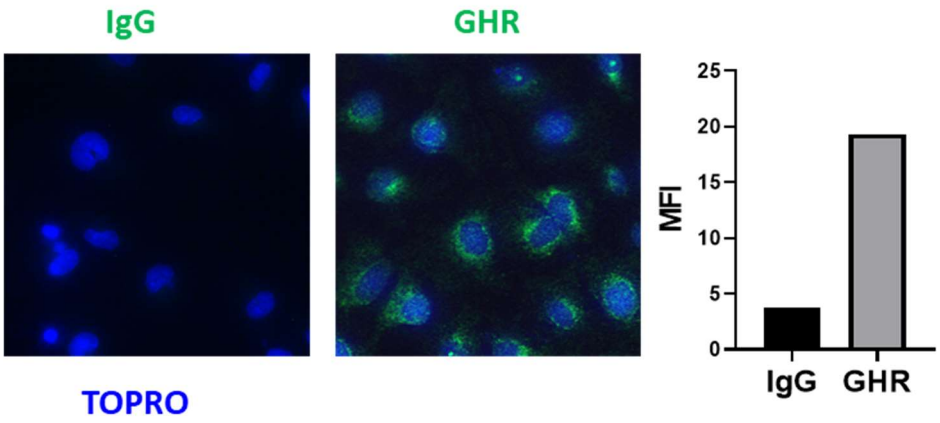

Supplemental figure 2: Images of cells stained with either IgG or GHR (green) and nuclear TOPRO staining (blue) at 63X magnification demonstrate the presence of GHR in OX161c1.

Chapter 5: GROWTH HORMONE INHIBITION IN A PRECLINICAL SETTING of ADPKD

5.1 Introduction

To examine the effects of inhibiting growth hormone signalling in a whole organism model of ADPKD, Octreotide and Ruxolitinib were tested in homozygous $Pkd1^{nl/nl}$ mice and WT littermate controls (Happé *et al*., 2013). The somatostain analogue Octreotide acts upstream of the GHR to inhibit growth hormone release at the pituitary level and Ruxolitinib acts downstream of the GHR by inhibiting JAK2, both drugs inhibit within the same pathway (GHR/JAK2/STAT5). In this chapter these two treatments will be studied for the effects on inhibition of growth hormone signalling and PKD progression *in vivo*.

In previous preclinical studies of Octreotide in ADPKD rodent models a range of dosing routes have been used such as gavage, intraperitoneal (IP) injection and subcutaneous injection and osmotic minipumps, as well as a range of doses from 20 µg/kg – 8 mg/kg per day (Masyuk et al., 2007, Masyuk et al., 2013, Spirli et al., 2012, Kugita et al., 2017). The selected dose route was IP injection at a dose of 1 mg/kg/day for Octreotide.

Previous preclinical studies with Ruxolitinib to examine treatment of neoplasms have used doses of 30-90 mg/kg (Bhagwat et al., 2014, Reeves et al., 2017), whilst people with myelofibrosis are given Ruxolitinib (Jakavi) at a dose of 0.5 mg/kg.

The no observable adverse effect level (NOAEL) in rodents for Ruxolitinib is 50 mg/kg (European Medicines Agency: EMA/465846/2012,

https://www.ema.europa.eu/en/documents/assessment-report/jakavi-epar-public-assessment-report_en.pdf , July 20201) thus the dose of 50 mg/kg/day of Ruxolitinib was selected for treatment.

5.1.1 Aims

The aim of this chapter was to examine the effects of inhibition of growth hormone signalling on pathogenesis and progression in a mouse model of ADPKD using Octreotide and Ruxolitinib as upstream and downstream inhibitors of growth hormone signalling.

5.2 Effects of Octreotide treatment on progression of ADPKD in *Pkd1* $^{nl/nl}$ mice

To study whether Octreotide treatment was successfully administered and exerting its function in lowering serum growth hormone, the serum growth hormone levels were compared between treatment groups. Serum GH levels were not significantly altered between treatment groups when assessed on its own (Figure 5.1 A), despite a trend towards reduced serum GH levels which is more noticable in the female Pkd1$^{nl/nl}$ group (Figure 5.1 B). Due to the known variability in body weight with this mouse model, serum growth hormone was normalised to body weight. When serum GH is normalised to bodyweight there is a significant reduction in normalised GH of Octreotide-treated Pkd1$^{nl/nl}$ mice compared to saline-treated vehicle controls (Figure 5.1 C). When normalised GH was split by sex there was no significant reduction in the treated groups,

although similar to the serum GH there is a downward trend most noticable in the female Pkd1$^{nl/nl}$ group, though due to the small number of animals in this group this does not achieve statistical significance (Figure 5.1 D).

To determine the impact of Octreotide on disease progression in Pkd1$^{nl/nl}$ mice renal hypertrophy and renal function were assessed. It should be noted mice were of mixed sex and were approximately 4-6 weeks old during Octreotide dosing, hence as this is a mixed age group we anticipated increased variability of the results. There was no observable reduction in renal hypertrophy, measured as a ratio of kidney weight to body weight (KW:BW), between Octreotide and vehicle treatment groups in Pkd1$^{nl/nl}$ mice (Figure 5.1 E). To determine if there were any sex differences in response to Octreotide treatment the KW:BW was grouped by sex. In males the KW:BW is consistent between treatment groups. There appears to be a downward trend in KW:BW for the female Octreotide-treated Pkd1$^{nl/nl}$ compared to vehicle controls, however this result is not statistically significant and there is a low N number for this group (Figure 5.1 F). To assess renal function, serum levels of blood urea nitrogen (BUN) were measured and this revealed no difference between vehicle and Octreotide treatment groups when taken as a total (Figure 5.1 G) and when split by sex (Figure 5.1 H). Octreotide treatment did not affect renal growth or renal function in the WT control group (Supplemental figure 1).

When comparing untreated Pkd1$^{nl/nl}$ with WT littermate controls, the genotype differences were as expected with increased KW:BW and BUN levels indicating renal hypertrophy and decline of renal function. Serum growth hormone (GH) levels were compared between the Pkd1$^{nl/nl}$ and WT to determine any differences by genotype.

Concordant with previous findings from Fragiadaki *et al*. (2017) there is a trend of higher serum growth hormone levels in the $Pkd1^{nl/nl}$ group compared to the WT littermate controls. Although this result is not statistically significant, when serum GH was normalised to body weight, the $Pkd1^{nl/nl}$ group shows a significantly higher normalised GH level. There were no significant differences between Octreotide and vehicle treated WT mice for KW:BW or BUN suggesting safety of the drug (Supplemental figure 1).

The impact of Octreotide on renal fibrosis and cyst development were then examined using ImageJ measured as fibrotic index and cystic index. There were no significant differences between treatment groups in fibrotic index or cystic index in the $Pkd1^{nl/nl}$ mice (Figure 5.2). Cysts were categorised by small (5,000– 19,999 μm^2), medium (20,000 – 99,999 μm^2) and large (≥100,000 μm^2) to investigate treatment effects on cyst expansion (figure 5.2 D). A lower threshold of 5000 μm^2 was set in ImageJ as the minimum size cyst that would be measured, as to avoid including non-cysts as cysts and subsequent manual removal of these which introduces subjectivity and potential bias. The caveat to the minimum cyst size of 5000 μm^2 being set is that cysts smaller than this were not measured and so any change to the number of cysts <5000 μm^2 could not be assessed. There were no stark differences in the pattern of cyst size between males and females. When analysing percentage of medium cysts, the difference between vehicle and Octreotide treatment is approaching significance which may suggest a treatment impact on cyst expansion, although not on the total cyst progression measured in the kidney by cystic index.

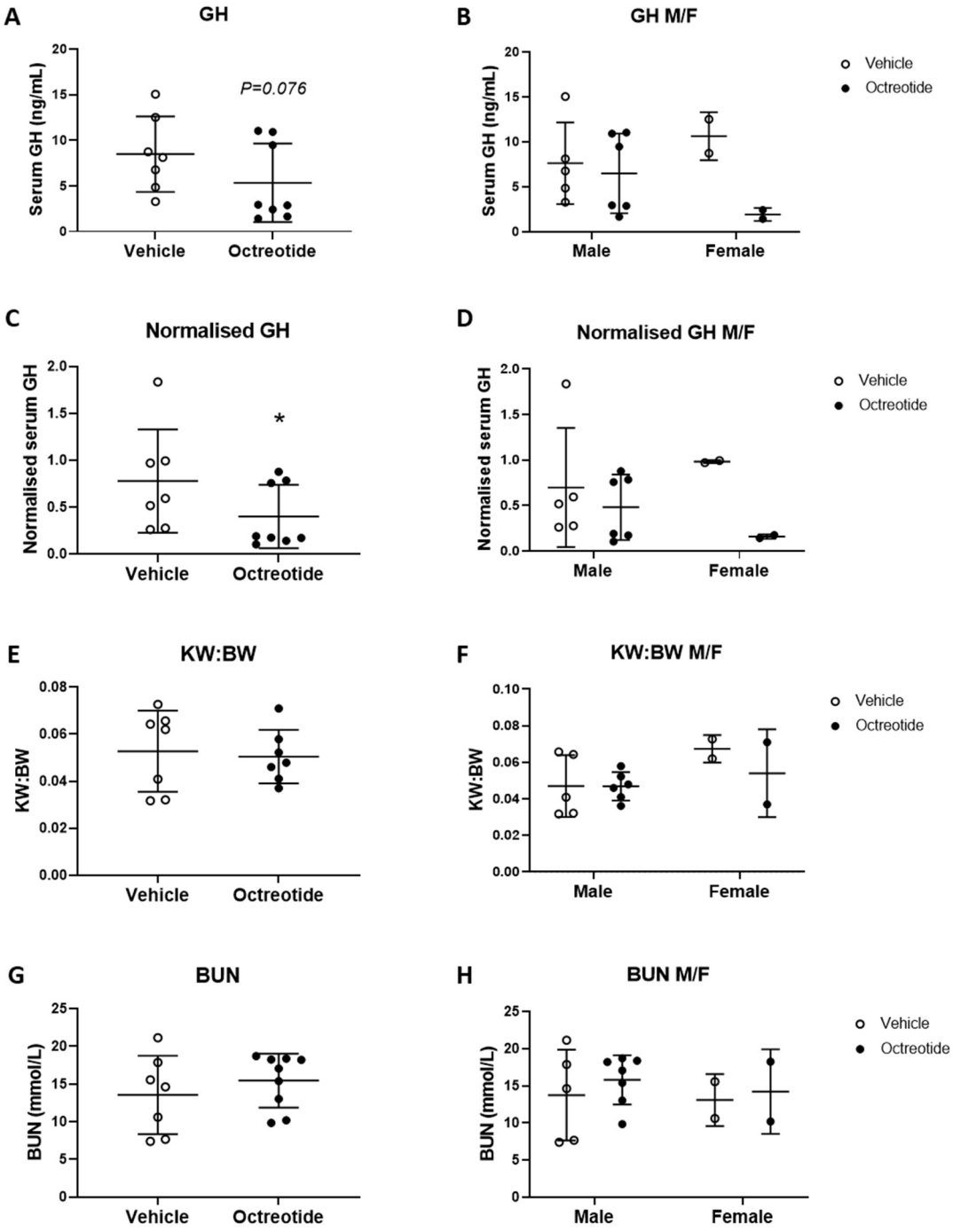

Figure 5.1 Octreotide reduces growth hormone levels but does not reduce renal hypertrophy or protect renal function

(A) Serum growth hormone levels (GH) display a trend in reduction with Octreotide treatment in Pkd1$^{nl/nl}$ mice (N=7) at a dose of 1 mg/kg compared to saline vehicle control (N=8). (B) Females appear to be more responsive to Octreotide treatment in terms of serum GH compared to males. (C) GH normalised to body weight in Pkd1$^{nl/nl}$ mice as a

mixed cohort shows significant reduction in serum GH in Octreotide-treated mice. (**D**) Reduction, though not significant is also observed when split by sex into male (N=11 total) or female groups (N=4 total) (M/F) (**E**) The Kidney weight to body weight (KW:BW) of $Pkd1^{nl/nl}$ mice was measured in Octreotide and saline vehicle treatment groups as a total then split by sex into male or female groups (**F**). (**G**) Serum levels of blood urea nitrogen (BUN) in $Pkd1^{nl/nl}$ mice comparing vehicle and Octreotide treated groups are shown as a total and by male and female only (**H**). No significant differences were observed between treatment groups for KW:BW or BUN.

Each plot point represents an individual mouse. Statistical significance is represented as asterisks. Mean ±SD is plotted. * P<0.05

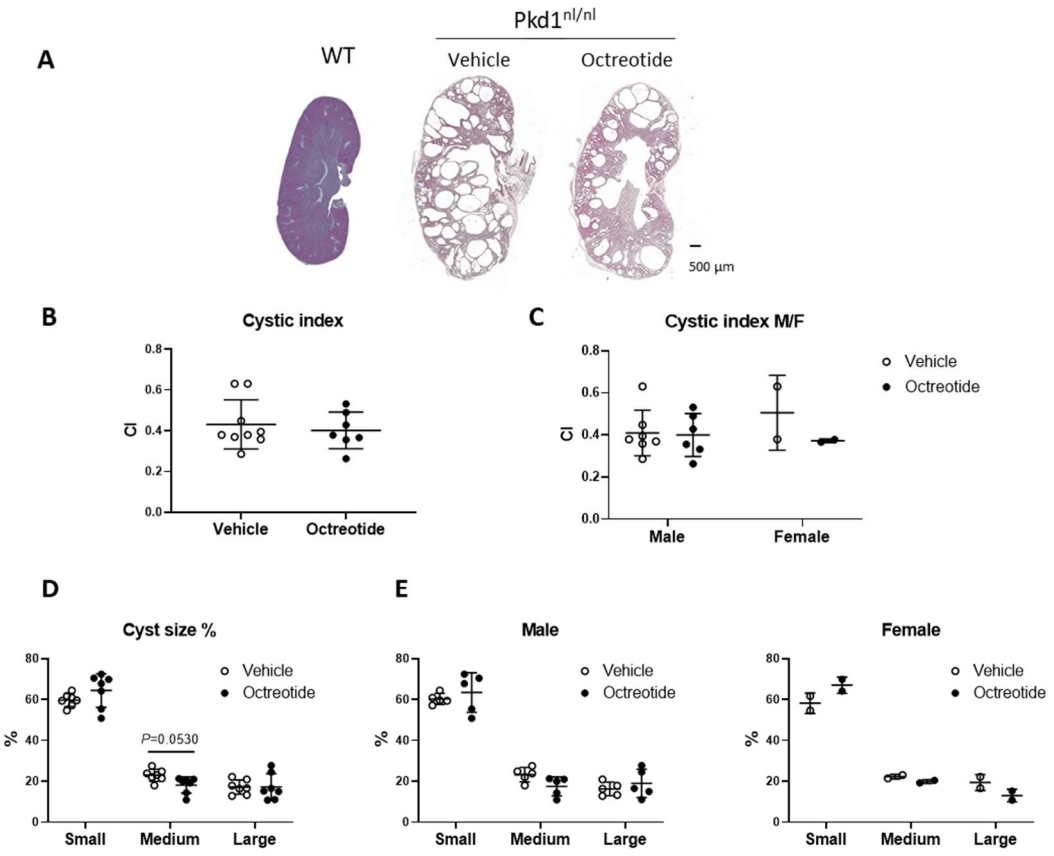

Figure 5.2 The impact of Octreotide on renal cysts and fibrosis in $Pkd1^{nl/nl}$ mice.

(**A**) Representative H&E stained kidneys from WT and Pkd1nl/nl treated with vehicle saline control or 1 mg/kg Octreotide. (**B**) Cystic index of the kidney of vehicle and

Octreotide-treated mice (C) cystic index split by male and female. (D) Percentage of cysts categorised as small (5,000– 19,999 µm^2), medium (20,000 – 99,999 µm^2) and large (⩾ 100,000 µm^2) (E) cyst size split by male and female. Each plot point represents an individual animal. Mean ±SD is plotted. A Mann-Whitney non-parametric t-test was used for cystic index treatment comparison and one-way ANOVA was used for cyst size treatment comparison to examine statistical significance.

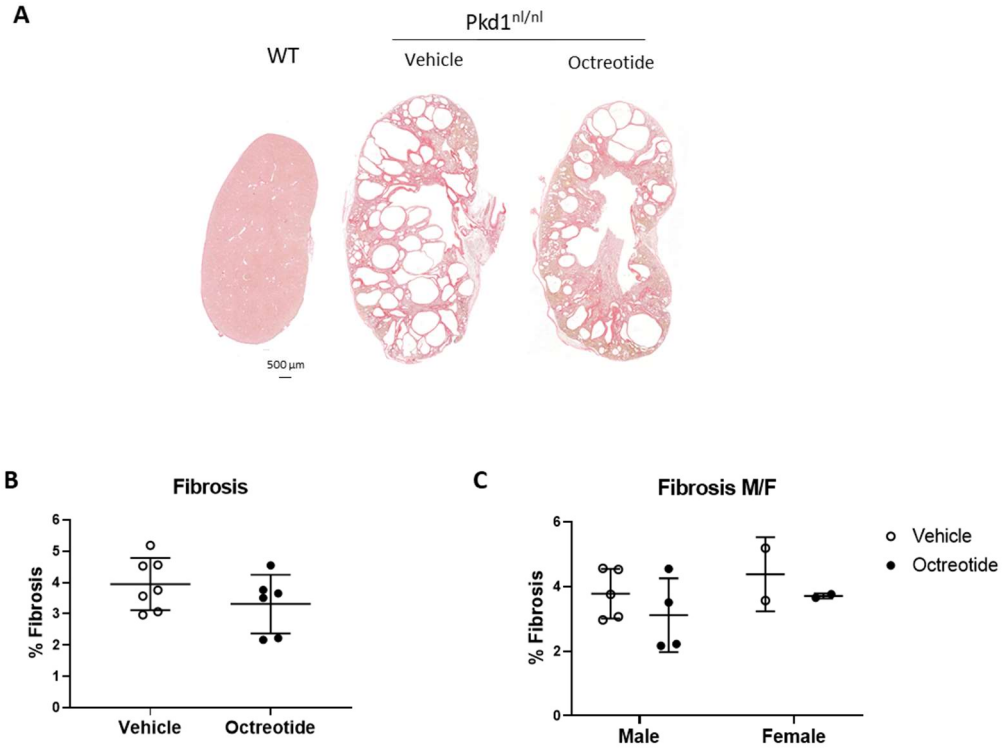

Figure 5.3 Octreotide shows a trend of reducing fibrosis in Pkd1$^{nl/nl}$ mice

(A) Representative image of picrosirius red (PSR) stained kidneys from WT and Pkd1nl/nl treated with vehicle saline control or 1 mg/kg Octreotide (B) The percentage of kidney fibrosis in Pkd1$^{nl/nl}$ mice treated with Octreotide or saline vehicle control (C) and split by male (M) and female (F) shows moderate reduction in fibrosis, though not significant. Each plot point represents an individual animal. Mean ±SD is plotted. Mann-whitney non-parametric t-test was used to examine statistical significance.

To determine whether the level of circulating growth hormone had an impact on cyst development or fibrosis, linear regression was used to assess growth hormone against (a) cystic index and (b) fibrosis. There is an upward trend, although not significant in growth hormone levels and cystic index, wherein as growth hormone levels increase so does the cystic index (Figure 5.4 A). When the animals are split by treatment this upward trend remains within both treatment groups though not significantly (Figure 5.4 B), this is due to smaller n number. The trend does become significant in the Octreotide group when assessed by treatment and looking at males only (Figure 5.4 C).

There is no statistically significant correlation observed between the levels of GH and renal fibrosis when considering all $Pkd1^{nl/nl}$ mice (Figure 5.4 D). Separation of the GH vs fibrosis by treatment as both a mixed cohort (Figure 5.4 E) and males only (Figure 5.4 F) shows a positive correlation between high GH levels and more renal fibrosis in vehicle treated mice, conversely a negative correlation is observed in the Octreotide-treated mice, though neither correlation is statistically significant.

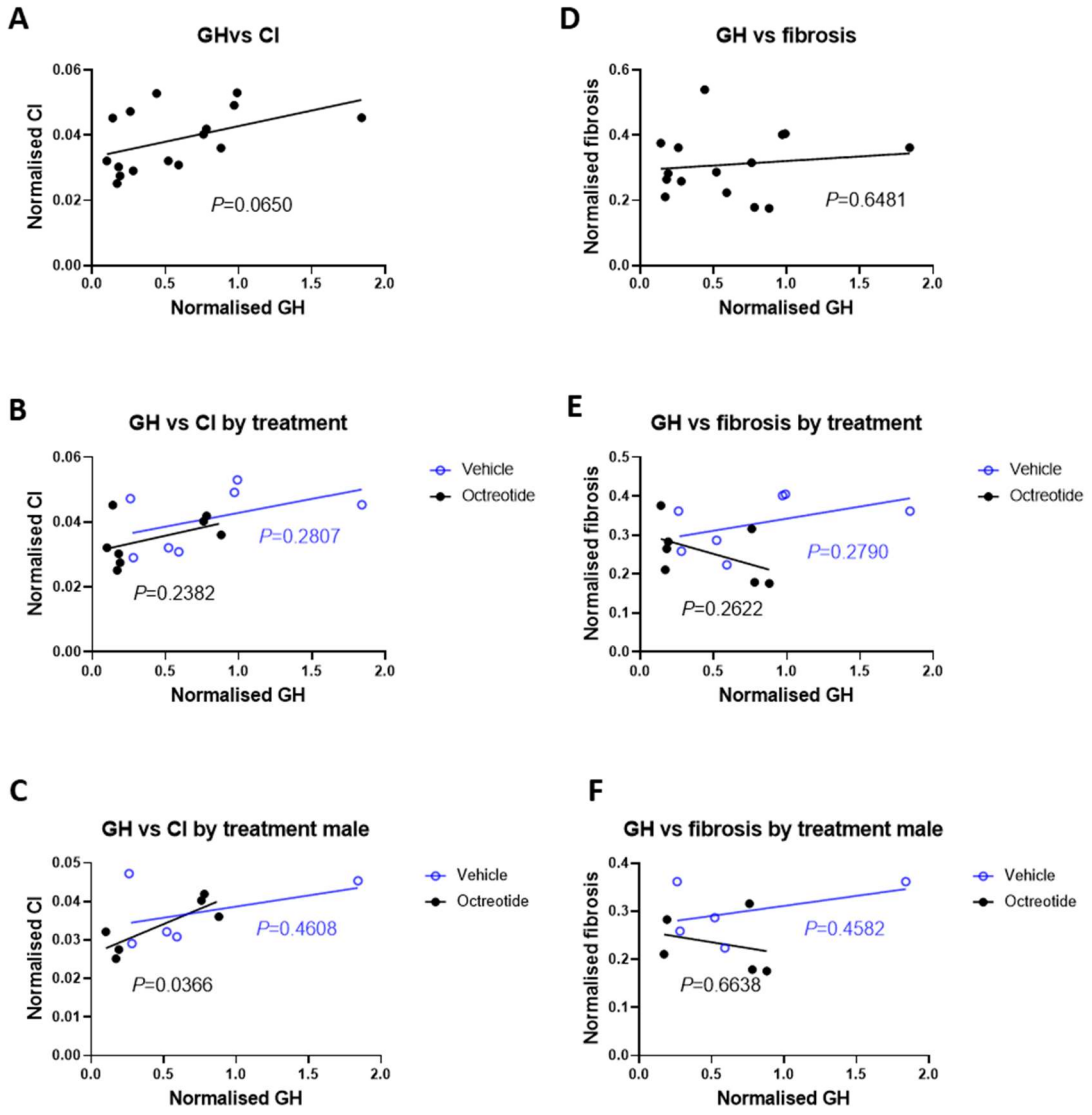

Figure 5.4 Stratified growth hormone data in PKD1nl/nl mice.

(A) Growth hormone compared cystic index shows an upward trend as a total and also shows an upward trend when split by treatment as a mixed cohort (B) and with males only (C), displaying statistical significance in the Octreotide treated-males. (D) Growth hormone compared to fibrosis shows a very minor upward trend. When split by treatment as a mixed cohort (E) and with males only (F) vehicle treated mice show an upward trend in fibrosis as GH increases whilst the opposite is true for the Octreotide-treated mice. Statistical significance and P values were determined from simple linear regression and whether the slope was significantly non-zero. Each plot point represents an individual animal.

5.3 GHR expression in Pkd1$^{nl/nl}$ mice and the impact of Octreotide treatment

To confirm the expression of the growth hormone receptor in the mouse kidneys and determine the localisation of the GHR, immunofluorescent staining was employed.

The mouse kidneys stained positively for presence of the growth hormone receptor indicating the capacity for renal cells to respond to growth hormone. In the WT kidneys the GHR stained noticeably most positively in the outer cortical region of the kidney. In Pkd1$^{nl/nl}$ kidneys GHR staining appeared to be primarily in the proximal tubular region based on proximity of the stained tubule to the glomerulus. Notably, GHR stained positively in the cyst-lining cells. There was an observed increase in the level of GHR fluorescence in Pkd1$^{nl/nl}$ mice when compared to wild-type littermates, suggesting that GHR levels maybe enhanced in disease (Figure 5.5). Yet Octreotide treatment did not affect the levels of tubular GHR expressed.

To explore the localisation of the GHR within the renal tubular segments, antibodies for aquaporin 1 (AQP1), aquaporin 2 (AQP2), and Tam-Horsfall protein (THP) also known as uromodulin were used to costain with the GHR. Within the murine nephron AQP1 is localised in the proximal convoluted tubule and descending thin limb of the loop of Henle, AQP2 is localised in the collecting ducts and THP is found in the thick ascending limb of the loop of Henle (Brandt et al., 2012) (Figure 5.6 A).

The GHR appears to be coincident more so with AQP1 than AQP2 or THP which supports what was initially observed of GHR being expressing more highly in the proximal tubular region of the nephron (Figure 5.6 B). Yet, there is GHR co-staining with AQP2 and THP

suggesting that GHR expression is not limited only to tubular epithelial cells but it is rather more widespread.

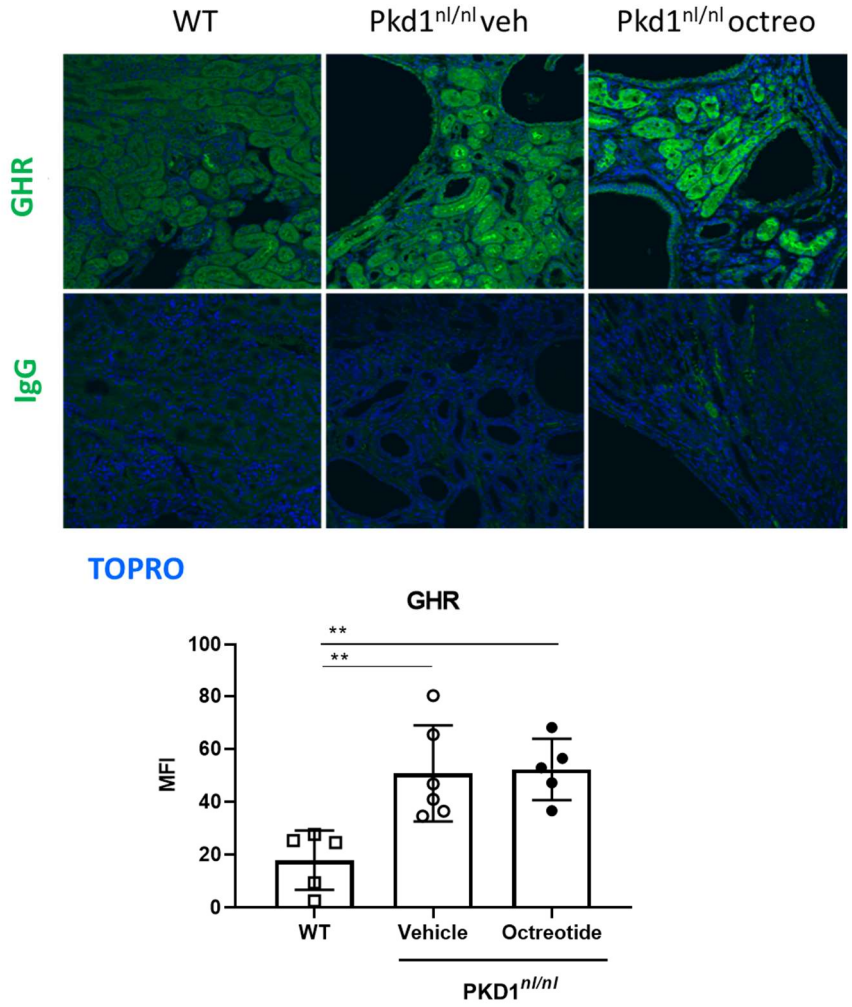

Figure 5.5 Immunofluorescent staining for growth hormone receptor in mouse kidneys
Growth hormone receptor (GHR) is expressed in the kidneys of WT and Pkd1$^{nl/nl}$ mice and appears to be expressed more highly in Pkd1$^{nl/nl}$ kidneys compared to WT wuantified as mean fluorescence intensity (MFI). Octreotide treatment doesn not affect renal GHR expression levels. GHR is also present in the cyst lining cells of Pkd1$^{nl/nl}$ kidneys.

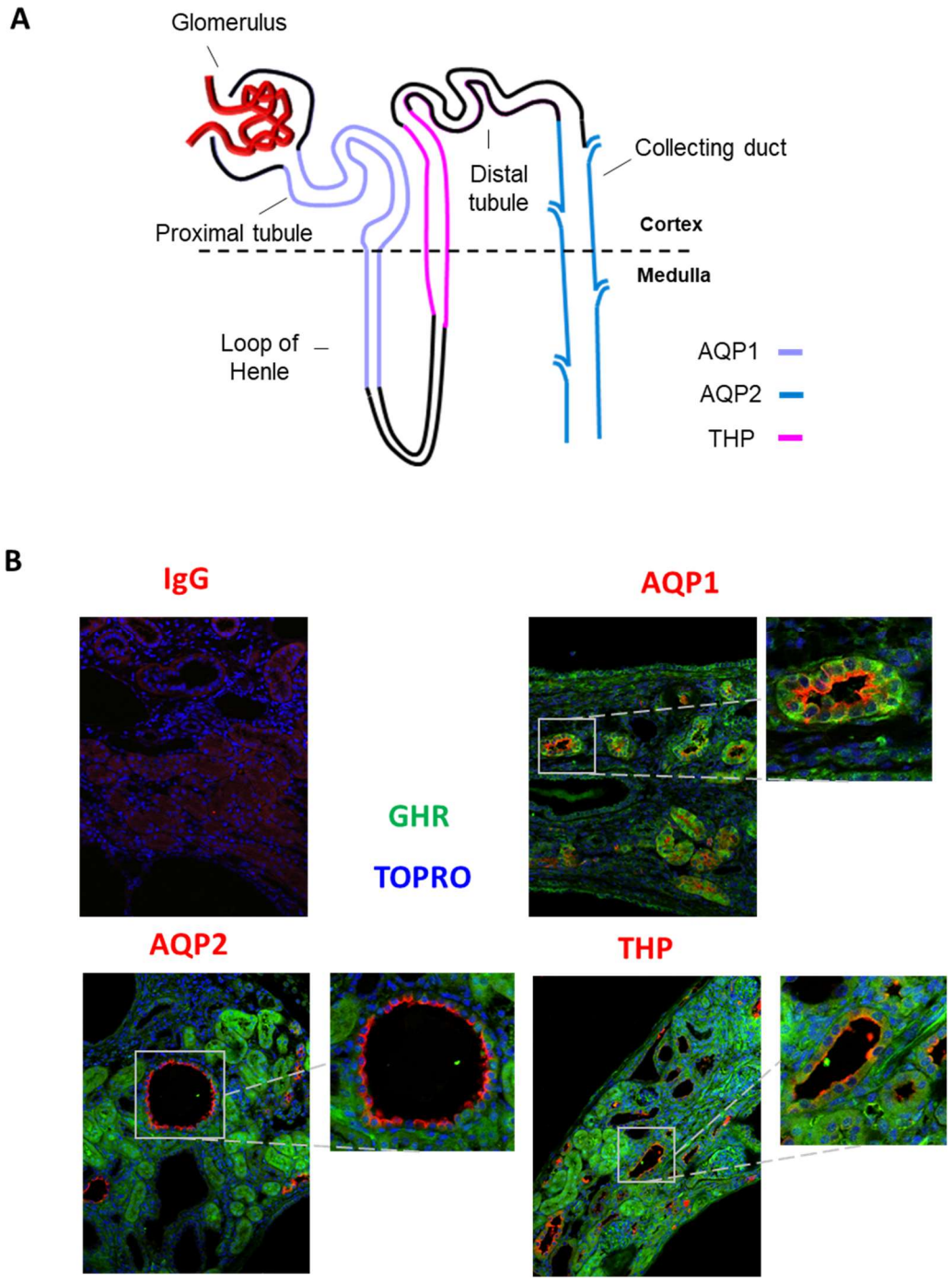

Figure 5.6 Localisation of the growth hormone receptor in the mouse kidney

(A) In the mouse nephron aquaporin 1 (AQP1, lilac) is located in the proximal distal tubule and descending thin limb, aquaporin 2 (AQP2, blue) is located in the collecting duct and Tamm-Horsfall protein (THP, pink) is located in the thick ascending limb. (B) Representative images of the cotrtical region of $Pkd1^{nl/nl}$ kidneys costained with GHR (green) and in red an IgG isotype control, AQP1, AQP2, or THP, taken at 20X magnification.

5.4 Ruxolitinib reduces renal hypertrophy and protects renal function in $Pkd1^{nl/nl}$ mice

The JAK inhibitor Ruxolitinib was used as a downstream inhibitor of GH-GHR signal transduction to study how this will impact disease progression in a mouse model of ADPKD. The same mouse model was used though dosing was performed at a later timepoint of ages 6-8 weeks than the age of dosing for Octreotide. The later timepoint for dosing was chosen so as to avoid the peak of disease which happens at ~4 weeks in this mouse model (Happe et al., 2013). $Pkd1^{nl/nl}$ mice were dosed with either 50 mg/kg/day Ruxolitinib through intraperitoneal injection or vehicle controls of equal volume, alongside wild-type littermate controls.

There is a trend of reduced kidney weight to body weight ratio and blood urea nitrogen in $Pkd1^{nl/nl}$ mice treated with Ruxolitinib compared to vehicle controls indicating that JAK inhibition may protect renal function and slow renal hypertrophy (Figure 5.7).

There were no significant differences between Ruxolitinib-treated WT mice compared to vehicle controls in BUN or KW:BW which indicates that the drug is not nephrotoxic when given at the dose and time point studied.

Ruxolitinib is known to reduce spleen size (Verstovsek et al., 2017) which my data corroborates shown as reduced diameter of the spleen, indicating successful dosing of the Ruxolitinib (Figure 5.8). Spleen enlargement is observed in people with ADPKD compared to controls (Yin et al., 2019) so Ruxolitinib could provide an additional benefit of reducing enlarged spleen volume.

The cystic index of Ruxolitinib-treated $Pkd1^{nl/nl}$ mice appears to be relatively similar to the vehicle controls as a mean, though there is a wide variation which is a product of this particular animal model (Figure 5.9 A). There were no statistically significant differences in the cyst size pattens between treatment groups when measuring the percentage of small, medium and large cysts, in which the variability within a treatment group becomes more apparent in the small and large cyst categories (Figure 5.9 B)

Despite limited impact on cyst development, a moderate reduction in fibrosis was observed in Ruxolitinib-treated $Pkd1^{nl/nl}$ mice compared to vehicle controls which adds to the evidence that Ruxolitinib may protect renal function. (Figure 5.10).

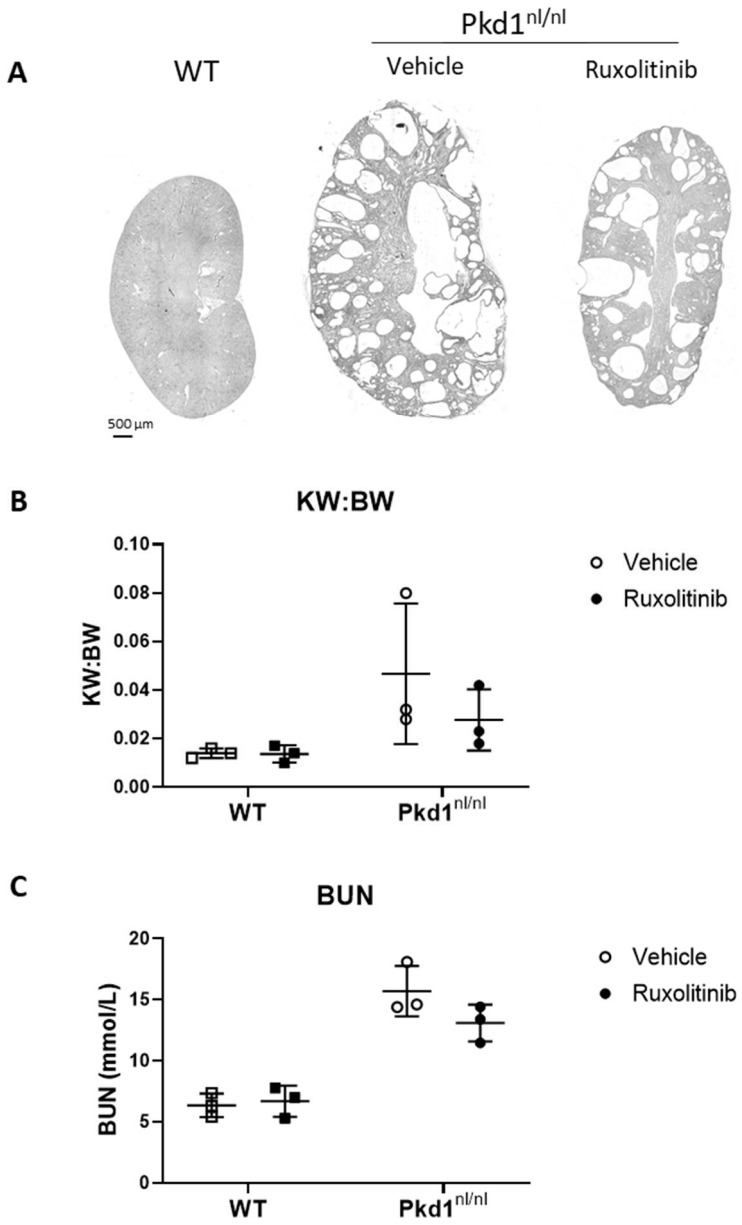

Figure 5.7 Ruxolitinib reduces renal hypertrophy and blood urea nitrogen in Pkd1$^{nl/nl}$ mice

(A) Representative images of kidneys from Pkd1$^{nl/nl}$ and WT mice treated with vehicle control or 50 mg/kg Ruxolitinib (B) The Kidney weight to body weight (KW:BW) of Pkd1$^{nl/nl}$ and WT mice was measured in Ruxolitinib and vehicle treatment groups. (C) Serum levels of blood urea nitrogen (BUN) in Pkd1$^{nl/nl}$ and WT mice comparing vehicle and Ruxolitinib treated groups. Though there is a downward trend in Ruxolitinib-treated Pkd1$^{nl/nl}$ mice, no significant differences were observed between treatment groups for KW:BW or BUN. Each plot point represents an individual mouse. Mean ±SD is plotted.

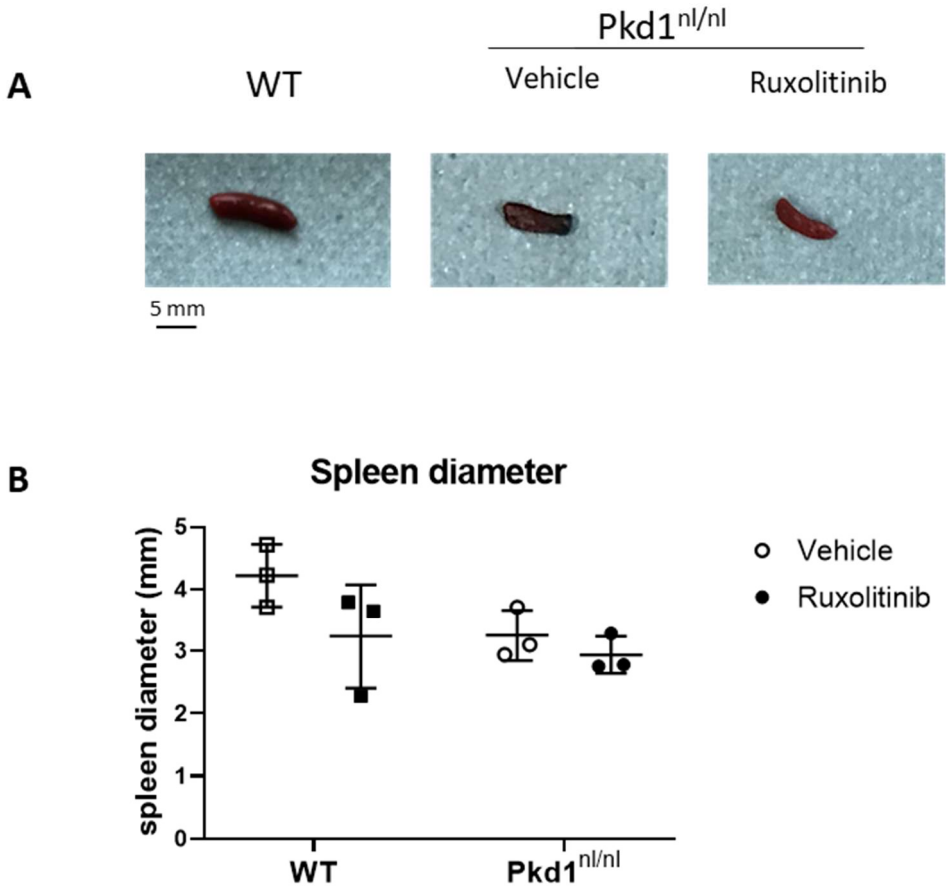

Figure 5.8 Ruxolitinib reduces spleen diameter

(A) Representative images of spleens that were measured with ImageJ (B) Spleen diameter was measured in $Pkd1^{nl/nl}$ and WT mice treated with vehicle control or 50 mg/kg Ruxolitinib which displayed a modest reduction in spleen diameter with Ruxolitinib treatment compared to vehicle control. Each plot point represents an individual mouse. Mean ±SD is plotted.

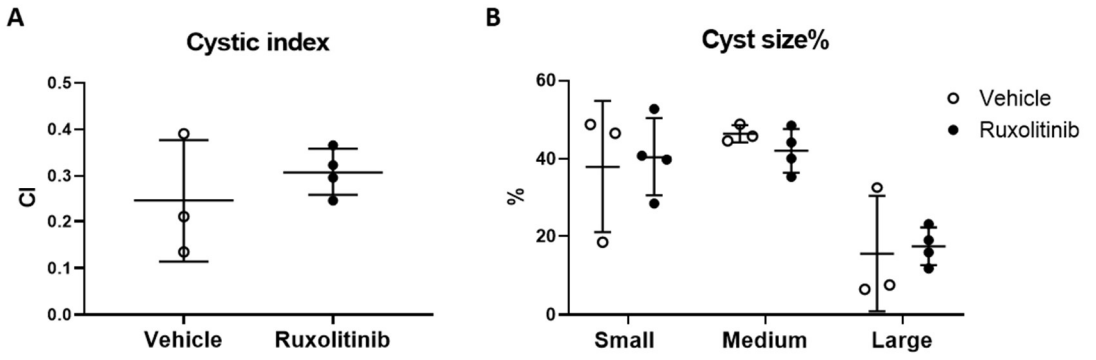

Figure 5.9 Ruxolitinib does not appear to affect the cystic index in Pkd1$^{nl/nl}$ mice

(A) Cystic index is relatively similar with Ruxolitinib treatment (50 mg/kg) (N=4) compared to vehicle control (N=3) in Pkd1$^{nl/n\ l}$ mice (B) Percentage of cysts categorised as small (5,000– 19,999 µm^2), medium (20,000 – 99,999 µm^2) and large ($\geqslant$100,000 µm^2) is relatively similar between treatment groups. Each plot point represents an individual mouse. Mean ±SD is plotted A Mann-Whitney non-parametric t-test was used for cystic index treatment comparison and one-way ANOVA was used for cyst size treatment comparison to examine statistical significance.

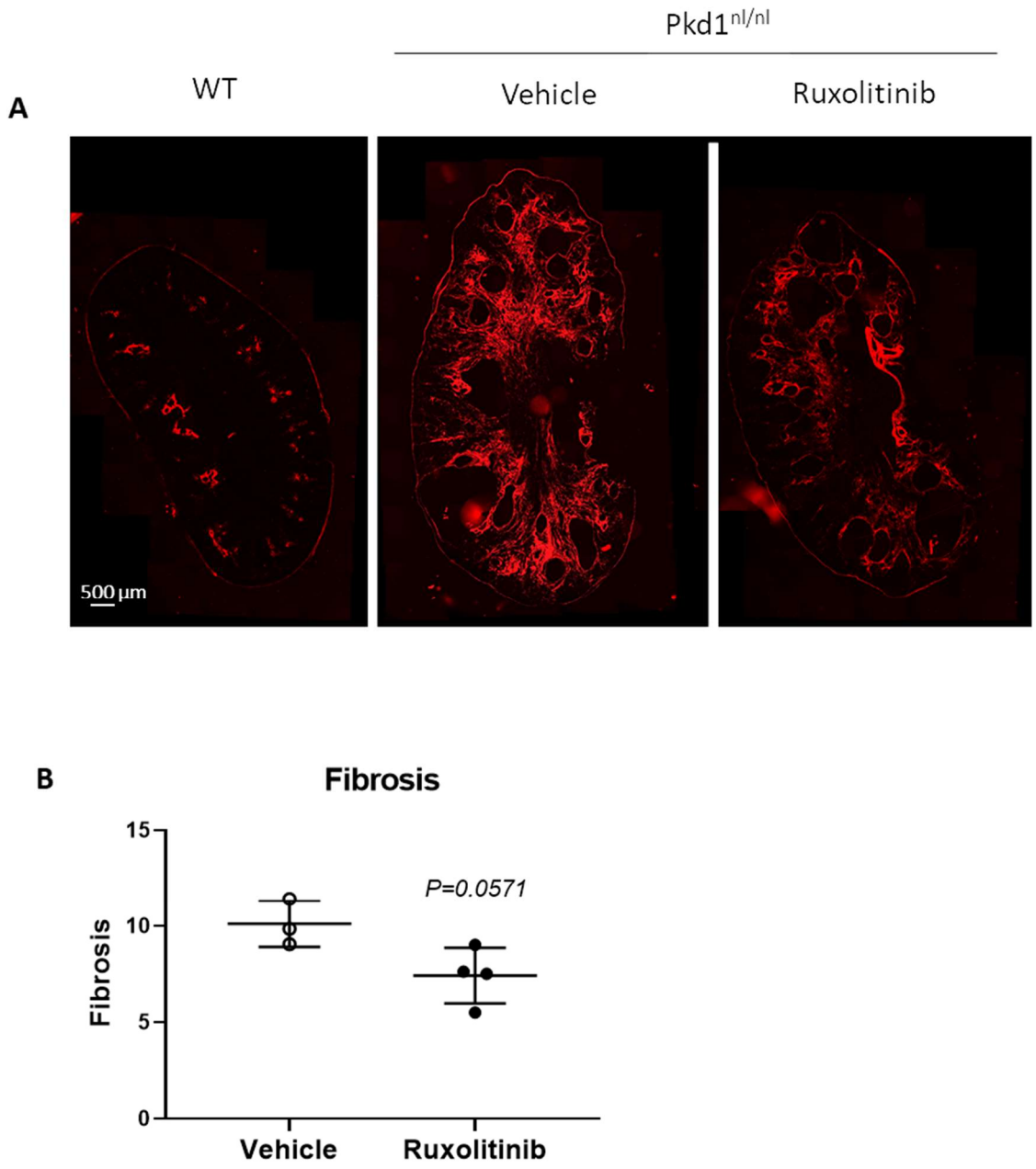

Figure 5.10 Ruxolitinib reduces fibrosis in Pkd1$^{nl/nl}$ mice

(A) Representative images of fibrosis from polarised light of picrosirius red stained kidneys from WT and Pkd1nl/nl treated with vehicle control or 50 mg/kg Ruxolitinib. (B) Fibrosis (%) red measured with ImageJ) is reduced with Ruxolitinib treatment (50 mg/kg) (N=4) compared to vehicle control (N=3) in Pkd1$^{nl/nl}$, (Each plot point represents an individual mouse. Mean ±SD is plotted. A Mann-Whitney non-parametric t-test was used to examine statistical significance.

5.5 Discussion

5.5.1 General overview

In this chapterthe impact of inhibiting growth hormone signalling upstream and downstream of the growth hormone receptor (GHR) was assessed for its effect on progression of ADPKD in a genetically orthologous *in vivo* model of disease through dosing $Pkd1^{nl/nl}$ mice with either 1 mg/kg Octreotide at ages 4-6 weeks, 50 mg/kg at ages 6-8 weeks, or vehicle controls alongside wild-type (WT) littermate controls. Upstream inhibition of GH signalling with Octreotide reduced the total circulating levels of GH, though it did not significantly reduce renal hypertrophy assessed as kidney weight: body weight ratio (KW:BW), or renal damage assessed using serum blood urea nitrogen (BUN). Downstream inhibition of GH signalling with the JAK1/JAK2 inhibitor Ruxolitinib in a novel study testing Ruxolitinib as a treatment in an *in vivo* ADPKD model revealed a trend in reduction of KW:BW and BUN in $Pkd1^{nl/nl}$ mice compared to vehicle controls.

There appeared to be minimal impact on cyst development and cystic growth assessed using cystic index of the kidney in $Pkd1^{nl/nl}$ mice treated with Octreotide compared to vehicle controls. Nonetheless, there was a modest trend in reduction in fibrosis with Octreotide treatment. Similarly, despite Ruxolitinib-treated $Pkd1^{nl/nl}$ mice displaying little change in cystic index, a moderate reduction in fibrosis approaching significance was observed compared to vehicle controls.

Interestingly, renal expression of the GHR is significantly higher in the cortical regions of $Pkd1^{nl/nl}$ mice compared to WT, particularly in the proximal tubular region, and the GHR

expression does not appear to be impacted by Octreotide treatment even though circulating GH is lowered.

5.5.2 Effects of Octreotide treatment on progression of ADPKD in *Pkd1 nl/nl* mice

The somatostatin analogue Octreotide directly suppresses pituitary secretion of growth hormone as well as hypothalamic release of growth hormone releasing hormone (Masuda *et al*., 1989). Though Octreotide at the dose and time point tested in this chapter did not significantly alter progression of ADPKD in the $Pkd1^{nl/nl}$ mouse model, Octreotide has previously been shown to reduce hepato-renal cystorgenesis and hypertrophy in preclinical PKD rodent models (Masyuk *et al*., 2007; Masyuk *et al*., 2013).

In clinical trials, Octreotide initially slowed renal hypertrophy after one year, shown by reduced total kidney volume conpared to placebo controls, but by three years there was no significant difference in TKV between the treatment and control groups, (Caroli *et al*., 2013). In a follow up study, TKV was significantly lowered at one and three years in the Octreotide-treated group, but did not significantly affect estimated glomerular filtration rate (eGFR) decline in patients with later stage kidney disease, though progression to end stage renal failure (ESRF) was reduced with Octreotide treatment (Perico *et al*, 2019). The renoprotective effect of Octreotide is thought to be due to its inhibitory effects on adenosine 3',5'-cyclic monophosphate (cAMP) via binding the Gi protein-coupled somatostatin receptors (SSTRs) (Hogan *et al*., 2010). It has been suggested that the reason the beneficial effects of Octreotide may be negated with long-term treatment is due to downregulation of SSTRs (Lin *et al*., 2018). A relatively recent meta-analysis of somatostatin analogues in ADPKD concluded that somatostatin analogues effectively

reduce TKV in ADPKD, nonetheless there was no overall improvement in eGFR (Griffiths et al., 2020). This indicates that although TKV is an accepted renal function biomarker for prognosis by regulatory bodies such as the European Medicines Agency (EMA) and Food and Drug Agency (FDA) (Perrone et al., 2017), reduction in TKV does not necessarily equal protection of renal function.

In addition to Octreotide, alternative somatostatin analogues have been tested in ADPKD including lanreotide and pasireotide (Kugita et al., 2017, Masyuk et al., 2013, Gevers et al., 2015).

It has been postulated that the renoprotective mechanism of action in successfully slowing progression of disease that has been observed with somatostatin analogue treatment is the same as the vasopressin receptor antagonist tolvaptan, namely reduction of intracellular cAMP (Hogan et al., 2010). Intracellular cAMP has a demonstrable role in pathogenic ADPKD mechanisms such as proliferation and cystogenesis (Yamaguchi et al., 1997, Yamaguchi et al., 2000, Hanaoka and Guggino, 2000) and both tolvaptan and Octreotide effectively lower cAMP (Masyuk et al., 2007, Gattone et al., 2003). In a hypomorphic *PKD1* model pasireotide and tolvaptan independently reduced cystic growth and in combination had an additive effect in delaying disease progression with significant reduction in cystic and fibrotic volume (Hopp et al., 2015). Clinical trials to examine the efficacy of combined treatment of tolvaptan and Octreotide-LAR in a clinical setting are ongoing (https://clinicaltrials.gov/ct2/show/NCT03541447, July 2021). Whilst the additive renoprotective effect of combined treatment could be solely due to the impact of each drug on cAMP being more thorough and robust, alternatively, it could indicate

mechanisms beyond the effects of cAMP involved in slowing disease progression such as inhibition of growth hormone release and downstream growth hormone signalling.

The purpose of the Octreotide *in vivo* experiments performed in this chapter were to reexamine the mechanism of Octreotide in ADPKD progression through the lens of its impact on growth hormone as opposed to its actions on SST receptors and cAMP, though the two cannot be uncoupled. A significant reduction in circulating GH was observed when normalised to body weight in Octreotide-treated $Pkd1^{nl/nl}$ mice compared to vehicle controls and there did appear to be a trend toward positive correlation between circulating GH levels and cystic index of the kidney. Despite this the parameters of renal hypertrophy, function, cystogenesis and fibrosis were not significantly altered with Octreotide treatment at the dose given and the timepoint studied which opposes what has previously been described for Octreotide in other preclinical rodent models of ADPKD.

The Pkd1 neolox mouse used in my *in vivo* studies is advantageous as it is genetically orthologous to human ADPKD. These mice exhibit rapid development of disease which is a double-edged sword as only a short period of time required to develop advanced disease can be useful in as it allows for time-efficient research, but also has the disadvantage of being difficult to reach an early enough timepoint with drug treatments to impede disease progression. Octreotide has not previously been tested in this preclinical ADPKD mouse model in published data which may, in part, account for the discordant lack of effect observed in slowing ADPKD progression in the $Pkd1^{nl/nl}$ mouse compared to previous published data. Nonetheless, the impact of Octreotide on growth

hormone and growth hormone signalling as a potential contributor in the efficacy of delaying ADPKD progression in previous published studies should not be discounted.

5.5.3 GHR expression in Pkd1$^{nl/nl}$ mice and the impact of Octreotide treatment

Immunofluorescent staining displays that renal GHR expression appears to be upregulated in the cortical regions of Pkd1$^{nl/nl}$ kidneys versus WT, particularly in the proximal tubular region and in cyst lining cells. One might speculate that the elevation of renal GHR expression observed in Pkd1$^{nl/nl}$ kidneys versus WT could be associated with the increase in serum growth hormone that is also observed between these two groups which cannot be ruled out at this stage. In opposition of this hypothesis is that there is no observable reduction in GHR expression in Pkd1$^{nl/nl}$ kidneys treated with Octreotide compared to vehicle controls despite reduction in circulating growth hormone.

Nevertheless, even though the cause of upregulated renal GHR in this ADPKD model is unknown, it is possible that it contributes towards increased GH signalling within the kidney which would require further exploration.

5.5.4 Ruxolitinib reduces renal hypertrophy and protects renal function in Pkd1$^{nl/nl}$ mice

As the JAK1/Jak2 inhibitor Ruxolitinib displayed the ability to modulate GH-induced proliferation and cystogenesis *in vitro* as shown in chapter 4, the efficacy of Ruxolitinib

was tested *in vivo* to assess its ability in slowing progression of disease. There was a trend towards reduced renal hypertrophy and protection of renal function with lower KW:BW and BUN in Ruxolitinib-treated $Pkd1^{nl/nl}$ mice compared to vehicle controls. However, the N numbers are too low to see statistical significance, power calculations based on the BUN values between treatment groups of $Pkd1^{nl/nl}$ mice estimates that each treatment group requires N=7 for statistical power. As observed with Octreotide treatment, Ruxolitinib treatment does not significantly alter the cystic index compared to vehicle controls. Nevertheless, there is a clear trend towards modest reduction in fibrosis with Ruxolitinib treatment which approaches statistical significance compared to vehicle controls. Together the reduction in fibrosis and BUN illustrates the potential for Ruxolitinib in protecting renal function.

The trend of reduced fibrosis and BUN despite no change in cystic index suggests that fibrosis may be a larger contributor to renal function decline, at least in this mouse model at this stage of disease.

The mechanism underlying the observed reduction in fibrosis is currently unknown. Fibrosis is a process of excessive accumulation of extracellular matrix proteins such as collagen in response to injury due to either reduction in matrix production or induction of matrix breakdown (Herrera et al., 2018). Growth hormone has been shown to induce epithelial to mesenchymal transition (EMT) wherein epithelial cells transdifferentiate into fibroblasts, leading to fibrosis progression due to increased matrix production (Kalluri and Weinberg, 2009, Brittain et al., 2017). This offers a possible mechanism through which growth hormone contributes towards fibrosis and Ruxolitinib reduces fibrosis through inhibition of GH signal transduction.

5.5.5 Conclusion

In summary, the elevated levels of circulating growth hormone and renal growth hormone receptor expression in cyst-lining cells in a model of ADPKD highlights the potential contribution of GH-GHR signalling towards ADPKD pathogenesis and progression in an *in vivo* setting. Moreover, inhibition of GH-GHR-JAK2 signalling with the use of somatostatin analogues or Ruxolitinib show potential in reducing renal fibrosis and protecting renal function.

5.6 Supplemental figures

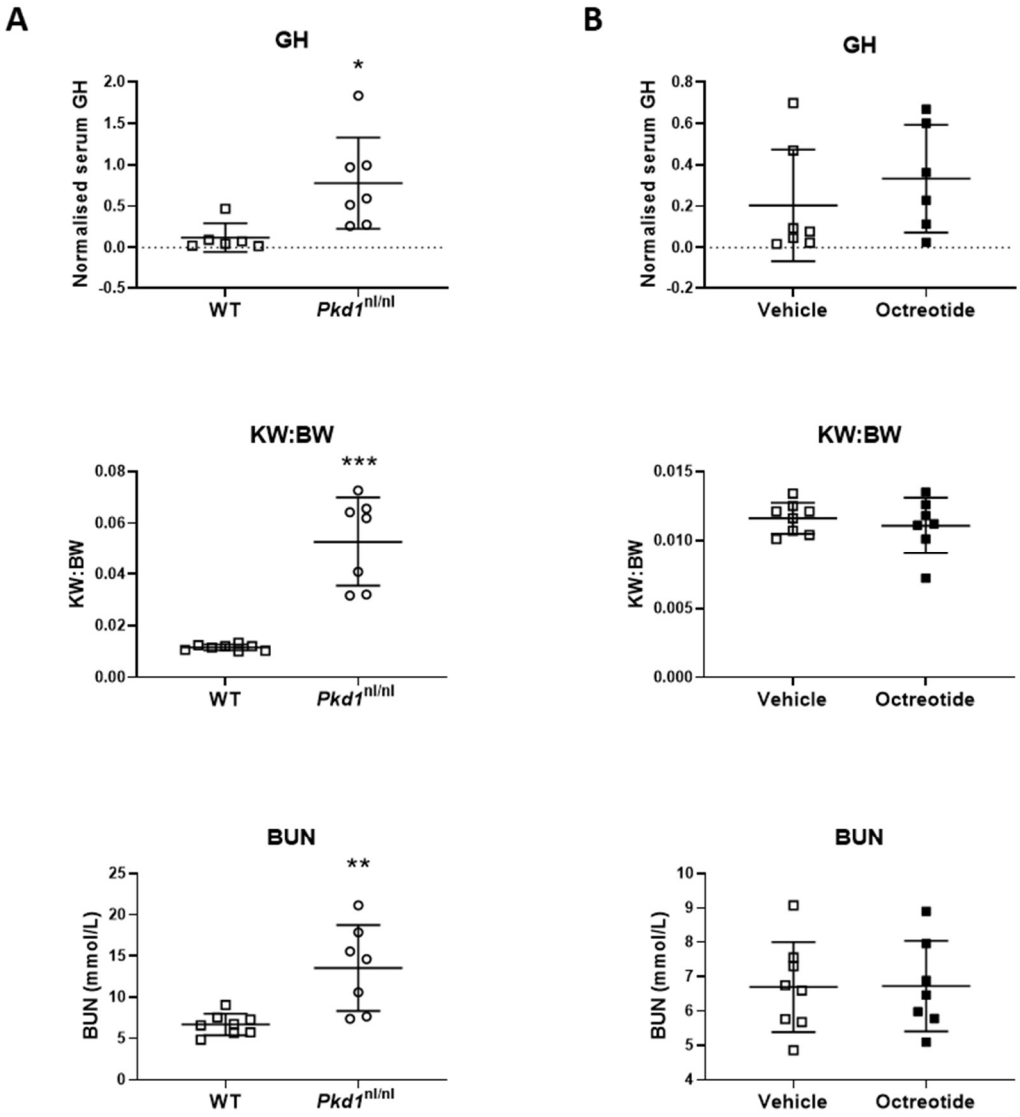

Supplemental figure 3: Genotype differences of untreated WT and Pkd1$^{nl/nl}$ mice and Octreotide treatment in WT mice

(A) Genotype differences in serum growth hormone (GH), kidney weight to body weight ratio (KW:BW) and blood urea nitrogen (BUN) of saline treated WT (N=8) and Pkd1$^{nl/nl}$ mice (N=7) shows the increase of all parameters in Pkd1$^{nl/nl}$ mice compared to WT. (B) Octreotide treatment in WT mice (N=7) has no impact on GH, KW:BW, or BUN compared to vehicle controls(N=8).

Chapter 6: Discussion

Autosomal dominant polycystic kidney disease (ADPKD) pathogenesis involves dysregulation of multiple cellular signalling pathways as a result of disruption to polycystin function. Defining the specific pathogenic signalling pathways and their influence in disease development and progression is an ongoing process.

Aberrant upregulation of circulating growth hormone and activated nuclear STAT5 alongside increased JAK2 expression has been observed in models of ADPKD (Fragiadaki et al., 2017, Patera et al., 2019), suggesting that GH-GHR-JAK2-STAT5 signalling is dysregulated in ADPKD and could be contributing towards pathogenesis.

The main objectives of the thesis were firstly to produce recombinant growth hormone analogues capable of either inducing or inhibiting growth hormone receptor signal transduction with the use of wild-type or mutant GHR antagonist analogue, respectively. The second aim was to investigate the effects of modulation of GH-GHR-JAK2-STAT5 signalling in *in vitro* models of PKD and examine the subsequent impact on proliferation and cystogenesis. The final objective was to analyse the impact of inhibition of GH-GHR-JAK2-STAT5 in an *in vivo* model of PKD and subsequent effect on cyst development, fibrosis, renal hypertrophy and renal function.

6.1 Expression, purification, and validation of bioactive recombinant growth hormone analogues

Analogues of the ~22 kDa isoform of human and mouse growth hormone were produced in bacterial and mammalian expression systems, respectively. Substitution of glycine to arginine, at the 120 position in hGH and the 118 position in mGH, in receptor binding site 2 of growth hormone generates a mutant growth hormone analogue which results in receptor antagonism. It was previously reported by Chen *et al* and Nass *et al* that the GH mutants Gly120Arg (human) and Gly118Arg (mouse) were unable to bind to one molecule of a GHR dimer, but still bind to the other GHR molecule of the dimer through receptor binding site 1, resulting in a competitive inhibitor of GHR (Chen et al., 1990, Nass et al., 2000a). While the specifics of the physical binding of the GH antagonist were not confirmed, their ability to inhibit GH-triggered signalling was examined, and it was demonstrated that they can potently inhibit STAT5 phosphorylation. In addition, the hGH-m12 recombinant protein was expressed which contains the Gly120Arg mutation but carries eight additional mutations at site 1 which increases its binding affinity to the receptor, making it a more potent inhibitor of GH. Furthermore, mGH-Gly118Arg fused to mouse growth hormone binding protein (mGHBP) was subcloned and expressed it as GH fusion to GHBP. This fusion protein was produced as the human analogue was previously shown to improve stability and delay clearance (Wilkinson et al., 2016), though this was not produced in large enough quantities for further testing.

The recombinant WT GH analogues were capable of inducing STAT5 activity evidenced by (a) increased tyrosine phosphoactivation, which was significantly above untreated

controls (b) increased 5x STAT5 luciferase activity, which reports on the transcriptional activity of STAT5 following GH stimulation and antagonism and (c) enhanced STAT5 target gene expression, specifically IGF1 and CCDN1. All these data together indicated that the laboratory made recombinant wild-type GH and the antagonists were properly refolded and bioactive as they triggered GHR signal transduction in kidney cells. As a similar response was observed in HEK293-GHR cells treated with GH antagonists between the luciferase assay for STAT5 activity and the western blot for pYSTAT5, the pYSTAT5 blot was used for subsequent testing of GH-STAT5 modulation with GH or GHA as a more time and cost-effective approach. The mouse and human GHAs were able to significantly reduce GH-induced STAT5 phosphoactivation in kidney cells. Inhibition of GH-STAT5 signalling with mutant GH analogues has previously been examined with a STAT5 luciferase assay and phosphotyrosine activation of STAT5 (Wilkinson et al., 2016, Petkovic et al., 2007, Maamra et al., 1999, Xu et al., 2011). Taken together, the successful expression of bioactive GH analogues with a proven capacity to modulate STAT5 activity in renal cells has provided the toolkit and necessary components to examine the effects of GH in Autosomal Dominant Polycystic Kidney Disease *in vitro* and *in vivo* models.

6.2 The effects of stimulation and inhibition of growth hormone signalling in *in vitro* models of ADPKD

The recombinant WT GH analogues were able to induce STAT5 phosphoactivation in relevant cellular models of human or mouse-derived ADPKD renal epithelial cells. The human GHAs significantly reduced GH-stimulated STAT5 phosphoactivation in SKI-001

cells. Meanwhile Ruxolitinib, a JAK inhibitor, was selected as an alternative mechanism of inhibiting GH-JAK2-STAT5 signalling which would corroborate the GH antagonist effects and provide a comparison of effectiveness of the new GH antagonists when compared with Ruxolitinib which is an approved drug with very well known kinetics of JAK/STAT pathway inhibition. As expected from previously published literature (Bartalucci et al., 2017, Nitulescu et al., 2017, Sapre et al., 2019) Ruxolitinib significantly reduced phosphoactivation of STAT5 downstream of GH in the isogenic murine F1 Pkd1 +/+ and F1 Pkd1 -/- cells, suggesting successful disruption of GH-JAK2-STAT5 signalling.

Development of cysts is the definitive hallmark of ADPKD, therefore the impact of stimulating and inhibiting GH signalling was studied using independent cellular models of ADPKD capable of forming cysts in a 3D environment (SKI-001, OX161c1, F1 Pkd1 +/+, and F1 Pkd1 -/-). The *in vitro* cyst assays revealed the novel finding that stimulation of cells with exogenous growth hormone promotes cyst expansion in all four cell types, exceeding the cystic growth of untreated cells over time to a significant degree in the human SKI-001 and OX161c1 cells. Inhibition of GH signalling either through drug treatment of GHA or Ruxolitinib or genetic modulation through GHR or STAT5 knockdown resulted in significant reduction of GH-induced cystic growth which provides strong evidence that GH is promoting cystic growth via the GHR-JAK2-STAT5 pathway.

Hyperproliferation is a key pathological mechanism in ADPKD which contributes towards cyst expansion. Growth hormone signalling via JAK2-STAT5 promotes proliferation through upregulation of pro-proliferative molecules involved in cell cycle progression such as cyclin D1 (CCND1), cyclin D2 (Matsumura et al., 1999, Friedrichsen et al., 2003), and c-MYC (Murphy et al., 1987), or indirectly via insulin-like growth factor 1 (IGF-1)

which promotes proliferation via the IGF1 receptor (Hakuno and Takahashi, 2018). Treatment with exogenous GH resulted in a significant increase in proliferating cells compared to untreated controls, alongside significant upregulation of the pro-proliferative STAT5 targets CCND1 and IGF-1 in human ADPKD models. These findings expand our current understanding of GH signalling and contribute further to the previous understanding that GH (in GH overexpressing transgenic mice) enhanced hepatic proliferation (Miquet et al., 2008). The finding that GH enhances renal cell proliferation in cells with Pkd1 deficiency is consistent with the finding that renal epithelial cells have widespread and diffuse expression of growth hormone receptor and are hence primed to respond to GH. Furthermore, addition of GHA or Ruxolitinib abrogated GH-induced proliferation and STAT5 target expression, suggesting that the effect of GH is directly on the epithelial cells and does not necessarily require hepatic production of IGF-1. Together this provides mechanistic insight into GH-induced cyst expansion via increased proliferation downstream of GH-JAK2-STAT5 signalling.

6.3 Growth hormone inhibition in a preclinical setting of ADPKD

Octreotide, a somatostatin analogue (SSA) has previously been tested in preclinical and clinical trials for ADPKD and was found to be effective in reducing hepatic and renal cystogenesis, total kidney volume and total liver volume, indicating delayed hypertrophy and disease progression, as well as a delay in Octreotide-treated people with ADPKD reaching end stage-renal failure compared to control (Hogan et al., 2010, Masyuk et al.,

2013, Perico et al., 2019, Caroli et al., 2013, Griffiths et al., 2020, Masyuk et al., 2007). Given the variability of response in these clinical trials, the type of PKD mutation that each individual person with ADPKD had was not analysed or presented so it would be interesting to know the type of PKD mutations to gain further understanding of mechanism and potential differences in response to treatment. Octreotide has been shown to lower levels of circulating cyclic AMP (cAMP) in these trials. Indeed, the kidneys express somatostatin receptors and it has been proposed that Octreotide binds kidney somatostatin receptors blocking cAMP release.

Octreotide was tested in a genetically orthologous hypomorphic Pkd1 mouse model to inhibit pituitary growth hormone secretion and examine Octreotide treatment through the lens of growth hormone signalling effects rather than an assumption of cAMP being the mechanism of effect on PKD pathogenesis (Figure 6.1). Octreotide (1 mg/kg) or saline vehicle controls were administered to both $Pkd1^{nl/nl}$ mice and WT littermate controls. The WT mice had no discernible differences in KW:BW and BUN between Octreotide and vehicle groups, indicating the drug is well tolerated without adverse effects on the kidney in healthy mice. Within the $Pkd1^{nl/nl}$ mice Octreotide significantly reduced serum growth hormone levels indicating the drug was effective in reducing pituitary growth hormone secretion.

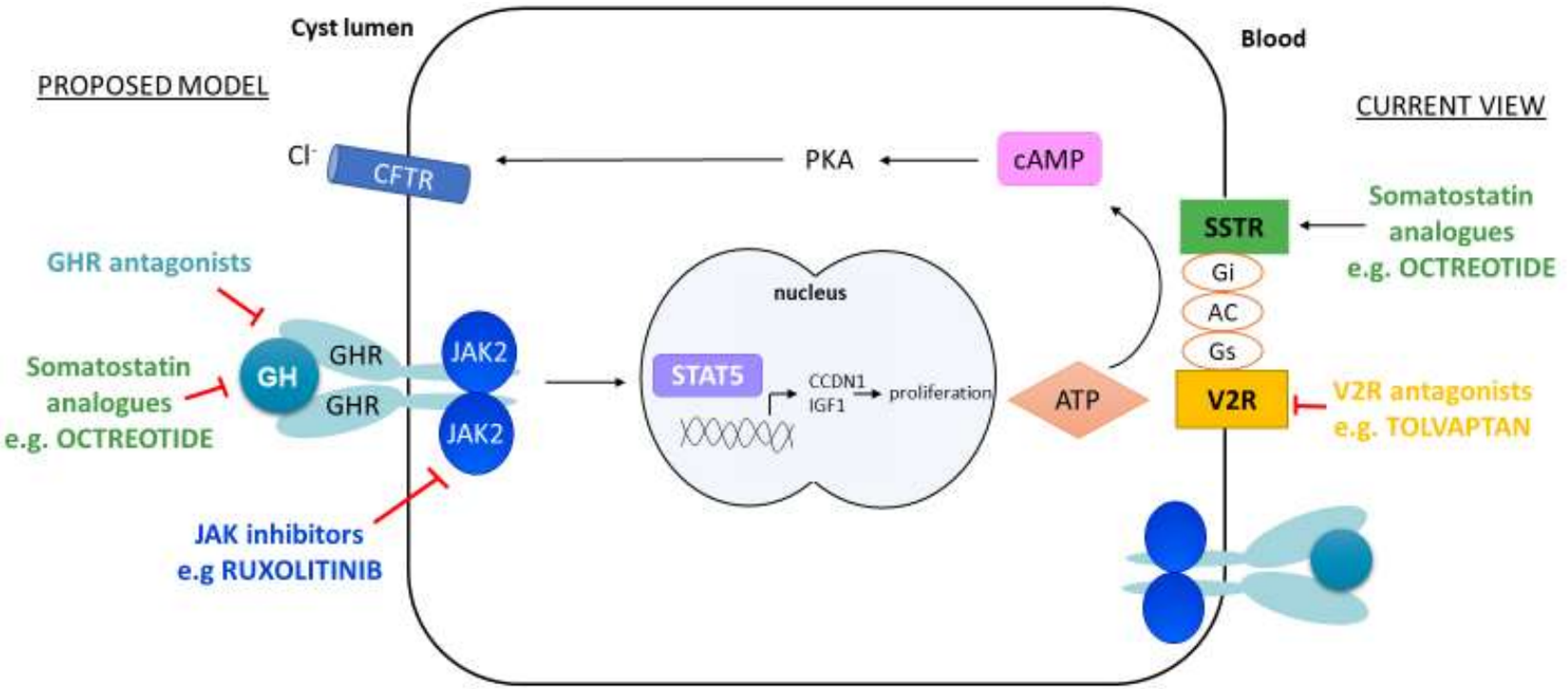

Figure 6.1 The proposed model versus the current view of cystogenic pathways in the kidney

The current view of cystogenic pathways proposes that in ADPKD intracellular cyclic AMP is elevated leading to increased proliferation and luminal fluid secretion via activation of protein kinase A (PKA) and chloride (Cl^-) secretion (Yamaguchi et al., 2000), which is inhibited through antagonism of the Gs-coupled vasopressin 2 receptor (V2R) e.g. with tolvaptan (Torres et al., 2012), or through somatostatin analogues e.g. Octreotide acting on the Gi-coupled somatostatin receptor (SSTR) (Hogan et al., 2010). In this thesis it is proposed that growth hormone (GH) stimulates proliferation via JAK2-STAT5, which is inhibited through growth hormone receptor (GHR) antagonists, JAK inhibitors e.g. Ruxolitinib, or somatostatin analogues inhibiting pituitary GH.

In contrast to what has previously been reported in preclinical rodent ADPKD rodent models treated with Octreotide, there was not a significant impact between treatment groups on the KW:BW, BUN, cystic index or fibrotic index, suggesting Octreotide does not slow disease progression in this particular mouse model at the dose and time point studied. There was a slight downward trend in renal fibrosis in response to Octreotide treatment.

Whilst reduced fibrosis could be a result of reduced circulating growth hormone with Octreotide treatment, as growth hormone has a known role in fibrosis via promoting epithelial to mesenchymal transition, the stratified data analysing the correlation between GH and kidney fibrosis does not support this conclusion. On the other hand, there was a significantly positive correlation between normalised circulating GH and the kidney cystic index of Octreotide-treated males, which suggests that GH is contributing towards renal cystic growth as has been established from my *in vitro* cyst assays.

However, despite the correlation between levels of growth hormone and renal cystic index, reduction of circulating GH with Octreotide did not impact the cystic index, which could suggest that there is a threshold of GH reduction required to affect renal cyst development that was not met, or it could be that the dose and time point of treatment was too advanced to impact the cystic aspect of disease, wherein the 4 week start point of treatment is when the Pkd1 neolox mice are at the peak of disease (Happe et al., 2013).

Ruxolitinib was studied in the same mouse model to further investigate the impact of inhibition of GH signalling, this time targeting downstream of the GHR by inhibiting JAK. The mice were treated at the age of 6 weeks to avoid the 4-week peak of disease but still allow for investigation of the advanced stage of disease. Treatment with Ruxolitinib (50 mg/kg) resulted in a clear trend of moderate reduction in renal hypertrophy and protecting renal

function through a reduction in serum BUN and renal fibrosis which approaches statistical significance compared to vehicle controls. Due to time limitations, including the impact of COVID-19 related restrictions, I was not in a position to increase the n number for Ruxolitinib treated mice. The fact that both Octreotide and Ruxolitinib show a trend in reducing fibrosis provides stronger evidence that the reduction in fibrosis is a result of altered GH signalling.

Despite the improvement in renal function, hypertrophy and fibrosis, cystic index was unaltered with Ruxolitinib treatment, but this could be due to the small number of animals tested and the inherent nature of variability of cystic presentation expected with these mouse models. It is of interest that fibrosis and kidney function show a clearer trend of improvement when compared with cystic index. This poses the question as to the relative contribution of renal hypertrophy, cystic index and renal fibrosis towards renal function decline. As observed in aforementioned Octreotide clinical trials, Octreotide reduced TKV and displayed an overall reduction in the number of patients with ADPKD reaching ADPKD after 3 years, but meta-analysis showed no overall improvement in the eGFR (Griffiths et al., 2020). Additionally, knockdown of STAT3 reduces cystic index but not KW:BW, due to impact on macrophage infiltration (Viau et al., 2020). Together, this suggests that, alongside other factors, KW:BW, cystic index and fibrosis are not invariably simultaneously impacted by treatment.

Yet another point to consider when interpreting the difference in impact of Ruxolitinib on renal fibrosis and cystic index is that it has been suggested that, at least for a time, when fibrosis is established there is regression in cystic growth (Happe et al., 2013). This offers potential explanation toward the dichotomy in renal fibrosis and cystic index in response to Ruxolitinib treatment, as the reduction in fibrosis caused by Ruxolitinib may impact the level of cyst regression whereas untreated mice with higher fibrosis may have increased levels of

cyst regression and so an impact of treatment on cystic index is not captured. Yet there is a clear trend towards improved renal function (as measured by blood urea nitrogen), suggesting that Ruxolitinib treatment and the accompanied reduction in fibrosis are beneficial for kidney function.

It is of interest to mention that Ruxolitinib caused a marked reduction in cystic growth in three dimensional in vitro experiments of renal epithelial cells, suggesting that inhibition of JAK/STAT signalling within renal epithelial cells *per se* is sufficient to reduce their innate ability to proliferate. On the other hand, Ruxolitinib treatment on the mouse model was performed after disease was already established and cysts had already formed, hence a direct comparison between the 2 models cannot be made. Moreover, within a whole organism system there are additional factors at play that may influence cell/cyst responses to any given drug including, drug metabolism, immune response and inflammation, in addition to the potential of compensatory mechanisms through interactions with other cells. For example, STAT3 activation in polycystic kidneys can occur through indirect mechanisms involving macrophages (Viau et al., 2020).

Expression of the growth hormone receptor is significantly increased in the proximal tubular region of kidneys of $Pkd1^{nl/nl}$ mice compared to WT mice. Importantly, GHR is expressed in cyst lining cells of the kidney. This data in combination with previous reported data of elevated expression of JAK2 (Patera et al., 2019), nuclear STAT5 and expression of cyclin D1 (Fragiadaki et al., 2017) in cyst lining renal epithelial cells of the $Pkd1^{nl/nl}$ mouse, and the *in vitro* data in SKI-001, provides supporting evidence that GH-GHR-JAK2-STAT5-CCND1 signalling is dysregulated in ADPKD and contributed towards pathogenesis.

6.4 Limitations

One of the limitations of this study is genetic variability within ADPKD and its effect on pathogenesis and cellular response which may not be fully represented within the scope of this study, though this was mitigated by use of a variety of cellular ADPKD models.

There is also the potential genetic drift with immortalised cellular ADPKD models over time and number of passages, which opens the possibility of deviating from the original genotype and introducing other genetic factors that could play a role in cellular response. The immortalised cell lines of cystic human renal epithelial cells may behave differently to primary cystic renal epithelial cells *in situ*. The use of several different ADPKD-derived cell lines helps mitigate the risk. Moreover, my conclusions were based on combined used of robust *in vitro* and *in vivo* models allowing me to examine the effects of GH inhibition using multiple models.

The Pkd1neolox mouse model is orthologous genetically to human ADPKD, but the severe and rapid onset of disease is different from what we see in humans wherein disease becomes more severe in middle age. Although because of the rapid onset of disease this was a pragmatic choice for a rodent model of PKD.

6.5 Future work

6.5.1 Cellular and animal studies

Future directions to build upon the work described in this thesis would be to express high levels of mouse growth hormone receptor antagonist and test the robust efficacy in cellular

and *in vivo* models of ADPKD in slowing disease progression. To ensure robust efficacy and that the effects observed within the Pkd1 neolox mouse model are not specific to this mouse model other models would need to be tested. Moreover, to test inhibition of growth hormone signalling in alternative rodent models and to take treatments forward into rabbits, non-human primates and then clinical trials to further test efficacy and toxicity.

It would be interesting to examine inhibition of the GH-GHR-JAK2-STAT5 axis at different levels of the signalling pathway (e.g. compare GH antagonism with Ruxolitinib) and to look at the effects on progression of disease to determine which method of inhibition has higher efficacy. *In vivo* genetic loss of STAT5 (i.e. kidney specific STAT5 knockout mice crossed with Pkd1 knockout) could be used to examine causal pathogenicity of STAT5. Even though genetic deletion of STAT5 is not going to provide a potential drug it will be a way to genetically determine its role in driving disease progression. If STAT5 was found to be a driver of ADPKD the newly generated STAT5 small molecule inhibitors may be worth testing in the ADPKD mouse models in addition to Octreotide and Ruxolitinib.

Additionally, the effect of combination of treatments could be tested to examine whether there is an additive benefit and establish whether the effects of Octreotide are indeed only via cAMP or alternative pathways (e.g. inhibition of JAK/STAT). Combination treatment of tolvaptan and Ruxolitinib or GHR antagonism could also be tested to examine whether there is a an additive benefit as has been performed for tolvaptan and Octreotide which has demonstrated additive renoprotective effects (Hopp et al., 2015).

Another future direction could be to investigate the effect of growth hormone on progression of disease not just in kidneys, but on extrarenal symptoms such as cardiovascular, liver and

spleen size. My study identified Ruxolitinib as a drug able to reduce the splenic size of ADPKD mice, this could be a beneficial effect that could be studied further.

6.5.2 Understanding the mechanism behind the increase in GH signalling and its impact on ADPKD pathogenesis

The findings presented within this thesis clearly show that growth hormone promotes proliferation and cystic growth, and in Pkd1-deficient mice (murine ADPKD model) growth hormone and downstream signalling is elevated compared to wild-type littermate controls. This provides a foundation to further explore the mechanism behind the increase in circulating growth hormone and expression of GHR in the cortical region of polycystic kidneys observed in the ADPKD model, whether this finding is seen in alternative models of ADPKD, and most importantly whether this is observed within human ADPKD is currently unknown and certainly worth further investigation.

It is worthwhile to comment on the fact that elevated circulating GH levels could be due to either an increase in GH production and/or a reduction in GH clearance by the kidneys. As the circulating levels of growth hormone are elevated, this points towards pituitary-secreted growth hormone as opposed to kidney-specific autocrine/paracrine growth hormone. There is currently no data on polycystin expression in the pituitary gland, though polycystin 2 expression in the pituitary has been reported in mice (Markowitz et al., 1999), so how pathogenic mutations in PKD genes or modifier mutations impact pituitary release of hormones (e.g. growth hormone, vasopressin) is unclear.

There is also the possibility that an increase in pituitary release is at the hypothalamic level. Though there is no data on hypothalamic expression of polycystins, an effect of ADPKD within

the brain has been observed with the formation of intracranial subarachnoid cysts (Krauer et al., 2012). Given that the elevated growth hormone is seen in serum, this could indicate modulation of GH release at the pituitary level. Hypothalamic growth hormone releasing hormone (GHRH) induces growth hormone release through binding to pituitary somatotroph GHRH receptors, leading to activation of adenylyl cyclase and production of cAMP, subsequently activating protein kinase A and influx of calcium, wherein increased cAMP and Ca^{2+} stimulates GH exocytosis (Holl et al., 1988, Draznin et al., 1988). Of note, polycystin mutation aberrantly increases cAMP, so whether this happens in the pituitary and could result in non-canonical release of GH from somatotrophs is unclear.

Alternatively, or perhaps in addition to increase in production of GH, reduction in GH clearance may contribute towards elevated serum GH. The kidney is the major organ of metabolic clearance of GH, and with chronic renal failure elevated levels of GH have been observed (Cameron et al., 1972). Renal function decline in ADPKD may lead to reduced GH clearance and subsequent accumulation of GH, leading to persistent longer-lasting impact of GH. As GH signalling has been shown to elevate proliferation and cystic growth *in vitro* and appears to influence fibrosis *in vivo*, all of which contribute towards renal function decline, GH may be exacerbating and accelerating disease progression in a positive feedback loop of renal function decline and GH accumulation. This is reflected by data from Fragiadaki *et al*., wherein older mice at a more advanced stage of disease at 10 weeks of age showed nearly double the levels of serum GH of 5 week old $Pkd1^{nl/nl}$ mice (Fragiadaki et al., 2017), indicating the increase in GH as kidney function declines.

The systemic effect of elevated GH is likely insufficient to cause cystic disease on its own, though people with acromegaly and transgenic GH overexpressing mice exhibit structural

changes to the kidney such as tubular dilatation and in a small number of cases formation of cysts (Fragiadaki et al., 2017, von Waldthausen et al., 2008, Yamamoto et al., 2016). On the other hand people with PKD that have renal transplantation do not develop cystic kidney post-transplantation (Kanaan et al., 2014). Thus, growth hormone on its own is not enough to fuel disease, but in already diseased kidney it may promote progression of disease in cells that have lost Pkd1 expression.

In addition to understanding the mechanism upstream of GH elevation, unpicking the precise mechanisms at play downstream of GH signalling through STAT5 in disease pathogenesis could be further explored. As an initial high throughput step, microarray analysis or next-generation RNA sequencing of STAT5 silenced ADPKD cells could be investigated to determine the impact on cellular signalling and mechanisms.

How the impact of growth hormone-STAT5 signalling links with IGF-1 in ADPKD requires further investigation, particularly as to whether the impact of modulation of GH signalling is dependent or independent of IGF-1 in ADPKD. IGF-1 is an established mediator of growth hormone activity and a known transcriptional target of STAT5 (Davey et al., 2001), corroborated by my data showing increased IGF-1 expression in response to GH stimulation in human-derived ADPKD renal epithelial cells in chapter 4. IGF-1 has been implicated in ADPKD pathogenesis, where deficiency in polycystin 1 was linked with an increase in cellular IGF-1 sensitivity, and subsequent IGF-1 induced hyperproliferation of cystic cells dependent on Ras/Raf- signalling (Parker et al., 2007). Furthermore IGF-1 expression is elevated in cystic lesion of a nonorthologous murine ADPKD mouse model (Nakamura et al., 1993). Though IGF-1 involvement in ADPKD pathogenesis may be downstream of GH, regulation of IGF-1

signalling in ADPKD has been associated with the metalloproteinase pregnancy associated plasma protein A (PAPP-A) resulting in cleavage of IGF-1 from IGF-1 binding protein resulting in increased IGF-1 bioactivity (Kashyap et al., 2020).

GH may also be influencing pathogenesis and progression of ADPKD independently of IGF-1, through alternative pro-proliferative STAT5 transcriptional targets such as cyclin D1 and c-MYC. The oncogenic transcription factor c-MYC is a downstream target of STAT5 which, when overexpressed in mice induces polycystic kidney disease (Trudel et al., 1998, Trudel et al., 1991), though a number signalling pathways and transcription factors have been demonstrated to regulate c-MYC in ADPKD (Cai et al., 2018, Lee et al., 2020).

Super enhancers (SEs) are clusters of enhancers that drive robust expression through higher density of transcriptional machinery and stronger binding. Super enhancers have been shown to undergo remodelling in PKD, resulting in considerable reprogramming of cellular metabolic processes during cystogenesis (Mi et al., 2020). The precise upstream signalling and activating transcription factors involved in alterations in the SE landscape in PKD is currently unknown. Li *et al*. have demonstrated that cytokines can induce STAT5 binding at SEs, with STAT5-mediated chromatin looping within SE-regulated genes (Li et al., 2017). This suggests a possibility of dysregulation of cytokine-induced STAT5 to alter the SE landscape in ADPKD, as a potential mechanism of STAT5-mediated pathogenesis, although the role of STAT5 with SEs in PKD is unknown. It would be interesting to explore the precise SE-associated transcripts that STAT5 associates with, whether this differs between healthy kidneys and ADPKD, and if STAT5 contributes towards SE-mediated metabolic reprogramming in ADPKD.

Together this highlights multiple future directions of study to provide mechanistic insight into GH-JAK2-STAT5 dysregulation in ADPKD pathogenesis.

6.5.3 The role of SNPs

Disease severity of ADPKD can be modified by single nucleotide polymorphisms (SNPs) which has been explored in a number of genes (Magistroni et al., 2003, Lee et al., 2003, Ramanathan et al., 2014, Lee et al., 2002, Liu et al., 2010). This opens up the possibility of SNPs in GH-GHR-JAK2-STAT5 potentially modifying ADPKD disease severity and impacting the phenotypic variability observed in ADPKD.

Polymorphisms in the GHR affect responsiveness to GH, for example an isoform of the GHR gene lacking exon 3 has up to 2 times higher growth acceleration in response to growth hormone compared to full length GHR (Dos Santos et al., 2004). SNPs involved in GH signalling have been associated with the risk of developing various cancers which, like ADPKD, is a disease driven by aberrant proliferation (Wagner et al., 2007, Le Marchand et al., 2002, Shi et al., 2014). Polymorphisms in the GHR and/or GH could potentially impact the contribution of GH signalling in ADPKD pathogenesis and the response to a GH inhibition, which may require a more personalised approach to treatment.

Interestingly, somatotroph pituitary adenomas with resulting GH production and acromegaly have been observed in a small number of cases of people with ADPKD (Otani et al., 2021, Ruggenenti et al., 2005, Syro et al., 2012). One of which was related to a polymorphism in the somatostatin receptor SSTR5, which the authors hypothesise there is a causal relationship between the somatotroph adenoma and ADPKD due to the proximity of SSTR5 and ADPKD on chromosome 16 (Syro et al., 2012).

6.6 Concluding statements

In this thesis I have demonstrated that growth hormone contributes towards significantly enhanced cell proliferation and cystogenesis in ADPKD via activating JAK2-STAT5 signalling, supporting the body of evidence that dysregulation of GH-GHR-JAK2-STAT5 plays a role in promoting ADPKD pathogenesis. Stimulation of human cystic cells with exogenous GH resulted in significantly increased expression of pro-proliferative STAT5 target genes, proliferation and cystic growth, which was blocked through GHR antagonism or JAK2 inhibition. My work has identified that GH affects kidney pathophysiology directly by enhancing JAK/STAT signalling. Inhibition along the GH/JAK2 axis in human cellular models of ADPKD and Pkd1 deficient mice has provided some evidence of renoprotection in the context of ADPKD. This provides a basis for targeting GH-JAK2-STAT5 signalling as novel treatments to be further explored in delaying progression of ADPKD.

APPENDIX

A Vectors

A.1 The pet21a+ circular plasmid vector map.

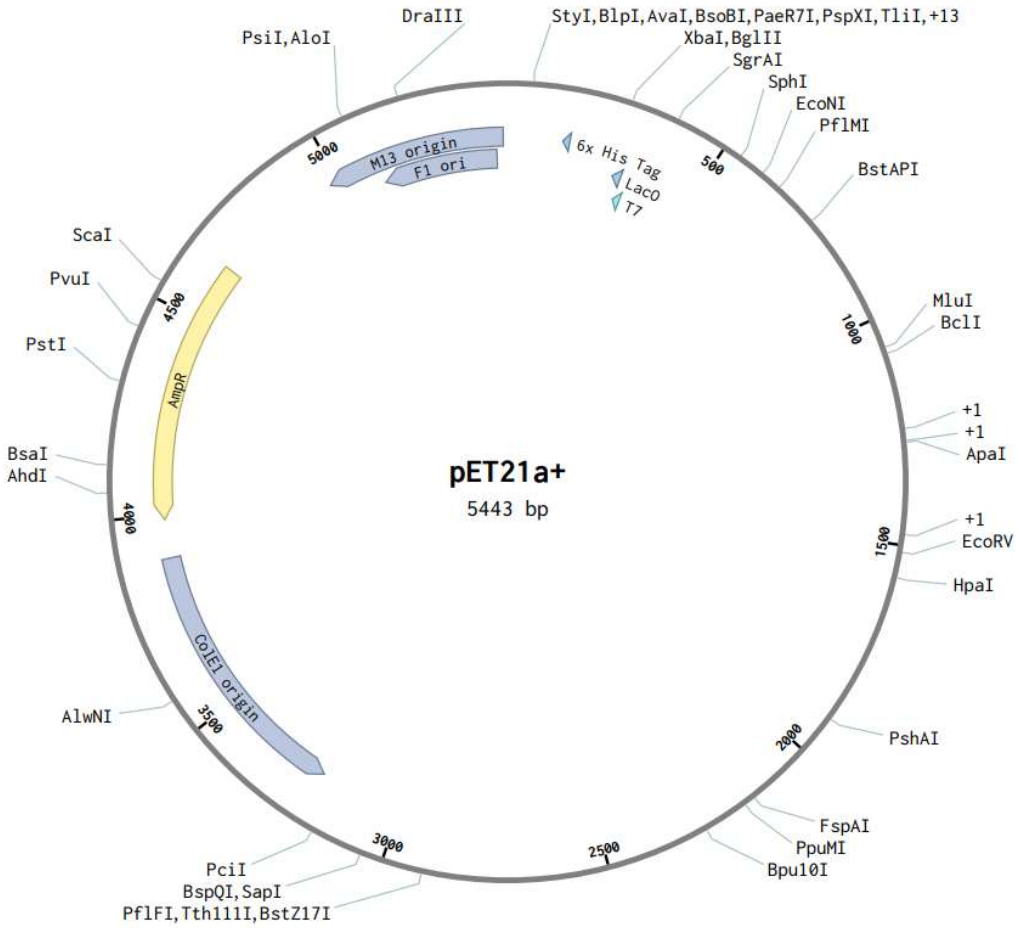

A.2 The pCEP4 circular plasmid vector map.

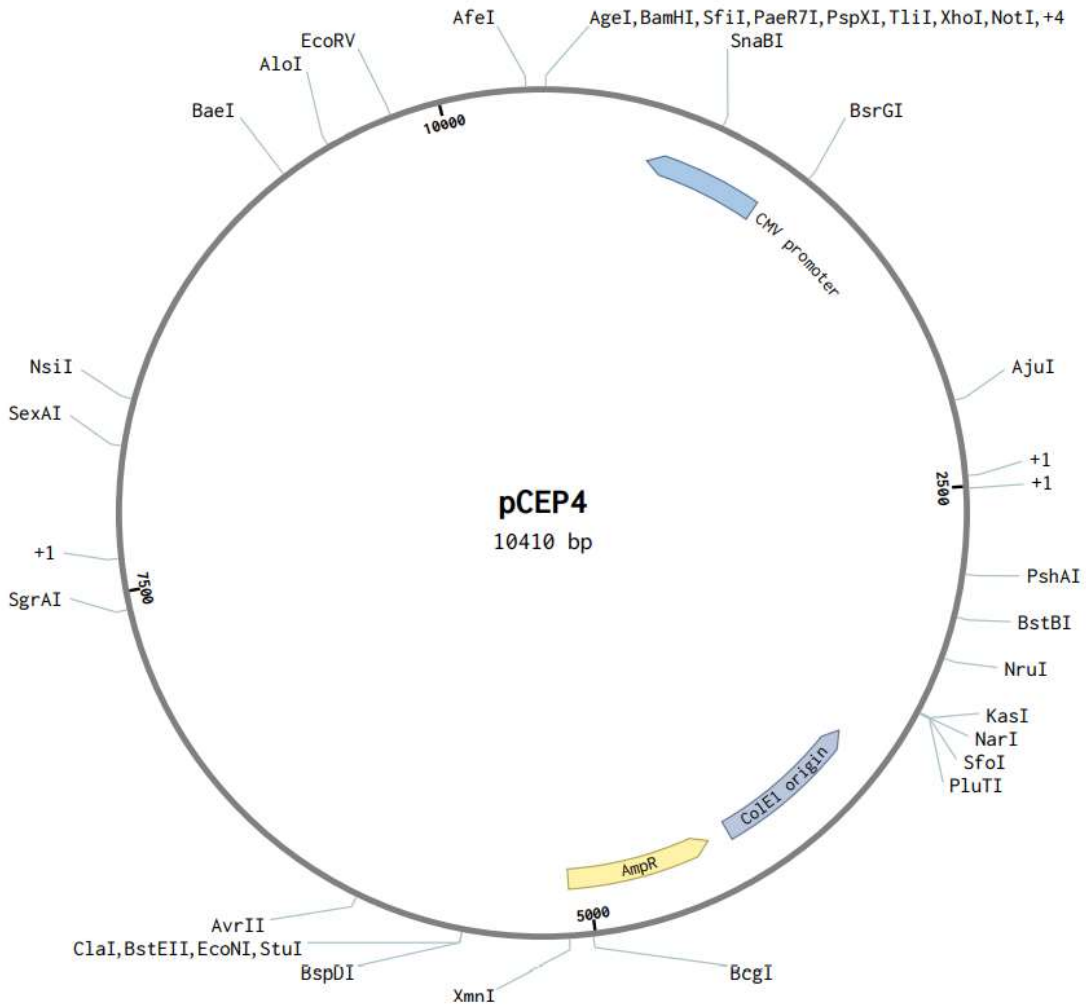

B Protein and DNA sequences

B.1 Amino acid and nucleotide sequence of recombinant hexahistidine-tagged wild-type human growth hormone.

```
atg ttc cca acc att ccc tta tcc agg ctt ttt gac aac gct atg ctc cgc gcc cat cgt
 M   F   P   T   I   P   L   S   R   L   F   D   N   A   M   L   R   A   H   R
ctg cac cag ctg gcc ttt gac acc tac cag gag ttt gaa gaa gcc tat atc cca aag gaa
 L   H   Q   L   A   F   D   T   Y   Q   E   F   E   E   A   Y   I   P   K   E
cag aag tat tca ttc ctg cag aac ccc cag acc tcc ctc tgt ttc tca gag tct att ccg
 Q   K   Y   S   F   L   Q   N   P   Q   T   S   L   C   F   S   E   S   I   P
aca ccc tcc aac agg gag gaa aca caa cag aaa tcc aac cta gag ctg ctc cgc atc tcc
 T   P   S   N   R   E   E   T   Q   Q   K   S   N   L   E   L   L   R   I   S
ctg ctg ctc atc cag tcg tgg ctg gag ccc gtg cag ttc ctc agg agt gtc ttc gcc aac
 L   L   L   I   Q   S   W   L   E   P   V   Q   F   L   R   S   V   F   A   N
agc ctg gtg tac ggc gcc tct gac agc aac gtc tat gac ctc cta aag gac cta gag gaa
 S   L   V   Y   G   A   S   D   S   N   V   Y   D   L   L   K   D   L   E   E
ggc atc caa acg ctg atg ggg agg ctg gaa gat ggc agc ccc cgg act ggg cag atc ttc
 G   I   Q   T   L   M   G   R   L   E   D   G   S   P   R   T   G   Q   I   F
aag cag acc tac agc aag ttc gac aca aac tca cac aac gat gac gca cta ctc aag aac
 K   Q   T   Y   S   K   F   D   T   N   S   H   N   D   D   A   L   L   K   N
tac ggg ctg ctc tac tgc ttc agg aag gac atg gac aag gtc gag aca ttc ctg cgc atc
 Y   G   L   L   Y   C   F   R   K   D   M   D   K   V   E   T   F   L   R   I
gtg cag tgc cgc tct gtg gag ggc agc tgt ggc ttc ctc gag cac cac cac cac cac cac
 V   Q   C   R   S   V   E   G   S   C   G   F   L   E   H   H   H   H   H   H
tga
 -
```

B.2 Amino acid and nucleotide sequence of recombinant hexahistidine-tagged Gly120Arg mutant human growth hormone. Gly120Arg mutation is highlighted in cyan.

```
atg ttc cca acc att ccc tta tcc agg ctt ttt gac aac gct atg ctc cgc gcc cat cgt
 M   F   P   T   I   P   L   S   R   L   F   D   N   A   M   L   R   A   H   R
ctg cac cag ctg gcc ttt gac acc tac cag gag ttt gaa gaa gcc tat atc cca aag gaa
 L   H   Q   L   A   F   D   T   Y   Q   E   F   E   E   A   Y   I   P   K   E
cag aag tat tca ttc ctg cag aac ccc cag acc tcc ctc tgt ttc tca gag tct att ccg
 Q   K   Y   S   F   L   Q   N   P   Q   T   S   L   C   F   S   E   S   I   P
aca ccc tcc aac agg gag gaa aca caa cag aaa tcc aac cta gag ctg ctc cgc atc tcc
 T   P   S   N   R   E   E   T   Q   Q   K   S   N   L   E   L   L   R   I   S
ctg ctg ctc atc cag tcg tgg ctg gag ccc gtg cag ttc ctc agg agt gtc ttc gcc aac
 L   L   L   I   Q   S   W   L   E   P   V   Q   F   L   R   S   V   F   A   N
agc ctg gtg tac ggc gcc tct gac agc aac gtc tat gac ctc cta aag gac cta gag gaa
 S   L   V   Y   G   A   S   D   S   N   V   Y   D   L   L   K   D   L   E   E
cgc atc caa acg ctg atg ggg agg ctg gaa gat ggc agc ccc cgg act ggg cag atc ttc
 R   I   Q   T   L   M   G   R   L   E   D   G   S   P   R   T   G   Q   I   F
aag cag acc tac agc aag ttc gac aca aac tca cac aac gat gac gca cta ctc aag aac
 K   Q   T   Y   S   K   F   D   T   N   S   H   N   D   D   A   L   L   K   N
tac ggg ctg ctc tac tgc ttc agg aag gac atg gac aag gtc gag aca ttc ctg cgc atc
 Y   G   L   L   Y   C   F   R   K   D   M   D   K   V   E   T   F   L   R   I
gtg cag tgc cgc tct gtg gag ggc agc tgt ggc ttc ctc gag cac cac cac cac cac cac
 V   Q   C   R   S   V   E   G   S   C   G   F   L   E   H   H   H   H   H   H
tga
 -
```

B.3 Amino acid and nucleotide sequence of recombinant hexahistidine-tagged B2036/m12 mutant human growth hormone. Gly120Arg is highlighted in cyan, and the site 1 H18D, H21N, R167N, K168A, D171S, K172R, E174S and I179T mutations are highlighted in yellow.

```
atg ttc cca acc att ccc tta tcc agg ctt ttt gac aac gct agt ctc cgc gcc gac cgt
 M   F   P   T   I   P   L   S   R   L   F   D   N   A   S   L   R   A   D   R
ctg aac cag ctg gcc ttt gac acc tac cag gag ttt gaa gaa gcc tat atc cca aag gaa
 L   N   Q   L   A   F   D   T   Y   Q   E   F   E   E   A   Y   I   P   K   E
cag aag tat tca ttc ctg cag aac ccc cag acc tcc ctc tgt ttc tca gag tct att ccg
 Q   K   Y   S   F   L   Q   N   P   Q   T   S   L   C   F   S   E   S   I   P
aca ccc tcc aac agg gag gaa aca caa cag aaa tcc aac cta gag ctg ctc cgc atc tcc
 T   P   S   N   R   E   E   T   Q   Q   K   S   N   L   E   L   L   R   I   S
ctg ctg ctc atc cag tcg tgg ctg gag ccc gtg cag ttc ctc agg agt gtc ttc gcc aac
 L   L   L   I   Q   S   W   L   E   P   V   Q   F   L   R   S   V   F   A   N
agc ctg gtg tac ggc gcc tct gac agc aac gtc tat gac ctc cta aag gac cta gag gaa
 S   L   V   Y   G   A   S   D   S   N   V   Y   D   L   L   K   D   L   E   E
cgc atc caa acg ctg atg ggg agg ctg gaa gat ggc agc ccc cgg act ggg cag atc ttc
 R   I   Q   T   L   M   G   R   L   E   D   G   S   P   R   T   G   Q   I   F
aag cag acc tac agc aag ttc gac aca aac tca cac aac gat gac gca cta ctc aag aac
 K   Q   T   Y   S   K   F   D   T   N   S   H   N   D   D   A   L   L   K   N
tac ggg ctg ctc tac tgc ttc aac gcc gac atg tca agg gtc tca aca ttc ctg cgc aca
 Y   G   L   L   Y   C   F   N   A   D   M   S   R   V   S   T   F   L   R   T
gtg cag tgc cgc tct gtg gag ggc agc tgt ggc ttc ctc gag cac cac cac cac cac cac
 V   Q   C   R   S   V   E   G   S   C   G   F   L   E   H   H   H   H   H   H
tga
 -
```

B.4 Amino acid and nucleotide sequence of recombinant hexahistidine-tagged wild-type mouse growth hormone codon-optimised for use in E. coli.

```
atg ttt ccc gcc atg ccc ttg tcc agt ctg ttt tct aat gct gtg ctc cga gcc cag cac
 M   F   P   A   M   P   L   S   S   L   F   S   N   A   V   L   R   A   Q   H
ctg cac cag ctg gct gct gac acc tac aaa gag ttc gag cgt gcc tac att ccc gag gga
 L   H   Q   L   A   A   D   T   Y   K   E   F   E   R   A   Y   I   P   E   G
cag cgc tat tcc att cag aat gcc cag gct gct ttc tgc ttc tca gag acc atc ccg gcc
 Q   R   Y   S   I   Q   N   A   Q   A   A   F   C   F   S   E   T   I   P   A
ccc aca ggc aag gag gag gcc cag cag aga acc gac atg gaa ttg ctt cgc ttc tcg ctg
 P   T   G   K   E   E   A   Q   Q   R   T   D   M   E   L   L   R   F   S   L
ctg ctc atc cag tca tgg ctg ggg ccc gtg cag ttc ctc agc agg att ttc acc aac agc
 L   L   I   Q   S   W   L   G   P   V   Q   F   L   S   R   I   F   T   N   S
ctg atg ttc ggc acc tcg gac cgt gtc tat gag aaa ctg aag gac ctg gaa gag ggc atc
 L   M   F   G   T   S   D   R   V   Y   E   K   L   K   D   L   E   E   G   I
cag gct ctg atg cag gag ctg gaa gat ggc agc ccc cgt gtt ggg cag atc ctc aag caa
 Q   A   L   M   Q   E   L   E   D   G   S   P   R   V   G   Q   I   L   K   Q
acc tat gac aag ttt gac gcc aac atg cgc agc gac gac gcg ctg ctc aaa aac tat ggg
 T   Y   D   K   F   D   A   N   M   R   S   D   D   A   L   L   K   N   Y   G
ctg ctc tcc tgc ttc aag aag gac ctg cac aaa gcg gag acc tac ctg cgg gtc atg aag
 L   L   S   C   F   K   K   D   L   H   K   A   E   T   Y   L   R   V   M   K
tgt cgc cgc ttt gtg gaa agc agc tgt gcc ttc ctc gag cac cac cac cac cac cac tga
 C   R   R   F   V   E   S   S   C   A   F   L   E   H   H   H   H   H   H   -
```

B.5 Amino acid and nucleotide sequence of recombinant hexahistidine-tagged Gly118Arg mutant mouse growth hormone. Gly118Arg mutation is highlighted in cyan codon-optimised for use in E. coli.

atg ttt ccc gcc atg ccc ttg tcc agt ctg ttt tct aat gct gtg ctc cga gcc cag cac

M F P A M P L S S L F S N A V L R A Q H

ctg cac cag ctg gct gct gac acc tac aaa gag ttc gag cgt gcc tac att ccc gag gga

L H Q L A A D T Y K E F E R A Y I P E G

cag cgc tat tcc att cag aat gcc cag gct gct ttc tgc ttc tca gag acc atc ccg gcc

Q R Y S I Q N A Q A A F C F S E T I P A

ccc aca ggc aag gag gag gcc cag cag aga acc gac atg gaa ttg ctt cgc ttc tcg ctg

P T G K E E A Q Q R T D M E L L R F S L

ctg ctc atc cag tca tgg ctg ggg ccc gtg cag ttc ctc agc agg att ttc acc aac agc

L L I Q S W L G P V Q F L S R I F T N S

ctg atg ttc ggc acc tcg gac cgt gtc tat gag aaa ctg aag gac ctg gaa gag cgc atc

L M F G T S D R V Y E K L K D L E E R I

cag gct ctg atg cag gag ctg gaa gat ggc agc ccc cgt gtt ggg cag atc ctc aag caa

Q A L M Q E L E D G S P R V G Q I L K Q

acc tat gac aag ttt gac gcc aac atg cgc agc gac gac gcg ctg ctc aaa aac tat ggg

T Y D K F D A N M R S D D A L L K N Y G

ctg ctc tcc tgc ttc aag aag gac ctg cac aaa gcg gag acc tac ctg cgg gtc atg aag

L L S C F K K D L H K A E T Y L R V M K

tgt cgc cgc ttt gtg gaa agc agc tgt gcc ttc ctc gag cac cac cac cac cac cac tga

C R R F V E S S C A F L E H H H H H H -

B.6 Amino acid and nucleotide sequence of recombinant hexahistidine-tagged wild-type mouse growth hormone codon-optimised for mammalian expression, from the site of signal peptide cleavage.

```
ttt ccc gcc atg ccc ttg tcc agt ctg ttt tct aat gct gtg ctc cga gcc cag cac ctg
 F   P   A   M   P   L   S   S   L   F   S   N   A   V   L   R   A   Q   H   L
cac cag ctg gct gct gac acc tac aaa gag ttc gag cgt gcc tac att ccc gag gga cag
 H   Q   L   A   A   D   T   Y   K   E   F   E   R   A   Y   I   P   E   G   Q
cgc tat tcc att cag aat gcc cag gct gct ttc tgc ttc tca gag acc atc ccg gcc ccc
 R   Y   S   I   Q   N   A   Q   A   A   F   C   F   S   E   T   I   P   A   P
aca ggc aag gag gag gcc cag cag aga acc gac atg gaa ttg ctt cgc ttc tcg ctg ctg
 T   G   K   E   E   A   Q   Q   R   T   D   M   E   L   L   R   F   S   L   L
ctc atc cag tca tgg ctg ggg ccc gtg cag ttc ctc agc agg att ttc acc aac agc ctg
 L   I   Q   S   W   L   G   P   V   Q   F   L   S   R   I   F   T   N   S   L
atg ttc ggc acc tcg gac cgt gtc tat gag aaa ctg aag gac ctg gaa gag ggc atc cag
 M   F   G   T   S   D   R   V   Y   E   K   L   K   D   L   E   E   G   I   Q
gct ctg atg cag gag ctg gaa gat ggc agc ccc cgt gtt ggg cag atc ctc aag caa acc
 A   L   M   Q   E   L   E   D   G   S   P   R   V   G   Q   I   L   K   Q   T
tat gac aag ttt gac gcc aac atg cgc agc gac gac gcg ctg ctc aaa aac tat ggg ctg
 Y   D   K   F   D   A   N   M   R   S   D   D   A   L   L   K   N   Y   G   L
ctc tcc tgc ttc aag aag gac ctg cac aaa gcg gag acc tac ctg cgg gtc atg aag tgt
 L   S   C   F   K   K   D   L   H   K   A   E   T   Y   L   R   V   M   K   C
cgc cgc ttt gtg gaa agc agc tgt gcc ttc ctc gag cac cac cac cac cac cac tga
 R   R   F   V   E   S   S   C   A   F   L   E   H   H   H   H   H   H   -
```

B.7 Amino acid and nucleotide sequence of recombinant hexahistidine-tagged Gly118Arg mutant mouse growth hormone codon-optimised for mammalian expression, from the site of signal peptide cleavage.

```
ttt ccc gcc atg ccc ttg tcc agt ctg ttt tct aat gct gtg ctc cga gcc cag cac ctg
 F   P   A   M   P   L   S   S   L   F   S   N   A   V   L   R   A   Q   H   L
cac cag ctg gct gct gac acc tac aaa gag ttc gag cgt gcc tac att ccc gag gga cag
 H   Q   L   A   A   D   T   Y   K   E   F   E   R   A   Y   I   P   E   G   Q
cgc tat tcc att cag aat gcc cag gct gct ttc tgc ttc tca gag acc atc ccg gcc ccc
 R   Y   S   I   Q   N   A   Q   A   A   F   C   F   S   E   T   I   P   A   P
aca ggc aag gag gag gcc cag cag aga acc gac atg gaa ttg ctt cgc ttc tcg ctg ctg
 T   G   K   E   E   A   Q   Q   R   T   D   M   E   L   L   R   F   S   L   L
ctc atc cag tca tgg ctg ggg ccc gtg cag ttc ctc agc agg att ttc acc aac agc ctg
 L   I   Q   S   W   L   G   P   V   Q   F   L   S   R   I   F   T   N   S   L
atg ttc ggc acc tcg gac cgt gtc tat gag aaa ctg aag gac ctg gaa gag aga atc cag
 M   F   G   T   S   D   R   V   Y   E   K   L   K   D   L   E   E   R   I   Q
gct ctg atg cag gag ctg gaa gat ggc agc ccc cgt gtt ggg cag atc ctc aag caa acc
 A   L   M   Q   E   L   E   D   G   S   P   R   V   G   Q   I   L   K   Q   T
tat gac aag ttt gac gcc aac atg cgc agc gac gac gcg ctg ctc aaa aac tat ggg ctg
 Y   D   K   F   D   A   N   M   R   S   D   D   A   L   L   K   N   Y   G   L
ctc tcc tgc ttc aag aag gac ctg cac aaa gcg gag acc tac ctg cgg gtc atg aag tgt
 L   S   C   F   K   K   D   L   H   K   A   E   T   Y   L   R   V   M   K   C
cgc cgc ttt gtg gaa agc agc tgt gcc ttc ctc gag cac cac cac cac cac cac tga
 R   R   F   V   E   S   S   C   A   F   L   E   H   H   H   H   H   H   -
```

B.8 Amino acid and nucleotide sequence of mouse growth hormone Gly118Arg fused to the mouse growth hormone binding protein from the site of signal peptide cleavage. The Gly118Arg mutation is highlighted in cyan. The Gly_4Ser linker is highlighted in red.

```
ttt ccc gcc atg ccc ttg tcc agt ctg ttt tct aat gct gtg ctc cga gcc cag cac ctg
 F   P   A   M   P   L   S   S   L   F   S   N   A   V   L   R   A   Q   H   L
cac cag ctg gct gct gac acc tac aaa gag ttc gag cgt gcc tac att ccc gag gga cag
 H   Q   L   A   A   D   T   Y   K   E   F   E   R   A   Y   I   P   E   G   Q
cgc tat tcc att cag aat gcc cag gct gct ttc tgc ttc tca gag acc atc ccg gcc ccc
 R   Y   S   I   Q   N   A   Q   A   A   F   C   F   S   E   T   I   P   A   P
aca ggc aag gag gag gcc cag cag aga acc gac atg gaa ttg ctt cgc ttc tcg ctg ctg
 T   G   K   E   E   A   Q   Q   R   T   D   M   E   L   L   R   F   S   L   L
ctc atc cag tca tgg ctg ggg ccc gtg cag ttc ctc agc agg att ttc acc aac agc ctg
 L   I   Q   S   W   L   G   P   V   Q   F   L   S   R   I   F   T   N   S   L
atg ttc ggc acc tcg gac cgt gtc tat gag aaa ctg aag gac ctg gaa gag aga atc cag
 M   F   G   T   S   D   R   V   Y   E   K   L   K   D   L   E   E   R   I   Q
gct ctg atg cag gag ctg gaa gat ggc agc ccc cgt gtt ggg cag atc ctc aag caa acc
 A   L   M   Q   E   L   E   D   G   S   P   R   V   G   Q   I   L   K   Q   T
tat gac aag ttt gac gcc aac atg cgc agc gac gac gcg ctg ctc aaa aac tat ggg ctg
 Y   D   K   F   D   A   N   M   R   S   D   D   A   L   L   K   N   Y   G   L
ctc tcc tgc ttc aag aag gac ctg cac aaa gcg gag acc tac ctg cgg gtc atg aag tgt
 L   S   C   F   K   K   D   L   H   K   A   E   T   Y   L   R   V   M   K   C
cgc cgc ttt gtg gaa agc agc tgt gcc ttc ctc gag gga ggc ggt gga tcc aca ccc gca
 R   R   F   V   E   S   S   C   A   F   L   E   G   G   G   G   S   T   P   A
acc ttg ggg aag gct tcc cct gtt ctg cag cgc atc aac ccg agc ttg ggg acg agt agc
 T   L   G   K   A   S   P   V   L   Q   R   I   N   P   S   L   G   T   S   S
tcg ggg aaa ccg cgt ttc acc aag tgt cgg tcc ccc gaa tta gaa act ttc tca tgt tat
 S   G   K   P   R   F   T   K   C   R   S   P   E   L   E   T   F   S   C   Y
tgg acc gag ggt gat aat cca gac tta aag acc cct ggc tct att cag ctt tat tat gct
 W   T   E   G   D   N   P   D   L   K   T   P   G   S   I   Q   L   Y   Y   A
aaa agg gaa tca cag agg cag gcg gcc cgc att gcc cat gag tgg acc caa gag tgg aaa
 K   R   E   S   Q   R   Q   A   A   R   I   A   H   E   W   T   Q   E   W   K
gag tgc cca gat tac gtg tct gca ggt aag aat agt tgt tat ttc aat agc tct tat act
 E   C   P   D   Y   V   S   A   G   K   N   S   C   Y   F   N   S   S   Y   T
```

```
tcc atc tgg atc cca tat tgc ata aag ctg act acc aac ggg gac ctg ctg gat caa aaa
 S   I   W   I   P   Y   C   I   K   L   T   T   N   G   D   L   L   D   Q   K
tgc ttt aca gta gat gaa att gta caa cct gat cca ccc atc ggc ctg aac tgg aca ttg
 C   F   T   V   D   E   I   V   Q   P   D   P   P   I   G   L   N   W   T   L
ctt aac att tca ctg aca ggt ata cgg ggg gac att caa gtt agt tgg cag cct cca ccc
 L   N   I   S   L   T   G   I   R   G   D   I   Q   V   S   W   Q   P   P   P
aat gcc gac gtg ctt aaa ggc tgg atc ata cta gaa tac gag atc cag tac aag gag gtc
 N   A   D   V   L   K   G   W   I   I   L   E   Y   E   I   Q   Y   K   E   V
aat gaa agc aaa tgg aag gtg atg ggc ccc att tgg ctc act tac tgc cct gtc tac tct
 N   E   S   K   W   K   V   M   G   P   I   W   L   T   Y   C   P   V   Y   S
ctc agg atg gac aag gaa cac gaa gtg cga gtg cga tcc cgg cag aga tcc ttt gaa aag
 L   R   M   D   K   E   H   E   V   R   V   R   S   R   Q   R   S   F   E   K
tac tca gag ttt tcg gag gtg ctg cgg gtg atc ttt cca cag aca aat atc cat cat cac
 Y   S   E   F   S   E   V   L   R   V   I   F   P   Q   T   N   I   H   H   H
cat cac cac tga tag taa
 H   H   H   -   -   -
```

B.9 Alignment of wild-type human growth hormone (Query 1) and mouse growth hormone (Sbject 1) using the ncbi BLAST protein alignment tool. + symbol indicates conservative substitution of amino acids with similar biochemical properties.

```
Identities:129/194(66%), Positives:154/194(79%), Gaps:3/194(1%)

Query  1    FPTIPLSRLFDNAMLRAHRLHQLAFDTYQEFEEAYIPKEQKYSFLQNPQTSLCFSESIPT  60
            FP +PLS LF NA+LRA  LHQLA DTY+EFE AYIP+ Q+YS +QN Q + CFSE+IP
Sbjct  1    FPAMPLSSLFSNAVLRAQHLHQLAADTYKEFERAYIPEGQRYS-IQNAQAAFCFSETIPA  59

Query  61   PSNREETQQKSNLELLRISLLLIQSWLEPVQFLRSVFANSLVYGASDSNVYDLLKDLEEG  120
            P+ +EE QQ++++ELLR SLLLIQSWL PVQFL  +F NSL++G SD  VY+ LKDLEEG
Sbjct  60   PTGKEEAQQRTDMELLRFSLLLIQSWLGPVQFLSRIFTNSLMFGTSD-RVYEKLKDLEEG  118

Query  121  IQTLMGRLEDGSPRTGQIFKQTYSKFDTNSHNDDALLKNYGLLYCFRKDMDKVETFLRIV  180
            IQ LM  LEDGSPR GQI KQTY KFD N  +DDALLKNYGLL CF+KD+ K ET+LR++
Sbjct  119  IQALMQELEDGSPRVGQILKQTYDKFDANMRSDDALLKNYGLLSCFKKDLHKAETYLRVM  178

Query  181  QCRS-VEGSCGFLE  193
            +CR  VE SC FLE
Sbjct  179  KCRRFVESSCAFLE  192
```

C Protein physical and chemical properties

Table C: Protein Parameters of mouse and human growth hormone. All parameters were predicted using the ExPASy protein parameters (ProtParam) tool, based on the amino acid sequences.

Proteins	Length	Theoretical pI	Mw (Da)	Extinction coefficient ($m^{-1}cm^{-1}$)[1]	Abs 0.1% (=1g/L)[1]
Mouse WT Growth Hormone	198	6.53	22906.14	15930	0.695
Mouse Gly118Arg Growth Hormone	198	6.82	23005.28	15930	0.692
Mouse Gly118Arg Growth Hormone fusion	469	7.14	53723.26	88810	1.653
Human WT Growth Hormone	200	5.83	23325.36	17420	0.747
Human Gly120Arg Growth Hormone	200	5.98	23424.50	17420	0.744
Human m12 Growth Hormone	200	5.62	23226.14	17420	0.750

[1] Calculated assuming that formation of disulphide bonds between the thiol groups of cysteine residues formed are reduced.

D Primers

ID	Oligonucleotide sequence	Corresponding figure
CMV for	CGCAAATGGGCGGTAGGCGTG	3.12, 3.16
EBV rev	GTGGTTTGTCCAAACTCATC	3.12
Fus for	AGGGAGGCGGTGGATCCACACCCGCAACCTTGGGGA	3.16
Fus rev	TGGATCCACCGCCTCCCTCGAGGAAGGCACAGCT	3.16
mGHR rev	TAGCCTAAGCTTAGGATCTTACTATCAGTGGT	3.16
Gly118Arg for	GCCTGGATGCGCTCTTCCAGG	3.12
Gly118Arg rev	TCTGATGCAGGAGCTGGAAG	3.12

References

Tolvaptan-Octreotide LAR Combination in ADPKD. https://ClinicalTrials.gov/show/NCT03541447.

ARAC, D., BOUCARD, A. A., BOLLIGER, M. F., NGUYEN, J., SOLTIS, S. M., SUDHOF, T. C. & BRUNGER, A. T. 2012. A novel evolutionarily conserved domain of cell-adhesion GPCRs mediates autoproteolysis. *Embo Journal,* 31**,** 1364-1378.

ARIZA, M., ALVAREZ, V., MARIN, R., AGUADO, S., LOPEZLARREA, C., ALVAREZ, J., MENENDEZ, M. J. & COTO, E. 1997. A family with a milder form of adult dominant polycystic kidney disease not linked to the PKD1 (16p) or PKD2 (4q) genes. *Journal of Medical Genetics,* 34**,** 587-589.

BAIK, M., YU, J. H. & HENNIGHAUSEN, L. 2011. Growth hormone-STAT5 regulation of growth, hepatocellular carcinoma, and liver metabolism. *Nutrition and Physical Activity in Aging, Obesity, and Cancer,* 1229**,** 29-37.

BALDIN, V., LUKAS, J., MARCOTE, M. J., PAGANO, M. & DRAETTA, G. 1993. CYCLIN D1 IS A NUCLEAR-PROTEIN REQUIRED FOR CELL-CYCLE PROGRESSION IN G(1). *Genes & Development,* 7**,** 812-821.

BAMBERGER, A. M., BAMBERGER, C. M., PU, L. P., PUY, L. A., LOH, Y. P. & ASA, S. L. 1995. EXPRESSION OF PIT-1 MESSENGER-RIBONUCLEIC-ACID AND PROTEIN IN THE HUMAN PLACENTA. *Journal of Clinical Endocrinology & Metabolism,* 80**,** 2021-2026.

BARTALUCCI, N., CALABRESI, L., BALLIU, M., MARTINELLI, S., ROSSI, M. C., VILLEVAL, J. L., ANNUNZIATO, F., GUGLIELMELLI, P. & VANNUCCHI, A. M. 2017. Inhibitors of the PI3K/mTOR pathway prevent STAT5 phosphorylation in &ITJAK2V617F &ITmutated cells through PP2A/CIP2A axis. *Oncotarget,* 8**,** 96710-96724.

BASTOS, A. P., PIONTEK, K., SILVA, A. M., MARTINI, D., MENEZES, L. F., FONSECA, J. M., FONSECA, II, GERMINO, G. G. & ONUCHIC, L. F. 2009. Pkd1 Haploinsufficiency Increases Renal Damage and Induces Microcyst Formation following Ischemia/Reperfusion. *Journal of the American Society of Nephrology,* 20**,** 2389-2402.

BAUMANN, G., AMBURN, K. D. & BUCHANAN, T. A. 1987. THE EFFECT OF CIRCULATING GROWTH HORMONE-BINDING PROTEIN ON METABOLIC-CLEARANCE, DISTRIBUTION, AND DEGRADATION OF HUMAN GROWTH-HORMONE. *Journal of Clinical Endocrinology & Metabolism,* 64**,** 657-660.

BEAR, J. C., MCMANAMON, P., MORGAN, J., PAYNE, R. H., LEWIS, H., GAULT, M. H. & CHURCHILL, D. N. 1984. AGE AT CLINICAL ONSET AND AT ULTRASONOGRAPHIC DETECTION OF ADULT POLYCYSTIC KIDNEY-DISEASE - DATA FOR GENETIC-COUNSELING. *American Journal of Medical Genetics,* 18**,** 45-53.

BELET, U., DANACI, M., SARIKAYA, S., ODABAS, F., UTAS, C., TOKGOZ, B., SEZER, T., TURGUT, T., ERDOGAN, N. & AKPOLAT, T. 2002. Prevalence of epididymal, seminal vesicle, prostate, and testicular cysts in autosomal dominant polycystic kidney disease. *Urology,* 60**,** 138-141.

BELIBI, F. A., REIF, G., WALLACE, D. P., YAMAGUCHI, T., OLSEN, L., LI, H., HELMKAMP, G. M. & GRANTHAM, J. J. 2004. Cyclic AMP promotes growth and secretion in human polycystic kidney epithelial cells. *Kidney International,* 66**,** 964-973.

BERELOWITZ, M., SZABO, M., FROHMAN, L. A., FIRESTONE, S., CHU, L. & HINTZ, R. L. 1981. SOMATOMEDIN-C MEDIATES GROWTH-HORMONE NEGATIVE FEEDBACK BY EFFECTS ON BOTH THE HYPOTHALAMUS AND THE PITUITARY. *Science,* 212**,** 1279-1281.

BERGAN-ROLLER, H. E. & SHERIDAN, M. A. 2018. The growth hormone signaling system: Insights into coordinating the anabolic and catabolic actions of growth hormone. *General and Comparative Endocrinology,* 258**,** 119-133.

BERGMANN, C., GUAY-WOODFORD, L. M., HARRIS, P. C., HORIE, S., PETERS, D. J. M. & TORRES, V. E. 2018. Polycystic kidney disease. *Nature Reviews Disease Primers,* 4.

BESSON, A., SALEMI, S., DELADOEY, J., VUISSOZ, J. M., EBLE, A., BIDLINGMAIER, M., BURGI, S., HONEGGER, U., FLUCK, C. & MULLIS, P. E. 2005. Short stature caused by a biologically inactive

mutant growth hormone (GH-C53S). *Journal of Clinical Endocrinology & Metabolism,* 90**,** 2493-2499.

BHAGWAT, N., KOPPIKAR, P., KELLER, M., MARUBAYASHI, S., SHANK, K., RAMPAL, R., QI, J., KLEPPE, M., PATEL, H. J., SHAH, S. K., TALDONE, T., BRADNER, J. E., CHIOSIS, G. & LEVINE, R. L. 2014. Improved targeting of JAK2 leads to increased therapeutic efficacy in myeloproliferative neoplasms. *Blood,* 123**,** 2075-2083.

BHUNIA, A. K., PIONTEK, K., BOLETTA, A., LIU, L. J., QIAN, F., XU, P. N., GERMINO, F. J. & GERMINO, G. G. 2002. PKD1 induces p21(waf1) and regulation of the cell cycle via direct activation of the JAK-STAT signaling pathway in a process requiring PKD2. *Cell,* 109**,** 157-168.

BJORKLUND, M., TAIPALE, M., VARJOSALO, M., SAHARINEN, J., LAHDENPERA, J. & TAIPALE, J. 2006. Identification of pathways regulating cell size and cell-cycle progression by RNAi. *Nature,* 439**,** 1009-1013.

BOGDANOVA, N., DWORNICZAK, B., DRAGOVA, D., TODOROV, V., DIMITRAKOV, D., KALINOV, K., HALLMAYER, J., HORST, J. & KALAYDJIEVA, L. 1995. GENETIC-HETEROGENEITY OF POLYCYSTIC KIDNEY-DISEASE IN BULGARIA. *Human Genetics,* 95**,** 645-650.

BOOTH, W. T., SCHLACHTER, C. R., POTE, S., USSIN, N., MANK, N. J., KLAPPER, V., OFFERMANN, L. R., TANG, C. B., HURLBURT, B. K. & CHRUSZCZ, M. 2018. Impact of an N-terminal Polyhistidine Tag on Protein Thermal Stability. *Acs Omega,* 3**,** 760-768.

BOUCHERON, C., DUMON, S., CONSTANTINO, S., SANTOS, R., MORIGGL, R., HENNIGHAUSEN, L., GISSELBRECHT, S. & GOUILLEUX, F. 1998. A single amino acid in the DNA binding regions of STAT5A and STAT5B confers distinct DNA binding specificities. *Journal of Biological Chemistry,* 273**,** 33936-33941.

BOZZOLA, M., DE BENEDETTI, F., DE AMICI, M., JOURET, B., TRAVAGLINO, P., PAGANI, S., CONTE, F. & TAUBER, M. 2003. Stimulating effect of growth hormone on cytokine release in children. *European Journal of Endocrinology,* 149**,** 397-401.

BRANDENBERGER, G. & WEIBEL, L. 2004. The 24-h growth hormone rhythm in men: sleep and circadian influences questioned. *Journal of Sleep Research,* 13**,** 251-255.

BRANDT, L. E., BOHN, A. A., CHARLES, J. B. & EHRHART, E. J. 2012. Localization of Canine, Feline, and Mouse Renal Membrane Proteins. *Veterinary Pathology,* 49**,** 693-703.

BRITTAIN, A. L., R, B., Y, Q. & J, K. J. 2017. Growth Hormone and the Epithelial-to-Mesenchymal Transition. *The Journal of Clinical Endocrinology & Metabolism*

BROOKS, A. J. & WATERS, M. J. 2010. The growth hormone receptor: mechanism of activation and clinical implications. *Nature Reviews Endocrinology,* 6**,** 515-525.

BROWN, J. H., BIHOREAU, M. T., HOFFMANN, S., KRANZLIN, B., TYCHINSKAYA, I., OBERMULLER, N., PODLICH, D., BOEHN, S. N., KAISAKI, P. J., MEGEL, N., DANOY, P., COPLEY, R. R., BROXHOLME, J., WITZGALL, R., LATHROP, M., GRETZ, N. & GAUGUIER, D. 2005. Missense mutation in sterile alpha motif of novel protein SamCystin is associated with polycystic kidney disease in (cy/+) rat. *Journal of the American Society of Nephrology,* 16**,** 3517-3526.

BRUN, M., MAUGEY-LAULOM, B., EURIN, D., DIDIER, F. & AVNI, E. F. 2004. Prenatal sonographic patterns in autosomal dominant polycystic kidney disease: a multicenter study. *Ultrasound in Obstetrics & Gynecology,* 24**,** 55-61.

BUSTAMANTE, J. J., GONZALEZ, L., CARROLL, C. A., WEINTRAUB, S. T., AGUILAR, R. M., MUNOZ, J., MARTINEZ, A. O. & HARO, L. S. 2009. O-Glycosylated 24 kDa human growth hormone has a mucin-like biantennary disialylated tetrasaccharide attached at Thr-60. *Proteomics,* 9**,** 3474-3488.

CABRITA, I., KRAUS, A., SCHOLZ, J. K., SKOCZYNSKI, K., SCHREIBER, R., KUNZELMANN, K. & BUCHHOLZ, B. 2020. Cyst growth in ADPKD is prevented by pharmacological and genetic inhibition of TMEM16A in vivo. *Nature Communications,* 11.

CAGNAZZO, F., GAMBACCIANI, C., MORGANTI, R. & PERRINI, P. 2017. Intracranial aneurysms in patients with autosomal dominant polycystic kidney disease: prevalence, risk of rupture, and management. A systematic review. *Acta Neurochirurgica,* 159**,** 811-821.

CAI, J., SONG, X. W., WANG, W., WATNICK, T., PEI, Y., QIAN, F. & PAN, D. J. 2018. A RhoA-YAP-c-Myc signaling axis promotes the development of polycystic kidney disease. *Genes & Development,* 32**,** 781-793.

CAI, Z. Q., MAEDA, Y., CEDZICH, A., TORRES, V. E., WU, G. Q., HAYASHI, T., MOCHIZUKI, T., PARK, J. H., WITZGALL, R. & SOMLO, S. 1999. Identification and characterization of polycystin-2, the PKD2 gene product. *Journal of Biological Chemistry,* 274**,** 28557-28565.

CAMERON, D. P., BURGER, H. G., CATT, K. J., WATTS, J. M. & GORDON, E. 1972. METABOLIC CLEARANCE OF HUMAN GROWTH-HORMONE IN PATIENTS WITH HEPATIC AND RENAL-FAILURE, AND IN ISOLATED PERFUSED PIG LIVER. *Metabolism-Clinical and Experimental,* 21**,** 895-+.

CANTERO, M. D., VELAZQUEZ, I. F., STREETS, A. J., ONG, A. C. M. & CANTIELLO, H. F. 2015. The cAMP Signaling Pathway and Direct Protein Kinase A Phosphorylation Regulate Polycystin-2 (TRPP2) Channel Function. *Journal of Biological Chemistry,* 290**,** 23888-23896.

CAROLI, A., PERICO, N., PERNA, A., ANTIGA, L., BRAMBILLA, P., PISANI, A., VISCIANO, B., IMBRIACO, M., MESSA, P., CERUTTI, R., DUGO, M., CANCIAN, L., BUONGIORNO, E., DE PASCALIS, A., GASPARI, F., CARRARA, F., RUBIS, N., PRANDINI, S., REMUZZI, A., REMUZZI, G., RUGGENENTI, P. & GRP, A. S. 2013. Effect of longacting somatostatin analogue on kidney and cyst growth in autosomal dominant polycystic kidney disease (ALADIN): a randomised, placebo-controlled, multicentre trial. *Lancet,* 382**,** 1485-1495.

CHAPIN, H. C. & CAPLAN, M. J. 2010. The cell biology of polycystic kidney disease. *Journal of Cell Biology,* 191**,** 701-710.

CHAPMAN, A. B., JOHNSON, A. M. & GABOW, P. A. 1994. PREGNANCY OUTCOME AND ITS RELATIONSHIP TO PROGRESSION OF RENAL-FAILURE IN AUTOSOMAL-DOMINANT POLYCYSTIC KIDNEY-DISEASE. *Journal of the American Society of Nephrology,* 5**,** 1178-1185.

CHAPMAN, A. B., STEPNIAKOWSKI, K. & RAHBARI-OSKOUI, F. 2010. Hypertension in Autosomal Dominant Polycystic Kidney Disease. *Advances in Chronic Kidney Disease,* 17**,** 153-163.

CHEBIB, F. T., HOGAN, M. C., EL-ZOGHBY, Z. M., IRAZABAL, M. V., SENUM, S. R., HEYER, C. M., MADSEN, C. D., GALL, E. C. L., BEHFAR, A., HARRIS, P. C. & TORRES, V. E. 2017. Autosomal Dominant Polycystic Kidney Patients May Be Predisposed to Various Cardiomyopathies. *Kidney International Reports,* 2**,** 913-923.

CHEN, W. Y., CHEN, N. Y., YUN, J., WAGNER, T. E. & KOPCHICK, J. J. 1994. IN-VITRO AND IN-VIVO STUDIES OF ANTAGONISTIC EFFECTS OF HUMAN GROWTH-HORMONE ANALOGS. *Journal of Biological Chemistry,* 269**,** 15892-15897.

CHEN, W. Y., WIGHT, D. C., WAGNER, T. E. & KOPCHICK, J. J. 1990. EXPRESSION OF A MUTATED BOVINE GROWTH-HORMONE GENE SUPPRESSES GROWTH OF TRANSGENIC MICE. *Proceedings of the National Academy of Sciences of the United States of America,* 87**,** 5061-5065.

CHEN, X. Z., SHAFER, A. W., YUN, J. S., LI, Y. S., WAGNER, T. E. & KOPCHICK, J. J. 1992. CONVERSION OF BOVINE GROWTH-HORMONE CYSTEINE RESIDUES TO SERINE AFFECTS SECRETION BY CULTURED-CELLS AND GROWTH-RATES IN TRANSGENIC MICE. *Molecular Endocrinology,* 6**,** 598-606.

CHIPMAN, J. J., ZERWEKH, J., NICAR, M., MARKS, J. & PAK, C. Y. C. 1980. EFFECT OF GROWTH-HORMONE ADMINISTRATION - RECIPROCAL CHANGES IN SERUM 1-ALPHA,25-DIHYDROXYVITAMIN-D AND INTESTINAL CALCIUM-ABSORPTION. *Journal of Clinical Endocrinology & Metabolism,* 51**,** 321-324.

CHOW, J. C., LING, P. R., QU, Z. S., LAVIOLA, L., CICCARONE, A., BISTRIAN, B. R. & SMITH, R. J. 1996. Growth hormone stimulates tyrosine phosphorylation of JAK2 and STAT5, but not insulin receptor substrate-1 or SHC proteins in liver and skeletal muscle of normal rats in vivo. *Endocrinology,* 137**,** 2880-2886.

CHRISTIANSEN, J. S., GAMMELGAARD, J., ORSKOV, H., ANDERSEN, A. R., TELMER, S. & PARVING, H. H. 1981. KIDNEY-FUNCTION AND SIZE IN NORMAL SUBJECTS BEFORE AND DURING GROWTH-HORMONE ADMINISTRATION FOR ONE WEEK. *European Journal of Clinical Investigation,* 11**,** 487-490.

COHEN, L. E., WONDISFORD, F. E. & RADOVICK, S. 1996. Role of Pit-1 in the gene expression of growth hormone, prolactin, and thyrotropin. *Endocrinology and Metabolism Clinics of North America,* 25**,** 523-&.

COLAO, A., PIVONELLO, R., AURIEMMA, R. S., DE MARTINO, M. C., BIDLINGMAIER, M., BRIGANTI, F., TORTORA, F., BURMAN, P., KOURIDES, I. A., STRASBURGER, C. J. & LOMBARDI, G. 2006. Efficacy of 12-month treatment with the GH receptor antagonist pegvisomant in patients with acromegaly resistant to long-term, high-dose somatostatin analog treatment: effect on IGF-I levels, tumor mass, hypertension and glucose tolerance. *European Journal of Endocrinology,* 154**,** 467-477.

CORNEC-LE GALL, E., AUDREZET, M. P., CHEN, J. M., HOURMANT, M., MORIN, M. P., PERRICHOT, R., CHARASSE, C., WHEBE, B., RENAUDINEAU, E., JOUSSET, P., GUILLODO, M. P., GRALL-JEZEQUEL, A., SALIOU, P., FEREC, C. & LE MEUR, Y. 2013. Type of PKD1 Mutation Influences Renal Outcome in ADPKD. *Journal of the American Society of Nephrology,* 24**,** 1006-1013.

COWLEY, B. D., RUPP, J. C., MUESSEL, M. J. & GATTONE, V. H. 1997. Gender and the effect of gonadal hormones on the progression of inherited polycystic kidney disease in rats. *American Journal of Kidney Diseases,* 29**,** 265-272.

CRISMAN, R. I. & RANDOLPH, T. W. 2009. Refolding of Proteins From Inclusion Bodies Is Favored by a Diminished Hydrophobic Effect at Elevated Pressures. *Biotechnology and Bioengineering,* 102**,** 483-492.

CUNNINGHAM, B. C., ULTSCH, M., DEVOS, A. M., MULKERRIN, M. G., CLAUSER, K. R. & WELLS, J. A. 1991. DIMERIZATION OF THE EXTRACELLULAR DOMAIN OF THE HUMAN GROWTH-HORMONE RECEPTOR BY A SINGLE HORMONE MOLECULE. *Science,* 254**,** 821-825.

DAOUST, M. C., REYNOLDS, D. M., BICHET, D. G. & SOMLO, S. 1995. EVIDENCE FOR A 3RD GENETIC-LOCUS FOR AUTOSOMAL-DOMINANT POLYCYSTIC KIDNEY-DISEASE. *Genomics,* 25**,** 733-736.

DARNELL, J. E., KERR, I. M. & STARK, G. R. 1994. JAK-STAT PATHWAYS AND TRANSCRIPTIONAL ACTIVATION IN RESPONSE TO IFNS AND OTHER EXTRACELLULAR SIGNALING PROTEINS. *Science,* 264**,** 1415-1421.

DAVEY, H. W., XIE, T., MCLACHLAN, M. J., WILKINS, R. J., WAXMAN, D. J. & GRATTAN, D. R. 2001. STAT5b is required for GH-induced liver Igf-I gene expression. *Endocrinology,* 142**,** 3836-3841.

DAVIES, F., COLES, G. A., HARPER, P. S., WILLIAMS, A. J., EVANS C. & COCHLIN D. 1991. Polycystic kidney disease re-evaluated: a population-based study . The Quarterly Journal of Medicine

DAVISON, Z., DE BLACQUIERE, G. E., WESTLEY, B. R. & MAY, F. E. B. 2011. Insulin-like Growth Factor-Dependent Proliferation and Survival of Triple-Negative Breast Cancer Cells: Implications for Therapy. *Neoplasia,* 13**,** 504-515.

DEALMEIDA, S., DEALMEIDA, E., PETERS, D., PINTO, J. R., TAVORA, I., LAVINHA, J., BREUNING, M. & PRATA, M. M. 1995. AUTOSOMAL-DOMINANT POLYCYSTIC KIDNEY-DISEASE - EVIDENCE FOR THE EXISTENCE OF A 3RD LOCUS IN A PORTUGUESE FAMILY. *Human Genetics,* 96**,** 83-88.

DELAFOSSE, L., XU, P. & DUROCHER, Y. 2016. Comparative study of polyethylenimines for transient gene expression in mammalian HEK293 and CHO cells. *Journal of Biotechnology,* 227**,** 103-111.

DELHASE, M., VERGANI, P., MALUR, A., HOOGHEPETERS, E. L. & HOOGHE, R. J. 1993. THE TRANSCRIPTION FACTOR PIT-1/GHF-1 IS EXPRESSED IN HEMATOPOIETIC AND LYMPHOID-TISSUES. *European Journal of Immunology,* 23**,** 951-955.

DELL, K. M. 2015. The role of cilia in the pathogenesis of cystic kidney disease. *Current Opinion in Pediatrics,* 27**,** 212-218.

DEVOS, A. M., ULTSCH, M. & KOSSIAKOFF, A. A. 1992. HUMAN GROWTH-HORMONE AND EXTRACELLULAR DOMAIN OF ITS RECEPTOR - CRYSTAL-STRUCTURE OF THE COMPLEX. *Science,* 255**,** 306-312.

DOS SANTOS, C., ESSIOUX, L., TEINTURIER, C., TAUBER, M., GOFFIN, V. & BOUGNERES, P. 2004. A common polymorphism of the growth hormone receptor is associated with increased responsiveness to growth hormone. *Nature Genetics,* 36**,** 720-724.

DRAZNIN, B., DAHL, R., SHERMAN, N., SUSSMAN, K. E. & STAEHELIN, L. A. 1988. EXOCYTOSIS IN NORMAL ANTERIOR-PITUITARY CELLS - QUANTITATIVE CORRELATION BETWEEN GROWTH-HORMONE RELEASE AND THE MORPHOLOGICAL FEATURES OF EXOCYTOSIS. *Journal of Clinical Investigation,* 81**,** 1042-1050.

DUBENDORFF, J. W. & STUDIER, F. W. 1991. CONTROLLING BASAL EXPRESSION IN AN INDUCIBLE T7 EXPRESSION SYSTEM BY BLOCKING THE TARGET T7 PROMOTER WITH LAC REPRESSOR. *Journal of Molecular Biology,* 219**,** 45-59.

ELLIOTT, R. W., LEE, B. K. & EICHER, E. M. 1990. LOCALIZATION OF THE GROWTH-HORMONE GENE TO THE DISTAL HALF OF MOUSE CHROMOSOME-11. *Genomics,* 8**,** 591-594.

FALKHEDEN, T. & WICKBOM, I. 1965. RENAL FUNCTION AND KIDNEY SIZE FOLLOWING HYPOPHYSECTOMY IN MAN. *Acta Endocrinologica,* 48**,** 348-+.

FARIA, A. C. S., VELDHUIS, J. D., THORNER, M. O. & VANCE, M. L. 1989. HALF-TIME OF ENDOGENOUS GROWTH-HORMONE (GH) DISAPPEARANCE IN NORMAL MAN AFTER STIMULATION OF GH SECRETION BY GH-RELEASING HORMONE AND SUPPRESSION WITH SOMATOSTATIN. *Journal of Clinical Endocrinology & Metabolism,* 68**,** 535-541.

FERRER, M., CHERNIKOVA, T. N., YAKIMOV, M. M., GOLYSHIN, P. N. & TIMMIS, K. N. 2003. Chaperonins govern growth of Escherichia coli at low temperatures. *Nature Biotechnology,* 21**,** 1266-1267.

FICK, G. M., DULEY, I. T., JOHNSON, A. M., STRAIN, J. D., MANCOJOHNSON, M. L. & GABOW, P. A. 1994. THE SPECTRUM OF AUTOSOMAL-DOMINANT POLYCYSTIC KIDNEY-DISEASE IN CHILDREN. *Journal of the American Society of Nephrology,* 4**,** 1654-1660.

FIRMBACHKRAFT, I., BYERS, M., SHOWS, T., DALLAFAVERA, R. & KROLEWSKI, J. J. 1990. TYK2, PROTOTYPE OF A NOVEL CLASS OF NONRECEPTOR TYROSINE KINASE GENES. *Oncogene,* 5**,** 1329-1336.

FRADKIN, A. H., BOAND, C. S., EISENBERG, S. P., ROSENDAHL, M. S. & RANDOLPH, T. W. 2010. Recombinant Murine Growth Hormone from E. coli Inclusion Bodies: Expression, High-Pressure Solubilization and Refolding, and Characterization of Activity and Structure. *Biotechnology Progress,* 26**,** 743-749.

FRAGIADAKI, M., LANNOY, M., THEMANNS, M., MAURER, B., LEONHARD, W. N., PETERS, D. J. M., MORIGGL, R. & ONG, A. C. M. 2017. STAT5 drives,abnormal proliferation in autosomal dominant polycystic kidney disease. *Kidney International,* 91**,** 575-586.

FRIEDRICHSEN, B. N., RICHTER, H. E., HANSEN, J. A., RHODES, C. J., NIELSEN, J. H., BILLESTRUP, N. & MOLDRUP, A. 2003. Signal transducer and activator of transcription 5 activation is sufficient to drive transcriptional induction of cyclin D2 gene and proliferation of rat pancreatic beta-cells. *Molecular Endocrinology,* 17**,** 945-958.

GABOW, P. A., JOHNSON, A. M., KAEHNY, W. D., KIMBERLING, W. J., LEZOTTE, D. C., DULEY, I. T. & JONES, R. H. 1992. FACTORS AFFECTING THE PROGRESSION OF RENAL-DISEASE IN AUTOSOMAL-DOMINANT POLYCYSTIC KIDNEY-DISEASE. *Kidney International,* 41**,** 1311-1319.

GABOW, P. A., KAEHNY, W. D., JOHNSON, A. M., DULEY, I. T., MANCOJOHNSON, M., LEZOTTE, D. C. & SCHRIER, R. W. 1989. THE CLINICAL UTILITY OF RENAL CONCENTRATING CAPACITY IN POLYCYSTIC KIDNEY-DISEASE. *Kidney International,* 35**,** 675-680.

GABOW, P. A., KIMBERLING, W. J., STRAIN, J. D., MANCOJOHNSON, M. L. & JOHNSON, A. M. 1997. Utility of ultrasonography in the diagnosis of autosomal dominant polycystic kidney disease in children. *Journal of the American Society of Nephrology,* 8**,** 105-110.

GATTONE, V. H., WANG, X. F., HARRIS, P. C. & TORRES, V. E. 2003. Inhibition of renal cystic disease development and progression by a vasopressin V2 receptor antagonist. *Nature Medicine,* 9**,** 1323-1326.

GERICH, J. E., LORENZI, M., BIER, D. M., TSALIKIAN, E., SCHNEIDER, V., KARAM, J. H. & FORSHAM, P. H. 1976. EFFECTS OF PHYSIOLOGIC LEVELS OF GLUCAGON AND GROWTH-HORMONE ON HUMAN CARBOHYDRATE AND LIPID-METABOLISM - STUDIES INVOLVING ADMINISTRATION OF EXOGENOUS HORMONE DURING SUPPRESSION OF ENDOGENOUS HORMONE-SECRETION WITH SOMATOSTATIN. *Journal of Clinical Investigation,* 57**,** 875-884.

GEVERS, T. J. G., HOL, J. C., MONSHOUWER, R., DEKKER, H. M., WETZELS, J. F. M. & DRENTH, J. P. H. 2015. Effect of lanreotide on polycystic liver and kidneys in autosomal dominant polycystic kidney disease: an observational trial. *Liver International,* 35**,** 1607-1614.

GHANAAT, F. & TAYEK, J. A. 2005. Growth hormone administration increases glucose production by preventing the expected decrease in glycogenolysis seen with fasting in healthy volunteers. *Metabolism-Clinical and Experimental,* 54**,** 604-609.

GIUSTINA, A., MAZZIOTTI, G. & CANALIS, E. 2008. Growth hormone, insulin-like growth factors, and the skeleton. *Endocrine Reviews,* 29**,** 535-559.

GJERSET, R. A., YEARGIN, J., VOLKMAN, S. K., VILA, V., ARYA, J. & HAAS, M. 1990. INSULIN-LIKE GROWTH FACTOR-I SUPPORTS PROLIFERATION OF AUTOCRINE THYMIC LYMPHOMA-CELLS WITH A PRE-T-CELL PHENOTYPE. *Journal of Immunology,* 145**,** 3497-3501.

GODFREY, R. J., MADGWICK, Z. & WHYTE, G. P. 2003. The exercise-induced growth hormone response in athletes. *Sports Medicine,* 33**,** 599-613.

GOEDDEL, D. V., HEYNEKER, H. L., HOZUMI, T., ARENTZEN, R., ITAKURA, K., YANSURA, D. G., ROSS, M. J., MIOZZARI, G., CREA, R. & SEEBURG, P. H. 1979. DIRECT EXPRESSION IN ESCHERICHIA-COLI OF A DNA-SEQUENCE CODING FOR HUMAN GROWTH-HORMONE. *Nature,* 281**,** 544-548.

GRAF, L., BORVENDEG, J., BARAT, E., HERMANN, I. & PATTHY, A. 1976. REACTIVITY AND BIOLOGICAL IMPORTANCE OF DISULFIDE BONDS IN HUMAN GROWTH-HORMONE. *Febs Letters,* 66**,** 233-237.

GRANTHAM, J. J., TORRES, V. E., CHAPMAN, A. B., GUAY-WOODFORD, L. M., BAE, K. T., KING, B. F., WETZEL, L. H., BAUMGARTEN, D. A., KENNEY, P. J., HARRIS, P. C., KLAHR, S., BENNETT, W. M., HIRSCHMAN, G. N., MEYERS, C. M., ZHANG, X. L., ZHU, F., MILLER, J. P. & INVESTIGATORS, C. 2006. Volume progression in polycystic kidney disease. *New England Journal of Medicine,* 354**,** 2122-2130.

GRETZ, N., ZEIER, M., GEBERTH, S., STRAUCH, M. & RITZ, E. 1989. IS GENDER A DETERMINANT FOR EVOLUTION OF RENAL-FAILURE - A STUDY IN AUTOSOMAL DOMINANT POLYCYSTIC KIDNEY-DISEASE. *American Journal of Kidney Diseases,* 14**,** 178-183.

GRIFFITHS, J., MILLS, M. T. & ONG, A. C. M. 2020. Long-acting somatostatin analogue treatments in autosomal dominant polycystic kidney disease and polycystic liver disease: a systematic review and meta-analysis. *Bmj Open,* 10.

HAJARNIS, S., LAKHIA, R., YHESKEL, M., WILLIAMS, D., SOROURIAN, M., LIU, X. Q., ABOUDEHEN, K., ZHANG, S. R., KERSJES, K., GALASSO, R., LI, J., KAIMAL, V., LOCKTON, S., DAVIS, S., FLATEN, A., JOHNSON, J. A., HOLLAND, W. L., KUSMINSKI, C. M., SCHERER, P. E., HARRIS, P. C., TRUDEL, M., WALLACE, D. P., IGARASHI, P., LEE, E. C., ANDROSAVICH, J. R. & PATEL, V. 2017. microRNA-17 family promotes polycystic kidney disease progression through modulation of mitochondrial metabolism. *Nature Communications,* 8.

HAKUNO, F. & TAKAHASHI, S. I. 2018. IGF1 receptor signaling pathways. *Journal of Molecular Endocrinology,* 61**,** T69-T86.

HAN, H. Y. 2018. RNA Interference to Knock Down Gene Expression. *Disease Gene Identification: Methods and Protocols, 2nd Edition,* 1706**,** 293-302.

HAN, Y. L., LEAMAN, D. W., WATLING, D., ROGERS, N. C., GRONER, B., KERR, I. M., WOOD, W. I. & STARK, G. R. 1996. Participation of JAK and STAT proteins in growth hormone-induced signaling. *Journal of Biological Chemistry,* 271**,** 5947-5952.

HANAHAN, D. & WEINBERG, R. A. 2011. Hallmarks of Cancer: The Next Generation. *Cell,* 144**,** 646-674.

HANAOKA, K. & GUGGINO, W. B. 2000. cAMP regulates cell proliferation and cyst formation in autosomal polycystic kidney disease cells. *Journal of the American Society of Nephrology,* 11**,** 1179-1187.

HANAOKA, K., QIAN, F., BOLETTA, A., BHUMIA, A. K., PIONTEK, K., TSIOKAS, L., SUKHATME, V. P., GUGGINO, W. B. & GERMINO, G. G. 2000. Co-assembly of polycystin-1 and-2 produces unique cation-permeable currents. *Nature,* 408**,** 990-994.

HANS, F. & DIMITROV, S. 2001. Histone H3 phosphorylation and cell division. *Oncogene,* 20**,** 3021-3027.

HAPPE, H., LEONHARD, W. N., VAN DER WAL, A., VAN DE WATER, B., LANTINGA-VAN LEEUWEN, I. S., BREUNING, M. H., DE HEER, E. & PETERS, D. J. M. 2009. Toxic tubular injury in kidneys from Pkd1-deletion mice accelerates cystogenesis accompanied by dysregulated planar cell polarity and canonical Wnt signaling pathways. *Human Molecular Genetics,* 18**,** 2532-2542.

HAPPE, H., VAN DER WAL, A. M., SALVATORI, D. C. F., LEONHARD, W. N., BREUNING, M. H., DE HEER, E. & PETERS, D. J. M. 2013. Cyst expansion and regression in a mouse model of polycystic kidney disease. *Kidney International,* 83**,** 1099-1108.

HARDING, P. A., WANG, X. Z., OKADA, S., CHEN, W. Y., WAN, W. & KOPCHICK, J. J. 1996. Growth hormone (GH) and a GH antagonist promote GH receptor dimerization and internalization. *Journal of Biological Chemistry,* 271**,** 6708-6712.

HARPER, M. E., BARRERASALDANA, H. A. & SAUNDERS, G. F. 1982. CHROMOSOMAL LOCALIZATION OF THE HUMAN PLACENTAL LACTOGEN-GROWTH HORMONE GENE-CLUSTER TO 17Q22-24. *American Journal of Human Genetics,* 34**,** 227-234.

HARRIS, P. C. 1999. Autosomal dominant polycystic kidney disease: clues to pathogenesis. *Human Molecular Genetics,* 8**,** 1861-1866.

HARRIS, P. C., BAE, K. T., ROSSETTI, S., TORRES, V. E., GRANTHAM, J. J., CHAPMAN, A. B., GUAY-WOODFORD, L. M., KING, B. F., WETZEL, L. H., BAUMGARTEN, D. A., KENNEY, P. J., CONSUGAR, M., KLAHR, S., BENNETT, W. M., MEYERS, C. M., ZHANG, Q., THOMPSON, P. A., ZHU, F., MILLER, J. P. & CONSORTIUM, C. 2006. Cyst number but not the rate of cystic growth is associated with the mutated gene in autosomal dominant polycystic kidney disease. *Journal of the American Society of Nephrology,* 17**,** 3013-3019.

HATEBOER, N., DIJK, M. A. V., BOGDANOVA, N., COTO, E., SAGGAR-MALIK, A. K., SAN MILLAN, J. L., TORRA, R., BREUNING, M., RAVINE, D. & EUROPEAN, P. D. K. P. D. K. S. G. 1999. Comparison of phenotypes of polycystic kidney disease types 1 and 2. *Lancet,* 353**,** 103-107.

HATTORI, N., SHIMATSU, A., SUGITA, M., KUMAGAI, S. & IMURA, H. 1990. IMMUNOREACTIVE GROWTH-HORMONE (GH) SECRETION BY HUMAN-LYMPHOCYTES - AUGMENTED RELEASE BY EXOGENOUS GH. *Biochemical and Biophysical Research Communications,* 168**,** 396-401.

HE, J., LI, Q. Y., FANG, S. Y., GUO, Y., LIU, T. X., YE, J. H., YU, Z. Q., ZHANG, R., ZHAO, Y. F., HU, X. X., BAI, X. Y., CHEN, X. M. & LI, N. 2015. PKD1 Mono-Allelic Knockout Is Sufficient to Trigger Renal Cystogenesis in a Mini-Pig Model. *International Journal of Biological Sciences,* 11**,** 361-369.

HEINE, A., HELD, S. A. E., DAECKE, S. N., WALLNER, S., YAJNANARAYANA, S. P., KURTS, C., WOLF, D. & BROSSART, P. 2013. The JAK-inhibitor ruxolitinib impairs dendritic cell function in vitro and in vivo. *Blood,* 122**,** 1192-1202.

HELLEBUST, H., UHLEN, M. & ENFORS, S. O. 1989. EFFECT OF PROTEIN FUSION ON THE STABILITY OF PROTEOLYTICALLY SENSITIVE SITES IN RECOMBINANT DNA PROTEINS. *Journal of Biotechnology,* 12**,** 275-284.

HERRERA, J., HENKE, C. A. & BITTERMAN, P. B. 2018. Extracellular matrix as a driver of progressive fibrosis. *Journal of Clinical Investigation,* 128**,** 45-53.

HERRINGTON, J., SMIT, L. S., SCHWARTZ, J. & CARTER-SU, C. 2000. The role of STAT proteins in growth hormone signaling. *Oncogene,* 19**,** 2585-2597.

HIAN, C. K., LEE, C. L. & THOMAS, W. 2016. Renin-Angiotensin-Aldosterone System Antagonism and Polycystic Kidney Disease Progression. *Nephron,* 134**,** 59-63.

HIGASHIHARA, E., NUTAHARA, K., KOJIMA, M., TAMAKOSHI, A., YOSHIYUKI, O., SAKAI, H. & KUROKAWA, K. 1998. Prevalence and renal prognosis of diagnosed autosomal dominant polycystic kidney disease in Japan. *Nephron,* 80**,** 421-427.

HILL, D. J., RILEY, S. C., BASSETT, N. S. & WATERS, M. J. 1992. LOCALIZATION OF THE GROWTH-HORMONE RECEPTOR, IDENTIFIED BY IMMUNOCYTOCHEMISTRY, IN 2ND TRIMESTER HUMAN FETAL TISSUES AND IN PLACENTA THROUGHOUT GESTATION. *Journal of Clinical Endocrinology & Metabolism,* 75**,** 646-650.

HINTZEN, C., EVERS, C., LIPPOK, B. E., VOLKMER, R., HEINRICH, P. C., RADTKE, S. & HERMANNS, H. M. 2008. Box 2 region of the oncostatin M receptor determines specificity for recruitment of Janus kinases and STAT5 activation. *Journal of Biological Chemistry,* 283**,** 19465-19477.

HIRAI, K., SHIMOMURA, T., MORIWAKI, H., ISHII, H., SHIMOSHIKIRYO, T., TSUJI, D., INOUE, K., KADOIRI, T. & ITOH, K. 2016. Risk factors for hypernatremia in patients with short- and long-term tolvaptan treatment. *European Journal of Clinical Pharmacology,* 72**,** 1177-1183.

HIRSCHBERG, R. & ADLER, S. 1998. Insulin-like growth factor system and the kidney: Physiology, pathophysiology, and therapeutic implications. *American Journal of Kidney Diseases,* 31**,** 901-919.

HO, K. Y., EVANS, W. S., BLIZZARD, R. M., VELDHUIS, J. D., MERRIAM, G. R., SAMOJLIK, E., FURLANETTO, R., ROGOL, A. D., KAISER, D. L. & THORNER, M. O. 1987. EFFECTS OF SEX AND AGE ON THE 24-HOUR PROFILE OF GROWTH-HORMONE SECRETION IN MAN - IMPORTANCE OF ENDOGENOUS ESTRADIOL CONCENTRATIONS. *Journal of Clinical Endocrinology & Metabolism,* 64**,** 51-58.

HOGAN, M. C., ABEBE, K., TORRES, V. E., CHAPMAN, A. B., BAE, K. T., TAO, C., SUN, H. L., PERRONE, R. D., STEINMAN, T. I., BRAUN, W., WINKLHOFER, F. T., MISKULIN, D. C., RAHBARI-OSKOUI, F., BROSNAHAN, G., MASOUMI, A., KARPOV, I. O., SPILLANE, S., FLESSNER, M., MOORE, C. G. & SCHRIER, R. W. 2015. Liver Involvement in Early Autosomal-Dominant Polycystic Kidney Disease. *Clinical Gastroenterology and Hepatology,* 13**,** 155-+.

HOGAN, M. C., MASYUK, T. V., PAGE, L. J., KUBLY, V. J., BERGSTRALH, E. J., LI, X. J., KIM, B., KING, B. F., GLOCKNER, J., HOLMES, D. R., ROSSETTI, S., HARRIS, P. C., LARUSSO, N. F. & TORRES, V. E. 2010. Randomized Clinical Trial of Long-Acting Somatostatin for Autosomal Dominant Polycystic Kidney and Liver Disease. *Journal of the American Society of Nephrology,* 21**,** 1052-1061.

HOLL, R. W., THORNER, M. O. & LEONG, D. A. 1988. INTRACELLULAR CALCIUM-CONCENTRATION AND GROWTH-HORMONE SECRETION IN INDIVIDUAL SOMATOTROPES - EFFECTS OF GROWTH HORMONE-RELEASING FACTOR AND SOMATOSTATIN. *Endocrinology,* 122**,** 2927-2932.

HOPP, K., HOMMERDING, C. J., WANG, X. F., YE, H., HARRIS, P. C. & TORRES, V. E. 2015. Tolvaptan plus Pasireotide Shows Enhanced Efficacy in a PKD1 Model. *Journal of the American Society of Nephrology,* 26**,** 39-47.

HOYBYE, C., CHANDRAMOULI, V., EFENDIC, S., HULTING, A. L., LANDAU, B. R., SCHUMANN, W. C. & WAJNGOT, A. 2008. Contribution of gluconeogenesis and glycogenolysis to hepatic glucose production in acromegaly before and after pituitary microsurgery. *Hormone and Metabolic Research,* 40**,** 498-501.

HUGHES, J., WARD, C. J., PERAL, B., ASPINWALL, R., CLARK, K., SANMILLAN, J. L., GAMBLE, V. & HARRIS, P. C. 1995. THE POLYCYSTIC KIDNEY-DISEASE-1 (PKD1) GENE ENCODES A NOVEL PROTEIN WITH MULTIPLE CELL RECOGNITION DOMAINS. *Nature Genetics,* 10**,** 151-160.

IBRAGHIMOVBESKROVNAYA, O., DACKOWSKI, W. R., FOGGENSTEINER, L., COLEMAN, N., THIRU, S., PETRY, L. R., BURN, T. C., CONNORS, T. D., VANRAAY, T., BRADLEY, J., QIAN, F., ONUCHIC, L. F., WATNICK, T. J., PIONTEK, K., HAKIM, R. M., LANDES, G. M., GERMINO, G. G., SANDFORD, R. & KLINGER, K. W. 1997. Polycystin: In vitro synthesis, in vivo tissue expression, and subcellular localization identifies a large membrane-associated protein. *Proceedings of the National Academy of Sciences of the United States of America,* 94**,** 6397-6402.

IDOWU, J., HOME, T., PATEL, N., MAGENHEIMER, B., TRAN, P. V., MASER, R. L., WARD, C. J., CALVET, J. P., WALLACE, D. P. & SHARMA, M. 2018. Aberrant Regulation of Notch3 Signaling Pathway in Polycystic Kidney Disease. *Scientific Reports,* 8.

IGLESIAS, C. G., TORRES, V. E., OFFORD, K. P., HOLLEY, K. E., BEARD, C. M. & KURLAND, L. T. 1983. EPIDEMIOLOGY OF ADULT POLYCYSTIC KIDNEY-DISEASE, OLMSTED COUNTY, MINNESOTA - 1935-1980. *American Journal of Kidney Diseases,* 2**,** 630-639.

IHLE, J. N. 1996. STATs: Signal transducers and activators of transcription. *Cell,* 84**,** 331-334.

ISHIKAWA, I., MAEDA, K., NAKAI, S. & KAWAGUCHI, Y. 2000. Gender difference in the mean age at the induction of hemodialysis in patients with autosomal dominant polycystic kidney disease. *American Journal of Kidney Diseases,* 35**,** 1072-1075.

JACKSONGRUSBY, L. L., PRAVTCHEVA, D., RUDDLE, F. H. & LINZER, D. I. H. 1988. CHROMOSOMAL MAPPING OF THE PROLACTIN GROWTH-HORMONE GENE FAMILY IN THE MOUSE. *Endocrinology,* 122**,** 2462-2466.

JAFFE, C. A., TURGEON, D. K., FRIBERG, R. D., WATKINS, P. B. & BARKAN, A. L. 1995. NOCTURNAL AUGMENTATION OF GROWTH-HORMONE (GH) SECRETION IS PRESERVED DURING REPETITIVE BOLUS ADMINISTRATION OF GH-RELEASING HORMONE - POTENTIAL INVOLVEMENT OF ENDOGENOUS SOMATOSTATIN - A CLINICAL RESEARCH-CENTER STUDY. *Journal of Clinical Endocrinology & Metabolism,* 80**,** 3321-3326.

JOHNSON, A. M. & GABOW, P. A. 1997. Identification of patients with autosomal dominant polycystic kidney disease at highest risk for end-stage renal disease. *Journal of the American Society of Nephrology,* 8**,** 1560-1567.

JOHNSON, V. & MAACK, T. 1977. RENAL EXTRACTION, FILTRATION, ABSORPTION, AND CATABOLISM OF GROWTH-HORMONE. *American Journal of Physiology,* 233**,** F185-F196.

KALLURI, R. & WEINBERG, R. A. 2009. The basics of epithelial-mesenchymal transition. *Journal of Clinical Investigation,* 119**,** 1420-1428.

KANAAN, N., DEVUYST, O. & PIRSON, Y. 2014. Renal transplantation in autosomal dominant polycystic kidney disease. *Nature Reviews Nephrology,* 10**,** 455-465.

KANAI, T., SEKI, S., JENKS, J. A., KOHLI, A., KAWLI, T., MARTIN, D. P., SNYDER, M., BACCHETTA, R. & NADEAU, K. C. 2014. Identification of STAT5A and STAT5B Target Genes in Human T Cells. *Plos One,* 9.

KAPLAN, S. L., SHEPARD, T. H. & GRUMBACH, M. M. 1972. ONTOGENESIS OF HUMAN FETAL HORMONES .1. GROWTH-HORMONE AND INSULIN. *Journal of Clinical Investigation,* 51**,** 3080-&.

KARIHALOO, A., KORAISHY, F., HUEN, S. C., LEE, Y., MERRICK, D., CAPLAN, M. J., SOMLO, S. & CANTLEY, L. G. 2011. Macrophages Promote Cyst Growth in Polycystic Kidney Disease. *Journal of the American Society of Nephrology,* 22**,** 1809-1814.

KASHYAP, S., HEIN, K. Z., CHINI, C. C. S., LIKA, J., WARNER, G. M., BALE, L. K., TORRES, V. E., HARRIS, P. C., OXVIG, C., CONOVER, C. A. & CHINI, E. N. 2020. Metalloproteinase PAPP-A regulation of IGF-1 contributes to polycystic kidney disease pathogenesis. *Jci Insight,* 5.

KIEPE, D., CIARMATORI, S., HOEFLICH, A., WOLF, E. & TONSHOFF, B. 2005. Insulin-like growth factor (IGF)-I stimulates cell proliferation and induces IGF binding protein (IGFBP)-3 and IGFBP-5 gene expression in cultured growth plate chondrocytes via distinct signaling pathways. *Endocrinology,* 146**,** 3096-3104.

KOJIMA, M., HOSODA, H., DATE, Y., NAKAZATO, M., MATSUO, H. & KANGAWA, K. 1999. Ghrelin is a growth-hormone-releasing acylated peptide from stomach. *Nature,* 402**,** 656-660.

KOPTIDES, M., HADJIMICHAEL, C., KOUPEPIDOU, P., PIERIDES, A. & DELTAS, C. C. 1999. Germinal and somatic mutations in the PKD2 gene of renal cysts in autosomal dominant polycystic kidney disease. *Human Molecular Genetics,* 8**,** 509-513.

KOPTIDES, M., MEAN, R., DEMETRIOU, K., PIERIDES, A. & DELTAS, C. C. 2000. Genetic evidence for a trans-heterozygous model for cystogenesis in autosomal dominant polycystic kidney disease. *Human Molecular Genetics,* 9**,** 447-452.

KOSLOWSKI, S., LATAPY, C., AUVRAY, P., BLONDEL, M. & MEIJER, L. 2020. An Overview of In Vivo and In Vitro Models for Autosomal Dominant Polycystic Kidney Disease: A Journey from 3D-Cysts to Mini-Pigs. *International Journal of Molecular Sciences,* 21.

KRAUER, F., AHMADLI, U., KOLLIAS, S., BLEISCH, J., RP, W., AL, S. & D, P. 2012. Growth of arachnoid cysts in patients with autosomal dominant polycystic kidney disease: serial imaging and clinical relevance. *Clinical Kidney Journal,* 5**,** 405-411.

KUGITA, M., NISHII, K., YAMAGUCHI, T., SUZUKI, A., YUZAWA, Y., HORIE, S., HIGASHIHARA, E. & NAGAO, S. 2017. Beneficial effect of combined treatment with octreotide and pasireotide in PCK rats, an orthologous model of human autosomal recessive polycystic kidney disease. *Plos One,* 12.

LAGER, D. J., QIAN, Q., BENGAL, R. J., ISHIBASHI, M. & TORRES, V. E. 2001. The pck rat: A new model that resembles human autosomal dominant polycystic kidney and liver disease. *Kidney International,* 59**,** 126-136.

LANDAU, D., DOMENE, H., FLYVBJERG, A., GRONBAEK, H., ROBERTS, C. T., ARGOV, S. & LEROITH, D. 1998. Differential expression of renal growth hormone receptor and its binding protein in experimental diabetes mellitus. *Growth Hormone & Igf Research,* 8**,** 39-45.

LANDRETH, K. S., NARAYANAN, R. & DORSHKIND, K. 1992. INSULIN-LIKE GROWTH FACTOR-I REGULATES PRO-B-CELL DIFFERENTIATION. *Blood,* 80**,** 1207-1212.

LANKTREE, M. B., GUIARD, E., LI, W. L., AKBARI, P., HAGHIGHI, A., ILIUTA, L. A., SHI, B., CHEN, C., HE, N., SONG, X. W., MARGETTS, E. E., INGRAM, A., KHALILI, O. R. O., PATERSON, A. R. & PEI, Y. R. 2019. Intrafamilial Variability of ADPKD. *Kidney International Reports,* 4**,** 995-1003.

LANOIX, J., DAGATI, V., SZABOLCS, M. & TRUDEL, M. 1996. Dysregulation of cellular proliferation and apoptosis mediates human autosomal dominant polycystic kidney disease (ADPKD). *Oncogene,* 13**,** 1153-1160.

LANTINGA-VAN LEEUWEN, I. S., DAUWERSE, J. G., BAELDE, H. J., LEONHARD, W. N., VAN DE WAL, A., WARD, C. J., VERBEEK, S., DERUITER, M. C., BREUNING, M. H., DE HEER, E. & PETERS, D. J. M. 2004. Lowering of Pkd1 expression is sufficient to cause polycystic kidney disease. *Human Molecular Genetics,* 13**,** 3069-3077.

LE MARCHAND, L., DONLON, T., SEIFRIED, A., KAAKS, R., RINALDI, S. & WILKENS, L. R. 2002. Association of a common polymorphism in the human GH1 gene with colorectal neoplasia. *Jnci-Journal of the National Cancer Institute,* 94**,** 454-460.

LEE, E. C., VALENCIA, T., ALLERSON, C., SCHAIRER, A., FLATEN, A., YHESKEL, M., KERSJES, K., LI, J., GATTO, S., TAKHAR, M., LOCKTON, S., PAVLICEK, A., KIM, M., CHU, T., SORIANO, R., DAVIS, S., ANDROSAVICH, J. R., SARWARY, S., OWEN, T., KAPLAN, J., LIU, K., JANG, G., NEBEN, S., BENTLEY, P., WRIGHT, T. & PATEL, V. 2019. Discovery and preclinical evaluation of anti-miR-17 oligonucleotide RGLS4326 for the treatment of polycystic kidney disease. *Nature Communications,* 10.

LEE, E. J., SEO, E., KIM, J. W., NAM, S. A., LEE, J. Y., JUN, J., OH, S., PARK, M., JHO, E. H., YOO, K. H., PARK, J. H. & KYUN, Y. 2020. TAZ/Wnt-beta-catenin/c-MYC axis regulates cystogenesis in polycystic kidney disease. *Proceedings of the National Academy of Sciences of the United States of America,* 117**,** 29001-29012.

LEE, J. G., AHN, C., YOON, S. C., PARK, J. H., EO, H. S., NO, J. J., KIM, K. H., LEE, E. J., HWANG, Y. H., HWANG, D. Y., KIM, Y. S., HAN, J. S., KIM, S., LEE, J. S. & KIM, S. H. 2003. No association of the TGF-beta(1) gene polymorphisms with the renal progression in autosomal dominant polycystic kidney disease (ADPKD) patients. *Clinical Nephrology,* 59**,** 10-16.

LEE, J. G., AHN, C., YOON, S. C., PARK, J. H., NO, J. J., MOON, C. S., SONG, E. K., HWANG, Y. H., HWANG, D. Y., KIM, Y. S., HAN, J. S., KIM, S. G., LEE, J. S. & KIM, S. H. 2002. The Glu/Asp polymorphism of ecNOS gene and the renal progression in Korean autosomal dominant polycystic kidney disease (ADPKD) patients. *Korean Journal of Genetics,* 24**,** 241-246.

LEE, K., BOCTOR, S., BARISONI, L. M. C. & GUSELLA, G. L. 2015. Inactivation Of Integrin-beta 1 Prevents the Development of Polycystic Kidney Disease after the Loss of Polycystin-1. *Journal of the American Society of Nephrology,* 26**,** 888-895.

LENTINE, K. L., XIAO, H. L., MACHNICKI, G., GHEORGHIAN, A. & SCHNITZLER, M. A. 2010. Renal Function and Healthcare Costs in Patients with Polycystic Kidney Disease. *Clinical Journal of the American Society of Nephrology,* 5**,** 1471-1479.

LEONHARD, W. N., VAN DER WAL, A., NOVALIC, Z., KUNNEN, S. J., GANSEVOORT, R. T., BREUNING, M. H., DE HEER, E. & PETERS, D. J. M. 2011. Curcumin inhibits cystogenesis by simultaneous interference of multiple signaling pathways: in vivo evidence from a Pkd1-deletion model. *American Journal of Physiology-Renal Physiology,* 300**,** F1193-F1202.

LEUNG, D. W., SPENCER, S. A., CACHIANES, G., HAMMONDS, R. G., COLLINS, C., HENZEL, W. J., BARNARD, R., WATERS, M. J. & WOOD, W. I. 1987. GROWTH-HORMONE RECEPTOR AND SERUM BINDING-PROTEIN - PURIFICATION, CLONING AND EXPRESSION. *Nature,* 330**,** 537-543.

LEUNG, K. C., DOYLE, N., BALLESTEROS, M., SJOGREN, K., WATTS, C. K. W., LOW, T. H., LEONG, G. M., ROSS, R. J. M. & HO, K. K. Y. 2003. Estrogen inhibits GH signaling by suppressing GH-induced JAK2 phosphorylation, an effect mediated by SOCS-2. *Proceedings of the National Academy of Sciences of the United States of America,* 100**,** 1016-1021.

LEWIS, U. J., LEWIS, L. J., SALEM, M. A. M., STATEN, N. R., GALOSY, S. S. & KRIVI, G. G. 1991. A RECOMBINANT-DNA-DERIVED MODIFICATION OF HUMAN GROWTH-HORMONE (HGH44-191) WITH ENHANCED DIABETOGENIC ACTIVITY. *Molecular and Cellular Endocrinology,* 78**,** 45-54.

LI, P., MITRA, S., SPOLSKI, R., OH, J., LIAO, W., TANG, Z. H., MO, F., LI, X. W., WEST, E. E., GROMER, D., LIN, J. X., LIU, C. Y., RUAN, Y. J. & LEONARD, W. J. 2017. STAT5-mediated chromatin interactions in superenhancers activate IL-2 highly inducible genes: Functional dissection of the Il2ra gene locus. *Proceedings of the National Academy of Sciences of the United States of America,* 114**,** 12111-12119.

LI, X. G., LUO, Y., STARREMANS, P. G., MCNAMARA, C. A., PEI, Y. & ZHOU, J. 2005. Polycystin-1 and polycystin-2 regulate the cell cycle through the helix-loop-helix inhibitor Id2. *Nature Cell Biology,* 7**,** 1202-1212.

LI, Y. S., KELDER, B. & KOPCHICK, J. J. 2001. Identification, isolation, and cloning of growth hormone (GH)-inducible interscapular brown adipose complementary deoxyribonucleic acid from GH antagonist mice. *Endocrinology,* 142**,** 2937-2945.

LIU, M., SHI, S., SENTHILNATHAN, S., YU, J., WU, E., BERGMANN, C., ZERRES, K., BOGDANOVA, N., COTO, E., DELTAS, C., PIERIDES, A., DEMETRIOU, K., DEVUYST, O., GITOMER, B., LAAKSO, M., LUMIAHO, A., LAMNISSOU, K., MAGISTRONI, R., PARFREY, P., BREUNING, M., PETERS, D. J. M., TORRA, R., WINEARLS, C. G., TORRES, V. E., HARRIS, P. C., PATERSON, A. D. & PEI, Y. 2010. Genetic Variation of DKK3 May Modify Renal Disease Severity in ADPKD. *Journal of the American Society of Nephrology,* 21**,** 1510-1520.

LIU, X. W., ROBINSON, G. W., WAGNER, K. U., GARRETT, L., WYNSHAWBORIS, A. & HENNIGHAUSEN, L. 1997. Stat5a is mandatory for adult mammary gland development and lactogenesis. *Genes & Development,* 11**,** 179-186.

LOMBARDI, G., COLAO, A., CUOCOLO, A., LONGOBARDI, S., DI SOMMA, C., ORIO, F., MEROLA, B., NICOLAI, E. & SALVATORE, M. 1997. Cardiological aspects of growth hormone and insulin-like growth factor-I. *Journal of Pediatric Endocrinology & Metabolism,* 10**,** 553-560.

LOW, S. H., VASANTH, S., LARSON, C. H., MUKHERJEE, S., SHARMA, N., KINTER, M. T., KANE, M. E., OBARA, T. & WEIMBS, T. 2006. Polycystin-1, STAT6, and pathway that transduces P100 function in a ciliary mechanosensation and is activated in polycystic kidney disease. *Developmental Cell,* 10**,** 57-69.

LU, C. X., KASIK, J., STEPHAN, D. A., YANG, S. H., SPERLING, M. A. & MENON, R. K. 2001. Grtp1, a novel gene regulated by growth hormone. *Endocrinology,* 142**,** 4568-4571.

LU, W. N., PEISSEL, B., BABAKHANLOU, H., PAVLOVA, A., GENG, L., FAN, X. H., LARSON, C., BRENT, G. & ZHOU, J. 1997. Perinatal lethality with kidney and pancreas defects in mice with a targetted Pkd1 mutation. *Nature Genetics,* 17**,** 179-181.

MAAMRA, M., FINIDORI, J., VON LAUE, S., SIMON, S., JUSTICE, S., WEBSTER, J., DOWER, S. & ROSS, R. 1999. Studies with a growth hormone antagonist and dual-fluorescent confocal microscopy demonstrate that the full-length human growth hormone receptor, but not the truncated isoform, is very rapidly internalized independent of Jak2-Stat5 signaling. *Journal of Biological Chemistry,* 274**,** 14791-14798.

MADURAWE, R. D., CHASE, T. E., TSAO, E. I. & BENTLEY, W. E. 2000. A recombinant lipoprotein antigen against Lyme disease expressed in E-coli: Fermentor operating strategies for improved yield. *Biotechnology Progress,* 16**,** 571-576.

MAGISTRONI, R., MANFREDINI, P., FURCI, L., LIGABUE, G., MARTINO, C., LEONELLI, M., SCAPOLI, C. & ALBERTAZZI, A. 2003. Epidermal growth factor receptor polymorphism and autosomal dominant polycystic kidney disease. *Journal of Nephrology,* 16**,** 110-115.

MALAS, T. B., FORMICA, C., LEONHARD, W. N., RAO, P., GRANCHI, Z., ROOS, M., PETERS, D. J. & T' HOEN, P. A. 2018. Meta-analysis of polycystic kidney disease expression profiles defines strong involvement of injury repair processes (vol 312, pg F806, 2017). *American Journal of Physiology-Renal Physiology,* 314**,** F140-F140.

MANGOOKARIM, R., UCHIC, M. E., GRANT, M., SHUMATE, W. A., CALVET, J. P., PARK, C. H. & GRANTHAM, J. J. 1989. RENAL EPITHELIAL FLUID SECRETION AND CYST GROWTH - THE ROLE OF CYCLIC-AMP. *Faseb Journal,* 3**,** 2629-2632.

MARKOWITZ, G. S., CAI, Y. Q., LI, L., WU, G. Q., WARD, L. C., SOMLO, S. & D'AGATI, V. D. 1999. Polycystin-2 expression is developmentally regulated. *American Journal of Physiology-Renal Physiology,* 277**,** F17-F25.

MASYUK, T. V., MASYUK, A. I., TORRES, V. E., HARRIS, P. C. & LARUSSO, N. F. 2007. Octreotide inhibits hepatic cystogenesis in a rodent model of polycystic liver disease by reducing cholangiocyte adenosine 3 ',5 '-cyclic monophosphate. *Gastroenterology,* 132**,** 1104-1116.

MASYUK, T. V., RADTKE, B. N., STROOPE, A. J., BANALES, J. M., GRADILONE, S. A., HUANG, B., MASYUK, A. I., HOGAN, M. C., TORRES, V. E. & LARUSSO, N. F. 2013. Pasireotide Is More Effective than Octreotide in Reducing Hepatorenal Cystogenesis in Rodents with Polycystic Kidney and Liver Diseases. *Hepatology,* 58**,** 409-421.

MATSUMURA, I., KITAMURA, T., WAKAO, H., TANAKA, H., HASHIMOTO, K., ALBANESE, C., DOWNWARD, J., PESTELL, R. G. & KANAKURA, Y. 1999. Transcriptional regulation of the cyclin D1 promoter by STAT5: its involvement in cytokine-dependent growth of hematopoietic cells. *Embo Journal,* 18**,** 1367-1377.

MCEWAN, P., WILTON, H. B., ONG, A. C. M., ORSKOV, B., SANDFORD, R., SCOLARI, F., CABRERA, M. C. V., WALZ, G., O'REILLY, K. & ROBINSON, P. 2018. A model to predict disease progression in patients with autosomal dominant polycystic kidney disease (ADPKD): the ADPKD Outcomes Model. *Bmc Nephrology,* 19.

MCPHERSON, E. A., LUO, Z. M., BROWN, R. A., LEBARD, L. S., CORLESS, C. C., SPETH, R. C. & BAGBY, S. P. 2004. Chymase-like angiotensin II-generating activity in end-stage human autosomal dominant polycystic kidney disease. *Journal of the American Society of Nephrology,* 15**,** 493-500.

MEHTA, A., HINDMARSH, P. C., STANHOPE, R. G., TURTON, J. P. G., COLE, T. J., PREECE, M. A. & DATTANI, M. T. 2005. The role of growth hormone in determining birth size and early postnatal growth, using congenital growth hormone deficiency (GHD) as a model. *Clinical Endocrinology,* 63**,** 223-231.

MI, Z. Y., SONG, Y. D., CAO, X. Y., LU, Y., LIU, Z. H., ZHU, X., GENG, M. J., SUN, Y. Z., LAN, B. X., HE, C. R., XIONG, H., ZHANG, L. R. & CHEN, Y. P. 2020. Super-enhancer-driven metabolic reprogramming promotes cystogenesis in autosomal dominant polycystic kidney disease. *Nature Metabolism,* 2**,** 717-+.

MIERENDORF, R. C., MORRIS, B. B., HAMMER, B. & NOVY, R. E. 1998. Expression and purification of recombinant proteins using the pET system. *Molecular Diagnosis of Infectious Diseases,* 13**,** 257-292.

MILUTINOVIC, J., RUST, P. F., FIALKOW, P. J., AGODOA, L. Y., PHILLIPS, L. A., RUDD, T. G. & SUTHERLAND, S. 1992. INTRAFAMILIAL PHENOTYPIC-EXPRESSION OF AUTOSOMAL DOMINANT POLYCYSTIC KIDNEY-DISEASE. *American Journal of Kidney Diseases,* 19**,** 465-472.

MIQUET, J. G., GONZALEZ, L., MATOS, M. N., HANSEN, C. E., LOUIS, A., BARTKE, A., TURYN, D. & SOTELO, A. I. 2008. Transgenic mice overexpressing GH exhibit hepatic upregulation of GH-signaling mediators involved in cell proliferation. *Journal of Endocrinology,* 198**,** 317-330.

MOCHIZUKI, T., WU, G. Q., HAYASHI, T., XENOPHONTOS, S. L., VELDHUISEN, B., SARIS, J. J., REYNOLDS, D. M., CAI, Y. Q., GABOW, P. A., PIERIDES, A., KIMBERLING, W. J., BREUNING, M. H., DELTAS, C.

C., PETERS, D. J. M. & SOMLO, S. 1996. PKD2, a gene for polycystic kidney disease that encodes an integral membrane protein. *Science,* 272**,** 1339-1342.

MORIGGL, R., GOUILLEUXGRUART, V., JAHNE, R., BERCHTOLD, S., GARTMANN, C., LIU, X. W., HENNIGHAUSEN, L., SOTIROPOULOS, A., GRONER, B. & GOUILLEUX, F. 1996. Deletion of the carboxyl-terminal transactivation domain of MGF-Stat5 results in sustained DNA binding and a dominant negative phenotype. *Molecular and Cellular Biology,* 16**,** 5691-5700.

MOSETTI, M. A., LEONARDOU, P., MOTOHARA, T., KANEMATSU, M., ARMAO, D. & SEMELKA, R. C. 2003. Autosomal dominant polycystic kidney disease: MR imaging evaluation using current techniques. *Journal of Magnetic Resonance Imaging,* 18**,** 210-215.

MURPHY, L. J., BELL, G. I. & FRIESEN, H. G. 1987. GROWTH-HORMONE STIMULATES SEQUENTIAL INDUCTION OF C-MYC AND INSULIN-LIKE GROWTH FACTOR-I EXPRESSION INVIVO. *Endocrinology,* 120**,** 1806-1812.

NAGAO, S., MORITA, M., KUGITA, M., YOSHIHARA, D., YAMAGUCHI, T., KURAHASHI, H., CALVET, J. P. & WALLACE, D. P. 2010. Polycystic kidney disease in Han:SPRD Cy rats is associated with elevated expression and mislocalization of SamCystin. *American Journal of Physiology-Renal Physiology,* 299**,** F1078-F1086.

NAKAMURA, T., EBIHARA, I., NAGAOKA, I., TOMINO, Y., NAGAO, S., TAKAHASHI, H. & KOIDE, H. 1993. GROWTH-FACTOR GENE-EXPRESSION IN KIDNEY OF MURINE POLYCYSTIC KIDNEY-DISEASE. *Journal of the American Society of Nephrology,* 3**,** 1378-1386.

NASS, R., TOOGOOD, A. A., HELLMANN, P., BISSONETTE, E., GAYLINN, B., CLARK, R. & THORNER, M. O. 2000a. Intracerebroventricular administration of the rat growth hormone (GH) receptor antagonist G118R stimulates GH secretion: Evidence for the existence of short loop negative feedback of GH. *Journal of Neuroendocrinology,* 12**,** 1194-1199.

NASS, R., TOOGOOD, A. A., HELLMANN, P., BISSONETTE, E., GAYLINN, B., CLARK, R. & THORNER, M. O. 2000b. Intracerebroventricular administration of the rat growth hormone (GH) receptor antagonist G118R stimulates GH secretion: evidence for the existence of short loop negative feedback of GH. *J Neuroendocrinol,* 12**,** 1194-9.

NAULI, S. M., ALENGHAT, F. J., LUO, Y., WILLIAMS, E., VASSILEV, P., LIL, X. G., ELIA, A. E. H., LU, W. N., BROWN, E. M., QUINN, S. J., INGBER, D. E. & ZHOU, J. 2003. Polycystins 1 and 2 mediate mechanosensation in the primary cilium of kidney cells. *Nature Genetics,* 33**,** 129-137.

NEUMANN, H. P. H., JILG, C., BACHER, J., NABULSI, Z., MALINOC, A., HUMMEL, B., HOFFMANN, M. M., ORTIZ-BRUECHLE, N., GLASKER, S., PISARSKI, P., NEEFF, H., KRAMER-GUTH, A., CYBULLA, M., HORNBERGER, M., WILPERT, J., FUNK, L., BAUMERT, J., PAATZ, D., BAUMANN, D., LAHL, M., FELTEN, H., HAUSBERG, M., ZERRES, K., ENG, C. & ELSE KROENER FRESENIUS, A. 2013. Epidemiology of autosomal-dominant polycystic kidney disease: an in-depth clinical study for south-western Germany. *Nephrology Dialysis Transplantation,* 28**,** 1472-1487.

NITULESCU, II, MEYER, S. C., WEN, Q. J., CRISPINO, J. D., LEMIEUX, M. E., LEVINE, R. L., PELISH, H. E. & SHAIR, M. D. 2017. Mediator Kinase Phosphorylation of STAT1 S727 Promotes Growth of Neoplasms With JAK-STAT Activation. *Ebiomedicine,* 26**,** 112-125.

O'HARE, M. J., BOND, J., CLARKE, C., TAKEUCHI, Y., ATHERTON, A. J., BERRY, C., MOODY, J., SILVER, A. R. J., DAVIES, D. C., ALSOP, A. E., NEVILLE, A. M. & JAT, P. S. 2001. Conditional immortalization of freshly isolated human mammary fibroblasts and endothelial cells. *Proceedings of the National Academy of Sciences of the United States of America,* 98**,** 646-651.

OLSAN, E. E., MUKHERJEE, S., WULKERSDORFER, B., SHILLINGFORD, J. M., GIOVANNONE, A. J., TODOROV, G., SONG, X. W., PEI, Y. & WEIMBS, T. 2011. Signal transducer and activator of transcription-6 (STAT6) inhibition suppresses renal cyst growth in polycystic kidney disease. *Proceedings of the National Academy of Sciences of the United States of America,* 108**,** 18067-18072.

OLSON, K., GEHANT, R., MUKKU, V., O'CONNELL, K., TOMLINSON, B., TOTPAL, K. & WINKLER, M. 1997. Preparation and characterization of poly(ethylene glycol)ylated human growth hormone antagonist. *Poly(Ethylene Glycol): Chemistry and Biological Applications,* 680**,** 170-181.

OLSON, K. C., FENNO, J., LIN, N., HARKINS, R. N., SNIDER, C., KOHR, W. H., ROSS, M. J., FODGE, D., PRENDER, G. & STEBBING, N. 1981. PURIFIED HUMAN GROWTH-HORMONE FROM ESCHERICHIA-COLI IS BIOLOGICALLY-ACTIVE. *Nature,* 293**,** 408-411.

ONG, A. C. M. & HARRIS, P. C. 2015. A polycystin-centric view of cyst formation and disease: the polycystins revisited. *Kidney International,* 88**,** 699-710.

ONG, A. C. M., WARD, C. J., BUTLER, R. J., BIDDOLPH, S., BOWKER, C., TORRA, P., PEI, Y. & HARRIS, P. C. 1999. Coordinate expression of the autosomal dominant polycystic kidney disease proteins, polycystin-2 and polycystin-1, in normal and cystic tissue. *American Journal of Pathology,* 154**,** 1721-1729.

ORSKOV, B., SORENSEN, V. R., FELDT-RASMUSSEN, B. & STRANDGAARD, S. 2012. Changes in causes of death and risk of cancer in Danish patients with autosomal dominant polycystic kidney disease and end-stage renal disease. *Nephrology Dialysis Transplantation,* 27**,** 1607-1613.

OTANI, D., MURAKAMI, T., MATSUBARA, T., HOJO, M., NAKAE, T., MORIYOSHI, K., YASODA, A., USUI, R., TATSUOKA, H., OGURA, M., INAGAKI, N. & YAMAMOTO, T. 2021. Acromegaly accompanied by diabetes mellitus and polycystic kidney disease. *Endocrine Journal,* 68**,** 103-110.

OWERBACH, D., RUTTER, W. J., MARTIAL, J. A., BAXTER, J. D. & SHOWS, T. B. 1980. GENES FOR GROWTH-HORMONE, CHORIONIC SOMATOMAMMOTROPIN, AND GROWTH HORMONE-LIKE GENE ON CHROMOSOME-17 IN HUMANS. *Science,* 209**,** 289-292.

PARKER, E., NEWBY, L. J., SHARPE, C. C., ROSSETTI, S., STREETS, A. J., HARRIS, P. C., O'HARE, M. J. & ONG, A. C. M. 2007. Hyperproliferation of PKD1 cystic cells is induced by insulin-like growth factor-1 activation of the Ras/Raf signalling system. *Kidney International,* 72**,** 157-165.

PARNELL, S. C., MAGENHEIMER, B. S., MASER, R. L., RANKIN, C. A., SMINE, A., OKAMOTO, T. & CALVET, J. P. 1998. The polycystic kidney disease-1 protein, polycystin-1, binds and activates heterotrimeric G-proteins in vitro. *Biochemical and Biophysical Research Communications,* 251**,** 625-631.

PATEL, V., WILLIAMS, D., HAJARNIS, S., HUNTER, R., PONTOGLIO, M., SOMLO, S. & IGARASHI, P. 2013. miR-17 similar to 92 miRNA cluster promotes kidney cyst growth in polycystic kidney disease. *Proceedings of the National Academy of Sciences of the United States of America,* 110**,** 10765-10770.

PATERA, F., CUDZICH-MADRY, A., HUANG, Z. & FRAGIADAKI, M. 2019. Renal expression of JAK2 is high in polycystic kidney disease and its inhibition reduces cystogenesis. *Scientific Reports,* 9.

PAUL, B. M., CONSUGAR, M. B., LEE, M. R., SUNDSBAK, J. L., HEYER, C. M., ROSSETTI, S., KUBLY, V. J., HOPP, K., TORRES, V. E., COTO, E., CLEMENTI, M., BOGDANOVA, N., DE ALMEIDA, E., BICHET, D. G. & HARRIS, P. C. 2014. Evidence of a third ADPKD locus is not supported by re-analysis of designated PKD3 families. *Kidney International,* 85**,** 383-392.

PEI, Y., PATERSON, A. D., WANG, K. R., HE, N., HEFFERTON, D., WATNICK, T., GERMINO, G. G., PARFREY, P., SOMLO, S. & ST GEORGE-HYSLOP, P. 2001. Bilineal disease and trans-heterozygotes in autosomal dominant polycystic kidney disease. *American Journal of Human Genetics,* 68**,** 355-363.

PERAL, B., ONG, A. C. M., SANMILLAN, J. L., GAMBLE, V., REES, L. & HARRIS, P. C. 1996. A stable, nonsense mutation associated with a case of infantile onset polycystic kidney disease 1 (PKD1). *Human Molecular Genetics,* 5**,** 539-542.

PEREZ-IBAVE, D. C., RODRIGUEZ-SANCHEZ, I. P., GARZA-RODRIGUEZ, M. D. & BARRERA-SALDANA, H. A. 2014. Extrapituitary growth hormone synthesis in humans. *Growth Hormone & Igf Research,* 24**,** 47-53.

PERICO, N., RUGGENENTI, P., PERNA, A., CAROLI, A., TRILLINI, M., SIRONI, S., PISANI, A., RICCIO, E., IMBRIACO, M., DUGO, M., MORANA, G., GRANATA, A., FIGUERA, M., GASPARI, F., CARRARA, F., RUBIS, N., VILLA, A., GAMBA, S., PRANDINI, S., CORTINOVIS, M., REMUZZI, A., REMUZZI, G. & GRP, A. S. 2019. Octreotide-LAR in later-stage autosomal dominant polycystic kidney disease (ALADIN 2): A randomized, double-blind, placebo-controlled, multicenter trial. *Plos Medicine,* 16.

PERRONE, R. D., MOUKSASSI, M. S., ROMERO, K., CZERWIEC, F. S., CHAPMAN, A. B., GITOMER, B. Y., TORRES, V. E., MISKULIN, D. C., BROADBENT, S. & MARIER, J. F. 2017. Total Kidney Volume Is a Prognostic Biomarker of Renal Function Decline and Progression to End-Stage Renal Disease in Patients With Autosomal Dominant Polycystic Kidney Disease. *Kidney International Reports,* 2**,** 442-450.

PETKOVIC, V., BESSON, A., THEVIS, M., LOCHMATTER, D., EBLE, A., FLUCK, C. E. & MULLIS, P. E. 2007. Evaluation of the biological activity of a growth hormone (GH) mutant (R77C) and its impact on GH responsiveness and stature. *Journal of Clinical Endocrinology & Metabolism,* 92**,** 2893-2901.

PONTING, C. P., HOFMANN, K. & BORK, P. 1999. A latrophilin/CL-1-like GPS domain in polycystin-1. *Current Biology,* 9**,** R585-R588.

PORATH, B., GAINULLIN, V. G., GALL, E. C. L., DILLINGER, E. K., HEYER, C. M., HOPP, K., EDWARDS, M. E., MADSEN, C. D., MAURITZ, S. R., BANKS, C. J., BAHETI, S., REDDY, B., HERRERO, J. I., BANALES, J. M., HOGAN, M. C., TASIC, V., WATNICK, T. J., CHAPMAN, A. B., VIGNEAU, C., LAVAINNE, F., AUDREZET, M. P., FEREC, C., LE MEUR, Y., TORRES, V. E., HARRIS, P. C., GENKYST STUDY, G., KIDNEY, H. P. P. & CONSORTIUM RADIOLOGIC IMAGING, S. 2016. Mutations in GANAB, Encoding the Glucosidase IIa Subunit, Cause Autosomal-Dominant Polycystic Kidney and Liver Disease. *American Journal of Human Genetics,* 98**,** 1193-1207.

QIAN, F., BOLETTA, A., BHUNIA, A. K., XU, H. X., LIU, L. J., AHRABI, A. K., WATNICK, T. J., ZHOU, F. & GERMINO, G. G. 2002. Cleavage of polycystin-1 requires the receptor for egg jelly domain and is disrupted by human autosomal-dominant polycystic kidney disease 1-associated mutations. *Proceedings of the National Academy of Sciences of the United States of America,* 99**,** 16981-16986.

QIAN, F., WATNICK, T. J., ONUCHIC, L. F. & GERMINO, G. G. 1996. The molecular basis of focal cyst formation in human autosomal dominant polycystic kidney disease type I. *Cell,* 87**,** 979-987.

QIANG, J., BAO, J. W., LI, H. X., CHEN, D. J., HE, J., TAO, Y. F. & XU, P. 2017. miR-1338-5p Modulates Growth Hormone Secretion and Glucose Utilization by Regulating ghitm in Genetically Improved Farmed Tilapia (GIFT, Oreochromis niloticus). *Frontiers in Physiology,* 8.

RAMANATHAN, G., ELUMALAI, R., PERIYASAMY, S. & LAKKAKULA, B. 2014. Role of Renin-Angiotensin-Aldosterone System Gene Polymorphisms and Hypertension-induced End-stage Renal Disease in Autosomal Dominant Polycystic Kidney Disease. *Iranian Journal of Kidney Diseases,* 8**,** 265-277.

RANE, S. G. & REDDY, E. P. 1994. JAK3 - A NOVEL JAK KINASE ASSOCIATED WITH TERMINAL DIFFERENTIATION OF HEMATOPOIETIC-CELLS. *Oncogene,* 9**,** 2415-2423.

REEDERS, S. T., BREUNING, M. H., DAVIES, K. E., NICHOLLS, R. D., JARMAN, A. P., HIGGS, D. R., PEARSON, P. L. & WEATHERALL, D. J. 1985. A HIGHLY POLYMORPHIC DNA MARKER LINKED TO ADULT POLYCYSTIC KIDNEY-DISEASE ON CHROMOSOME-16. *Nature,* 317**,** 542-544.

REEVES, P. M., ABBASLOU, M. A., KOOLS, F. R. W., VUTIPONGSATORN, K., TONG, X. Y., GAVEGANO, C., SCHINAZI, R. F. & POZNANSKY, M. C. 2017. Ruxolitinib sensitizes ovarian cancer to reduced dose Taxol, limits tumor growth and improves survival in immune competent mice. *Oncotarget,* 8**,** 94040-94053.

ROMEO, G., COSTA, G., CATIZONE, L., GERMINO, G. G., WEATHERALL, D. J., DEVOTO, M., RONCUZZI, L., ZUCCHELLI, P., KEITH, T. & REEDERS, S. T. 1988. A 2ND GENETIC-LOCUS FOR AUTOSOMAL DOMINANT POLYCYSTIC KIDNEY-DISEASE. *Lancet,* 2**,** 8-11.

ROSE, S. R., MUNICCHI, G., BARNES, K. M., KAMP, G. A., URIARTE, M. M., ROSS, J. L., CASSORLA, F. & CUTLER, G. B. 1991. SPONTANEOUS GROWTH-HORMONE SECRETION INCREASES DURING PUBERTY IN NORMAL GIRLS AND BOYS. *Journal of Clinical Endocrinology & Metabolism,* 73**,** 428-435.

ROSS, R. J. M., LEUNG, K. C., MAAMRA, M., BENNETT, W., DOYLE, N., WATERS, M. J. & HO, K. K. Y. 2001. Binding and functional studies with the growth hormone receptor antagonist, B2036-PEG

(pegvisomant), reveal effects of pegylation and evidence that it binds to a receptor dimers. *Journal of Clinical Endocrinology & Metabolism,* 86**,** 1716-1723.

RUGGENENTI, P., REMUZZI, A., ONDEI, P., FASOLINI, G., ANTIGA, L., ENE-IORDACHE, B., REMUZZI, G. & EPSTEIN, F. H. 2005. Safety and efficacy of long-acting somatostatin treatment in autosomal-dominant polycystic kidney disease. *Kidney International,* 68**,** 206-216.

SALARDI, S., ORSINI, L. F., CACCIARI, E., RIGHETTI, F., DONATI, S., MANDINI, M., CICOGNANI, A. & BOVICELLI, L. 1991. GROWTH-HORMONE, INSULIN-LIKE GROWTH FACTOR-I, INSULIN AND C-PEPTIDE DURING HUMAN FETAL LIFE - INUTERO STUDY. *Clinical Endocrinology,* 34**,** 187-190.

SALEM, M. A. M. & WOLFF, G. L. 1989. POTENTIATION OF RESPONSE TO INSULIN AND ANTI-INSULIN ACTION BY 2 HUMAN PITUITARY PEPTIDES IN LEAN AGOUTI A/A, OBESE YELLOW AVY/A, AND C57BL 6J-OB OB MICE. *Proceedings of the Society for Experimental Biology and Medicine,* 191**,** 113-123.

SAPRE, M., TREMBLAY, D., WILCK, E., JAMES, A., LEITER, A., COLTOFF, A., KOSHY, A. G., KREMYANSKAYA, M., HOFFMAN, R., MASCARENHAS, J. O. & GALLAGHER, E. J. 2019. Metabolic Effects of JAK1/2 Inhibition in Patients with Myeloproliferative Neoplasms. *Scientific Reports,* 9.

SASSIN, J. F., PARKER, D. C., MACE, J. W., GOTLIN, R. W., JOHNSON, L. C. & ROSSMAN, L. G. 1969. HUMAN GROWTH HORMONE RELEASE - RELATION TO SLOW-WAVE SLEEP AND SLEEP-WAKING CYCLES. *Science,* 165**,** 513-&.

SCHEFF, R. T., ZUCKERMAN, G., HARTER, H., DELMEZ, J. & KOEHLER, R. 1980. DIVERTICULAR-DISEASE IN PATIENTS WITH CHRONIC-RENAL-FAILURE DUE TO POLYCYSTIC KIDNEY-DISEASE. *Annals of Internal Medicine,* 92**,** 202-204.

SCHREM, H., SCHNEIDER, V., KUROK, M., GOLDIS, A., DREIER, M., KALTENBORN, A., GWINNER, W., BARTHOLD, M., LIEBENEINER, J., WINNY, M., KLEMPNAUER, J. & KLEINE, M. 2016. Independent Pre-Transplant Recipient Cancer Risk Factors after Kidney Transplantation and the Utility of G-Chart Analysis for Clinical Process Control. *Plos One,* 11.

SCHWARZ, J. M., MULLIGAN, K., LEE, J., LO, J. C., WEN, M., NOOK, M. A., GRUNFELD, C. & SCHAMBELAN, M. 2002. Effects of recombinant human growth hormone on hepatic lipid and carbohydrate metabolism in HIV-infected patients with fat accumulation. *Journal of Clinical Endocrinology & Metabolism,* 87**,** 942-945.

SHARP, C. K., ZELIGMAN, B. E., JOHNSON, A. M., DULEY, I. & GABOW, P. A. 1999. Evaluation of colonic diverticular disease in autosomal dominant polycystic kidney disease without end-stage renal disease. *American Journal of Kidney Diseases,* 34**,** 863-868.

SHI, J., TONG, J. H. & CAI, S. 2014. GH1 T1663A polymorphism and cancer risk: a meta-analysis of case-control studies. *Tumor Biology,* 35**,** 4529-4538.

SHILLINGFORD, J. M., MURCIA, N. S., LARSON, C. H., LOW, S. H., HEDGEPETH, R., BROWN, N., FLASK, C. A., NOVICK, A. C., GOLDFARB, D. A., KRAMER-ZUCKER, A., WALZ, G., PIONTEK, K. B., GERMINO, G. G. & WEIMBS, T. 2006. The mTOR pathway is regulated by polycystin-1, and its inhibition reverses renal cystogenesis in polycystic kidney disease. *Proceedings of the National Academy of Sciences of the United States of America,* 103**,** 5466-5471.

SHOAF, S. E., WANG, Z., BRICRUONT, P. & MOLLIKAARJUN, S. 2007. Pharmacokinetics, pharmacodynamics, and safety of tolvaptan, 1498 a nonpeptide AVP antagonist, during ascending single-dose studies in healthy subjects. *Journal of Clinical Pharmacology,* 47**,** 1498-1507.

SIMARD, M., MANTHOS, H., GIAID, A., LEFEBVRE, Y. & GOODYER, C. G. 1996. Ontogeny of growth hormone receptors in human tissues: An immunohistochemical study. *Journal of Clinical Endocrinology & Metabolism,* 81**,** 3097-3102.

SINGH, A., UPADHYAY, V., UPADHYAY, A. K., SINGH, S. M. & PANDA, A. K. 2015. Protein recovery from inclusion bodies of Escherichia coli using mild solubilization process. *Microbial Cell Factories,* 14.

SMIT, L. S., MEYER, D. J., BILLESTRUP, N., NORSTEDT, G., SCHWARTZ, J. & CARTERSU, C. 1996. The role of the growth hormone (GH) receptor and JAK1 and JAK2 kinases in the activation of Stats 1, 3, and 5 by GH. *Molecular Endocrinology,* 10**,** 519-533.

SOLAZZO, A., TESTA, F., GIOVANELLA, S., BUSUTTI, M., FURCI, L., CARRERA, P., FERRARI, M., LIGABUE, G., MORI, G., LEONELLI, M., CAPPELLI, G. & MAGISTRONI, R. 2018. The prevalence of autosomal dominant polycystic kidney disease (ADPKD): A meta-analysis of European literature and prevalence evaluation in the Italian province of Modena suggest that ADPKD is a rare and underdiagnosed condition. *Plos One,* 13.

SONODA, H. & SUGIMURA, A. 2008. Improved Solubilization of Recombinant Human Growth Hormone Inclusion Body Produced in Escherichia coli. *Bioscience Biotechnology and Biochemistry,* 72**,** 2675-2680.

SOTIROPOULOS, A., GOUJON, L., SIMONIN, G., KELLY, P. A., POSTELVINAY, M. C. & FINIDORI, J. 1993. EVIDENCE FOR GENERATION OF THE GROWTH HORMONE-BINDING PROTEIN THROUGH PROTEOLYSIS OF THE GROWTH-HORMONE MEMBRANE-RECEPTOR. *Endocrinology,* 132**,** 1863-1865.

SPIRLI, C., MORELL, C. M., LOCATELLI, L., OKOLICSANYI, S., FERRERO, C., KIM, A. K., FABRIS, L., FIOROTTO, R. & STRAZZABOSCO, M. 2012. Cyclic AMP/PKA-dependent Paradoxical Activation of Raf/MEK/ERK Signaling in Polycystin-2 Defective Mice Treated With Sorafenib. *Hepatology,* 56**,** 2363-2374.

SPITHOVEN, E. M., KRAMER, A., MEIJER, E., ORSKOV, B., WANNER, C., ABAD, J. M., ARESTE, N., LA TORRE, R. A., CASKEY, F., COUCHOUD, C., FINNE, P., HEAF, J., HOITSMA, A., DE MEESTER, J., PASCUAL, J., POSTORINO, M., RAVANI, P., ZURRIAGA, O., JAGER, K. J., GANSEVOORT, R. T., REGISTRY, E.-E., EURO, C. C. & WGIKD 2014. Renal replacement therapy for autosomal dominant polycystic kidney disease (ADPKD) in Europe: prevalence and survival-an analysis of data from the ERA-EDTA Registry. *Nephrology Dialysis Transplantation,* 29**,** 15-25.

STAGNER, E. E., BOUVRETTE, D. J., CHENG, J. & BRYDA, E. C. 2009. The polycystic kidney disease-related proteins Bicc1 and SamCystin interact. *Biochemical and Biophysical Research Communications,* 383**,** 16-21.

STALLONE, G., INFANTE, B., GRANDALIANO, G., BRISTOGIANNIS, C., MACARINI, L., MEZZOPANE, D., BRUNO, F., MONTEMURNO, E., SCHIRINZI, A., SABBATINI, M., PISANI, A., TATARANNI, T., SCHENA, F. P. & GESUALDO, L. 2012. Rapamycin for treatment of type I autosomal dominant polycystic kidney disease (RAPYD-study): a randomized, controlled study. *Nephrology Dialysis Transplantation,* 27**,** 3560-3567.

STUDIER, F. W. 2005. Protein production by auto-induction in high-density shaking cultures. *Protein Expression and Purification,* 41**,** 207-234.

SUEN, C. S. & CHIN, W. W. 1993. LIGAND-DEPENDENT, PIT-1 GROWTH-HORMONE FACTOR-I (GHF-1)-INDEPENDENT TRANSCRIPTIONAL STIMULATION OF RAT GROWTH-HORMONE GENE-EXPRESSION BY THYROID-HORMONE RECEPTORS INVITRO. *Molecular and Cellular Biology,* 13**,** 1719-1727.

SYRO, L. V., SUNDSBAK, J. L., SCHEITHAUER, B. W., TOLEDO, R. A., CAMARGO, M., HEYER, C. M., SEKIYA, T., URIBE, H., ESCOBAR, J. I., VASQUEZ, M., ROTONDO, F., TOLEDO, S. P. A., KOVACS, K., HORVATH, E., BABOVIC-VUKSANOVIC, D. & HARRIS, P. C. 2012. Somatotroph pituitary adenoma with acromegaly and autosomal dominant polycystic kidney disease: SSTR5 polymorphism and PKD1 mutation. *Pituitary,* 15**,** 342-349.

TAKAKURA, A., NELSON, E. A., HAQUE, N., HUMPHREYS, B. D., ZANDI-NEJAD, K., FRANK, D. A. & ZHOU, J. 2011. Pyrimethamine inhibits adult polycystic kidney disease by modulating STAT signaling pathways. *Human Molecular Genetics,* 20**,** 4143-4154.

TALBOT, J. J., SHILLINGFORD, J. M., VASANTH, S., DOERR, N., MUKHERJEE, S., KINTER, M. T., WATNICK, T. & WEIMBS, T. 2011. Polycystin-1 regulates STAT activity by a dual mechanism. *Proceedings of the National Academy of Sciences of the United States of America,* 108**,** 7985-7990.

TEGLUND, S., MCKAY, C., SCHUETZ, E., VAN DEURSEN, J. M., STRAVOPODIS, D., WANG, D. M., BROWN, M., BODNER, S., GROSVELD, G. & IHLE, J. N. 1998. Stat5a and Stat5b proteins have essential and nonessential, or redundant, roles in cytokine responses. *Cell,* 93**,** 841-850.

TELLMAN, M. W., BAHLER, C. D., SHUMATE, A. M., BACALLAO, R. L. & SUNDARAM, C. P. 2015. Management of Pain in Autosomal Dominant Polycystic Kidney Disease and Anatomy of Renal Innervation. *Journal of Urology,* 193**,** 1470-1478.

TENTLER, J. J., HADCOCK, J. R. & GUTIERREZHARTMANN, A. 1997. Somatostatin acts by inhibiting the cyclic 3',5'-adenosine monophosphate (cAMP)/protein kinase A pathway, cAMP response element-binding protein (CREB) phosphorylation, and CREB transcription potency. *Molecular Endocrinology,* 11**,** 859-866.

TORRA, R., BADENAS, C., DARNELL, A., NICOLAU, C., VOLPINI, V., REVERT, L. & ESTIVILL, X. 1996. Linkage, clinical features, and prognosis of autosomal dominant polycystic kidney disease types 1 and 2. *Journal of the American Society of Nephrology,* 7**,** 2142-2151.

TORRES, V. E., CHAPMAN, A. B., DEVUYST, O., GANSEVOORT, R. T., GRANTHAM, J. J., HIGASHIHARA, E., PERRONE, R. D., KRASA, H. B., OUYANG, J., CZERWIEC, F. S. & INVESTIGATORS, T. T. 2012. Tolvaptan in Patients with Autosomal Dominant Polycystic Kidney Disease. *New England Journal of Medicine,* 367**,** 2407-2418.

TORRES, V. E. & HARRIS, P. C. 2014. Strategies Targeting cAMP Signaling in the Treatment of Polycystic Kidney Disease. *Journal of the American Society of Nephrology,* 25**,** 18-32.

TORRES, V. E., WILSON, D. M., HATTERY, R. R. & SEGURA, J. W. 1993. RENAL STONE DISEASE IN AUTOSOMAL-DOMINANT POLYCYSTIC KIDNEY-DISEASE. *American Journal of Kidney Diseases,* 22**,** 513-519.

TRAINER, P. J., DRAKE, W. M., KATZNELSON, L., FREDA, P. U., HERMAN-BONERT, V., VAN DER LELY, A. J., DIMARAKI, E. V., STEWART, P. M., FRIEND, K. E., VANCE, M. L., BESSER, G. M., SCARLETT, J. A., THORNER, M. O., PARKINSON, C., KLIBANSKI, A., POWELL, J. S., BARKAN, A. L., SHEPPARD, M. C., MALDONADO, M., ROSE, D. R., CLEMMONS, D. R., JOHANNSON, G., BENGTSSON, B. A., STAVROU, S., KLEINBERG, D. L., COOK, D. M., PHILLIPS, L. S., BIDLINGMAIER, M., STRASBURGER, C. J., HACKETT, S., ZIB, K., BENNETT, W. F. & DAVIS, R. J. 2000. Treatment of acromegaly with the growth hormone-receptor antagonist pegvisomant. *New England Journal of Medicine,* 342**,** 1171-1177.

TRAN, U., ZAKIN, L., SCHWEICKERT, A., AGRAWAL, R., DOGER, R., BLUM, M., DE ROBERTIS, E. M. & WESSELY, O. 2010. The RNA-binding protein bicaudal C regulates polycystin 2 in the kidney by antagonizing miR-17 activity. *Development,* 137**,** 1107-1116.

TRUDEL, M., BARISONI, L., LANOIX, J. & D'AGATI, V. 1998. Polycystic kidney disease in SBM transgenic mice - Role of c-myc in disease induction and progression. *American Journal of Pathology,* 152**,** 219-229.

TRUDEL, M., DAGATI, V. & COSTANTINI, F. 1991. C-MYC AS AN INDUCER OF POLYCYSTIC KIDNEY-DISEASE IN TRANSGENIC MICE. *Kidney International,* 39**,** 665-671.

TSIOKAS, L., ARNOULD, T., ZHU, C. W., KIM, E., WALZ, G. & SUKHATME, V. P. 1999. Specific association of the gene product of PKD2 with the TRPC1 channel. *Proceedings of the National Academy of Sciences of the United States of America,* 96**,** 3934-3939.

TURCO, A. E., CLEMENTI, M., ROSSETTI, S., TENCONI, R. & PIGNATTI, P. F. 1996. An Italian family with autosomal dominant polycystic kidney disease unlinked to either the PKD1 or PKD2 gene. *American Journal of Kidney Diseases,* 28**,** 759-761.

UDY, G. B., TOWERS, R. P., SNELL, R. G., WILKINS, R. J., PARK, S. H., RAM, P. A., WAXMAN, D. J. & DAVEY, H. W. 1997. Requirement of STAT5b for sexual dimorphism of body growth rates and liver gene expression. *Proceedings of the National Academy of Sciences of the United States of America,* 94**,** 7239-7244.

VAN KERKHOF, P., GROVERS, R., DOS SANTOS, C. M. A. & STROUS, G. J. 2000. Endocytosis and degradation of the growth hormone receptor are proteasome-dependent. *Journal of Biological Chemistry,* 275**,** 1575-1580.

VERSTOVSEK, S., MESA, R. A., GOTLIB, J., GUPTA, V., DIPERSIO, J. F., CATALANO, J. V., DEININGER, M. W. N., MILLER, C. B., SILVER, R. T., TALPAZ, M., WINTON, E. F., HARVEY, J. H., ARCASOY, M. O., HEXNER, E. O., LYONS, R. M., PAQUETTE, R., RAZA, A., JONES, M., KORNACKI, D., SUN, K., KANTARJIAN, H. & INVESTIGATORS, C.-I. 2017. Long-term treatment with ruxolitinib for patients with myelofibrosis: 5-year update from the randomized, double-blind, placebo-controlled, phase 3 COMFORT-I trial. *Journal of Hematology & Oncology,* 10.

VERSTOVSEK, S., MESA, R. A., GOTLIB, J., LEVY, R. S., GUPTA, V., DIPERSIO, J. F., CATALANO, J. V., DEININGER, M. W. N., MILLER, C. B., SILVER, R. T., TALPAZ, M., WINTON, E. F., HARVEY, J. H., ARCASOY, M. O., HEXNER, E. O., LYONS, R. M., RAZA, A., VADDI, K., SUN, W., PENG, W., SANDOR, V., KANTARJIAN, H. & INVESTIGATORS, C.-I. 2015. Efficacy, safety, and survival with ruxolitinib in patients with myelofibrosis: results of a median 3-year follow-up of COMFORT-I. *Haematologica,* 100**,** 482-491.

VIAU, A., BAAZIZ, M., AKA, A., MAZLOUM, M., NGUYEN, C., KUEHN, E. W., TERZI, F. & BIENAIME, F. 2020. Tubular STAT3 Limits Renal Inflammation in Autosomal Dominant Polycystic Kidney Disease. *Journal of the American Society of Nephrology,* 31**,** 1035-1049.

VLAK, M. H. M., ALGRA, A., BRANDENBURG, R. & RINKEL, G. J. E. 2011. Prevalence of unruptured intracranial aneurysms, with emphasis on sex, age, comorbidity, country, and time period: a systematic review and meta-analysis. *Lancet Neurology,* 10**,** 626-636.

VON WALDTHAUSEN, D. C., SCHNEIDER, M. R., RENNER-MUELLER, I., RAULEDER, D. N., HERBACH, N., AIGNER, B., WANKE, R. & WOLF, E. 2008. Systemic overexpression of growth hormone (GH) in transgenic FVB/N inbred mice: an optimized model for holistic studies of molecular mechanisms underlying GH-induced kidney pathology. *Transgenic Research,* 17**,** 479-488.

WAGNER, K., HEMMINKI, K. & FORSTI, A. 2007. The GH1/IGF-1 axis polymorphisms and their impact on breast cancer development. *Breast Cancer Research and Treatment,* 104**,** 233-248.

WAHL, P. R., SERRA, A. L., LE HIR, M., MOLLE, K. D., HALL, M. N. & WUTHRICH, R. P. 2006. Inhibition of mTOR with sirolimus slows disease progression in Han : SPRD rats with autosomal dominant polycystic kidney disease (ADPKD). *Nephrology Dialysis Transplantation,* 21**,** 598-604.

WANG, X. F., WU, Y. H., WARD, C. J., HARRIS, P. C. & TORRES, V. E. 2008. Vasopressin directly regulates cyst growth in polycystic kidney disease. *Journal of the American Society of Nephrology,* 19**,** 102-108.

WANG, Y., LANGLEY, R. J., TAMSHEN, K., JAMIESON, S. M., LU, M., MAYNARD, H. D. & PERRY, J. K. 2020. Long-Acting Human Growth Hormone Receptor Antagonists Produced in E. coli and Conjugated with Polyethylene Glycol. *Bioconjugate Chemistry,* 31**,** 1651-1660.

WARD, C. J., PERAL, B., HUGHES, J., THOMAS, S., GAMBLE, V., MACCARTHY, A. B., SLOANESTANLEY, J., BUCKLE, V. J., KEARNEY, L., HIGGS, D. R., RATCLIFFE, P. J., HARRIS, P. C., ROELFSEMA, J. H., SPRUIT, L., SARIS, J. J., DAUWERSE, H. G., PETERS, D. J. M., BREUNING, M. H., NELLIST, M., BROOKCARTER, P. T., MAHESHWAR, M. M., CORDEIRO, I., SANTOS, H., CABRAL, P., SAMPSON, J. R., JANSSEN, B., HESSELINGJANSSEN, A. L. W., VANDENOUWELAND, A. M. W., EUSSEN, B., VERHOEF, S., LINDHOUT, D. & HALLEY, D. J. J. 1994. THE POLYCYSTIC KIDNEY-DISEASE-1 GENE ENCODES A 14-KB TRANSCRIPT AND LIES WITHIN A DUPLICATED REGION ON CHROMOSOME-16. *Cell,* 77**,** 881-894.

WATKINS, P. B., LEWIS, J. H., KAPLOWITZ, N., ALPERS, D. H., BLAIS, J. D., SMOTZER, D. M., KRASA, H., OUYANG, J., TORRES, V. E., CZERWIEC, F. S. & ZIMMER, C. A. 2015. Clinical Pattern of Tolvaptan-Associated Liver Injury in Subjects with Autosomal Dominant Polycystic Kidney Disease: Analysis of Clinical Trials Database. *Drug Safety,* 38**,** 1103-1113.

WATNICK, T., HE, N., WANG, K. R., LIANG, Y., PARFREY, P., HEFFERTON, D., ST GEORGE-HYSLOP, P., GERMINO, G. & PEI, Y. 2000. Mutations of PKD1 in ADPKD2 cysts suggest a pathogenic effect of trans-heterozygous mutations. *Nature Genetics,* 25**,** 143-144.

WAXMAN, D. J., RAM, P. A., PARK, S. H. & CHOI, H. K. 1995. INTERMITTENT PLASMA GROWTH-HORMONE TRIGGERS TYROSINE PHOSPHORYLATION AND NUCLEAR TRANSLOCATION OF A LIVER-EXPRESSED, STAT 5-RELATED DNA-BINDING PROTEIN - PROPOSED ROLE AS AN

INTRACELLULAR REGULATOR OF MALE-SPECIFIC LIVER GENE-TRANSCRIPTION. *Journal of Biological Chemistry,* 270**,** 13262-13270.

WEI, S., TANAKA, H., KUBO, T., ONO, T., KANZAKI, S. & SEINO, Y. 1997. Growth hormone increases serum 1,25-dihydroxyvitamin D levels and decreases 24,25-dihydroxyvitamin D levels in children with growth hormone deficiency. *European Journal of Endocrinology,* 136**,** 45-51.

WIDEMAN, L., WELTMAN, J. Y., HARTMAN, M. L., VELDHUIS, J. D. & WELTMAN, A. 2002. Growth hormone release during acute and chronic aerobic and resistance exercise - Recent findings. *Sports Medicine,* 32**,** 987-1004.

WILKINSON, I. R., PRADHANANGA, S. L., SPEAK, R., ARTYMIUK, P. J., SAYERS, J. R. & ROSS, R. J. 2016. A long-acting GH receptor antagonist through fusion to GH binding protein. *Scientific Reports,* 6.

WILKS, A. F., HARPUR, A. G., KURBAN, R. R., RALPH, S. J., ZURCHER, G. & ZIEMIECKI, A. 1991. 2 NOVEL PROTEIN-TYROSINE KINASES, EACH WITH A 2ND PHOSPHOTRANSFERASE-RELATED CATALYTIC DOMAIN, DEFINE A NEW CLASS OF PROTEIN-KINASE. *Molecular and Cellular Biology,* 11**,** 2057-2065.

WILLEY, C. J., BLAIS, J. D., HALL, A. K., KRASA, H. B., MAKIN, A. J. & CZERWIEC, F. S. 2017. Prevalence of autosomal dominant polycystic kidney disease in the European Union. *Nephrology Dialysis Transplantation,* 32**,** 1356-1363.

WILSON, P. D., SHERWOOD, A. C., PALLA, K., DU, J., WATSON, R. & NORMAN, J. T. 1991. REVERSED POLARITY OF NA+-K+-ATPASE - MISLOCATION TO APICAL PLASMA-MEMBRANES IN POLYCYSTIC KIDNEY-DISEASE EPITHELIA. *American Journal of Physiology,* 260**,** F420-F430.

WOOD, T. J. J., SLIVA, D., LOBIE, P. E., PIRCHER, T. J., GOUILLEUX, F., WAKAO, H., GUSTAFSSON, J. A., GRONER, B., NORSTEDT, G. & HALDOSEN, L. A. 1995. MEDIATION OF GROWTH HORMONE-DEPENDENT TRANSCRIPTIONAL ACTIVATION BY MAMMARY-GLAND FACTOR STAT-5. *Journal of Biological Chemistry,* 270**,** 9448-9453.

WU, G. Q., MARKOWITZ, G. S., LI, L., D'AGATI, V. D., FACTOR, S. M., GENG, L., TIBARA, S., TUCHMAN, J., CAI, Y. Q., PARK, J. H., VAN ADELSBERG, J., HOU, H., KUCHERLAPATI, R., EDELMANN, W. & SOMLO, S. 2000. Cardiac defects and renal failure in mice with targeted mutations in Pkd2. *Nature Genetics,* 24**,** 75-78.

WU, G. Q., TIAN, X., NISHIMURA, S., MARKOWITZ, G. S., D'AGATI, V., PARK, J. H., YAO, L. L., LI, L., GENG, L., ZHAO, H. Y., EDELMANN, W. & SOMLO, S. 2002. Trans-heterozygous Pkd1 and Pkd2 mutations modify expression of polycystic kidney disease. *Human Molecular Genetics,* 11**,** 1845-1854.

WU, M., WAHL, P. R., LE HIR, M., WACKERLE-MEN, Y., WUTHRICH, R. P. & SERRA, A. L. 2007. Everolimus retards cyst growth and preserves kidney function in a rodent model for polycystic kidney disease. *Kidney & Blood Pressure Research,* 30**,** 253-259.

XU, J., ZHANG, Y., BERRY, P. A., JIANG, J., LOBIE, P. E., LANGENHEIM, J. F., CHEN, W. Y. & FRANK, S. J. 2011. Growth Hormone Signaling in Human T47D Breast Cancer Cells: Potential Role for a Growth Hormone Receptor-Prolactin Receptor Complex. *Molecular Endocrinology,* 25**,** 597-610.

YAMAGUCHI, T., NAGAO, S., KASAHARA, M., TAKAHASHI, H. & GRANTHAM, J. J. 1997. Renal accumulation and excretion of cyclic adenosine monophosphate in a murine model of slowly progressive polycystic kidney disease. *American Journal of Kidney Diseases,* 30**,** 703-709.

YAMAGUCHI, T., PELLING, J. C., RAMASWAMY, N. T., EPPLER, J. W., WALLACE, D. P., NAGAO, S., ROME, L. A., SULLIVAN, L. P. & GRANTHAM, J. J. 2000. cAMP stimulates the in vitro proliferation of renal cyst epithelial cells by activating the extracellular signal-regulated kinase pathway. *Kidney International,* 57**,** 1460-1471.

YAMAMOTO, M., MATSUMOTO, R., FUKUOKA, H., IGUCHI, G., TAKAHASHI, M., NISHIZAWA, H., SUDA, K., BANDO, H. & TAKAHASHI, Y. 2016. Prevalence of Simple Renal Cysts in Acromegaly. *Internal Medicine,* 55**,** 1685-1690.

YANG, L. P. H. & KEATING, G. M. 2010. Octreotide Long-Acting Release (LAR) A Review of its Use in the Management of Acromegaly. *Drugs,* 70**,** 1745-1769.

YAO, Z. J., CUI, Y. Z., WATFORD, W. T., BREAM, J. H., YAMAOKA, K., HISSONG, B. D., LI, D., DURUM, S. K., JIANG, Q. O., BHANDOOLA, A., HENNIGHAUSEN, L. & O'SHEA, J. J. 2006. Stat5a/b are essential for normal lymphoid development and differentiation. *Proceedings of the National Academy of Sciences of the United States of America,* 103**,** 1000-1005.

YHESKEL, M., LAKHIA, R., COBO-STARK, P., FLATEN, A. & PATEL, V. 2019. Anti-microRNA screen uncovers miR-17 family within miR-17 similar to 92 cluster as the primary driver of kidney cyst growth. *Scientific Reports,* 9**,** 11.

YIN, X., PRINCE, W. K., BLUMENFELD, J. D., ZHANG, W., DONAHUE, S., BOBB, W. O., RENNERT, H., ASKIN, G., BARASH, I. & PRINCE, M. R. 2019. Spleen phenotype in autosomal dominant polycystic kidney disease. *Clinical Radiology,* 74.

YOSHIDA, A., ISHIOKA, C., KIMATA, H. & MIKAWA, H. 1992. RECOMBINANT HUMAN GROWTH-HORMONE STIMULATES B-CELL IMMUNOGLOBULIN-SYNTHESIS AND PROLIFERATION IN SERUM-FREE MEDIUM. *Acta Endocrinologica,* 126**,** 524-529.

YU, S. Q., HACKMANN, K., GAO, J. G., HE, X. B., PIONTEK, K., GONZALEZ, M. A. G., MENEZES, L. F., XU, H. X., GERMINO, G. G., ZUO, J. & QIAN, F. 2007. Essential role of cleavage of Polycystin-1 at G protein-coupled receptor proteolytic site for kidney tubular structure. *Proceedings of the National Academy of Sciences of the United States of America,* 104**,** 18688-18693.

YU, T. M., CHUANG, Y. W., YU, M. C., CHEN, C. H., YANG, C. K., HUANG, S. T., LIN, C. L., SHU, K. H. & KAO, C. H. 2016. Risk of cancer in patients with polycystic kidney disease: a propensity-score matched analysis of a nationwide, population-based cohort study. *Lancet Oncology,* 17**,** 1419-1425.

ZITTEMA, D., BOERTIEN, W. E., VAN BEEK, A. P., DULLAART, R. P. F., FRANSSEN, C. F. M., DE JONG, P. E., MEIJER, E. & GANSEVOORT, R. T. 2012. Vasopressin, Copeptin, and Renal Concentrating Capacity in Patients with Autosomal Dominant Polycystic Kidney Disease without Renal Impairment. *Clinical Journal of the American Society of Nephrology,* 7**,** 906-913.